

The Design and
Optimisation of a
Reflective Concentrator
Photovoltaic Generation
System



John Lasich

Doctor of Philosophy

VICTORIA UNIVERSITY OF TECHNOLOGY



3 0001 00684 7133

2010
VU

**The Design and Optimisation of a Reflective Concentrator
Photovoltaic Generation System**

Volume I

By John Lasich, BSc



Centre for Environmental Safety and Risk Engineering
Victoria University
Melbourne, Australia

2009

Dedication

This is dedicated to my wife Sue who helped me make the first CPV modules on the kitchen table in 1991 and whose undying faith and support has allowed me to bring this technology into being.

Declaration of the Candidate

I, John Lasich, declare that the PhD thesis entitled The Design and Optimisation of a Reflective Concentrator Photovoltaic Generation System is no more than 100,000 words in length including quotes and exclusive of tables, figures, appendices, bibliography, references and footnotes. This thesis contains no material that has been submitted previous, in whole or in part, for the award of any other academic degree or diploma. Except where otherwise indicated, this thesis is my own work.

Signature:

Date: 20/10/10

Acknowledgements

I gratefully appreciate the help and support from the many people who have helped and assisted me in this endeavour and the writing of this thesis including Pierre Verlinden, who has been a champion of CPV over the last 20 years, Chantha Chey and Annelene Dethlefsen for great assistance with the manuscript and the research team at Solar Systems (past and present) including; Dave Edwards, George Ganakas, Igor Varfolomeev, Neel Kaila, Mark Wright, Michael Volk, Ian Connaughton, Ian Bennier, Robbert Veerman, Huon Kendall, the Cleeve family, Astrid Lasich, Vincent Kelly and my ever patient and supportive supervisor Prof. Graham Thorpe. The cooperation of the folks at Spectrolab is also appreciated in particular Dave Lillington, Raed Sherif, Jeff Kinsey, Nassen Karam, Jim Ermer and Peter Hebert. Thanks also go to Julia Birch for helping me put the final ‘wraps’ on a sixteen year thesis. The support from my son, Zoran, for coolly fixing IT roadblocks and my daughter Astrid for continued moral support also deserves special acknowledgement. I thank you all.

Abstract

In these uncertain times having a clean, secure and definable energy supply will be a key ingredient necessary to provide a platform to underpin and stabilise our financial and economic systems while removing one of the greatest causes of political conflict.

The solar energy resource is widespread and can provide more than a thousand fold for our energy needs for the foreseeable future. To effectively harness this energy a number of challenges must be met to overcome shortcomings and inertia including aspects of a technical, social and political nature.

The researcher has focused this work on solving the key issue of the relatively high cost of solar power compared to that which society has come to accept for our present fossil fuel based energy.

Although it could be possible to use political means to lead the process there appears to be insufficient will and cooperation at a global level to effect this by politics alone. Put simply we could have the major countries ramp up their selling price of energy forms (which are limited or polluting) to a level where clean renewable energy can compete. (Probably about three times the present price). The additional revenue would be used to develop clean renewable energy and appliances for the demand side users who will naturally become more efficient (Also creating a new efficiency industry).

The resulting situation would see customers paying 3 times as much for energy but with 3 times the efficiency; their cost/comfort quotient would remain the same. With this achieved, new industries would become established around renewable and the demand on our earthly resources relieved so that they can be used to address other challenges such as provision of food for an exponentially growing population and perseveration of our worlds ecology.

These issues and options have been discussed for the last 30 years (Lasich, 1976). To date only a few percent of our power is generated from clean renewable energy

sources. This is a clear sign our politicians, businessmen and the community need more options to expeditiously tackle our energy challenges if we are to avoid a crisis.

The researcher has attempted to move us one step closer to a solution by providing a scientific solution which could significantly reduce the cost of solar power and therefore harness the power of enterprise by making it economically viable to make a profit from selling clean renewable power systems. The rest will follow.

This work has shown that there is a new pathway to lower the cost of solar power using a high concentration PV system with a separate collector and ‘dense array’ receiver which has been shown to work reliably, achieve high efficiency and have the potential for low cost. During this research a number of challenges had to be met including:

- Developing and cooling a photovoltaic receiver which could work efficiently and reliably in a concentrated light beam which can melt steel
- Developing the first ‘back contact’ multijunction CPV cell
- Developing and correlating a realistic ray tracing/receiver model
- Developing an optical system which can deliver an evenly distributed light beam to the PV cells at 500 suns intensity
- Tracking and managing the system to maintain high performance over long periods of varied weather conditions and loads
- Monitoring and measuring the performance and reliability of these subsystems requiring new techniques and metrics to be developed

All of the above problems were solved resulting in a new ‘reflective-dense array’ technology with a peak DC STC efficiency of more than 28% at 36kW. The researcher believes this system may have the highest long term performance published for any solar power system at 22% average annual AC efficiency (Lasich, 2009) and the system:

- Has operated for 6 years with quantified output (using multijunction cells for the last 3 years) producing over 4 GWh in total with 1.5 GWh from multijunction cells.
- Has potential for low capital cost $\$4/W_{AC}$ at 50MW/year and less than $\$2/W$ at 500MW/year with an unsubsidised LCOE at $\$100/MWh$. This is competitive with coal fired power stations which account for their pollution.
- Has a maximum scope for continued improvement in performance since the efficiency of a small area of cells can continue to increase at the present rate of 1% absolute per year with little influence on the system cost.
- Has scope for two different formats of CPV as a dish or central receiver and has diverse application for cogeneration or other high value applications such as hydrogen production for storage or fuel. The peak efficiency for cogeneration is estimated to be 60%.

During the journey of this research, a number of other discoveries were made in relation to this unique CPV system with reflective collector optics and a separate receiver/energy converter, including:

- Containment of all the complex components of CVP modules, monitoring and secondary optics in a small demountable receiver
- Has a very low manufacturing cost at less than one tenth of the plant cost for a 'one sun' PV module plant for a given production rate.
- Can be fully monitored and managed 'on line' at low cost resulting in reduced O&M and high average efficiency
- Can be simply upgraded by changing the receiver in less than one hour.
- Reflective optics with a single receiver, are more efficient than refractive optics with many targets because; 1. Mirrors have a reflectivity of 95% whereas lenses have transmission up to 90%, 2. alignment is less critical for many mirrors aimed at a single target and 3. feedback can be used to almost perfectly align a single solar beam with the needs of a single array of CPV cells.

- CPV systems have the lowest embodied energy of any solar power system (approx 1 year) being comparable to wind turbines but with a far greater resource available.
- With the power output of the CPV modules being more than 1000 times greater than the typical thin film module (of the same area), CPV is unlikely to be constrained by limited supplies of exotic materials.
- The modular dense array receiver can be deployed at any scale from a single module 500W receiver in a small dish to a 256 modules in a 140kW receiver for a central receiver. With 40% efficient cells a 1 MW dense array is just 6 m². This allows a great degree of pre-fabrication and pre-commissioning for large scale roll out.
- Reflective concentrator systems with a high power single beam as developed by the researcher for CPV are versatile and can be used for other applications which do not include PV. This gives greater value to the concentrator system technology.
- The 140 kW central receiver 'HCPV' system produced a peak DC efficiency of 25% (equivalent to 22 % AC) which is possibly the highest efficiency recorded for a central receiver system.

The sum of these findings is that a CPV system with reflective optics and a separate dense array PV receiver is the most efficient of any solar power technology and has a clear pathway to a competitive cost. With its unique potential for continuous improvement and diverse application this is likely to be one of those technologies which can take our world one step closer to the 'balance' we need for sustained occupation of this planet.

Table of Contents

Dedication	i
Declaration of the Candidate	ii
Acknowledgements	iii
Abstract	iv
CHAPTER 1. INTRODUCTION	1
1.1 <i>The Energy Context in the World and in Australia</i>	1
1.2 <i>The Intellectual Framework of this Research</i>	9
CHAPTER 2. EXPLORATION OF ALTERNATIVE DESIGNS	12
2.1 <i>Introduction</i>	12
2.2 <i>Flat Plate PV</i>	14
2.3 <i>Concentrating Solar Thermal (CST)</i>	17
2.4 <i>Low Concentration CPV</i>	19
2.5 <i>CPV Using Trough Concentrators</i>	20
CHAPTER 3. OUTLINE OF SYSTEM PHILOSOPHY & IDENTIFICATION OF MAJOR COMPONENTS	29
3.1 <i>System Components: Philosophy, Realisation and Results</i>	31
3.2 <i>Dish Solar Concentrator (small – 20m²)</i>	31
3.2.1 <i>Characterisation and Optimisation of a 20m² Concentrator Dish</i>	31
3.2.2 <i>Primary Concentrator Optics</i>	32
3.2.3 <i>The Sun</i>	35
3.2.4 <i>Reflection Errors</i>	36
3.2.5 <i>Mirror Reflectivity and Mirror Dead Space</i>	39
3.2.6 <i>Correlation of prediction with measured results</i>	40
3.2.7 <i>Secondary Optics</i>	44
3.3 <i>The Photovoltaic Receiver</i>	48
3.4 <i>Solar Cell Array</i>	50
CHAPTER 4. SOLAR CELLS SUITABLE FOR HIGH CONCENTRATION – THEORY & PRACTICE	53
4.1 <i>Theory of Operation of Solar Cells</i>	53
4.2 <i>Maximum Theoretical Efficiency of Solar Cells</i>	56
4.3 <i>Current World Record Efficiencies</i>	59
4.4 <i>Simulation of 35kW Multi-Junction Receiver</i>	59
4.4.1 <i>Spectral Response and Quantum Efficiency of Triple-Junction Solar Cells</i>	59
4.4.2 <i>Direct Solar Spectrum</i>	61
4.4.3 <i>Calculation of the Photo-Generated Current</i>	62
4.4.4 <i>Effect of non-uniformity of light</i>	65
4.4.5 <i>Sensitivity to Atmospheric Parameters</i>	66
4.4.6 <i>Reliability of Multijunction Receiver</i>	71
4.4.7 <i>Future High-Performance Receivers</i>	71

4.5	<i>Temperature Coefficients</i>	76
4.6	<i>Cell Types</i>	77
4.7	<i>Future projections for cell efficiency</i>	78
CHAPTER 5. 130m² DISH CPV SYSTEM		79
5.1	<i>Primary Optics</i>	81
5.2	<i>Mirror Panels</i>	81
5.3	<i>Dish Frame</i>	88
5.4	<i>Receiver</i>	88
5.4.1	<i>Secondary Optics</i>	89
5.4.2	<i>Cell Array and Modules</i>	89
5.4.3	<i>Heat Sinks and Thermal Considerations</i>	92
5.5	<i>Monitoring</i>	97
5.6	<i>Tracking System</i>	101
5.7	<i>Balance of System</i>	109
5.8	<i>Raytrace Modelling</i>	109
5.9	<i>Actual Performance</i>	116
CHAPTER 6. LONG TERM PERFORMANCE/ENERGY PREDICTIONS/ENERGY COST		118
6.1	<i>Relationship to Instantaneous Performance and Definitions</i>	118
6.2	<i>Nominal Target Performances – 130m² Dish and Modules and Cells</i>	119
6.3	<i>Definitions</i>	120
6.4	<i>TRANSOP Estimated for 130m² Dish for 2008</i>	122
6.5	<i>EPR and Average System Efficiency</i>	122
6.6	<i>Energy & Performance Analysis</i>	123
6.7	<i>Levelised Cost of Energy (LCOE) Model</i>	126
CHAPTER 7. RELIABILITY		132
7.1	<i>Operation and Maintenance</i>	132
7.2	<i>Modules</i>	132
7.3	<i>Accelerated Testing</i>	133
7.4	<i>Damp Heat and High Temperature Soak</i>	133
7.5	<i>Thermal Cycling</i>	134
7.6	<i>UV Exposure</i>	135
7.7	<i>Humidity Freeze tests</i>	135
7.8	<i>Observed Cell Degradations</i>	135
7.9	<i>Mirrors</i>	136
7.10	<i>Mechanicals</i>	137
7.11	<i>Maintenance</i>	137
CHAPTER 8. FUTURE WORK AND PROJECTIONS		138
8.1	<i>Limits on the Minimum Cost</i>	138
8.2	<i>Possible Performance Improvements for MkV 130m² Dish</i>	138
8.3	<i>Infant Mortality</i>	139
8.4	<i>Optical Efficiency</i>	140
8.5	<i>Increased Concentration Ratio</i>	140
8.6	<i>Control Maximum Power Point, Tracking Optimisation</i>	140
8.7	<i>Parasitics Reduction</i>	140
8.8	<i>Power Matching</i>	141
8.9	<i>Enhanced Monitoring, Replacement and Possible Recycling of Cells/Modules</i>	141
8.10	<i>Other Formats</i>	142
8.11	<i>HCPV</i>	142
8.12	<i>Small Domestic</i>	147
8.13	<i>Other Applications</i>	147
8.14	<i>Cogeneration</i>	147

8.14.1	PV Power and Low Temperature Heat	147
8.14.2	Spectrum Splitting	147
8.15	<i>Thermal Applications</i>	149
8.16	<i>Correlation of Efficiency Improvements with Sales</i>	150
8.17	<i>Embedded Energy and Energy Payback Ratio</i>	150

CHAPTER 9. PROJECTS DESIGNED AND BUILT BY THE RESEARCHER AND CO-WORKERS	151
CHAPTER 10. CONCLUSIONS	153
CHAPTER 11. REFERENCES	156
CHAPTER 12. APPENDICES	165
CHAPTER 13. LIST OF ACRONYMS	179

CHAPTER 1.

INTRODUCTION

1.1 *The Energy Context in the World and in Australia*

Today, energy is one of the most important resources on earth. With a suitable supply of energy it is possible to produce most of the other resources we require for survival, for example fresh water which in turn can be used to produce food. Globally, we consumed over ten trillion (10^{13}) kWh of fossil derived energy in 2007 (IEA, 2009) and spent several trillion dollars per year to buy it. Presently, energy is mostly used to make our lives easier, to harvest food, to run cars, to power TVs and other appliances and to power the industries that make these cars and appliances.

For those pleasures, we discharge over thirty billion (3×10^{10}) tonnes (IEA, 2009) of greenhouse gases into our atmosphere each year, resulting in a concomitant temperature rise of 0.8°C over the last one hundred years, and seemingly in climatic disturbances with increased frequency and range, from droughts to cyclones, which result in famine and devastation.

Such is our addiction to energy that wars have been (and are being) fought to seize or maintain secure supplies.

All this trouble and our fossil energy is relatively affordable for present industrialised users, but as supply is running out, the total cost of fossil energy will keep increasing (particularly if it is true as many believe that we are already half way through the oil reserves)! (Strahan, 2007)

Clearly the sourcing, ownership and utilisation of energy have a significant impact on our living.

At present consumption rates, it is predicted that the reserves of oil and gas will last between 40 to 60 years (BP Global, 2009) and coal will last for 120 years. In fact, our consumption rates are increasing at an exponential rate and our resources will be consumed in shorter time spans. The remaining resource will become progressively more expensive since the 'easy' accessible product is 'tapped' first.

War, famine, disaster and hedonism are all linked to our present energy consumption. Most people in the world are 'touched' by energy every day (mostly positively). Soon it will be linked to survival! For many, energy could change from being a commodity to a luxury, or for others from being a luxury to a necessity. Our exponentially increasing population will make this problem more acute.

An example of other impacts of own energy practices is exemplified by our coal fired power stations in Victoria is reported in *The Age*, 2009. Our power stations consume approximately one third of Melbourne's water (125 billion liters of water per year).

We have been aware of these issues for over 30 years (Lasich, J 1976). Clearly there is need for a change.

Increasing proportions of our energy use will be allocated to survival processes such as desalination to produce potable water, water table reduction to 'desalt' degraded land and production of fertiliser to make (presently mild climate) deserts available for food production.

If we were looking for an 'energy' solution to these problems of higher prices, increasing pollution, global devastation, wars and political domination driven by increasingly scarce resources, the answer may lie with solar energy.

The earth receives 7×10^{17} kWh of sunlight per year (Avallone and Baumeister, 1987) (the average diameter of Earth is 7,918.78 miles or 12,670 km. The apparent disk area of the Earth is 126,079,077 km². The extra-terrestrial solar radiation is 1.367 kW/m² some of which is reflected or transformed to heat. For 24 hours and 365 days, this becomes: 1.5×10^{18} kWh of sunlight per year. If the sun's rays are attenuated to 1 kWm², the amount of energy is 1.1×10^{18} kWh). This is an upper limit because atmospheric absorption at the edge of the disk is more important than at the centre of the Earth disk of radiant energy from the sun, and this is 7,000 times more energy than we presently consume. Solar radiation is also widely available in useful quantities for power generation for most of the world's population.

A solar energy system based on PV cells placed in a sunny climate, having an efficiency of 25% and a packing factor of 50% would require a total area of just 520km x 520km to supply the world's energy needs (see Figure 1-1). This represents a total area of less than 1% of the world's arid lands. It is thus evident that, in principle, solar power is capable of supplying all our energy needs and reducing pollution problems during humankind's likely habitation of the planet.



Figure 1-1: The area shaded in yellow indicates the area required to provide the world's total energy needs using current solar technology being developed by the researcher with an average efficiency of 25% and with a packing factor of 50%.

Considering there are many high population zones with main power grids within 500km from sunny deserts, it is likely that if the technical requirements of efficiency, reliability and compatibility can be met then solar power has the potential to make a real contribution to the world's energy. The main barriers are cost and our natural resistance to change.

We have inherited energy practices from processes which were available and most profitable at the time they were being developed approximately 100 years ago for oil, cars, steam engines and electricity. At that time no-one was in a position to measure the amount of oil available and 'smoke' was good being an indication of enterprise and progress!

Now it is time to develop energy harvesting and generation and consumption processes which are appropriate for our present and future needs considering sustainability and pollution levels. The significant advances in technology that have occurred over the last 100 years can be used to assist in this quest.

Presently, there is no single organisation or body that has the responsibility or power to bring about the necessary change. There are however, a number of initiatives, which support the development of clean renewable energy such as the Kyoto Protocol.

Australia's response has been to pass legislation, which will require that by 2010 of all energy used in Australia, 2% must be produced from renewable sources. This amounts to approximately 4 GW of new renewable energy (Electricity Supply Association of Australia Limited) delivering 9,500 GWh in Australia by 2010. This target has been increased to 20 % which translates to 45,000 GWh by 2020. The Asia-Pacific partnership on clean development or AP6 treaty is also being established between Australia, USA, India, China, South Korea and Canada for the purpose of fostering technology which enables greenhouse gas abatement.

A critical mass of three components – social conscience or the *Zeitgeist* raising an awareness of resource limitations and pollution issues, increases in costs of traditional energy and improvements in technological performance of new methods is necessary to tip the scales in favour of clean renewable energy. That is to say, reach a point when more than half of the new energy infrastructure that is built is clean and renewable. A positive shift in any of these three components will require a lesser shift in the other two.

Social awareness is strongly influenced by fashion, which is driven by the media and the views of leaders in society.

Presently 'green' is coming into vogue and thus renewable energy receives some considerable coverage in the media which helps to raise the profile of the world's ecology. For example, the film "An Inconvenient Truth" won an Oscar in 2007 for Best Documentary and Al Gore has received the 2007 Nobel Peace for his efforts to raise awareness of global pollution.

The cost of traditional fuel is substantially a matter of supply and demand. The rapid increase of oil price during 2006 and 2007 is an example of the classic economics law of supply and demand combined with speculation. The high demand for energy in China, added to the already high demand in established industrial and developed countries, has recently exceeded the worldwide oil reserves discovery rate.

While these first two elements are beyond the influence of most individuals, and are influenced by global economics and political forces, the renewable technology component may be significantly influenced by an individual researcher.

To achieve this goal of increased use of clean sustainable energy, it will be necessary to enlist the inspiration of invention and to excite the impetus of commerce to marshal the necessary resources to carry such new technology to the marketplace and into use.

The challenge is thus to produce a solar energy conversion system which can be competitive in price and performance with present expectations. This will allow commercial enterprise to profitably bring new products to the people.

If this can be achieved a substantial market is open to those who are successful and there will be a shift in our energy 'diet'. Once the trend has changed one can anticipate a virtuous cycle where profits from sales of clean renewable energy technology will stimulate more research and development – resulting in cheaper and more reliable products. This will lead to broader markets, higher sales and more profit – and so on! In these circumstances a contribution may be made towards reducing our energy shortage and pollution problems.

To trigger these events the researcher must demonstrate that clean renewable energy can be competitive with existing fossil fuels, or at least with 'clean' fossil fuel. The researcher proposes that this can be achieved through the use of concentrated solar energy and photovoltaic cells. The intent of this work is to detail a pathway to capability and ultimately profitability, including the design and demonstration of technology for large scale grid connected power stations. The proposal is to combine high technology photovoltaic cells with low-cost commonly available materials such as glass, steel and concrete to create high performance, low cost solar power systems.

A large-area solar collector is made of low-cost mirrors which beam concentrated sunlight to a small-area, high-efficiency multi-junction photovoltaic module or receiver, which can produce a high power output.

This type of system has the potential to be cheaply manufactured and deployed since most of the plant consists of standard industrial building components and uses processes which are highly developed for large scale infrastructure.

For this project, a target has been set to achieve system efficiency greater than any commercially available solar power system whether it be flat plate PV or thermal, i.e. greater than any existing solar-to-AC-electricity conversion technology. Furthermore, it will have the potential to have a similar or lower cost per square meter. This would result in a lower cost per kWh produced and be a significant step towards the initiation of a renewable energy avalanche. A sample from the review of available PV Module products is included in Appendix 5 with the Sun Power 315 module having the highest efficiency at 19% at 25°C, 1000 W/m² and spectrum AM 1.5g. This indicates an average annual system efficiency of approximately 15% allowing for balance of system and operation losses. Although short term efficiency data for Stirling systems has been reported (Mancini, 1968), the candidate could not find any long term data to use as a bench mark.

To advance the exploitation of the solar energy resource for wide application, it is necessary to reduce the cost of utilisation to a point where the technology is competitive with traditional forms. This will occur in certain markets first. Typically, this will be in remote area power applications and in sunny locations where high-cost diesel energy is used to generate electricity. An analysis by the researcher of the cost of generating electricity using diesel indicates the cost per kWh of electricity ranges from \$0.25 to \$1.00 depending on the cost of diesel, location and the size and age of plant. It is estimated that this market in Australia is 450 MW (Blakers A, 1991).

In the capture and utilisation of solar energy, there are five main steps:

1. Collection (interception);
2. Conversion (to a useful form, in practice to electricity);
3. Storage;
4. Transmission; and
5. Consumption.

In the case of an array of traditional photovoltaic (PV) panels, the “collection” of solar energy is achieved by placing solid-state solar cells in the natural pathway of sunshine.

The conversion is effected by the photovoltaic effect at the p-n junction(s) within the solar cell where an electrical current is generated. A useful voltage is developed by the

For this project, a target has been set to achieve system efficiency greater than any commercially available solar power system whether it be flat plate PV or thermal, i.e. greater than any existing solar-to-AC-electricity conversion technology. Furthermore, it will have the potential to have a similar or lower cost per square meter. This would result in a lower cost per kWh produced and be a significant step towards the initiation of a renewable energy avalanche. A sample from the review of available PV Module products is included in Appendix 5 with the Sun Power 315 module having the highest efficiency at 19% at 25°C, 1000 W/m² and spectrum AM 1.5g. This indicates an average annual system efficiency of approximately 15% allowing for balance of system and operation losses. Although short term efficiency data for Stirling systems has been reported (Mancini, 1968), the candidate could not find any long term data to use as a bench mark.

To advance the exploitation of the solar energy resource for wide application, it is necessary to reduce the cost of utilisation to a point where the technology is competitive with traditional forms. This will occur in certain markets first. Typically, this will be in remote area power applications and in sunny locations where high-cost diesel energy is used to generate electricity. An analysis by the researcher of the cost of generating electricity using diesel indicates the cost per kWh of electricity ranges from \$0.25 to \$1.00 depending on the cost of diesel, location and the size and age of plant. It is estimated that this market in Australia is 450 MW (Blakers A, 1991).

In the capture and utilisation of solar energy, there are five main steps:

1. Collection (interception);
2. Conversion (to a useful form, in practice to electricity);
3. Storage;
4. Transmission; and
5. Consumption.

In the case of an array of traditional photovoltaic (PV) panels, the “collection” of solar energy is achieved by placing solid-state solar cells in the natural pathway of sunshine.

The conversion is effected by the photovoltaic effect at the p-n junction(s) within the solar cell where an electrical current is generated. A useful voltage is developed by the

series connection of many cells with the current (and thus power) generated being proportional to the area of the cell and intensity of sunlight impinging on that area.

The ‘transfer’ of the electrical power is by standard DC wiring and switchgear to a number of different loads, typically

1. Battery storage
2. Direct consumption as DC power
3. Inversion to AC power for
 - a) Direct stand-alone use by AC appliances
 - b) Connection to the power grid for distribution throughout the consumer system

The research reported in this thesis is concerned with increasing efficiency and reducing cost of the first two steps, collection and conversion.

While storage of electricity at large scale does not have a simple solution, the issue may be avoided initially by targeting applications that are grid connected and can consume all available power generated in daylight hours. This will allow time for the development of appropriate storage technologies, such as fly wheels, bulk electrolyte batteries developed by companies such as ZBB and other methods using hydrogen (Lasich, 1992) for short, medium and long term storage respectively. Opportunities also exist to cooperate with existing or modified hydro power which is already connected to national grids. In Australia, there is approximately 10 GW peak of hydro capacity of which about 2.24 GW (Tumut Three 1.5 GW, Wivenhoe 0.5 GW, Kangaroo Valley 0.16 GW and Bendeela 0.08 GW) is already configured as ‘pumped hydro’ and is capable of acting as a large storage of electrical energy. The total energy storage capacity provided in Australia by ‘pumped hydro’ is currently 73 GWh (Kangaroo Valley 47 GWh, Tumut Three 20.3 GWh, Wivenhoe 5 GWh and Bendeela 0.65 GWh). Ironically some of this capacity has been used to perform the conversion of ‘black’ into ‘green’ by using off-peak power from coal stations at AU\$0.02/kWh to pump the water up and to sell the ‘green’ hydro power at a premium price. The round trip efficiency can be up to 70% for this process. The total grid-connected generating capacity in Australia is about 44.9 GW and has an annualized availability of 61.5% (ESA, 2007). The total production of electrical energy in Australia is 200,000 GWh pa. If we assume that the Clean Energy target of 20% by 2020 requires

50% storage and that the round-trip efficiency of the energy storage is 60%, we would need about 30GWh of energy storage. To provide this daily energy storage with pumped hydro, we can assume in first approximation that the water would be pumped for 8 hours and that the electricity generation would occur during the next 16 hours, with an efficiency of 85% for each process. Therefore, the water pumping and electricity generation capacity of this 'pumped hydro' scheme would be 3.8GW and 1.9GW respectively. In other words, the pumped hydro storage and generation capacity already exists in Australia and is at the level required to sustain a 20% portfolio target for renewable energy. The remaining challenge would be to effect practical implementation considering existing allocations.

In the European Union (EU) and in the US, the situation is similar. There are 32 GW and 19.5 GW of pumped hydro generating capacity, accounting for 5.5% and 2.5% of the total electricity generation, respectively in the EU and the US.

Another important consideration is that Australia's existing hydro generation scheme acting as a source of energy is becoming severely limited because the water reserves are currently at less than 10% of their long term levels. With climate changes due to global warming, this situation may not improve. Therefore, hydropower may be forced to take on a new role as 'storage' instead of a 'source'.

If we consider the problem beyond that, for example to a penetration of up to 50% by 2050 (the IPCC target), it is quite probable that the industry will be of sufficient size to deal with the problem. For example, if we achieve a 20% penetration with pumped hydro storage at \$5 per Watt for the renewable energy source and assuming a capacity factor of 27%, a typical average for wind and solar energy, there will be approximately 17 GW of renewable energy installed capacity at a value of \$85 billion. It is reasonable to expect that an industry of this scale would be able to make progress with the storage issue.

It is also to be noted that a significant part of the load (residential or industrial) that is currently ON at night to benefit from lower electricity prices, could be switched to mid-day operation to be in phase with solar electricity generation. This would not increase the overloading of the network providing that the solar electricity generation is well distributed.

The estimated development cost of a process patented by the researcher for high-efficiency production of storable hydrogen (McConnell RI, 2005; Lasich, 1993, Patent No. 5658448; Lasich, 1993, Patent No. 731495) is \$75 million to reach commercialisation.

In Australia, there is over 1 GW of remote diesel-powered grids where solar power without storage could be applied (NTPAWA, 2002). Where the solar energy converter produces electricity, the issues of transfer and consumption are relatively simple from a technical perspective because high-power inverters are available to provide compatible connection to standard three-phase high-voltage transmission lines. Standard electrical appliances and machinery can then consume the solar energy in the usual manner.

In relation to grid connection of renewable power, the Chairman of the Energy Supply Association of Australia (ESAA) has stated that the Australian grid can cope with up to 10% 'non-dispatchable' renewable energy. This is equal to approximately 5GW of renewable power without storage. The Director of Operations at Southern California Edison also stated that their grid could accommodate up to 15% (of their 30GW grid) of renewable power without storage.

1.2 *The Intellectual Framework of this Research*

The underlying philosophy for achieving the objectives outlined above is based on the following argument:

For clean solar power to become a significant energy source, the cost of solar power must be reduced. The present cost is too high for the following two reasons:

1. The solar radiation is a very dilute energy source and a large area of solar flux must be intercepted to capture useful amounts of energy.

This "large area" requirement is the major contributor to the cost of all solar energy systems. About 92% of the current market for photovoltaic modules is supplied by crystalline silicon PV modules (mono-crystalline and poly-crystalline silicon). In these modules, about 50% of the manufacturing cost is due to the semiconductor material (the silicon wafer). The other 50% is due to the solar cell manufacturing process, glass, encapsulation, junction box, wires, connectors, etc.

2. The average annual system conversion efficiency is low, typically about 10% at system level compared to 25% for brown coal and 35% for black coal.

Presently available photovoltaic panels, for example, are deployed such that the area of the energy conversion device is essentially equal to the collection area. The sophisticated and intense processing required to produce solar cells makes these conversion devices expensive, and with the entire collector panel being populated with cells the whole panel or 'module' is expensive, typically costing about \$500/m² and producing power at about AU\$0.50 per kWh. While thin film modules are cheaper per square meter the efficiency is considerably lower.

Furthermore, a substantial part of the energy, which has been collected at great expense, is wasted, e.g. flat plate photovoltaic systems (arrays of solar panels) with efficiencies of typically 12% waste 88% of the intercepted solar energy.

When viewed from this perspective, it is clear that, while a high cost is paid to intercept the solar radiation, we do not capitalise on this energy that has been intercepted. The energy conversion step is grossly inefficient, particularly in the production of electricity - the highest value energy form.

Efforts to reduce cost by increasing conversion efficiency of flat plate solar panels have not shown any marked advantage over lower efficiency panels. This is substantially because the cells cover a large area (nominally equal to interception area) and the increase in efficiency is outweighed by the increase in cost as detailed in the literature review.

A solution to this problem lies in the separation of the 'collection' from the 'conversion' and then reducing the size of the converter. The use of solar energy concentration where the energy converter is small in relation to the collector area allows for high efficiency at low incremental cost to the system. For example, the energy converter for a parabolic dish solar concentrator operating at 500 suns may have an area that is only 0.2% of the size of the collector and still deliver excellent performance. An efficiency of about double that of typical PV panel systems can be achieved (Lasich, J 1994).

This scenario allows for a relatively large expenditure per unit area of the energy conversion device to produce a high efficiency converter, which has the effect of increasing the entire system efficiency, but at small marginal increase in system cost.

The remainder of the system is concerned only with energy collection and has a cost an order of magnitude less per square meter than active devices, such as solar cells.

While conceptually this approach is straightforward, many practical issues, such as providing a uniform radiation intensity onto the receiver cells and the extraction of heat from solar cells that are illuminated with a high flux solar beam, must be dealt with. This thesis presents some of the researcher's work that has been carried out to address, and indeed solve these problems leading to the production of a novel and fully operational dish concentrator-photovoltaic (CPV) system.

The essential requirements for a technology which could meet the above objectives and be the basis of a sustainable long term industry would have the following characteristics:

- High efficiency (target greater than 20% annual system efficiency);
- Be easy to deploy and manufacture anywhere in the world – using standard practices and commonly available materials such as building, car parts, glass, steel and concrete. These materials are used in industries such as the construction and automobile industries.
- Accessible to most people – on existing grids in new infrastructure; and
- Similar or longer lifetime to existing power sources (20 to 50 years).

Additional features:

- Able to be easily upgraded as technology advances;
- Environmentally safe;
- Capable of cogeneration (for example to produce heat as well as electricity);
- Have low embodied energy (less than 1 year energy payback time);
- Support a profitable business; and
- Be adaptable to incorporate new technologies as they emerge.

CHAPTER 2. EXPLORATION OF ALTERNATIVE DESIGNS

2.1 Introduction

There is a range of approaches and technologies for capturing and converting solar energy for the use of humankind. These range from the simplest ‘passive’ methods such as ‘day lighting’ which uses the orientation and architecture of a building to efficiently capture natural light and heat thereby reducing the need for as much other (external) energy to provide these requirements. This approach allows consumers of energy to make a contribution to reducing the pollution of our environment and the depletion of our fossil energy supplies without having to buy or be expert in solar technology.

At the complex end of the scale a solar power station could produce electricity for light and heat. If a cogeneration stage were added it is also possible to produce heat as a by-product and enhance the overall system efficiency.

This observation raises an important big picture aspect of the energy/pollution challenge that demand-side management can and will need to play a significant role in assisting (generally more expensive) clean and renewable technologies become mainstream.

Consider if the average consumers could maintain their lifestyle while using half the amount of energy then the cost of that energy could be doubled and the balance of satisfaction is maintained for the customer. This would then mean that the challenge of reducing the cost of clean renewable energy resources is significantly reduced and thus much more achievable.

Low energy houses designed by the researcher and others have been shown to easily be able to halve their demand for external energy.

The ‘technology tree’ in Figure 2-1 shows the main branches of solar technology. This review will focus on technologies which are suitable for large scale solar power generation for connection to existing grids. Small scale ‘rooftop PV’ solar panel installations are not included because any grid connected customer solar power from a central station will be about half the cost of that from a small roof top installation. Presently the researcher has observed from the market place a typical cost of a roof top system is about \$12/Watt resulting in a Levelised Cost Of Energy (LCOE) of about \$0.50/kWh whereas the typical

cost of a central power station is about \$4/W to \$6/W with an LCOE of \$0.25. A separate study by the Arizona Public Service (APS) which has installed over 10 MW of solar power systems both as roof top and as central station has confirmed this (Kurtz, 2004).

It should be noted that the researcher has quoted performances and costs for various technologies and systems as they have been available to illustrate certain points. These values can vary considerably depending on location, scale, specific commercial factors and the economic background against which a project might be framed. The global financial crisis has also had a (possible temporary) downward pressure on solar power system prices in the last year.

The use of solar tracking is a method that can be used to enhance the performance of most solar technologies. While it does not increase the 'peak' output it increases the ability of the collector to capture more energy from the sun and thus increase the 'Capacity Factor'. The 'Active' nature of tracked systems also makes them more appropriate for central power stations where effective monitoring Operations and Maintenance (O&M) can be effected by expert mechanised operations servicing a large field of solar collectors.

The technologies reviewed will include;

- Flat plate one sun PV, fixed and tracked
- Low concentration CPV (2 suns)
- Medium concentration CPV (approx 25 suns) Troughs
- Medium concentration solar thermal power (CSP) Troughs
- High concentration Solar thermal (CSP) Central Receiver
- Dish concentrator Stirling engines

The Solar Energy Technology Tree (Fig. 2-1) shows the main solar energy conversion methods and how they relate.

Many of the conversion methods suffer limitations – through either thermodynamic efficiency limitations, due to low concentration (troughs), materials limitations due to high temperature (Dish Stirling) or high cost due to the need for a large area of expensive materials (PV panels).

The objective is to evaluate what has been done, identifying the limitations of each technology and then synthesise a combination of sub-technologies to create a new solar power station concept which can have high efficiency and low cost.

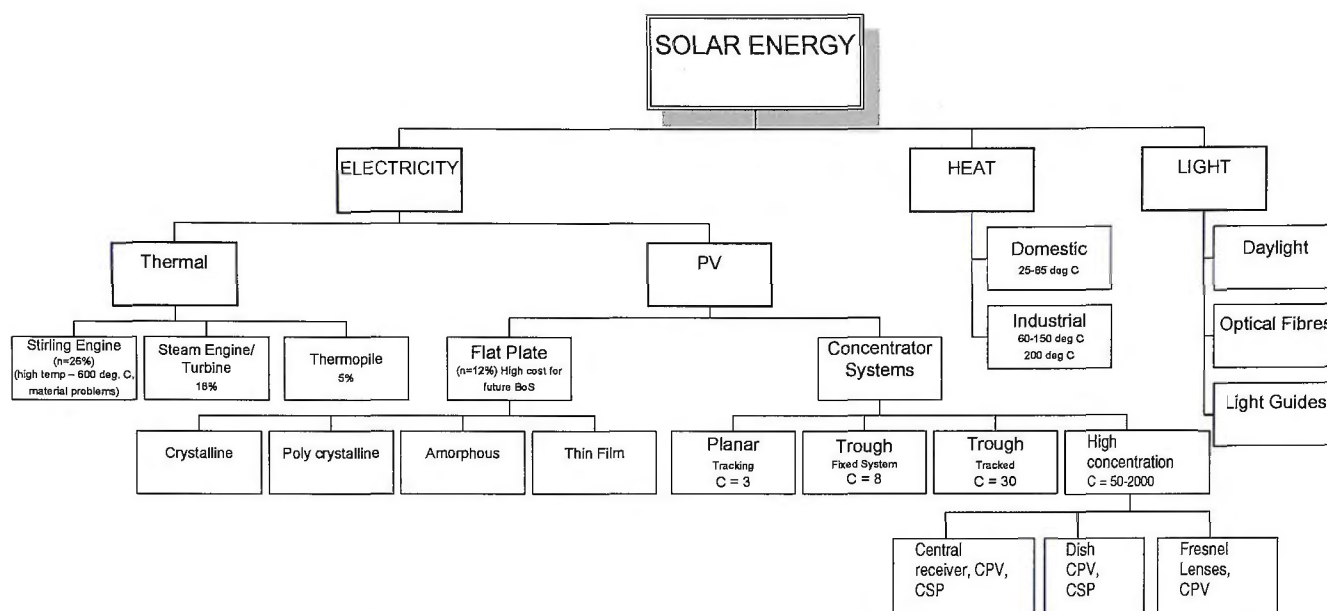


Figure 2-1: Solar Energy Technology Tree. The efficiencies are approximate average annual efficiencies.

To date, the most successful solar power technologies have been ‘flat plate’ photovoltaic panels (PV) and Concentrating Solar Thermal (CST) in the form of troughs.

2.2 Flat Plate PV

The familiar ‘solar panel’ has been very successful in niche markets for remote and small scale power. Although the cost is relatively high compared to the traditional carbon based grid power, high reliability and convenience have driven this market to the extent that sales have increased at an annually compounded rate of 35 % pa over the last 7 years to present annual global sales of over 6 GW with a total of more than 10 GW sold (Photon International, 2007). The main sub technologies of PV include single and polycrystalline, and thin films which include amorphous silicon, cadmium telluride (CdTe), and copper indium gallium diselenide (CIGS). Fig 2-2 shows a 100 kW flat plate installation.



Figure 2-2: A typical ‘flat plate’ installation showing a fixed array of solar panels. The ‘system’ efficiency is typically 8% to 10%, sunlight to AC power, allowing for series mismatch, wiring loss and increase cell temperature.

In all cases the gradual cost reductions have arisen principally from improved know-how of production methods. It can be seen from Figure 2-3 that there is a ‘roll off’ of solar cell record efficiencies as compiled by NREL. Although this is a \$15 billion/year market the rate of efficiency improvement for champion cell used in the flat plate’ PV market has diminished over the last ten to 20 years. The module efficiency has roughly tracked this trend at about 65% of the champion cell efficiency. (SunPower is a notable exception). This reflects the natural nexus between efficiency and cost for flat plate PV technologies where the cost of increasing the efficiency is balanced by the value of that improvement and thus the focus has generally been more on cost reduction per m^2 of panel. This is exemplified by comparing two technologies from the high and low efficiency ends of the performance spectrum. At the present time, panels with single crystal cells which are naturally more efficient and have a higher cost per unit area can be compared to CdTe low efficiency, low unit area cost panels and we find they have a similar levelised cost of energy (LCOE). The ‘SunPower 315’ panel is 19.3% efficient (maximum at STC of

1000W/M² and 25 deg C) and a ‘First Solar’ thin film panel has an efficiency of just 10.7% (maximum) at STC. With this cost down strategy the trend of the thin film per unit area panel cost will soon approach the cost of the complement materials which make up the panel, while the high efficiency SunPower panel will remain competitive at almost twice the cost per m². Thus there will be a lower cost/m² limit which will be reached as set by the glass, encapsulant, connections and mounts. Once ‘balance of module’ costs dominate, only efficiency advances can then significantly improve the cost per Watt. One would thus expect to see increased effort to cause an upward trend in the record efficiency for CdTe and an improvement in the ratio between champion cells and the typical module efficiency which is presently at about 60% for CdTe.

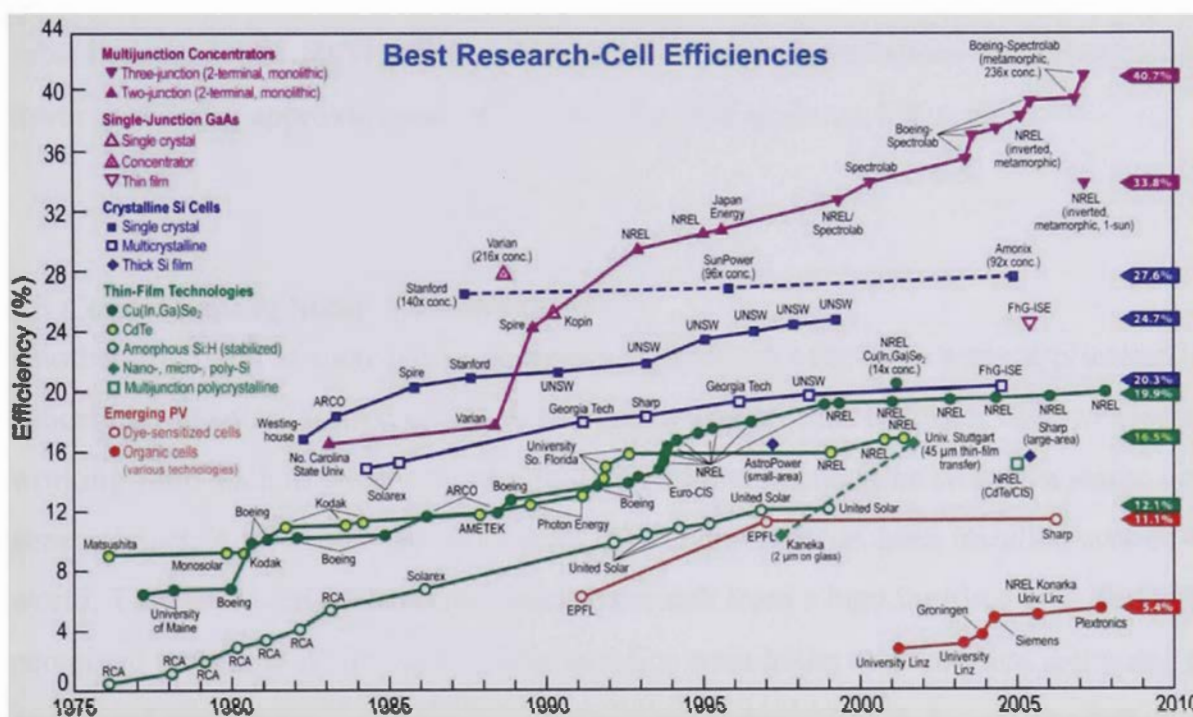


Figure 2-3: World Record Cell Efficiencies from NREL. It is clear that all flat plate technologies show a ‘roll off’ in efficiency over time whereas multijunction concentrator cells continue to increase.

As solar power moves from niche to mainstream it will need to compete with clean fossil energy which will cost about \$0.05/kWh for the base electricity plus about \$0.05 for the carbon capture and storage (CCS) or payment of carbon tax (through renewable energy certificates REC’s presently trading at about \$0.04/kWh) resulting in a cost of approximately \$0.10 per kWh of electricity. To make a comparison to this energy cost the metric known as levelized cost of energy (LCOE) was developed and is defined as the total cost of ownership of the power generating asset over this lifetime divided by the total amount of energy produced over its lifetime. The LCOE is based on complete SYSTEM

cost and performance. This includes the balance of system (BoS) to support the solar panels, collect and invert the power and the capitalised cost of operations and maintenance (O&M).

It is important to note that the BoS is a significant portion of the capital cost and particularly for low efficiency systems where the total area of collector is large the BoS can be of the order of 50% of the system cost. This also points to the need for efficiency improvement to reduce the BoS cost which is substantially area related. A side by side comparison is shown in the LCOE table in section 6.6 on present cost versus future requirement needing more efficiency.

The capacity weighted installed cost of PV systems completed in 2008 dollars without subsidies was US\$7.50/Watt DC (Wiser 2009). Larger installations were also considerably lower cost being approximately 30% lower for MW scale vs. kW scale.

2.3 Concentrating Solar Thermal (CST)

Another approach to solar power generation specifically for large scale applications is concentrating solar thermal (CST) where concentrated solar energy is used to heat a working fluid such as steam to power a conventional heat engine such as a steam turbine-generator set. Approximately 600MW of this technology has been installed around the world. This approach is attractive because the risk from a banking/financing perspective is perceived to be low. With the power generation train being conventional technology developed and proven over a hundred years the relatively simple trough concentrator is just heating a fluid, in this way most of the 'unknowns' are removed and the risk can be quantified and managed. Figure 2-4 and 2-5 show some photos taken by the researcher at one of the 'SEGS' installations in the Mojave desert in California. This plant is 80MW (part of a total of 345MW) and consists of 2,200,000 m² of glass mirror trough collectors focusing at 26 suns concentration on to a tube with selective solar absorber and evacuated glass envelope to minimise heat loss. The absorber temperature is approximately 390°C heating an industrial heat transfer oil which exchanges its energy with water to produce steam. The 'power block' is conventional with turbine, generator, step up transformer, cooling and air-water separation unit.

While this technology has paved the way for solar concentrators it has a relatively low efficiency and has a thermodynamic 'hard stop' due to the relatively low temperatures

which can be achieved with trough concentrators at a maximum theoretical concentration of 100 X and a practical limit of about 30 X. The peak efficiency is approximately 22% with an average annual system efficiency of 14%-18% (Kreith & Goswami, 2007) resulting from concentrator optics of 76%, absorber 96%, turbine 37%, generator 97% and parasitic losses of 15% to pump the working fluid around the field, run the cooling system and other auxiliaries.

Other factors which affect the average annual efficiency include availability (typically 98%), dirt on collectors, and low sun times when full operation temperature cannot be achieved. A further reduction in output ranging from 100% to 64% depends on these factors (Kreith & Goswami, 2007). The 'average' efficiency is lower than the 'peak' due to transients and the fact that insufficiently high temperatures can be sustained if the solar irradiance is below 300W/m^2 . It is interesting to note that at the time of visiting the plant, the 'control' system to maintain the working fluid temperature included human observation of the sky condition and approaching cloud, anticipating the required flow rate of the collector, and manually adjusting the flow rate through the collector in accordance with the observed temperature, in other words, a control system relied on 'bio feedback'. The substantial thermal inertia in the system assists this process by damping the response and minimising oscillation.

Other limitations of this technology include the requirement of a minimum scale for deployment. To achieve a sufficiently high economic efficiency, it is necessary to have a minimum scale of about 50MW. This is mainly due to the turbine efficiency/scale characteristic requiring large scale for high efficiency. PV and CPV systems are independent of scale.

Positive aspects to this approach relate to dispatchability. The ability to 'co-fire' the system with a complementary gas boiler and use thermal storage mean that the capacity factor can be increased and that there is flexibility to deliver power when tariffs are attractive. This may considerably improve the economics for CSP projects which can take advantage of these aspects.



Figure 2-4: Solar thermal trough concentrators at the Solar Energy Generating System (SEGS) plant in California, USA (photo taken by JB Lasich, 1996).



Figure 2-5: Solar Energy Generating System (SEGS) plant in California, USA looking at the 'field' from the power block (photo taken by JB Lasich, 1996)

2.4 Low Concentration CPV

At first glance the option of low concentration CPV of say 2 to 5 suns sounds attractive since it is theoretically possible to reduce the expensive PV cell area by a factor of 2 to 5 times. However the complications of tracking and elevated module temperature can negate much of the value gained from the reduced cell area. The researcher's experience with the 2 sun CPV unit (Figure 2-6) indicated that although the output was increased by

approximately two times, the cost was also two times. It was also noted that the cell temperature exceeded 100°C and could lead to module degradation (as in the Carrisa plains experience (Czanderna, 1996)) where the ethylene vinyl acetate (EVA) laminate degraded and turned brown reducing the output. The researcher used a Solarex panel with silicone laminate and experienced no significant reduction in output over several years.

The researcher believes further work on this low technology approach is warranted. Dr Lew Frass of US company JX Crystals have made some interesting progress in this area.



Figure 2-6: Photo of a 2 sun concentration built by the researcher. The system has 4 planar reflectors set at 30 degrees from the normal to the solar panel in the centre. Tracking was achieved by using a shadow band east-west with a seasonal tilt in the N-S direction.

2.5 CPV Using Trough Concentrators

Trough concentrators have been well developed for solar thermal applications with approximately 3.1 million m^2 installed worldwide, resulting in a total generating capacity of about 600 MW.

The concept of using an established concentrator technology with PV cells appears attractive at first glance with a 25 times the concentration, the cell area can be reduced by almost 25 times compared to flat plate PV and the thermal challenge is less daunting. The option for co-generation also exists. Several developments are underway in the area. They include the EUCLIDES project in Tenerife (see Figure 2-7 and 2-8), a passively cooled system for the production of electricity only and the CHAPS system built and tested by the ANU (Smeltink, 2005) which was an actively cooled method also capable of providing domestic or industrial heat. Both systems used modified 'one-sun' silicon cells.

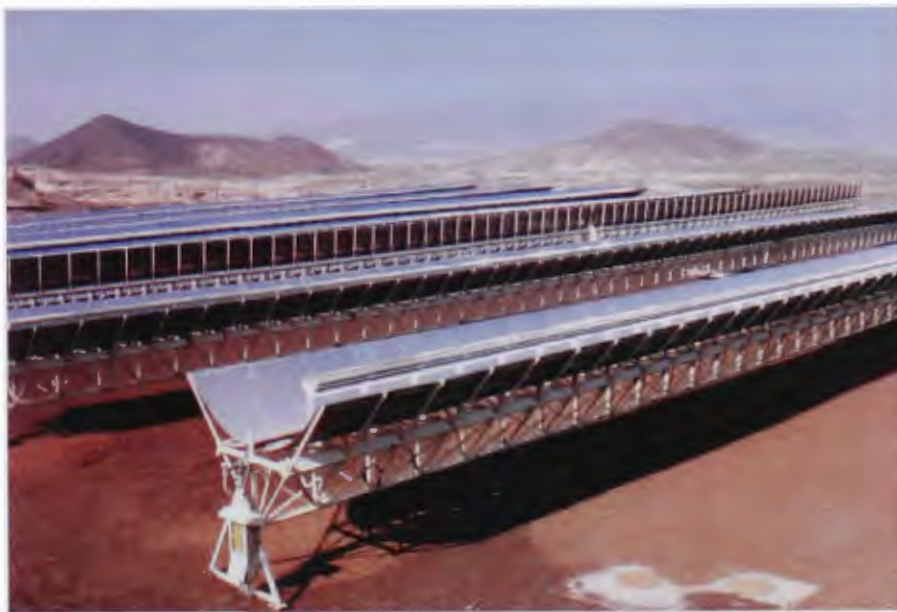


Figure 2-7: Euclides CPV troughs in Tenerife



Figure 2-8: EUCLIDES note the extended collector to allow for seasonal sun angle changes.

The researcher also built and tested two generations of CPV troughs (Figure 2-9 and 2-10). The second generation CPV trough in Figure 2-10 incorporated silicon cells and water cooling. This experience showed that while a trough needs to only be tracked in one axis and the heat transfer requirements through the cell is only $2.5\text{W}/\text{cm}^2$ the effort and cost of engineering such a system is high and the benefits appear to be limited. A number of second order effects detract from the performance including end losses. If the system is tracked only on one axis there are parts of the PV receiver which are not illuminated as a result of seasonal changes. Parasitic losses can be high – up to 10% - because of the very long receiver necessary to support a long ‘string’ of cells. Flux distribution losses also are significant (Coventry, 2005) since about 500 large cells must be connected in series to produce a potential of 250 volts. It is very difficult to keep the necessary, precise and uniform concentrated solar power on every cell of a receiver that may exceed 20m in length unlike solar thermal where this effect is insignificant. Further discoveries after building a small 2-axis tracking dish with a concentration of 500 times showed that once the designer has committed to a tracking system, two axes are not significantly more problematic than one axis. There are significant advantages to be gained from 2-axis tracking including: collection of more energy; ability to deliver high concentration; allowing the area of expensive solar cells to be reduced by a further factor of 20. Once the significant challenge of removing heat from the cells of $50\text{kW}/\text{m}^2$ was achieved, the cooling system and parasitic power requirements are smaller. The researcher developed a laminate of cell-ceramic-metal heat sink capable of transferring $50\text{kW}/\text{m}^2$ from the CPV cells to a coolant fluid with a ΔT of less than 20°C between the cell and the coolant. This laminate incorporated (Lasich, 2001, Patent No. 7076965B2) the necessary flexibility in the system to accommodate different thermal expansion coefficients for the different materials.



Figure 2-9: PV trough concentrator – Peak power = 45Watts built by the researcher in 1978. The system also produced hot water. The trough was formed from bright stainless steel with a reflectivity of 65%



Figure 2-10: Second generation CPV trough built by the researcher using bright anodised aluminium reflectivity of 85% including silicon solar cells. The system is designed and built by the researcher and tested on his premises.

The following Table 2-1 shows the side by side comparative performance and cost for a sample of solar power generators, by a range of different methods.

Technologies represented include:

- Photovoltaic panels;
- Solar thermal troughs;
- Dish Stirling;
- Central receiver thermal; and
- Researcher's system, Reflective Dense Array concentrator photovoltaics (CPV).
- Lens based CPV

Other technologies which show potential for high performance and low cost include crystalline silicon on glass (CSG) and 'sliver' cells which greatly enhance the number of watts which can be generated from a silicon wafer. The following graph, Figure 2-11, shows the researcher's estimate of future trends of average annual system efficiency for the leading technologies compared to the CPV technology developed by the researcher.

Organisation	Technology	Plant Size MW	Cost AU\$/W	Future Expectation/Target		Comments
				Efficiency	Cost/W	
Solar Systems Fully optimised for large scale project using the researcher's technology.	Heliostat CPV System and present efficiency	150 (design)	\$2.74 targeted at 150MW	24% annual efficiency with 42% cells and 76% optical efficiency.	1.80	Central receiver configuration with heliostats beaming concentrated light at 500 times to multi-junction concentrator cells. Prototype 140kW field recorded 25% peak efficiency (Lasich, 2009)
Luz USA 'SEGS' Plants	Thermal troughs up to 400°C	345 installed and running since 1985	≈ \$5.50/W gas assisted	Limited by max temp to 22% peak and annual average efficiency of 14-18% (Kreith and Goswami, 2007)		Best loop efficiency 60-70% annual, peak optical=78% for 'SEGS' V. People from this project formed a new company called Bright Source Energy to develop central receiver systems to overcome efficiency limitations of troughs.
Amonix	Lens CPV	10 MW	~\$4/W	20% estimated annual average	~2.20	Fresnel lenses have lower efficiency than reflective optics
Solucar Spain	Thermal central receiver 250 °C 14% annual target.	10 (installed) 20 (design)	\$5.72/W \$4.60/W predicted	Could be up to 20% for high temperature of 550°C		Average annual efficiency ~15% predicted @ 250 °C steam temperature
Researchers CPV System powering Solucar 10MW central receiver design	HCPV Average annual efficiency 22% predicted with 42% cells and optimised optics.	15 (design)	\$3.94 Rough estimate for SS PV in Solucar 'PS10'	24%		Estimate based on present Solucar 10MW thermal station refitted with Researchers PV DenseArray receiver.
20 leaders of flat plate PV industry	Flat plate PV systems 12%-14% efficient	2500/year	\$7.50 in 2008-9	16%-18% peak	5	Efficiency has not increased much in 10 years apart from SunPower. The increased cost seems to outweigh the advantages.
Researcher	Dish PV Peak 25% Average annual 22% (Lasich 2009)	1.5MW	\$3.50/W	Average annual efficiency of 30%	2.20	The same components used in dish CPV can be used in the heliostat central receiver form (see top of page).

Table 2-1: Technology Comparison as seen by the Researcher (efficiency based on total projected collector area)

Projected Annualised AC Energy Efficiency of solar power stations

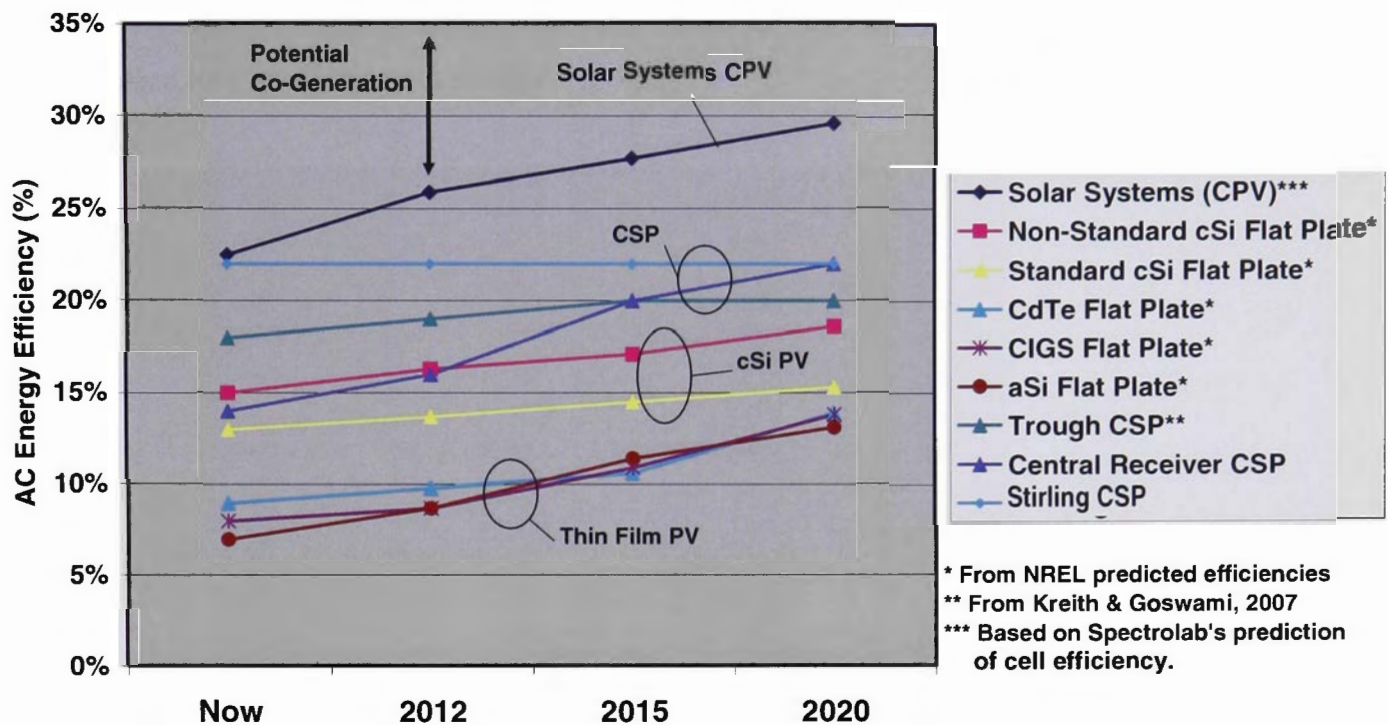


Figure 2-11: This graph shows the trends for average annual system efficiency estimated by the researcher. The estimations for PV technologies are based on NREL estimations for the cell efficiency. (Von Roedern, B 2008, Von Roedern, B 2005, Sopori, B 2007, Kieys, B 2007, Friedman, D 2007, Roedern, B 2007). Stirling system efficiency estimated from Mancini, 1968 and Kreith, 2007.

The literature review has highlighted a common theme, that is, regardless of the technology both efficiency and cost per m^2 play key roles in achieving low LCOE for solar power systems. For example it can be shown that for a given low efficiency flat plate system (say 8% system efficiency from a 10.6% efficient panel) there is the minimum cost/Watt below which the system cost cannot fall even if the solar cell is 'free'. The balance of the panel and the system are fixed essentially by the area of collector required. The only way the cost can be reduced further is to reduce the area of the system, and that requires an increase of efficiency. For a thin film cadmium telluride panel where say 1/3 of the panel cost is related to the solar cells and the panel is half of the system cost only a further one sixth or 16% cost reduction can be made even if the cost of the cells were to be zero. This statement assumes that 'volume' effects on common elements like 'white glass' are similar for all solar technologies and thus other relativities would be similar.

This finding is a major driver which supports the development of a system which can be low cost per m^2 AND have a very high efficiency.

A high concentration CPV system with high efficiency solar cells has the potential to achieve this. Figure 2-12 shows the Amonix CPV system which uses thousands of distributed 500X lens-cell couplets incorporated into five 'Megamodules' which are passively cooled and mounted on a tracker.



Figure 2-12: Amonix lens based CPV technology installed in Spain

The researcher has chosen to use a separate 'reflective collector' and PV 'dense array' 'receiver' or 'converter' with a single focus and active cooling for the following reasons;

- A glass mirror is the simplest collector there is, it contains no active components and also has the highest optical efficiency (up to 97%). Millions of m² have been proven for CSP over 20 years. There are also many experienced suppliers
- A small dense array CPV receiver contains all the complex components in a single box for easy monitoring, maintenance and upgrade. The manufacturing overhead is a fraction of other CPV of the same capacity
- Active cooling, while more complex than passive cooling, will significantly reduce maximum cell temperatures and cycle amplitudes thus increasing cell life

- The probability of successfully aligning one concentrated beam with one PV receiver using feedback from the cells is much greater than for aligning (and keeping aligned) thousands of lens-cell couplets on a single tracker. This will lead to higher average annual efficiency.
- This approach also allows flexibility of application where a central receiver format can be used . Co-generation using waste heat contained in the coolant or spectrum splitting for high grade heat are also possible.

CHAPTER 3. OUTLINE OF SYSTEM PHILOSOPHY & IDENTIFICATION OF MAJOR COMPONENTS

The arguments presented in the introductory chapters highlight the tension between obtaining high conversion efficiencies and the resulting high cost of PV cells.

A possible way forward is to develop a design which can have high efficiency at a low cost.

The system philosophy is developed by considering the points below:

- Presently, electricity generated from solar energy is too expensive for most applications.
- The reason for this is that even for the most economic systems the conversion is very inefficient, typically 12% (system) and that the “converter” solar cells are very expensive per square meter resulting in a large area of high unit cost components.
- To overcome this problem, firstly increase efficiency.
- In the past, this required increasing the cost of the active components which is a large percentage cost of the system.
- This results in higher efficiency, but at higher cost – resulting in no net gain.
- To avoid this problem, separate the collector and the converter, use a large, inexpensive reflector to collect and concentrate energy to a small high efficiency receiver and concentrator to produce electricity.
- High concentration reduces receiver cost – this must be optimised by considering optical efficiency and tracking accuracy as well as removal of high flux thermal energy.
- Because the solar energy is concentrated into a small area, a number of processes can be economically used to extract further useful power from the solar beam (even though these processes maybe expensive on a per unit area basis).
- Processes which can utilise concentrated sunlight include:

- Photovoltaics
- Thermoelectronics
- Thermophotovoltaics
- Thermal processes that:
 - generate electricity via a heat engine
 - drive chemical reactions (thermochemical reaction)
 - used as thermal energy for 'heating', which simply raise the temperature of a process.
- With the world record efficiency at 41.6% for multi-junction concentrator cells (reported by Spectrolab) and increasing at a rate of approximately 1.0% absolute per year (Kurtz,S 2008), it is now clear that the photovoltaic converter has the greatest potential for high efficiency.

The challenge is to make them operate efficiently and reliably at high concentration and create a design which can also be low cost. The approach will be to develop a system with a separate collector and a PV concentrator. The collector must have potential for low cost and the converter must have the highest possible efficiency. (Since the time of writing, Spectrolab have announced an increase to 41.6% for a latticed matched triple junction cell.)

The main components are:

- The collector or concentrator (primary optics)
- The receiver containing:
 - Solar cell array
 - Secondary optics
 - Heat extraction system
 - Monitoring system
- Tracking system
 - Mechanical
 - Electrical
 - Software
- Heat rejection system

3.1 System Components: Philosophy, Realisation and Results

In the literature review, the researcher examined the merits and challenges of five different approaches to solar power generation and concluded that although high concentration CPV had some significant challenges it also offered the greatest potential for the lowest cost. In order to produce new evidence to support this thesis the researcher has designed, built and tested several high concentration CPV systems beginning with 3.4kW, a 20m² faceted dish and ‘dense array’ CPV receiver operating at approximately 270 suns. The second case considers a 35kW, 130m² unit being a production prototype known as a CS500 (concentrator system running at 500 suns).

3.2 Dish Solar Concentrator (small – 20m²)

3.2.1 Characterisation and Optimisation of a 20m² Concentrator Dish

A number of dishes have been used by the researcher for development of concentrator photovoltaic (CPV) systems.

Although the researcher has maintained the same underlying philosophy throughout the research, its realisation has evolved over time as experience has been gained. One of the early systems developed was a 20m² faceted dish.

This is described here as it exemplifies features that must be considered when designing systems. In particular it highlights a specific design that illustrates the process and relationships between primary concentrator optics, secondary optics, cell array, tracking and cooling system.

This was the first multi-kW realisation of a CPV system by the researcher, producing a nominal 3.4kWe. While the performance of this dish/receiver design was excellent achieving 20% DC efficiency (Verlinden *et al*, 2001) and it verified the ray trace model developed by the researcher and co-worker, G. Ganakas (see Chapter 5), the potential of this system to achieve low cost was limited due to the large number of individual mirror facets required to be cut, attached and aligned. A commercial version (CS500) was developed to address the cost and issues and it is reported in detail in Chapter 5.

There are four main areas that need to be addressed when developing a PV dish solar concentrator design: the primary concentrator optics, the photovoltaic receiver and secondary optics, the receiver cooling system and the sun tracking system. There are many interrelated characteristics of the system where each must be optimised without seriously compromising the others. For cases where a PV array is located near the dish focal zone, the ‘shape’ of the incident energy beam needs to be characterized and modified with secondary optics, especially when the PV cells in the receiver are connected in series to achieve high voltage. A series connected PV array that is unevenly illuminated can have its peak power output reduced by more than 50%. Series connections are necessary to obtain a usable, high voltage, DC power output typically 240V to 600V. Managing the flux distribution on the solar cell array is a significant part of the art and can mean the difference between success and failure.

3.2.2 Primary Concentrator Optics

The primary concentrator is modelled on an existing dish, which was originally used in a solar thermal power application. The original dish consisted of a steel rimmed fibreglass shell as the main mirror support structure. The shape was paraboloidal with a diameter of 5.05 meters, a focal length of 1.81 meters, a rim angle of approximately 70 degrees and a projected mirror area of 19.83m². The dish contained approximately 2300 mirrored glass tiles most of which were the same size. These tiles, as will be seen later, did not produce a sufficiently coherent beam characteristic and so the dish was resurfaced with an increased number of smaller and accurately aimed and configured mirror tiles. The tiles were trapezoidal in shape and arranged in 30 concentric circles. The tile average widths (circumferentially) vary from 10.4cm in the outer ring to 4.4cm inner ring. The tile heights (radially) are approximately 10.2 ±0.2 cm except for the 12 outer rings which are half this height. This tile height reduction served to reduce the size of the image of each tile at high rim angles and thus maintain a tightly focused beam around the focal zone. This was needed so that all available energy could be captured by the relatively small aperture of the secondary optics. The number of tiles is 3127. The exact placement of each mirror tile was determined using a computer ray-tracing model (‘PV Trace developed by the researcher and co-worker G Ganakas). The mirrors were modelled mathematically as a number of

concentric, segmented circles that are inscribed on a paraboloidal surface. Figure 3-1 and 3-2 show the side and front profile of the modelled mirror surface geometry.

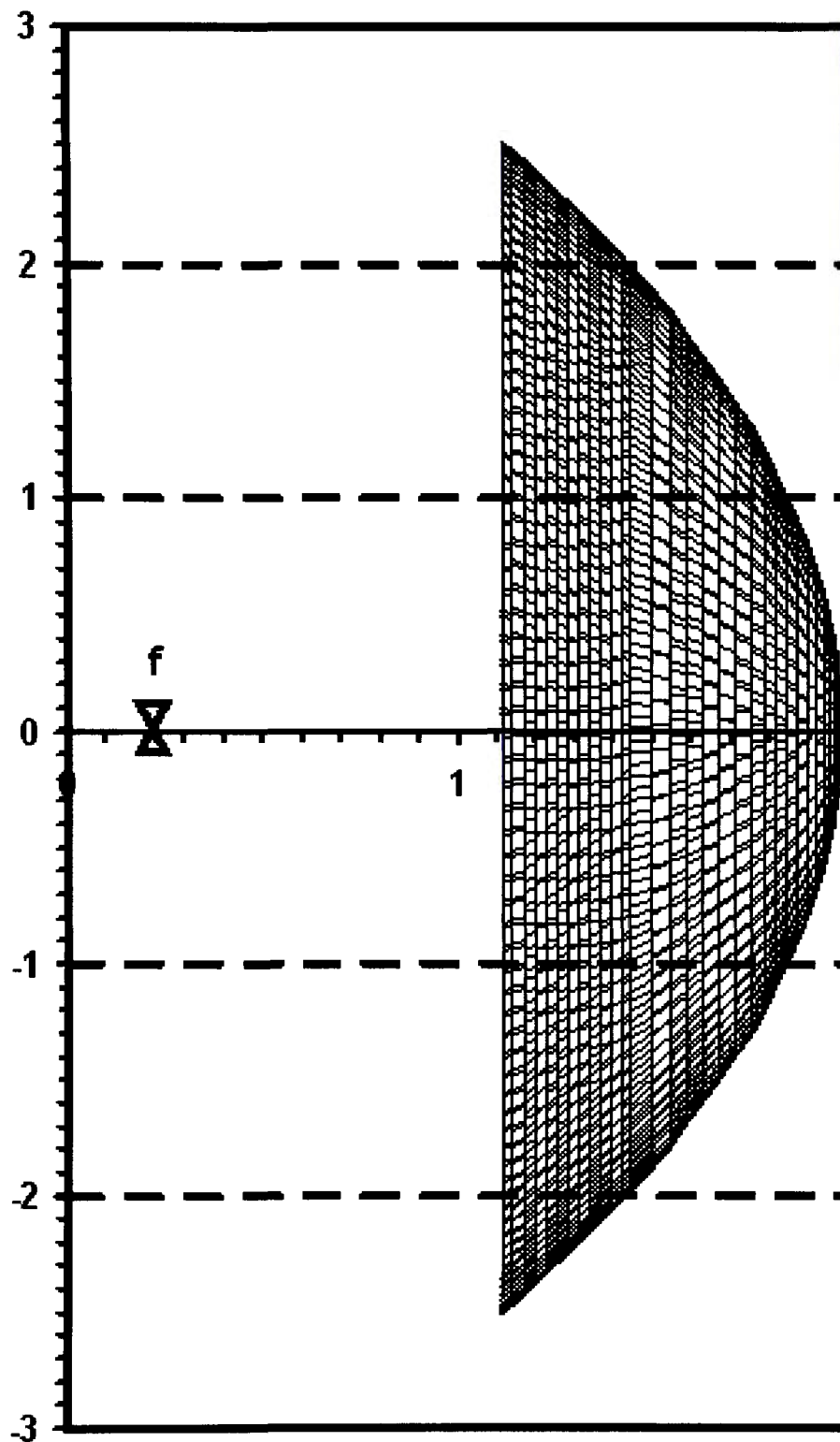


Figure 3-1: Side profile of the modelled 20m² PV dish concentrator (units are in meters).

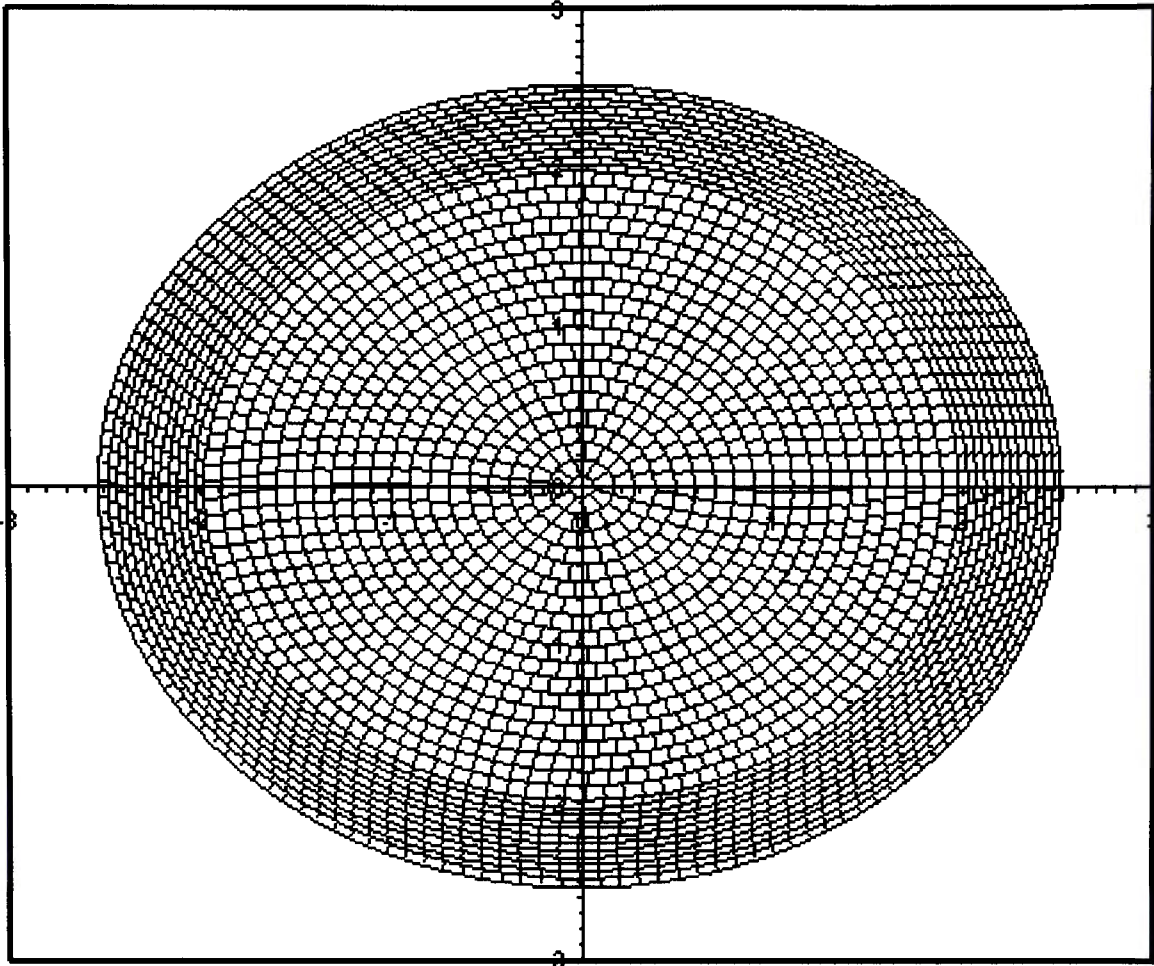


Figure 3-2: Front profile of the modelled PV dish concentrator (units are in meters).

The mathematical model was programmed in BASIC. A ray tracing code was used to predict variations in flux that impinge on the receiver surface. The code generates many random 'light' rays that are reflected by the mirror tile surfaces. The resultant energy distribution is a summation of all rays intercepted by the sampling region and the accumulated counts on each sampling point are subsequently multiplied by the calculated ray power to give overall energy intensity. This number is then divided by the small area (resolution) of the sampling region to give a power density value.

The result produced is an instantaneous power density map that can be displayed as a two dimensional contour or a three dimensional surface plot.

The mathematical code uses the principle of reflection whereby light rays (vectors), incident on a given surface are modelled using the formula:

$$\mathbf{A}' = 2(\mathbf{A} \cdot \mathbf{B} / \mathbf{B} \cdot \mathbf{B})\mathbf{B} - \mathbf{A} \quad (1)$$

where an incoming ray in Euclidean space is described by the vector $\mathbf{A} = a\mathbf{i} + b\mathbf{j} + c\mathbf{k}$: a, b, c are real numbers and a surface of which the normal component vector at the intercept point is described by $\mathbf{B} = d\mathbf{i} + e\mathbf{j} + f\mathbf{k}$: d, e, f are real numbers. The reflected image of the vector \mathbf{A} is \mathbf{A}' with respect to the non-zero surface vector \mathbf{B} . For a faceted parabolic dish, we find the gradient vector \mathbf{B} of each facet by considering 3 points that make up the facet. If we have a plane through three points, $\mathbf{a} (x_1, y_1, z_1)$, $\mathbf{b} (x_2, y_2, z_2)$ and $\mathbf{c} (x_3, y_3, z_3)$ then the vector \mathbf{B} in this case may be found by determining a normal vector to the plane which is given by the vector product of \mathbf{ab} and \mathbf{ac} .

3.2.3 The Sun

The Sun's shape can be modelled as a disk of small but non-zero radius. Because the sun's disk has a diameter and is not a point source, it illuminates a point on a reflector surface as a cone of rays rather than a single narrow beam. The angular distribution of energy with respect to the central ray (the ray emanating from the centre of the sun) is known the "sunshape". Usually the sunshape is modelled as a flat, uniform "disk". More accurate models of the sunshape include uniform disks with Gaussian-like tails or allow experimentally measured data to be incorporated into the ray-tracing program. The flat disk model is a good approximation, although it does not take into account the small percentage of energy emitted by the corona. In this application the ray tracer showed no significant difference between 'pill box' and Gaussian errors in the resultant distributions when modelling PV concentrators with diameters greater than 1 meter. A 'pill box' sun shape has been used in this model and the angular deviation of incoming rays will be no more than 0.265 degrees.

3.2.4 Reflection Errors

Slope Errors

Reflection errors are errors that cause a reflected ray to deviate from its ideal path. An attempt has been made to incorporate this error into the model. A real reflector differs from a perfect reflector in many respects. One example is that of "waviness" which can exist on the reflector surface and indicates the flatness of the glass superstrate on which the silver mirror surface is applied. This is known as "slope error". Surface roughness also contributes to reflection error causing ambiguity in the actual direction of the surface normal and results in a diffuse reflection. The diffusion and "waviness" error of a reflective surface is assumed to be completely random and is modelled as a 'pill box' distribution for the primary concentrator. Also, the degree of error for mirror-pointing accuracy was estimated from mirror alignment maps ascertained after the mirror tiles were laid and cured (see Figure 3.3). This mirror-pointing estimate was produced using the laser-mapper aligner built by the researcher and G Ganakas shown in Figure 3-4. The errors associated with dish tracking can also affect the beam displacement and to some extent, its shape. This error was found to be minimal and not to significantly alter the resultant beam shape. This is because with the 'active' tracking developed by the researcher ensures that the dish tracking error is less than 0.1° and the 'off-axis' effects are insignificant. (See section 5.6)



Figure 3-3: The researcher laying mirror tiles for the 20m² test dish.



Figure 3-4: Robotic laser mapping alignment system to align mirrors for 20m² dish with 3127 faceted mirrors.

Surface Roughness

The surface roughness of the mirrors was determined using a comparative measurement of a laser beam spread. Firstly, the beam width of an LED laser beam was measured at a distance from the source of 40m. The same laser beam was then reflected from a sample mirror where the reflected beam length was 40m and the incident beam length was less than 1m. The width of the reflected beam was measured at 40m distance from the sample mirror. This process was repeated several times with different mirrors and found to result in a similar beam width, indicating a spread of typically $\pm 0.005^\circ$. This effect is insignificant and has little effect on the modelling since it is approximately two orders of magnitude smaller than the sun width.

The ‘waviness’ or slope error was not considered in this model due to the small size of the tiles. The pointing error or the pointing direction of each tile was accurately known using laser mapping measurements of the optics from previous dish constructions. This data was used directly in the simulation to define the mirror direction vectors (Lasich, 2001, AUS 2002244529B2).

Figure 3-5 shows the reflection of solar radiation and the reflection of incident rays by a flat surface and the resultant cone of errors.

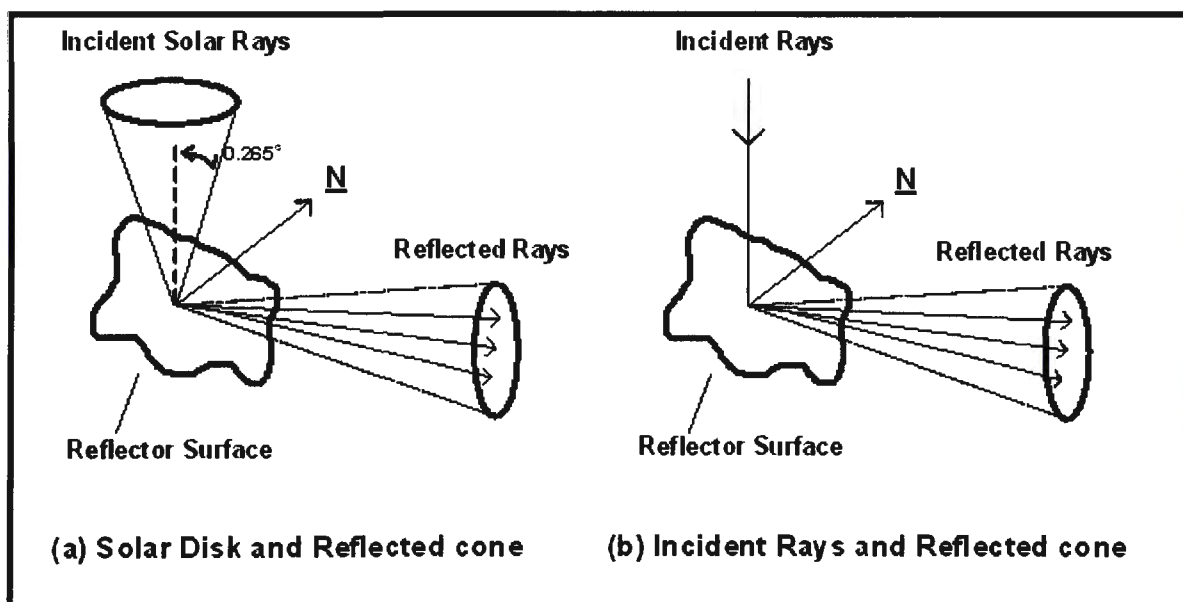


Figure 3-5: The reflection of solar radiation off a perfectly flat surface and (b) the reflection of incident radiation off a surface with symmetrical error.

3.2.5 Mirror Reflectivity and Mirror Dead Space

The reflectivity associated with an optical surface is not perfect and so a method for describing this parameter is necessary. Apart from the directional errors described above there are also losses due to dead space between mirrors and the actual reflectivity of the mirror itself. For a back surface mirror this reflectivity is made up of two components, the reflectivity of the silver backing layer and the absorption of the glass through which the light travels (twice). For the resurfaced dish, new high performance 1 mm thick low iron glass with the manufacturers specification of 95% solar weighted average was used and an allowance of 1% was also allowed for scratching and soiling.

The overall profile of the mirror tiles are modelled to have a uniform reflective loss and occur as a statistical loss of rays in the computer model. Reflectivity values may be assigned for all optical components. The actual dish contains gaps between the mirrors whereas the simulated dish does not. Figure 3-6 shows an exaggerated view of the 'dead' space in the actual dish compared to the simulated one. Instead of modelling the actual 'dead' space geometrically (which was not practical), the absence of reflective area caused by this space was incorporated onto the overall dish reflectivity number. The 'dead' space was approximated by experimental measurement. Another loss incorporated into the dish reflectivity number relates to the shading of incoming sunlight by the three struts which hold the receiver in place. Shading caused by the receiver is calculated by the computer model. Both the real and simulated dishes have a 50 cm diameter, circular area located in the dish centre which is un-mirrored.

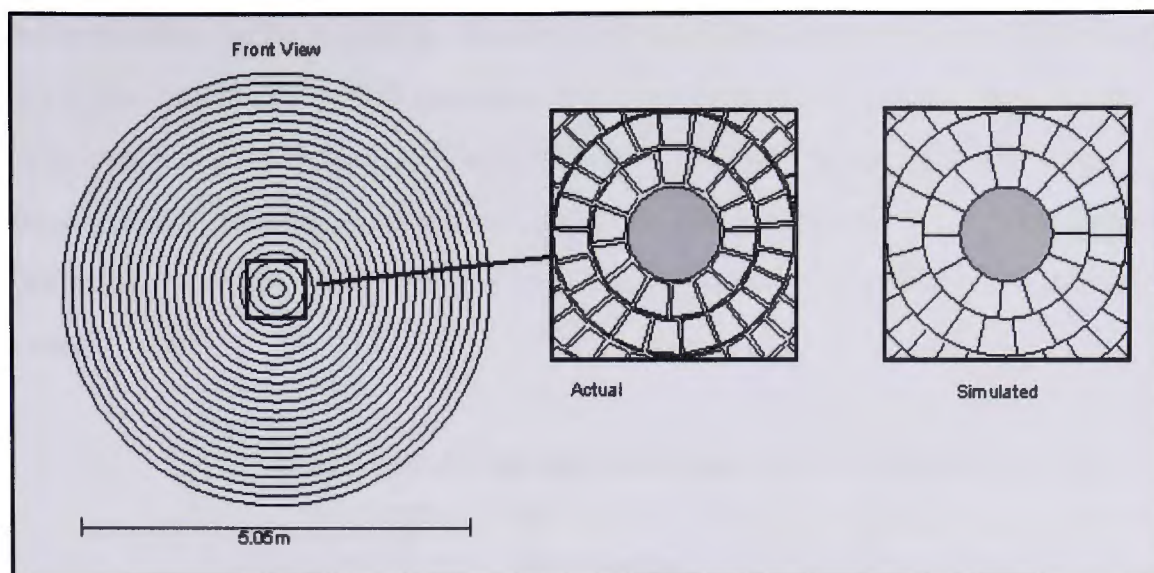


Figure 3-6: Diagram showing the difference between the actual and simulated dish

3.2.6 Correlation of prediction with measured results

The first comparison of measured and predicted performance for the 20m² dish was done with an aged dish which had been exposed to the weather for 12 years. The resultant flux distribution produced by the computer model was compared with experimental values (Figure 3-7). The experimental data was taken using a GaAs solar cell made by Varian. The cell was soldered to a copper tube in which cooling water was allowed to flow is shown in Figure 3-8. The cell and tube were moved across the focal plane of the dish while current measurements were taken. The GaAs cell characteristics are well known and supplied by the manufacturer Varian being 5.0amps (Werthen 1994) at a solar flux of 1000 suns. The current measurements were converted to power density values. The slightly lower intensities seen in the peak experimental values were possibly due to the presence of dirt and corrosion in and around some of the aged mirror tiles. The aged dish reflectivity was determined by adjusting the modelled reflectivity until it the predicted light power delivered to the receiver matched with the calorifically measured 12 kW of light absorbed at the receiver. (The reflectivity of the receiver was set at 10%). The correlation between the predicted and measured beam shape indicates that the model correctly predicts the character of the beam. The shape is essentially Gaussian, with a 'flat top' which is characterised by the flat mirror tiles. The peak value also matches reasonably well considering that the calorific test was indicative only. The asymmetry in the measured result may be a result of macroscopic change in the dish shape due to gravity as the orientation of the dish was approximately 20° from vertical during measurement, but was

positioned horizontal during mapping. Another source of this asymmetry could be mirror reflectivity reduction, due to partial corrosion resulting from the 12 years of weathering while it was positioned horizontally. The total power delivered to the focal plane was approximately 12kW, indicating an average mirror reflectivity of only 70%. The starting reflectivity would have been approximately 84% being typical of the 'bathroom mirror' that was used.

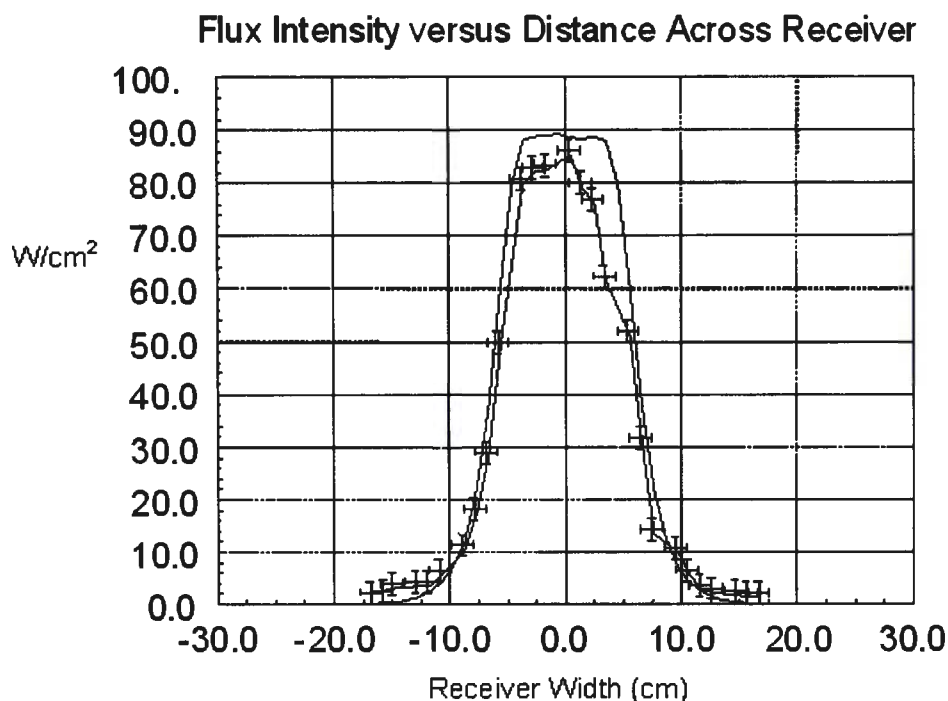


Figure 3-7: Intensity profile of the simulated solar flux distribution - Simulation Versus Measured Data (Side Profile) of a 5m diameter, 70 degree rim angled, 1.81m focal length dish containing approximately 2300 flat mirrored tiles (the original dish with total power approximately 12kW equating to an average reflectivity of 70%)



Figure 3-8: Solar Flux measurement 'wand' with variant GaAs concentration cell soldered to cooling tube (designed and constructed by the researcher)

The dish was later re-mirrored using high reflectivity mirrors (94%), with a smaller tile size on the outer 12 rings.

The mirror reflectivity and optical losses for the real dish and the numbers used for the simulated dish are:

(a) Real Dish

Dish diameter	= 5.04 m ²
Dish aperture area	= 19.95 m ²
Dish tiled area	= 19.75 m ² (Dish aperture minus unused area in dish centre)
Projected mirror area	= 19.48 m ² (Dish tiled area minus gaps between mirrors)
Mirror tile reflectivity	= 94.0% (for silver backed glass)
Shading by receiver	= 1.90%
Shading by support struts	= 0.36%
The ratio of mirror tile gaps area to total tile area	= 1.41%
Mirror roughness error	= 0.005 degrees

(b) Simulated dish

Dish diameter	= 5.04 m ²
Dish aperture area	= 19.95 m ²
Dish tiled area	= 19.75 m ² (Dish aperture minus unused area in dish centre)
Projected mirror area	= 19.75 m ²
Mirror tile reflectivity	= 94.0% - shading by support struts – loss due to gaps in between mirror tiles = 94.0% - 0.36% - 1.41% = 92.5%
Mirror roughness error	= 0.005 degrees 'pill box'

Figure 3-9 below shows the results of a ray-trace simulation for an incident solar radiation intensity of 1000 W/m².

Solar Flux Distribution Seen at The Focal Plane of a 5m Diameter Dish

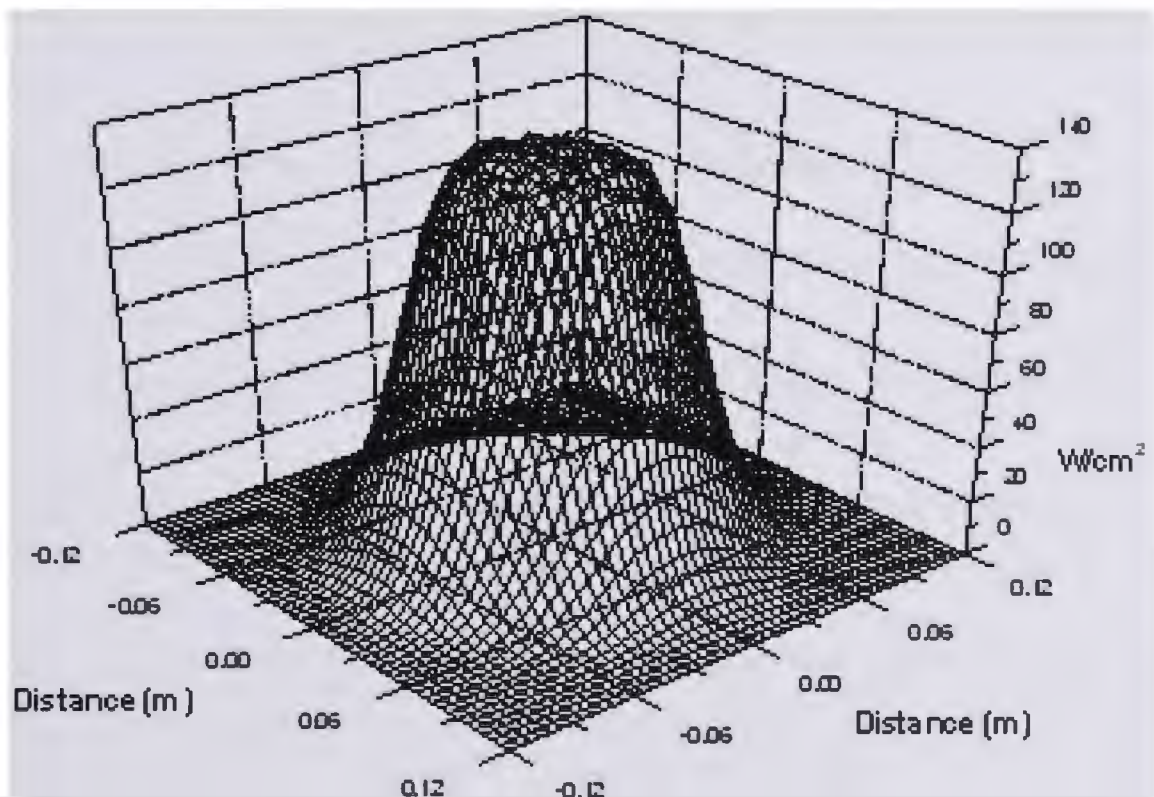


Figure 3-9: Simulated flux distribution seen at the focal plane of a 5m diameter, 70 degree rim angled, 1.81m focal length dish containing approximately 3100 flat mirrored tiles. The peak flux intensity is 134 Watts/cm². The total 'light' power delivered is approximately 17kW. It can be seen that virtually all of the flux falls within a distance of ± 0.06 m from the centre.

3.2.7 Secondary Optics

To be useful at large scale, it is necessary to have a system capable of producing several kilowatts or megawatts of power. With the practical power output for available solar concentrator cells being in the order of 20 Watts (at 0.7V for silicon and 2.6V for multi-junction), it is thus necessary to form an ‘array’ of hundreds of cells to achieve this power level. Electrical power transmission losses (I^2R) also require a high voltage to deliver significant power efficiently. This in turn requires a high voltage – in the order of hundreds of volts, meaning that hundreds of cells must be connected in series. To avoid ‘series mismatch’ and obtain the maximum power from a series-connected array of solar cells, it is necessary to have a uniform flux distribution of light delivered across the array.

For a ‘one-sun’ situation, this is generally very easy. All the cells must be located in the same plane and ensure no cell should be shaded.

For the case of concentrated sunlight however, the beam presented from our faceted parabolic dish is far from uniform, showing a range of intensity over two orders of magnitude (Figure 3-7 and 3-9). This would result in a significant drop in power output due to ‘series mismatch’ (elucidated in Section 4.4.4 which discusses the sensitivity of series strings of solar cells to varied flux distributions.).

Considering these factors, it is necessary to develop secondary optics which:

1. Capture as much of the concentrated beam as possible thus maximising the overall optical efficiency and
2. Deliver as much concentrated light as possible, evenly to the array of cells.

In keeping with the philosophy of targeting the highest efficiency at lowest cost, a ‘receiver’ containing an array of solar cells with secondary optics was chosen to:

- be as small as possible while still collecting most of the solar beam (Figure 3-9 indicates a radius of 12cm will achieve this);
- have secondary optics to ‘modify’ the primary concentrated beam and deliver it ‘evenly’ to an array of solar cells;
- be square to minimise complexity and cost;

- have a voltage that will be high enough to deliver the electrical power to efficiently transfer the power; and
- operate at an intensity which the solar concentrator cells can survive safely and efficiently (maximum 500 suns).

Considering the available solar cells with a size of 1.5cm x 1cm and the above requirements, it was concluded that a Photovoltaic Receiver (PV Rx) containing 384 series-connected cells would provide the necessary voltage of 265V (384 x 0.7V/cell) and cover an area of 24cm x 24cm being sufficient to capture most of the beam.

For this scenario, a simplistic calculation for the electrical power P_e , output for a perfect dish and receiver (assuming all reflected light is captured by the cells) would be:

$$P_e = \text{optical power reflected to the receiver } (P_L) \times \text{average cell efficiency } (\eta_{\text{cell}})$$

$$\text{or } P_e = P_L \times \eta_{\text{cell}}$$

$$\text{where } \eta_{\text{cell}} = 0.22 \text{ or } 22\%$$

$$\text{i.e. } P_e = 17\text{kW} \times 0.22 = 3.74 \text{ kW}$$

This calculation assumes that all reflected light hits the cell array, there is no series-mismatch and the secondary optics has no loss. This is the maximum ideal possible output. A more realistic model for the power output would include optical losses in the flux modification and series-mismatch, since the flux distribution will not be perfectly 'even'.

Three other factors can be used in combination with a 'flux modifier' to assist with 'shaping' the flux delivered to the cell array:

1. Position of the flux modifier aperture plane in relation to the dish focal plane;
2. Individual primary mirror facets may be pointed to another target point (within the flux modifier) other than the focal point; and
3. Individual facets may have a focal length different to the system focal length.

Constraints governing design of the flux modifier include:

1. The 'exit' must be the same shape and size as the cell array to prevent loss of concentrated modified flux;
2. The cost must be low;
3. Weight must be low since the receiver is supported on a cantilever at the focus of the dish; and
4. 'Modified' rays should approach the cell array at an angle of inclination of less than 60% to minimise 'surface' reflection from the cell/cover glass face according to the Fresnel equation.

Compromises must also be made considering:

- Reflectivity and cost;
- Length and number of ray bounces; and
- Flux modifier angle and approach of the reflected beam to cell face.

With these criteria established, it is then possible to proceed with the design of the secondary optics named the 'flux modifier' (FM).

The optimisation of the FM design was developed using our own code ray trace program called 'PV Trace'. The main steps of the process are shown below.

The target is to achieve an average intensity of 17kW for a receiver size of 24cm x 24cm = 29.5W/cm² or about 300 suns.

Considering the flux shape shown in Figure 3-9 (at the focal plane) the peak flux is approximately 120W/cm². The first step is to reduce this by moving the receiver 10cm back from the focal plane so that the peak is now approximately 27W/cm². (See Figure 3-10).

Figure 3-11 shows the effect on the flux distribution of moving the receiver back behind the focus and applying the reflective 'flux modifier' plates to reflect the 'crossed over' beam back onto the 'cell face' (Figure 3-10 without flux modifier). Figure 3-12 shows what the receiver flux modifier configuration will look like.

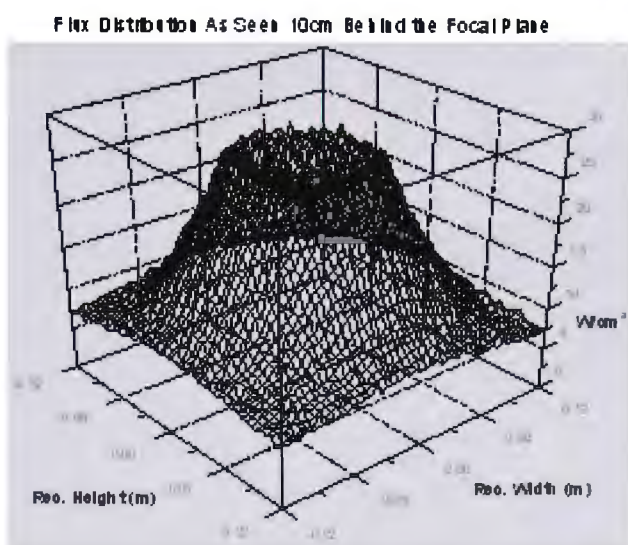


Figure 3-10: Simulated flux distribution as seen 10cm behind the focal plane of a 5m diameter dish. There is no secondary optics used here.

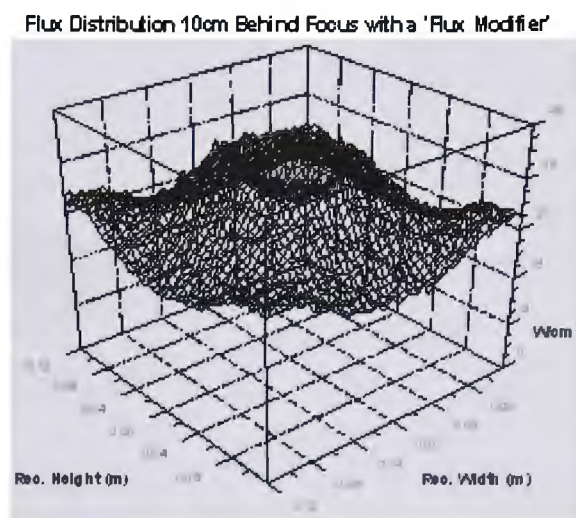


Figure 3-11: Simulated flux distribution as in Figure 3-10 with the addition of a 'flux modifier'.

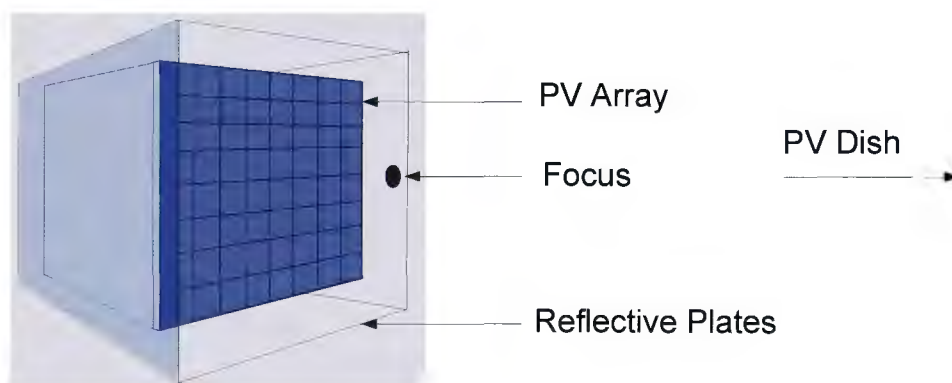


Figure 3-12: The PV dense array surrounded by 4 highly reflective plates placed behind the focal point of a 5m, diameter dish.

The graph in Figure 3-11 is a more even flux distribution, but would still result in a significant series mismatch loss. To improve this further, the precise direction of a number of mirror tiles were systematically adjusted in the ray trace model by trial and error until they produced a more even distribution (note: round beam into square hole). Figure 3-13 shows the effect on the flux distribution by re-pointing 944 mirror tiles. The mirror tiles in the 5th to 10th outer rings (counting from the outer most rings of mirrors) that were pointing towards the corners of the receiver were moved away and re-pointed towards the

centre of the edge of the receiver. All mirror tiles from the 23rd to 26th rings were pointed outwards to reduce the ‘doughnut’ shape that can be seen in Figure 3-10 and Figure 3-11.

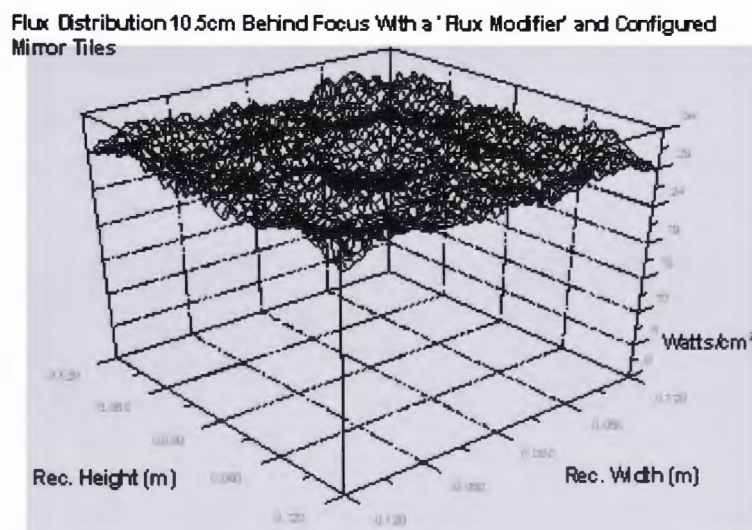


Figure 3-13: Simulated flux distribution as seen 10cm behind the focal plane of a 5m diameter dish. The beam has been changed using a ‘flux modifier’ and by configuring the direction of a number of mirror tiles. The incident solar intensity is $1000\text{W}/\text{m}^2$ which produced an average irradiance of $29.48\text{Watts}/\text{cm}^2$ with a nominal mirror activity of 94%. Total power is 17kW optical.

3.3 The Photovoltaic Receiver

The essential constraints that define the size and shape of a photovoltaic receiver are based on the properties of the solar cell device. These properties include:

- (i) the cell size (available and practical),
- (ii) the voltage and current output (required),
- (iii) the cell efficiency,
- (iv) the operating conditions of the cell and
- (v) the cost and availability.
- (vi) cooling considerations,
- (vii) power extraction.
- (viii) the ability to cool the cells (this limits the concentration ratio)

The devices most suited for this dish concentrator at the time of the initial experiments were found to be a 124 micron thick, back-contacted, silicon solar cell manufactured by Sun Power Inc. The cells measure 10mmx15mm in size and are grouped together to form a 60mm x 60mm, 6 x 4 cell, series connected module. An arrangement of 4 x 4 modules

makes up the entire receiver. The module size was chosen for ease of handling. All modules are series connected and the cell number totals 384. All cells are series connected. A basic calculation yields the predicted power output of the entire receiver (average cell efficiency x incident power). The results are shown in Table 3-1. The cell efficiency is based on flash tests and the expected solar radiation intensity (irradiance) is taken from in field results for Dish #2 at White Cliffs (Verlinden *et al*, 2001).

Number of Cells	Irradiance (Watts/cm ²)	Receiver Area (cm ²)	Incident Power on receiver (kW)	Average Cell Efficiency (%)	Predicted Power (kW)	Actual Power
384 cells in series	25.3	576	14.6	24.7	3.59	3.44

Table 3-1: The predicted and actual power output from a Photovoltaic receiver containing 384 series-connected cells with an incident solar beam irradiance of 25 Watts/cm² and a 39°C cell temperature.

The power predicted in Table 3-1 however, does not take into account the reduction in power output caused by the variation in flux intensity across the receiver. Generally, reduced flux intensity on any one cell connected in series with a group of other cells will have a reduced current and cause the current of entire array to be reduced. The actual power output therefore, may be substantially less. A measure of the performance of the actual system will be indicated by how close the actual performance is to the predicted 3.59 kW. The actual output was measured at 3.44 kW showing that the loss due to flux variation was 4.4%.

Figure 3-14 shows a prototype receiver in a dish concentrator system 'on sun'. Prototype and production receivers are also shown in Figures 3-15 and 3-16.

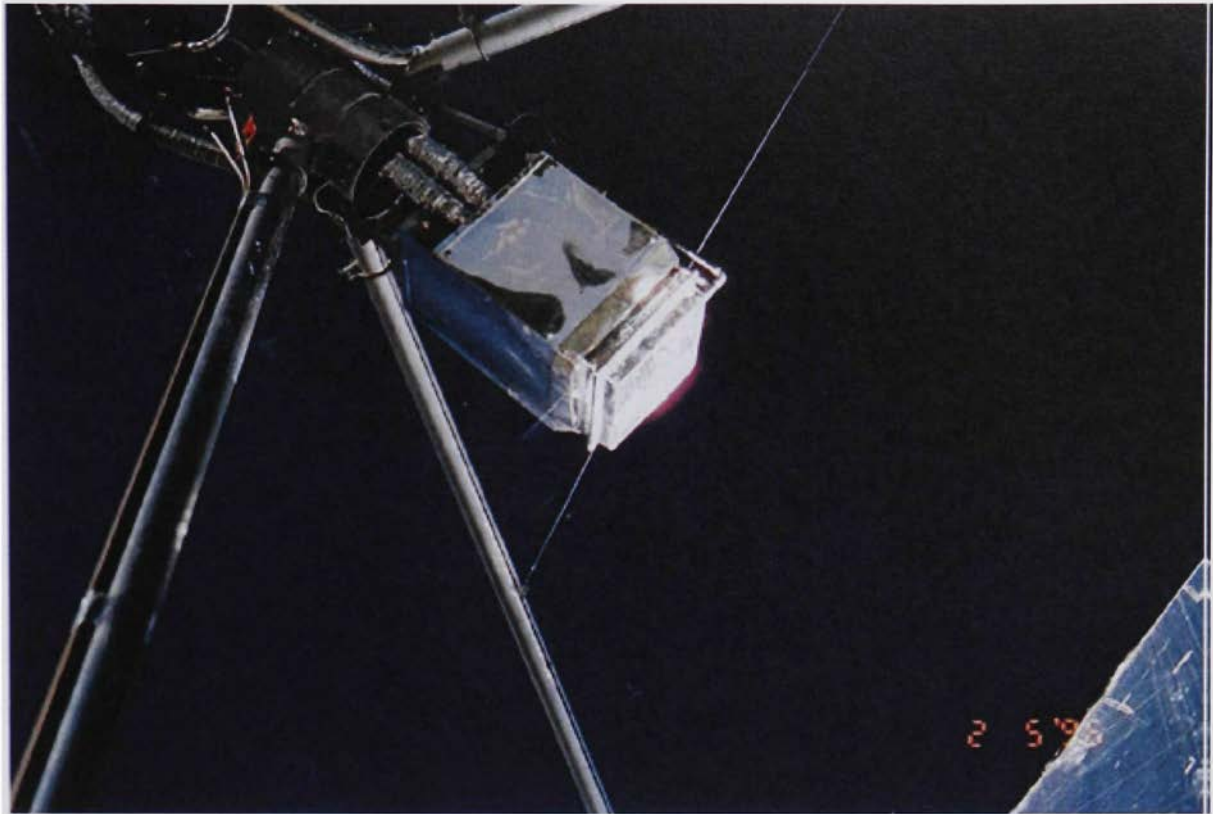


Figure 3-14: Photo of 3.3 kW prototype receivers 'on sun'.

3.4 Solar Cell Array

The design, performance and reliability of the solar cell array in a photovoltaic concentrator system is key to success for a CPV system. It must however be matched to the collector optics. The collector area is composed of non-expensive mirrors concentrating the sunlight onto a small area of expensive and very efficient solar cell array. The ratio of the projected aperture of the mirrors to the solar cell area is called the geometrical concentration ratio. The geometrical concentration ratio does not take into account optical losses due to non-perfect reflectivity of mirrors, light absorption, dirt on mirrors, imperfection of mirrors and spillage of light. The ratio of the average power reaching the solar cell surface to the direct sunlight incident power density is called the optical concentration ratio, which takes into account the optical losses mentioned above. At first sight, it seems obvious that, if the concentration ratio increases, the solar cell array will represent a smaller part of the whole system cost. In terms of cost per unit power (\$/Watt), the overall cost of the concentrator PV system should also decrease as the concentration ratio increases, providing that the solar cell efficiency and the optical system efficiency do not decrease, and that the cost of the cooling system or the tracking system do not increase. Practically speaking, the efficiency of every solar cell peaks at a particular intensity or concentration ratio (C_{max}). From an economical point of view, the cost per power ratio of a concentrator PV system

will reach the lowest point at a concentration ratio (C_{opt}) a little greater than C_{max} . The optimum concentration ratio C_{opt} is very difficult to determine a priori and, in real situations, the concentration ratio is often limited by the practical design of the thermal management and the reliability of the system.

Another interesting aspect of any concentrator PV system is that, because the solar cell array represents a small portion of the overall system cost (10% to 20%), but the solar cell, being the “engine” of the PV system, has great potential to reduce the cost of the produced electrical energy and increases as the concentration ratio increases. Thus a high concentration (if it can be achieved) is a strong lever for cost reduction.

In the next chapter (Chapter 4), we will study the theoretical ideal efficiencies or efficiency limits of solar cells, select the best solar cell for the concentrator system, established the required specifications of solar cells for a high-concentration PV system and study their electrical characteristics. We will also present the performance and reliability results of the solar cell array: an efficient multi-junction III-V solar cell array.



Figure 3-15: 3.3kW Prototype Dish with CPV Receiver ‘On Sun’



Figure 3-16: 'Whitecliffs' 3.7kW production dish receiver. This is the 'production' version of the prototype shown in Figure 3-14

CHAPTER 4. SOLAR CELLS SUITABLE FOR HIGH CONCENTRATION – THEORY & PRACTICE

4.1 Theory of Operation of Solar Cells

Solar cells are made by a p-n junction (diode) in a semiconductor material characterized by a valence band, of which almost all the energy states are filled with electrons, a conduction band, of which almost all the energy states are unoccupied, and by a forbidden band separating the valence and conduction bands, called bandgap. If the energy of the photons ($h\nu$, where h is the Planck constant and ν the frequency of light) is greater than the energy necessary to cross the bandgap (E_g), the photons will be absorbed by the semiconductor material, each photon generating one electron-hole pair. The excess energy of the photon, i.e. the difference between the energy of the photon and the bandgap, is converted into phonon energy, which causes the crystal lattice to heat.

The generated electrons and holes are separated by diffusion and finally by the internal electric field created by the p-n junction, the electrons flowing toward the n-type region and the holes flowing toward the p-type region. The current of electrons and holes is proportional to the intensity of light. At 500X concentration, the electrical current generated by the solar cell is 500 times greater than at one sun.

One can say that the solar cell is practically a current source. However, because it is also a p-n junction diode, as the voltage increases, the diode will divert part of the generated current in opposite direction. The diode current increases exponentially with the voltage. In its most simple form, the electrical model of a solar cell is a current source I_{ph} in parallel with a diode, with two resistances representing the series resistance R_s , due to electrical contacts and internal resistivity, and the shunt resistance R_{sh} , due to current leakage across the diode (see Figure 4-1).

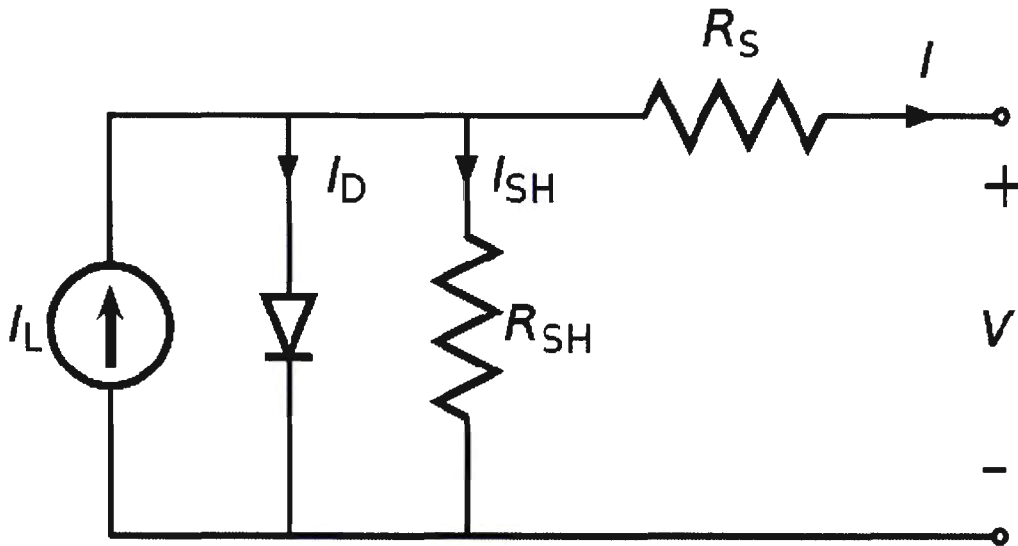


Figure 4-1: Electrical Model of a Solar Cell

The photogenerated current I_{ph} is proportional to the incident power density P_i and the area of the cell A_c , the ratio of these being called “Responsivity” R .

$$I_{ph} = R \cdot P_i \cdot A_c$$

The diode current I_D is given by:

$$I_D = I_0 \cdot (\exp(q V_D / nkT) - 1) = I_0 \cdot (\exp(q (V + R_s \cdot I) / nkT) - 1)$$

where I_0 is the saturation current of the diode, representing all the carrier recombination mechanisms inside the device, V_D is the voltage across the diode, T is the absolute temperature, k is the Boltzmann constant, n is the diode ideality factor, V and I are the solar cell voltage and current respectively and q the charge of the electron .

Therefore, the current-voltage equation of the solar cell is given by:

$$I = I_{ph} - I_0 \cdot (\exp(q (V + R_s \cdot I) / nkT) - 1) - (V + R_s \cdot I) / R_{sh}$$

At short-circuit condition, it becomes:

$$I_{sc} = I_{ph} - I_0 \cdot (\exp(q \cdot R_s \cdot I_{sc}) / nkT) - (R_s \cdot I_{sc}) / R_{sh} \approx I_{ph}$$

and is almost proportional to the light intensity.

At open-circuit condition, it becomes:

$$V_{oc} = nkT/q \cdot \ln ((I_{ph} - V_{oc}/R_{sh}) / I_o + 1) \approx nkT/q \cdot \ln (I_{ph} / I_o)$$

and is approximately proportional to the logarithm of the light intensity.

The generated power is the product of voltage and current. The generated power is zero at both short-circuit and open-circuit conditions and is maximum somewhere between I_{sc} and V_{oc} . The maximum power point is located on the I-V curve of the solar cell at a voltage V_{mp} and current I_{mp} :

$$P_{mp} = I_{mp} \cdot V_{mp}$$

The exact determination of P_{mp} , I_{mp} and V_{mp} depends strongly on the light intensity and the solar cell parameters, such as I_o , R_s , R_{sh} , and temperature. As a first approximation, for solar cells with a high efficiency, low series resistance and high shunt resistance, I_{mp} is about 90% to 95% of the short-circuit current I_{sc} , and $(V_{oc} - V_{mp})$ is almost constant and equal to:

$$(V_{oc} - V_{mp}) \approx nkT/q \cdot \ln (10 \text{ to } 20) \approx 0.178V \text{ to } 0.232V$$

In the particular case of a triple junction solar cell, the ideality factor n is approximately 1 for each cell.

Another way to express efficiency as a function of I_{sc} and V_{oc} is:

$$P_{mp} = I_{sc} \cdot V_{oc} \cdot FF$$

where FF is called “fill factor”, representing the squareness of the cell I-V curve:

$$FF = I_{mp} \cdot V_{mp} / (I_{sc} \cdot V_{oc})$$

The solar cell efficiency is given by:

$$\eta = P_{mp} / (A_c \cdot P_i) = I_{mp} \cdot V_{mp} / (A_c \cdot P_i) = I_{sc} \cdot V_{oc} \cdot FF / (A_c \cdot P_i)$$

Because I_{sc} and I_{mp} are essentially proportional to the incident power density P_i , whereas V_{oc} , V_{mp} and FF are essentially proportional to the logarithm of P_i , it results that the efficiency η also increases as the logarithm of the incident power density P_i . Therefore, the theoretical efficiency of a concentrator solar cell increases with the concentration ratio. This is true until the power loss due to the series resistance R_s becomes significant, causing a decrease in fill factor FF and a decrease in efficiency.

In a simplified form, the efficiency of a solar cell can be expressed as a function of the incident power density. Assuming that the shunt resistance is infinite, it can be approximately calculated by using the following equation:

$$\eta = R \cdot V_{oc} \cdot FF \approx R \cdot V_{oc} \cdot FF_0 \cdot (1 - 1.1 R_s \cdot I_{sc} / V_{oc})$$

$$\eta \approx R \cdot nkT/q \cdot \ln(R \cdot A_c \cdot P_i / I_0) \cdot FF_0 \cdot (1 - 1.1 R_s \cdot R \cdot A_c \cdot P_i / \{nkT/q \cdot \ln(R \cdot A_c \cdot P_i / I_0)\})$$

where R is the responsivity of the cell and FF_0 is the fill factor calculated with very low series resistance.

It is essential that solar cells designed for high concentration ratio have very low series resistance. In practice, a solar cell designed for one-sun operation (with a series resistance of, say, $1.0 \Omega\text{cm}^2$) will not see its efficiency increase with the concentration ratio because its series resistance is large and the I^2R_s loss dominates. While designing a cell for CPV application, one of the most important parameters to optimise is the series resistance. A fill factor of around 85%+ at $50\text{W}/\text{cm}^2$ may be achieved with a series resistance, R_s of around $0.02 \Omega\text{cm}^2$.

4.2 Maximum Theoretical Efficiency of Solar Cells

The theoretical maximum efficiency of solar cells is a function of the following variables:

T_s is the temperature of the external surface of the sun ($T_s \sim 5800 \text{ K}$),

T_c is the temperature of the cell,

T_a is the ambient surrounding the cell,

Following the second law of thermodynamics, the efficiency of an ideal heat engine (Carnot cycle) is:

$$\eta_C = 1 - T_a/T_s$$

If T_a is 300 K and T_s 5800 K, the maximum efficiency of any thermodynamical system, including solar cells, would be 95%.

Alternative derivations of the maximum efficiency have been presented by the following:

Curzon-Ahlborn (1975):

$$\eta_{CA} = 1 - (T_a/T_s)^{1/2}$$

Henry (1980):

$$\eta_H = 1 - (4/3) (T_a/T_s)$$

Landsberg (1998)

$$\eta_L = 1 - (4/3) (T_a/T_s) + (1/3) (T_a/T_s)^4$$

and the photo-thermal efficiency of Müser (1957):

$$\eta_{PTM} = [1 - (T_c/T_s)^4] [1 - T_a/T_c]$$

where the cell temperature T_c is calculated by:

$$4 T_c^5 - 3 T_a T_c^4 - T_a T_s^4 = 0$$

Under the same conditions ($T_a \sim 300$ K and $T_s \sim 6000$ K), the ideal efficiencies or efficiency limits are:

$$\eta_C = 95\%$$

$$\eta_H \sim \eta_L = 93.3\%$$

$$\eta_{PTM} = 85\%$$

$$\eta_{CA} = 77.6\%$$

The ideal efficiency formula presented by Henry is an approximation of Landsberg and is valid for ambient temperatures lower than $0.4 T_s$, as shown on Figure 4-2.

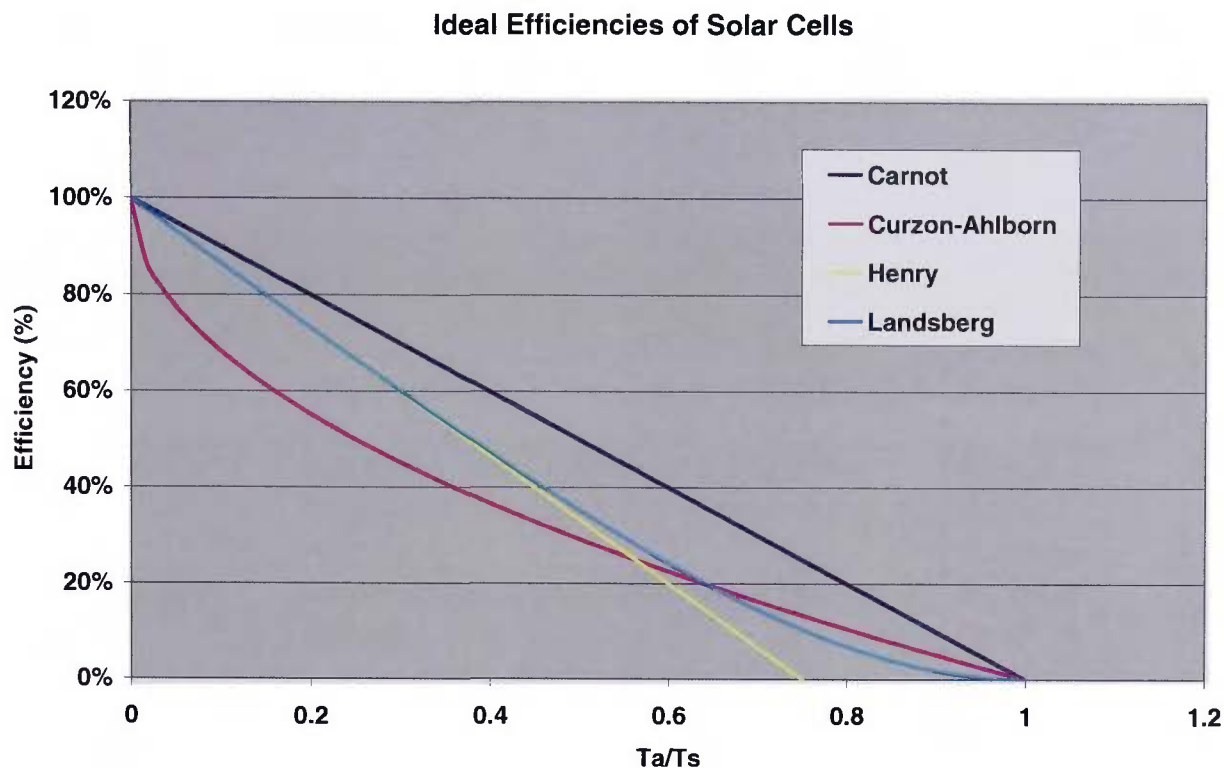


Figure 4-2: Theoretical ideal efficiencies as a function of the ambient to source temperature ratio.

The above formulae represent the predicted performance of ideal systems. In order to consider likely maximum performance, the bandgap of the semiconductor E_g needs to be taken into account to bridge the gap between thermodynamics that deals with macroscopic system and detailed mechanisms encapsulated by solid-state physics. Shockley and Queisser (1961) presented a detailed balance of the efficiency limit for p-n junction solar cells.

Maximum Efficiency	Particular situation	Calculated or proposed by
30%	Limit efficiency for a single-junction solar cell at 1 sun. Detailed balance.	Shockley and Queisser (1961)
31%	Single-junction solar cell at 1 sun. Ideal case	Henry (1980)
37%	Ideal single-junction solar cell at 1000 suns concentration	Henry (1980)
43%	Single-junction solar cell at 1 sun if multiple electron-hole pairs can be created by one photon	Werner et al (1994).
50%	Ideal dual-junction solar cell at 1000 suns	Henry (1980)
56%	Ideal triple-junction solar cell at 1000 suns	Henry (1980)
72%	Ideal 36-junction solar cell at 1000 suns	Henry (1980)

86.8%	Infinite number of junctions at maximum concentration ratio (46,300 X)	Landsberg (1998)
-------	--	------------------

Table 4-1: Maximum efficiency prediction for a range of cell configurations.

4.3 Current World Record Efficiencies

The currently best reported efficiencies are recorded in 'Progress in Photovoltaics' (Green, 2009):

Efficiency	Solar Cell Type	Author, Laboratory or Company
24.7%	Single-junction crystalline Si solar cell at 1 sun	Zhao, UNSW
25.1%	Single-junction GaAs solar cell at 1 sun	Kopin
27.6%	Single-junction crystalline Si solar cell at 92 suns	Slade, Amonix
28.3%	Single-junction crystalline Si solar cell at 100 suns	Swanson, Stanford (1998)
32.0%	Triple-junction GaInP/GaInAs/Ge solar cell at 1 sun	King, Spectrolab (2005)
41.1%	Triple-junction GaInP/GaInAs/Ge solar cell at 200 suns	Bett, Fraunhofer ISE

Table 4-2: World Record Solar Cell Efficiency for different types of cells. Spectrolab have recently announced 41.6% for a multijunction concentrator cell.

4.4 Simulation of 35kW Multi-Junction Receiver

4.4.1 Spectral Response and Quantum Efficiency of Triple-Junction Solar Cells

A multijunction solar cell was developed to increase the efficiency by capturing more of the solar spectrum. Figure 4-3 shows the concept of the cell stack and the spectral response. The Spectral Response SR of a solar cell is expressed in A/W and is the ratio of the photocurrent of a solar cell and the incident power of the light. It typically vanishes when the energy of the photons is smaller than the bandgap of the semiconductor material or when the wavelength of the light is greater than the maximum wavelength that the semiconductor can absorb.

The theoretical Spectral Response (SR) of a solar cell is given by:

$$SR = q\lambda/hc$$

where q is the electron charge (1.602×10^{-19} C), λ is the wavelength of the light, h is the Planck constant (6.626×10^{-34} J.sec) and c the speed of light (2.998×10^8 m/sec). The above equation corresponds to the assumption that every photon absorbed by the semiconductor will give one (and only one) electron-hole pair.

The External Quantum Efficiency (EQE) is the real (or measured) spectral response of a solar cell (or ratio of the photo-generated current and the incident power) divided by the theoretical spectral response ($q\lambda/hc$). The External Quantum Efficiency is typically smaller than 1 and goes to zero for photon energies smaller than the bandgap E_g of the semiconductor material (long wavelengths). It also vanishes for short wavelengths if the light is filtered by a layer of material deposited on top of the cell. For example, the top cell filters the light for the middle cell and, the anti-reflection coating and window layer filter the light for the top cell (See Figure 4.4).

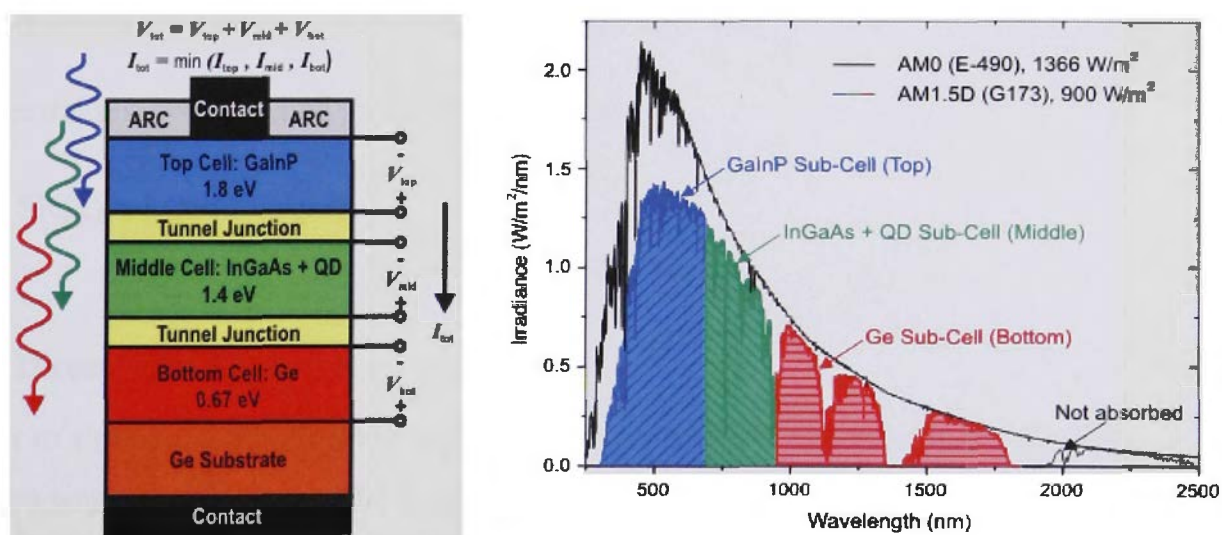


Figure 4-3: Multijunction cell concept

External Quantum Efficiency of Top and Middle cell of a Triple-Junction Solar Cell

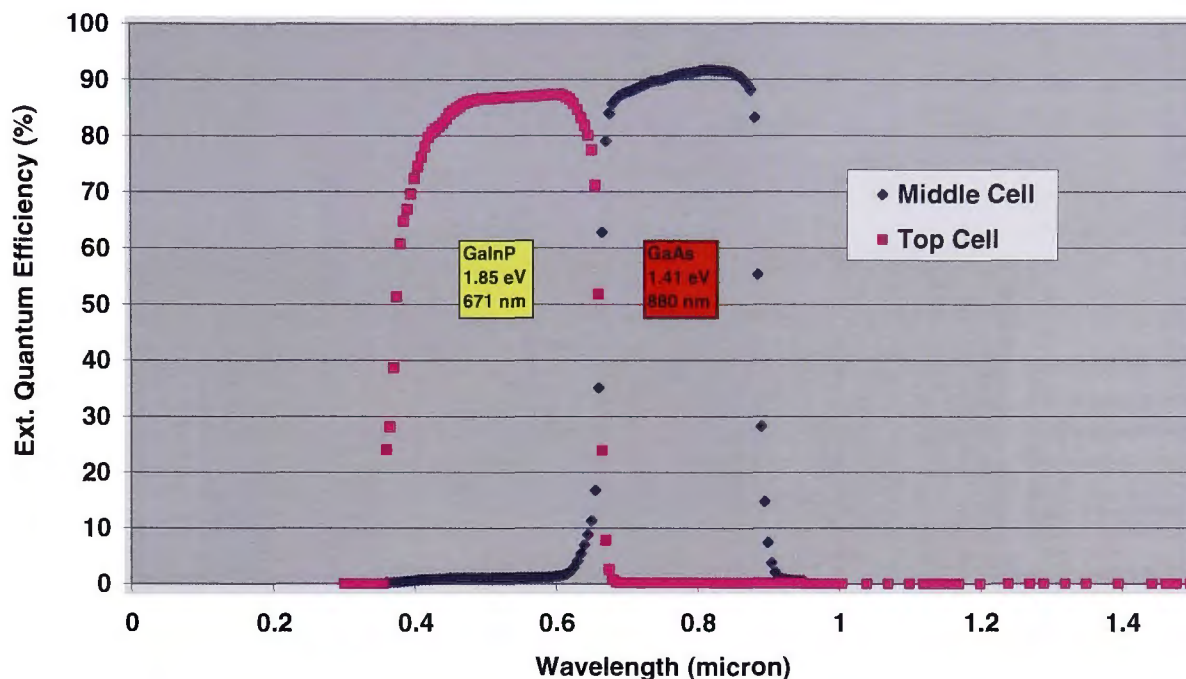


Figure 4-4: Measured external quantum efficiency (EQE) of the two top junction of a triple-junction solar cell from Spectrolab Inc. The top (GaInP) cell has a band edge of 671 nm, which requires a photon energy of 1.8 eV, and the middle (GaAs) cell has a band edge 880 nm and requires a photon energy of 1.41 eV.

The External Quantum Efficiency of the germanium solar cell is not represented on the graph. The germanium cell ($E_g = 0.67$ eV) response extends up to about 1.85 micron and is not the limiting photocurrent of the triple-junction solar cell.

The spectral response of each junction is given by:

$$SR(\lambda) = EQE(\lambda) \cdot q\lambda/hc$$

4.4.2 Direct Solar Spectrum

In order to simulate the performance of the multijunction PV receiver, the direct solar spectrum was simulated using the irradiance model developed by Bird (1984). The model is programmed into an Excel spreadsheet that is available from the NREL website. It simulates the direct and diffuse solar spectrum based on several input parameters, the most important being the day, time, latitude, longitude, pressure (or altitude), and the atmospheric parameters such as ozone concentration, aerosol (index of turbidity) and

precipitable water optical depth. Figure 4-5 shows a partial view of the spreadsheet developed by Myers (2000) at NREL. Only the direct part of the solar spectrum is considered in the case of concentrator PV systems since they cannot concentrate diffuse light.

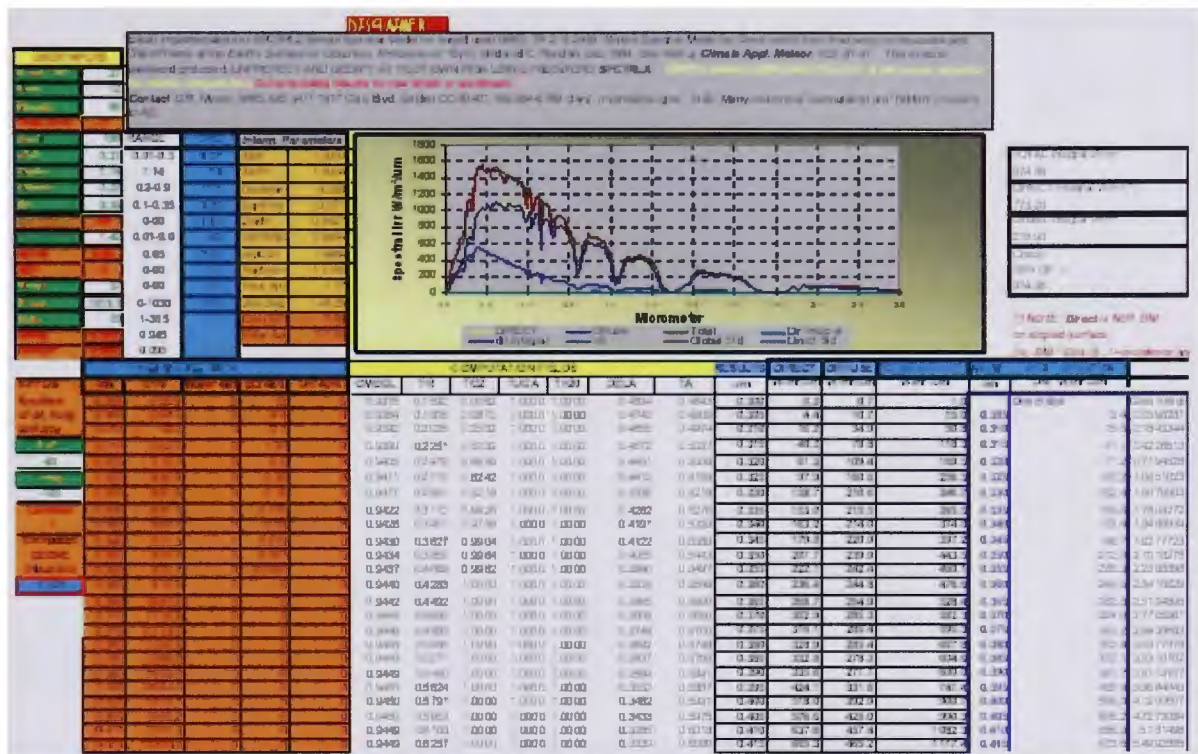


Figure 4-5: Partial view of the Excel spreadsheet developed by NREL providing the direct and diffuse solar spectrum calculated for a cloudless atmosphere following Bird's (1984) model.

The total incident power density is given by:

$$P_i = \int_0^{\infty} H_{sd}(\lambda) \cdot d\lambda$$

where $H_{sd}(\lambda)$ is the direct solar spectrum given by Bird's model.

4.4.3 Calculation of the Photo-Generated Current

Using, the direct solar spectrum given by Bird's (1984) model and the measured quantum efficiency of the two top junctions of the triple junction solar cell of Spectrolab, the photo-generated current of each junction I_{phi} of the triple-junction solar cell is then individually determined by:

$$I_{\text{phi}} = A_c \cdot \int_0^{\infty} \text{SR}_i(\lambda) \cdot H_{\text{sd}}(\lambda) \cdot d\lambda$$

Where $\text{SR}_i(\lambda)$ is the measured spectral response of each individual junction, A_c is the total solar cell area and $H_{\text{sd}}(\lambda)$ is the direct solar spectrum.

Because all three junctions of a monolithic triple-junction solar cell are series connected, the photo-generated current of the stack is the minimum photo-generated current of all three junctions.

$$I_{\text{ph}} = \text{minimum} (I_{\text{ph1}}, I_{\text{ph2}}, I_{\text{ph3}})$$

In the particular case of the GaInP/GaInAs/Ge triple-junction, the germanium junction is far from being the limiting junction. Therefore, only the current of the two top junctions need to be calculated. Usually, for terrestrial application the GaInP top junction is the limiting one.

The responsivity of the solar cell is given by:

$$R = I_{\text{ph}} / (A_c \cdot P_i)$$

It is typically 0.13 to 0.14 A/W for a high-efficiency triple-junction GaInP/GaInAs/Ge solar cell illuminated with a direct solar spectrum of AM1.5D (ASTM G173-03). For comparison, a typical responsivity of a high-efficiency silicon solar cell is around 0.39 A/W. Of course, the triple-junction cell provides a much greater voltage (~3.15 V at open-circuit condition) than the silicon solar cell (~0.83 V) at 500 suns.

Bird's (1984) model can generate the direct solar spectrum at any location and at any time of the year. The integration of the product of the solar spectrum with the measured spectral response of the two top junction of the solar cell allows calculating the photo-generated current of the multi-junction solar cell to be accelerated at any moment of the year.

The daily Energy Production Rate (EPR) is defined as the total energy production by a CPV system, expressed in kWh divided by the unit of solar direct normal energy received during the same period, expressed in kWh/m². The EPR can be calculated using the method explained above. The simulated EPR for Solar Systems commercial 35kW dish system as a

function of the date over one year is presented in Figure 4-6, along with the peak DC power output at noon and the DC power at noon, normalized to a DNI of 1 kW/m^2 .

Interestingly EPR, which is expressed in unit of kWh/kWh/m^2 or simply m^2 , also represents the equivalent projected area of a solar conversion system with 100% efficiency. As a consequence, the ratio of EPR and the actual projected area of the CPV system is the energy efficiency of the CPV system.

Figure 4-7 represents the calculated daily energy production for the same CPV dish for 12 different days of the year, without clouds.

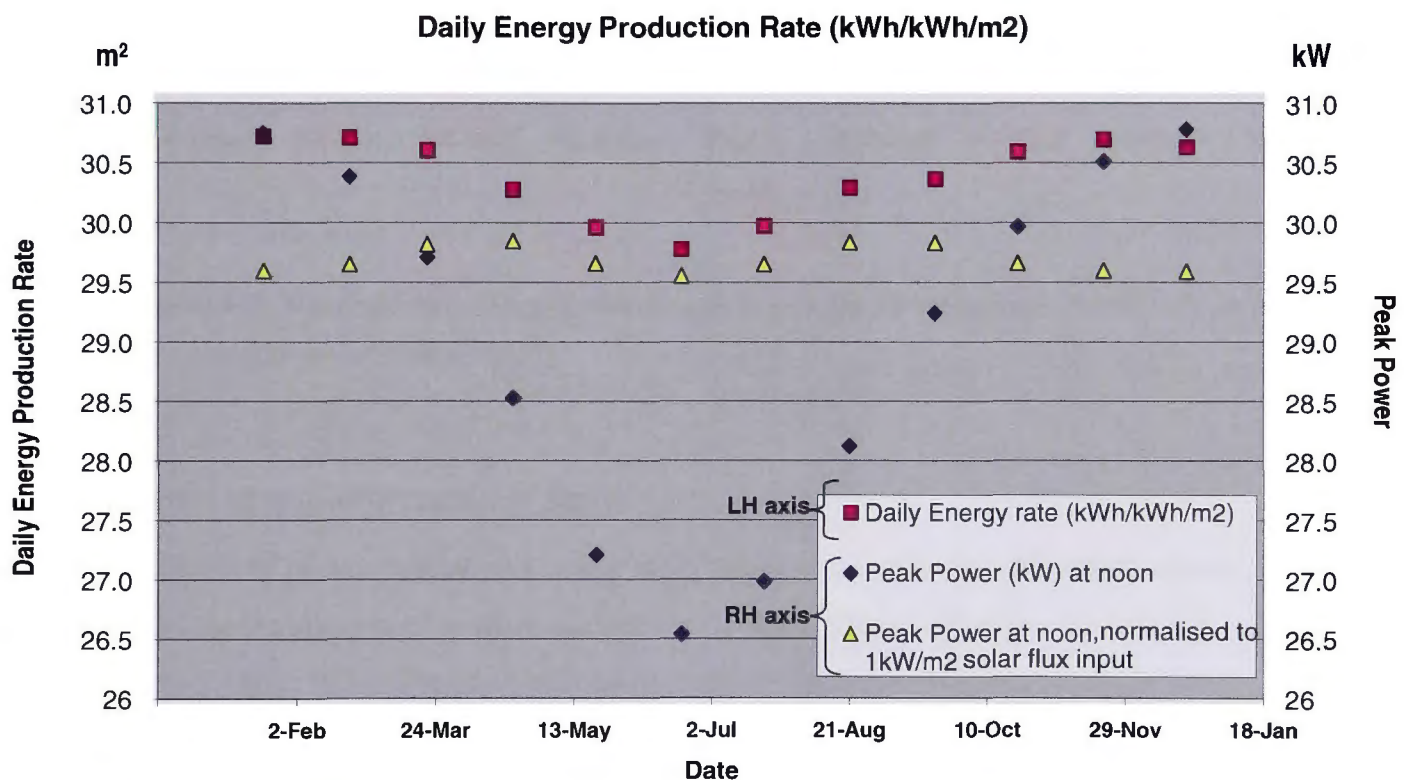


Figure 4-6: Simulated daily energy production for Solar Systems commercial 35.0 kW CPV dish, as well as peak DC power output at noon (real and normalized to a DNI of 1.00 kW/m^2), for 12 particular dates of the year, without clouds. In relation to the ‘Daily Energy rate’: this has a unit of m^2 and represents the number of square meters of collector required to deliver the charted amount of power at 100% efficiency. Coincidentally, the magnitude of this parameter is also equivalent to the average power output when the incident flux is 1000 W/m^2 .

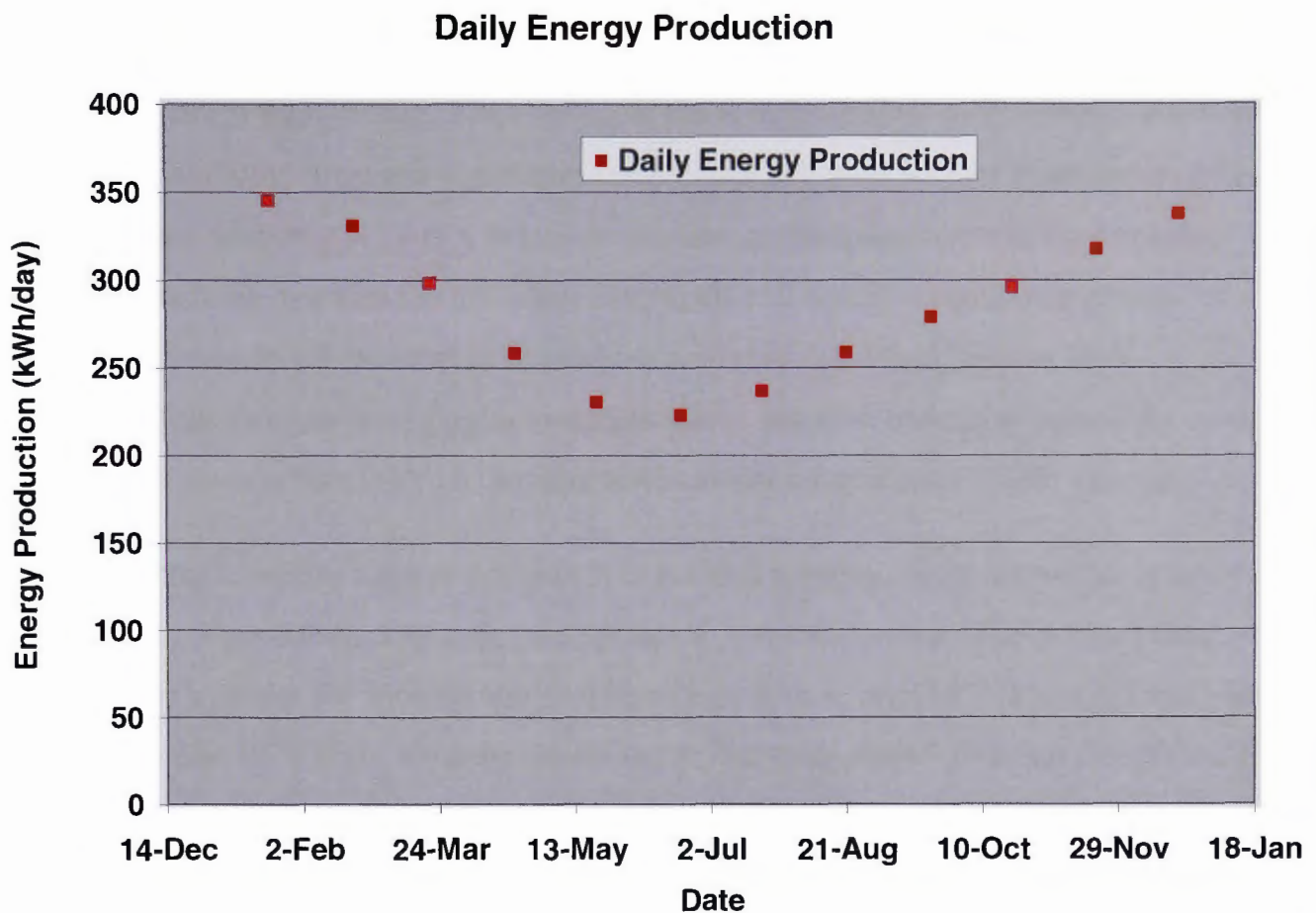


Figure 4-7: Simulated daily energy production of Solar Systems commercial 35 kW CPV dish unit for 12 days in a year without clouds.

4.4.4 Effect of non-uniformity of light

The simulation of power output of a dense array receiver like the one presented above assumes an ideal situation of perfect uniformity of light. This is of course not always possible. In general, almost perfect uniformity can be achieved, but this comes with a penalty in optical efficiency and cost. Therefore, in the design process of a CPV system, there is a trade-off between uniformity and optical efficiency.

In a PV system where many solar cells are interconnected in series, the non-uniformity of illumination is responsible for a significant power loss. This comes from the fact that solar cells are essentially current sources, as described above. The maximum current in a string of current sources is the current of the weakest source. In other words, if one cell in the series-interconnected string of cells is less illuminated than the others, it is equivalent to all of the cells being poorly illuminated, resulting in a significant power loss much greater than just the lack of light over one cell.

There is another issue associated with light non-uniformity, which is more related to reliability. In a series string, if one cell is in the dark or poorly illuminated, the other cells will have to run at high voltage, close to V_{oc} . If the voltage applied to the module is low or close to I_{sc} condition, there is a significant risk that the cell with weaker illumination will be reverse biased. Not only is there a risk of destruction of that particular cell by damaging reverse breakdown, but also the low-illuminated cell will absorb a significant amount of power (generated by all the other cells) and become very hot. Multijunction III-V compound solar cells are very fragile and particularly sensitive to reverse bias. They cannot sustain large reverse bias ($>5V$) or large reverse current without irreversible damage.

A typical solution to this kind of problem is to connect a bypass diode across the number of cells capable of producing a voltage corresponding to the maximum reverse bias voltage of any cell. For a silicon PV module, this is typically 12 cells or about 8V. For a module made of multijunction III-V cells, the cells are so fragile that each one of them must be protected by a bypass diode. The bypass diode prevents a reverse voltage greater than 1V being applied to the solar cell. It also allows the larger current generated by the other cells to flow through the series string.

In the particular case of the 35kW CPV dish, there are 24 cells in series in a module and 64 modules with sub arrays of either 8 or 16 modules in series in a receiver. Each cell within a module is protected by a bypass diode. An additional protection is provided by connecting in parallel several modules to form a sub-array. The location of the modules within a sub-array and the way a receiver is partitioned into sub-arrays is optimized taking into account the symmetry in light distribution within the receiver area. Each sub-array is also protected by a by-pass diode. Finally, in order to prevent current from flowing from one group of modules to another module connected in parallel, each module is also protected by a blocking diode.

4.4.5 Sensitivity to Atmospheric Parameters

At this point, it is very important to note that, even if the theoretical efficiency of a multijunction solar cell increases with the number of junctions, at the same time the sensitivity of the efficiency to changes in solar spectrum also increases. For example, a single-junction solar cell, such as a silicon solar cell, absorbs a large portion of the solar spectrum. Small changes in the solar spectrum due to change in Air Mass (AM) or Aerosol

Optical Depth (AOD) or precipitable Water Optical Thickness (WOT) do not have a great influence on the responsivity of a single-junction solar cell. In fact the responsivity of a silicon solar cell increases with the Air Mass index. Unlike single-junction solar cells, multijunction solar cells have several junctions that are monolithically series connected, each of them absorbing a different small part of the solar spectrum, and that are optimised in bandgap and thickness for one specific solar spectrum, usually the standard ASTM G173D with an AM index of 1.5. As seen previously, the optimisation of a multijunction solar cell consists in balancing the photogenerated current of each individual junction in such way that their theoretical photogenerated currents are equal for the nominal solar spectrum (AM1.5D). When the solar spectrum is different from that the nominal spectrum, the responsivity of the cell decreases. For example, for a GaInP/GaInAs/Ge triple-junction cell, the top GaInP junction would become limiting if the Air Mass index increased from the nominal 1.5 value, whereas the middle GaInAs junction would become limiting if the Air Mass index decreases below 1.5.

The following graphs (see Figures 4-8 to 4-13) show the sensitivity of the cell responsivity to atmospheric parameters such as Air Mass, Aerosol Optical Depth (AOD), precipitable Water Optical Thickness (WOT) and ozone. In particular the impact of WOT on the MJ cell responsivity deserves a short explanation because it is counter-intuitive. The presence of water in the atmosphere results in optical absorption of the sunlight in wavelength bands located in the Infra-Red region of the spectrum, centred on the following wavelengths: 937nm, 1120nm, 1400nm and 1880nm (see Figure 4-12). These absorption bands are all located in the portion of the spectrum that is absorbed by the germanium sub-cell. In other words, if the water in the atmosphere increases, the absorption bands will be deeper. It will result in a lower broadband incident power density and a lower photogenerated current for the germanium sub-cell. The other sub-cells will be not affected. Since the germanium sub-cell is already generating excess current compared to the other two sub-cells, the total current of the multijunction cell is actually not affected. This results in a greater responsivity because of a greater ratio of current to incident power. Inversely, if WOT decreases, the incident power density increases but the MJ cell current does not change, resulting in a lower responsivity as shown on Figure 4-12.

Sensitivity to Air Mass

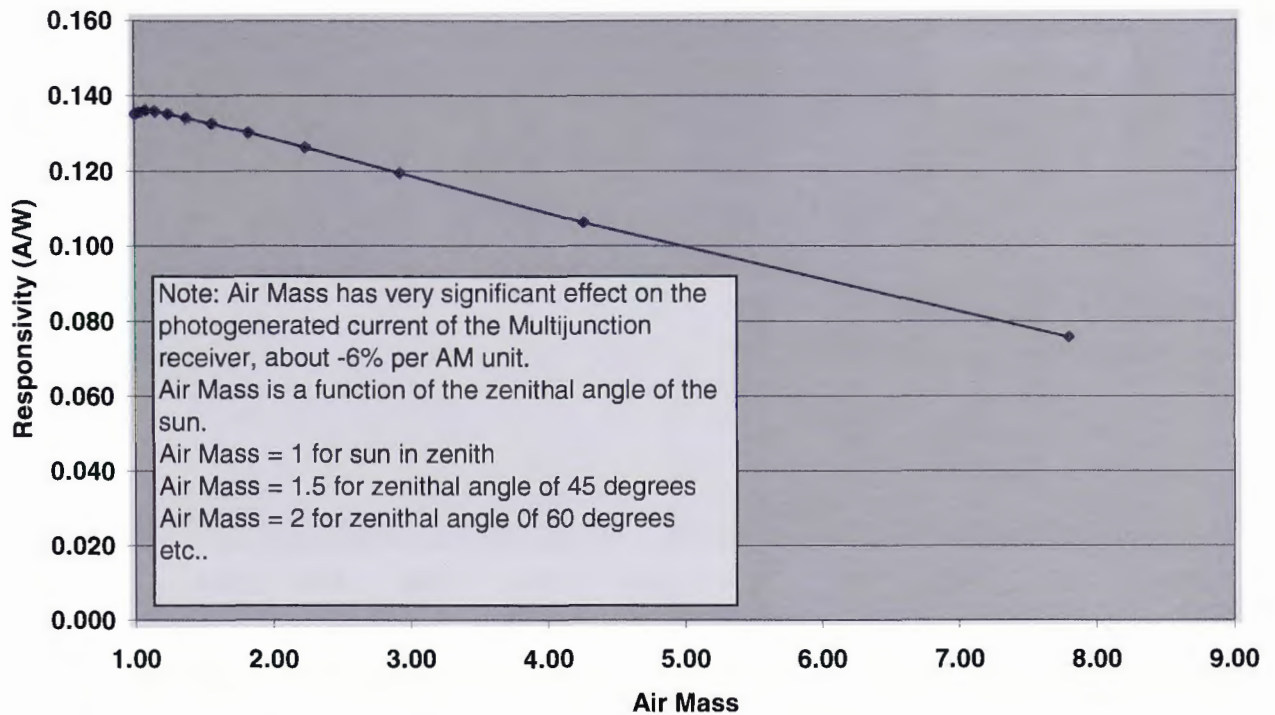


Figure 4-8: Sensitivity of responsivity of a GaInP/GaInAs/Ge triple-junction solar cell to Air Mass (Calculated result)

Cell Responsivity vs Air Mass (low AOD 0.085)

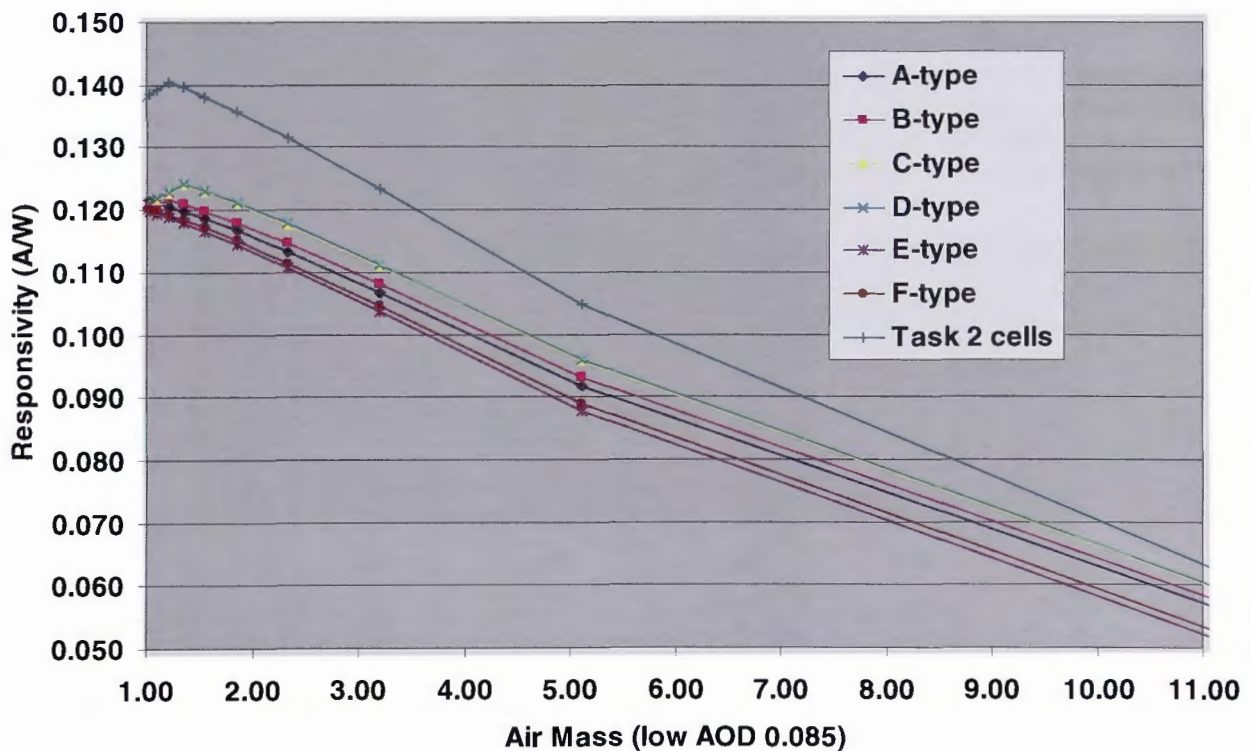


Figure 4-9: Simulated responsivity vs. Air Mass for different triple-junction solar cells. The different types represent a range of epitaxial growths, grid deposition methods and designs.

Hermannsburg - 2W - 31 May 2008

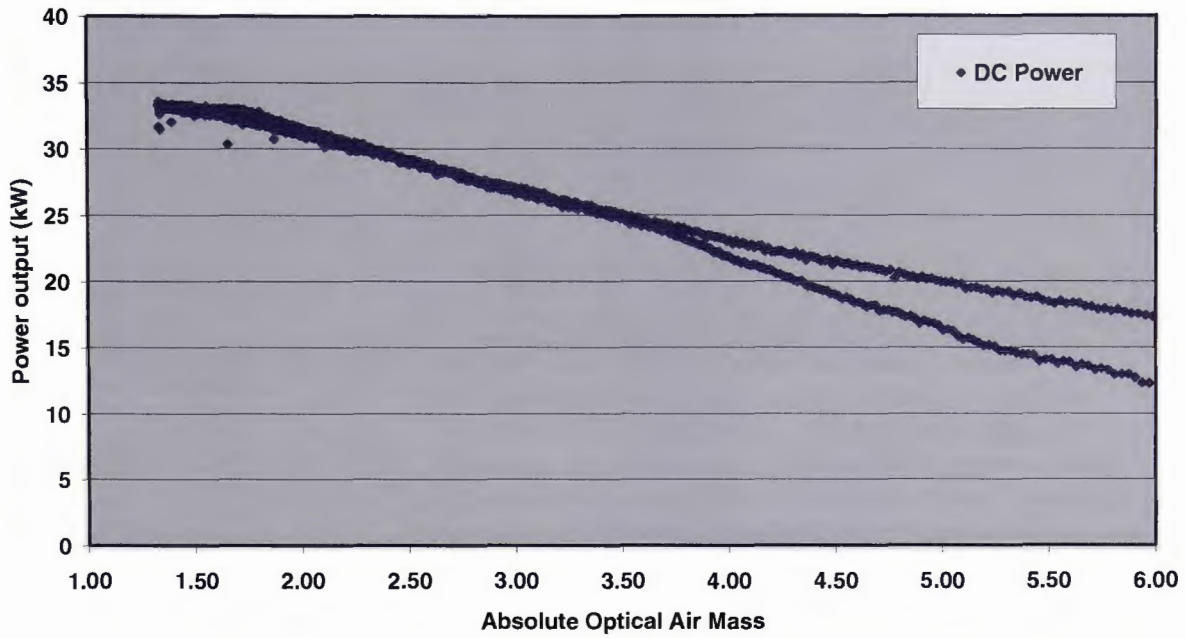


Figure 4-10: Measured DC power output of commercial 35kW dish versus Air Mass at Hermannsburg, Northern Territory, Australia.

Sensitivity to AOD (Aerosol Optical Depth or Turbidity factor)

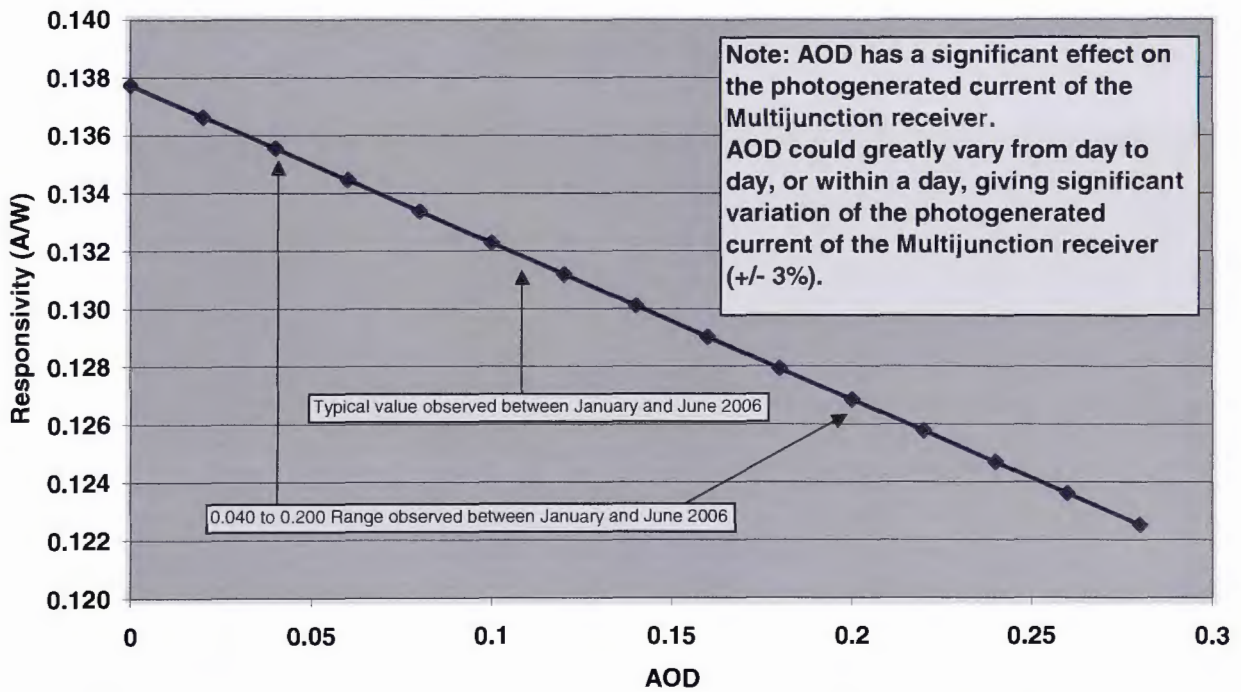


Figure 4-11: Simulated responsivity of triple-junction solar cell versus Aerosol Optical Depth (AOD). The air mass is 1.5.

Effect of Precipitable Water Optical Thickness (WOT) on Responsivity

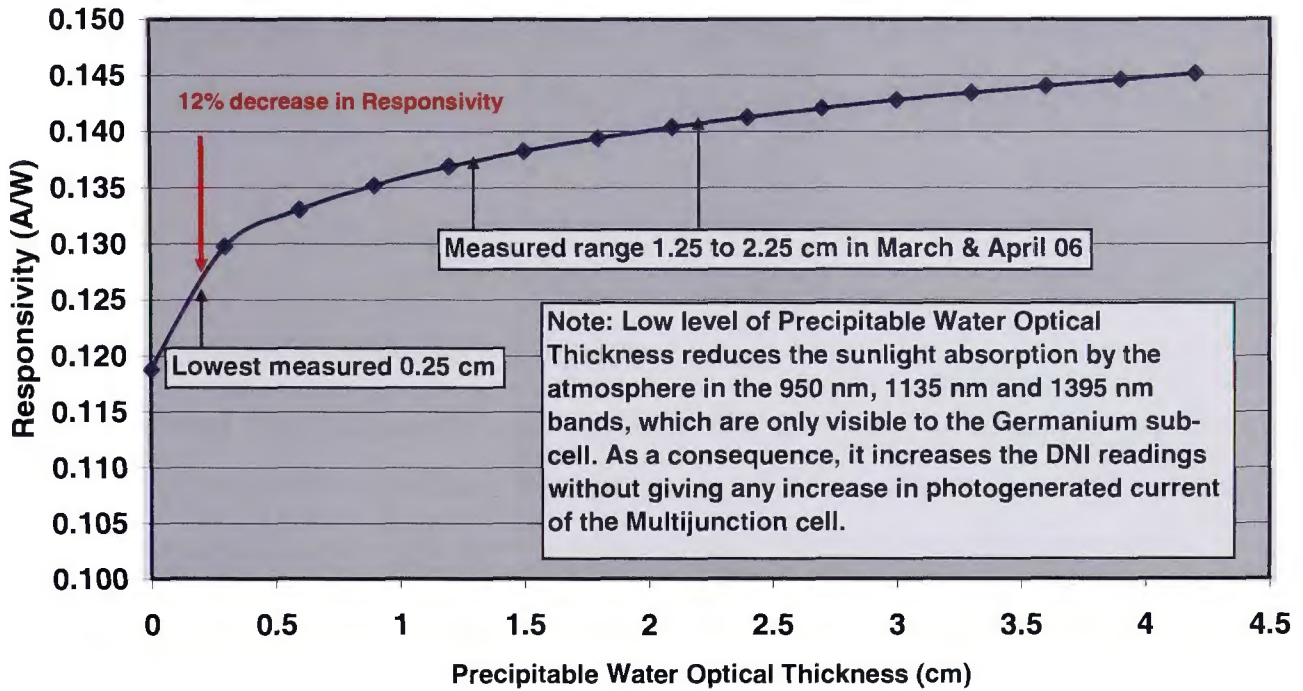


Figure 4-12: Simulated responsivity of triple-junction solar cell versus precipitable Water Optical Thickness (WOT)

Sensitivity to Ozone

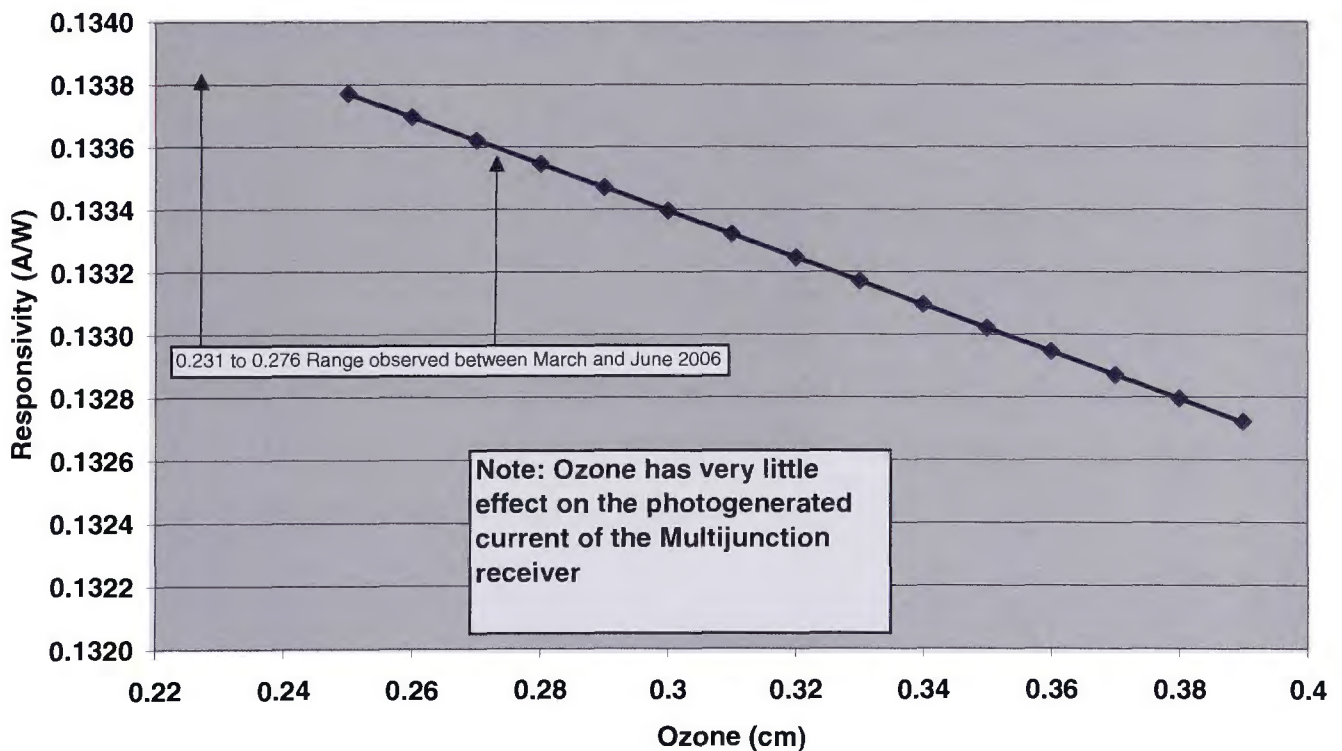


Figure 4-13: Simulated responsivity of triple-junction solar cell versus Ozone.

4.4.6 Reliability of Multijunction Receiver

The receiver reliability has a major influence on the system reliability with the ‘model’ being the main ‘active’ components. Chapter 7 examines the reliability assessment and measurement.

4.4.7 Future High-Performance Receivers

Looking forward to the development of very high efficiency solar cells, a larger number of junctions will have to be considered. The following graphs show the different possibilities of multijunction solar cells, with increasing number of junctions, assuming that each compound III-V semiconductor material would be grown on and lattice-matched to a germanium substrate (see Figures 4-14 to 4-18). Following the current GaInP/GaAs/Ge triple-junction solar cell, the possible future multijunction cells are:

- 4-Junctions: 1.85eV GaInP / 1.41eV GaAs / 1.0eV GaInNAs / 0.67eV Ge with a potential efficiency of about 42% in production
- 5-Junctions: 2.0eV AlGaInP / 1.8eV GaInP / 1.6eV AlGaInAs / 1.41eV GaInAs / 1.1eV GaInNAs / 0.67eV Ge with a potential efficiency of about 43% in production

From early simulations, it seems that five junctions would be the maximum number of junctions acceptable for terrestrial CPV applications. If the number of junctions is increased above five the efficiency of the solar cell may increase but the annual production of energy may not. Multijunction cells with more than 5 junctions, the sensitivity to atmospheric parameters (AM, AOD, WOT) may be so great that the efficiency would decrease quickly for any solar spectrum departing from the standard AM1.5D.

Direct Solar Spectrum Irradiance – AM1.5D, ASTM G173-03

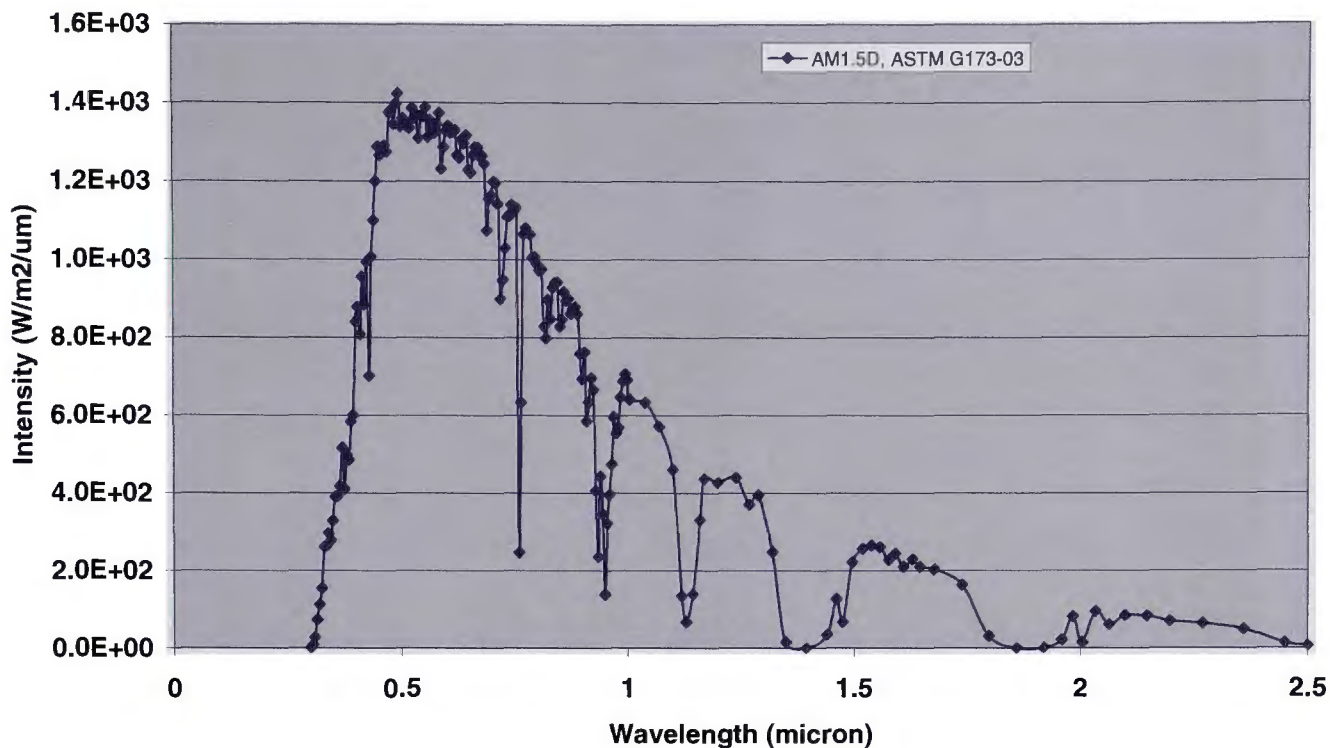


Figure 4-14: Direct solar spectrum (ASTM G173D) with AM1.5

The following figures 4-15 to 4-18 show the spectral partition for 1, 2, 3, 4 and 5 junction stacks.

Solar Spectrum Partition for 1-Junction Terrestrial Solar Cell based on Direct Solar Spectrum AM1.5D

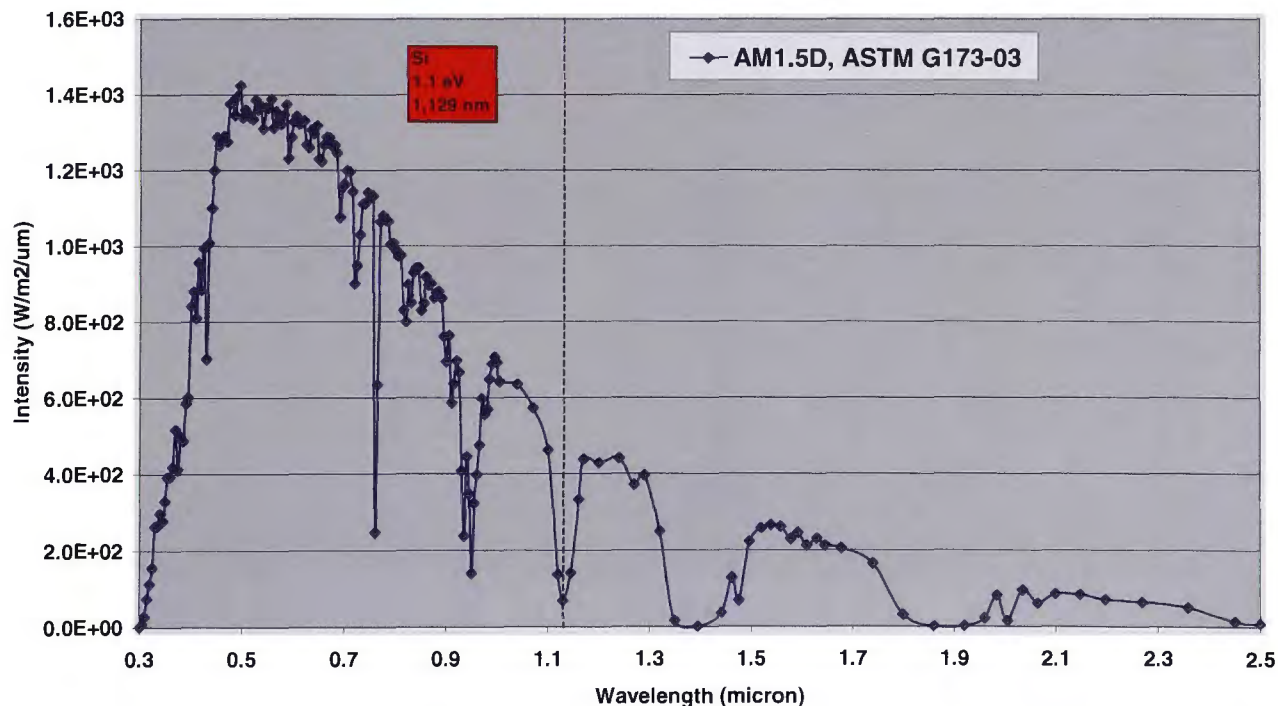


Figure 4-15: A single junction solar cell made of silicon is almost ideal with a bandgap of 1.1 eV and absorbing all the photons up to 1129 nm.

Solar Spectrum Partition for 3-Junction Terrestrial Solar Cell
based on Direct Solar Spectrum AM1.5D

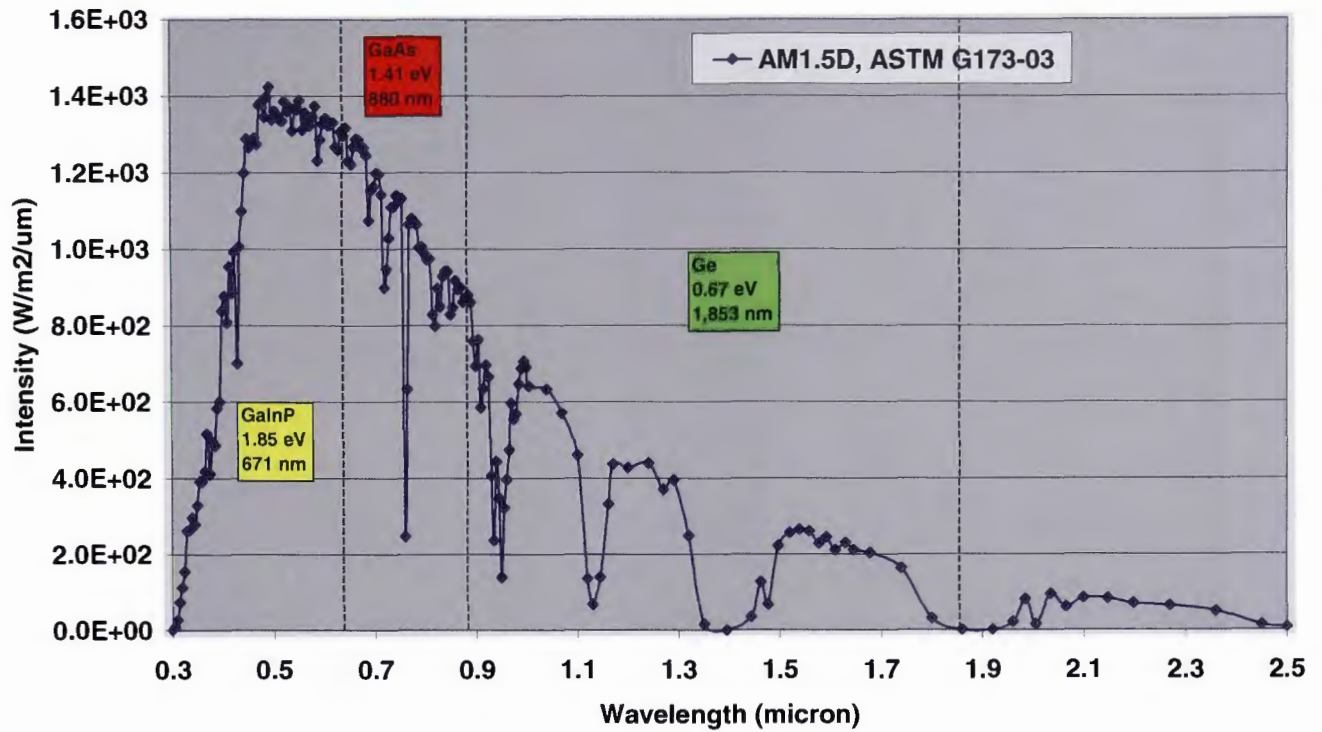


Figure 4-16: Solar spectrum partition for the current GaInP/GaAs/Ge triple junction solar cell.

Solar Spectrum Partition for 4-Junction Terrestrial Solar Cell
based on Direct Solar Spectrum AM1.5D

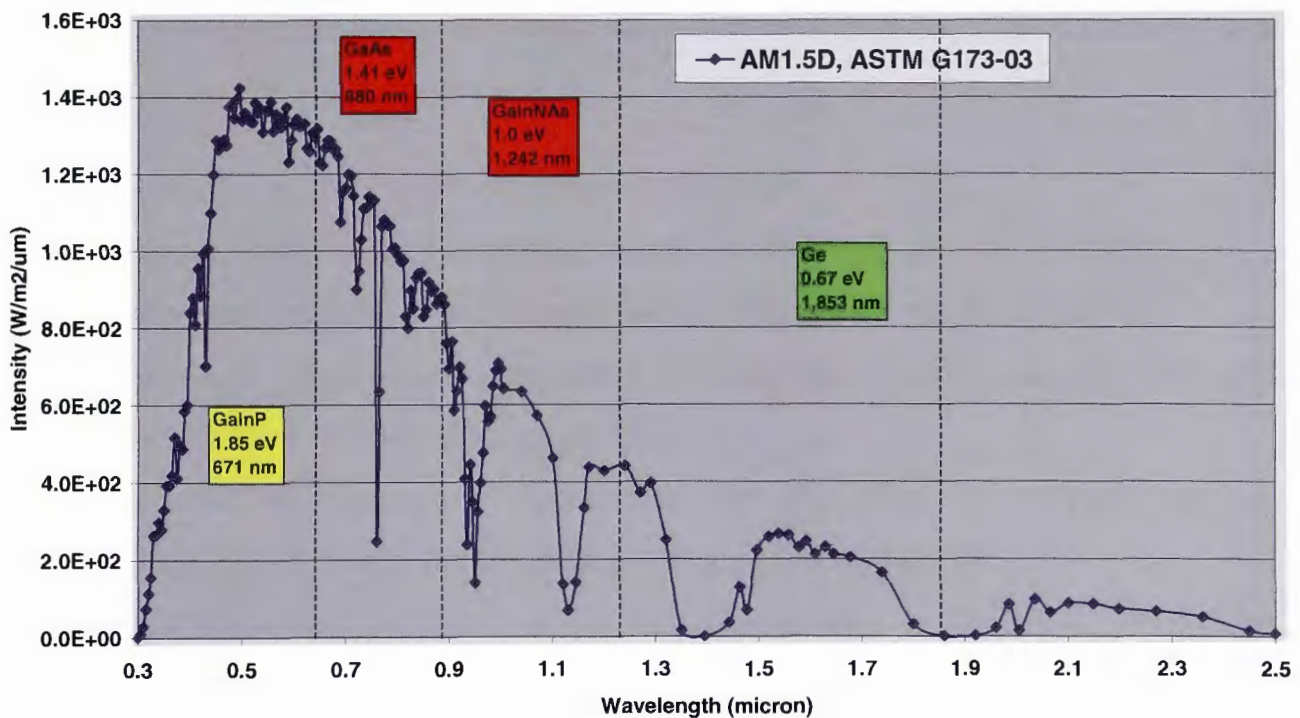


Figure 4-17: Possible partition of the solar spectrum for a GaInP/GaAs/GaInNAs/Ge quadruple-junction solar cell

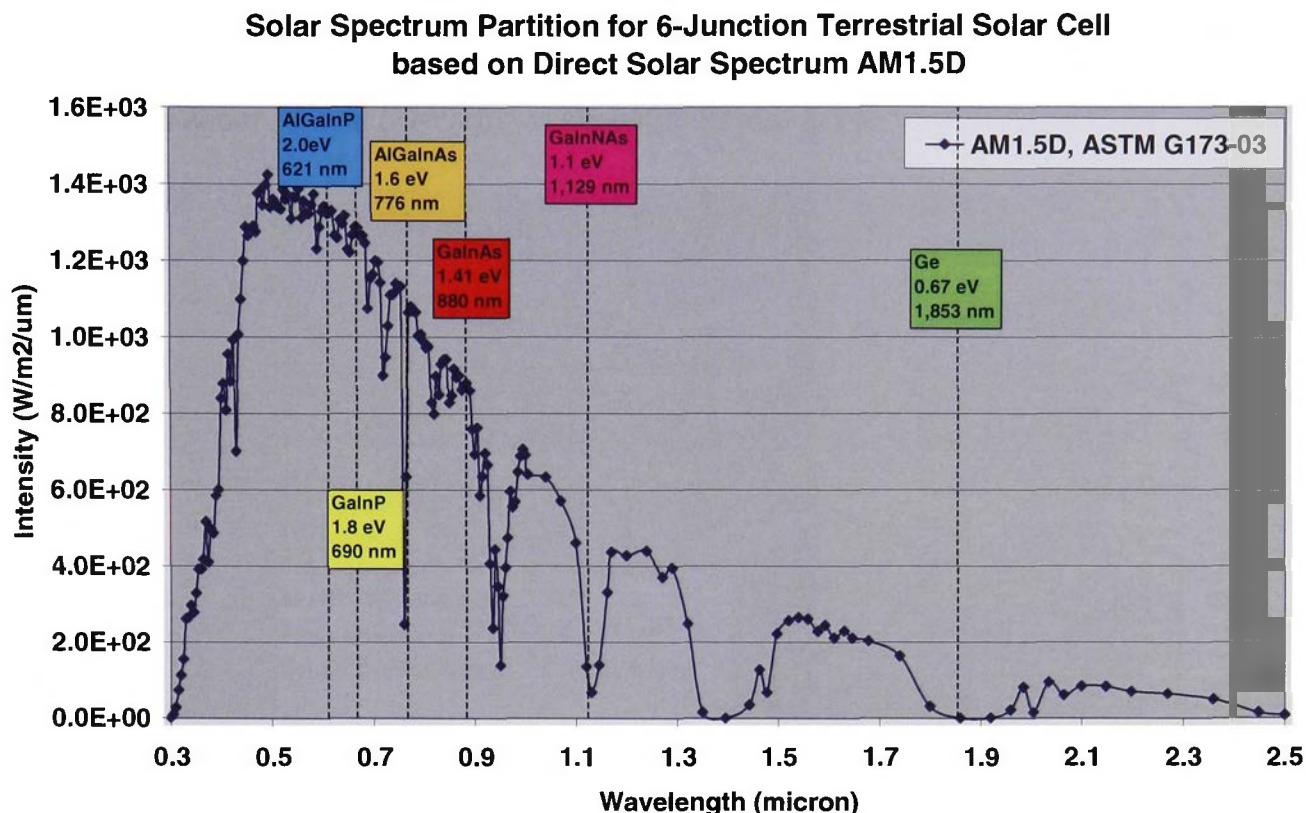


Figure 4-18: Possible partition of the solar spectrum for a AlGaInP/GaInP/AlGaInAs/GaInAs/GaInAs/Ge 5-junction solar cell

Between the efficiency of champion laboratory cells and the real average efficiency of production solar cells for dense array application there is usually a difference of about 10% relative (or about 4% absolute) due to:

- Efficiency distribution in large volume production;
- Larger cells than world record cell (impact on series resistance and shading);
- Dense array cells can have only one busbar (impact on series resistance);
- “Total area” efficiency is considered for dense array cells instead of “dedicated area” efficiency for world record cells; and
- World record efficiency is measured at peak-efficiency incident power density, nominal power density for real cells is about 2 to 3 times greater.

Although the maximum world record efficiency for a triple-junction GaInP/GaAs/Ge solar cell is 41.1% at about 20W/cm², the efficiency of assembled dense array modules in production is about 37% at 50W/cm² as shown in Figure 4-19.

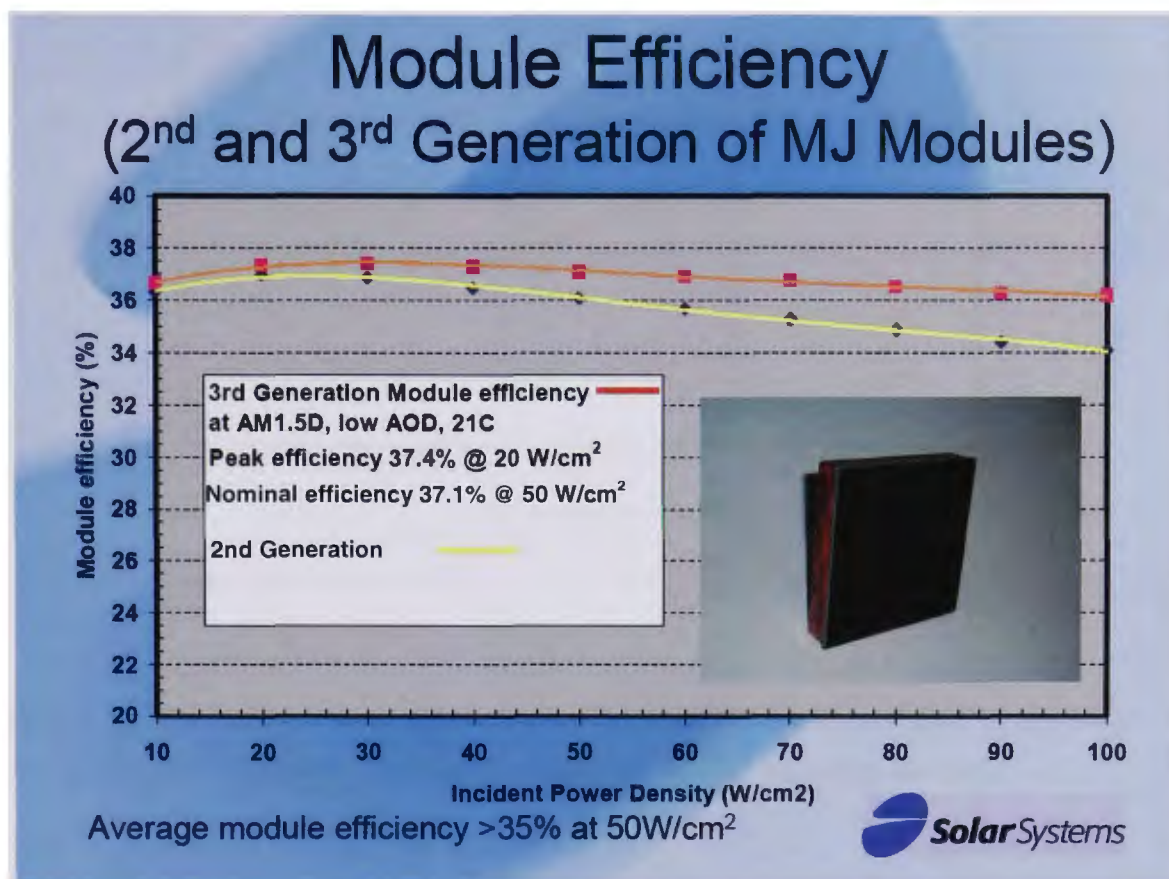


Figure 4-19: Efficiency of 36 cm² dense array modules with triple-junction solar cells versus incident power density for the two latest generations of modules, demonstrating an efficiency of 37% at 50W/cm².

The natural efficiency increases with concentration and is shown more clearly in Figure 4-20 where the efficiency increases with the product of current and voltage. The current increases linearly with intensity and the voltage increases with the log of intensity. The voltage follows the form:

$$V_{oc} = a \ln C + b$$

and the current follows:

$$I_{sc} = \alpha C$$

where C= concentration ratio and a, b and α are constants.

The efficiency ‘falls off’ at about 250 suns as the series resistance becomes a more significant loss than the gain in voltage at high intensity.

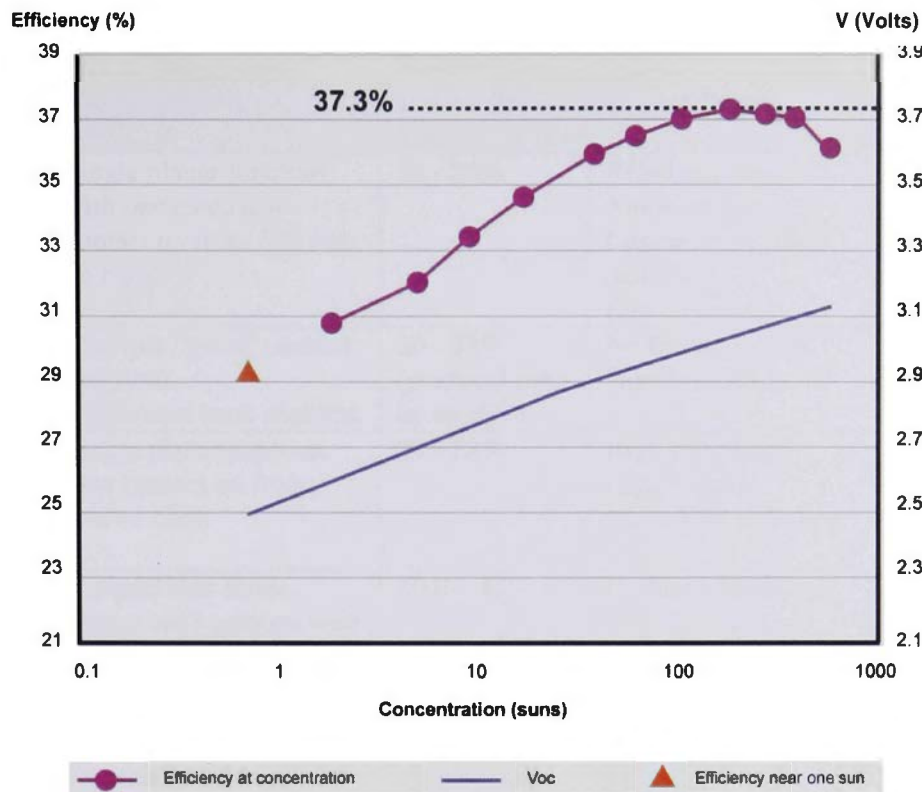


Figure 4-20: Efficiency Versus Concentration. This graph shows the gain in efficiency with concentration (and V_{oc} increases) until series resistance ‘swamps’ the voltage increase.

4.5 Temperature Coefficients

The temperature coefficient of dense array modules containing the GaInP/GaAs/Ge triple-junction solar cells was measured both at the US National Renewable Laboratories (NREL) using a continuous concentrated beam up to 600kW/m^2 and in the laboratory using a flash illumination system. In the first case, keeping the intensity constant, the cooling flow rate of water was progressively reduced and the open-circuit voltage of the module was measured as a function of the cell temperature. In the second case, the modules were first placed in an oven at 60°C , then the performance of the module (current, voltage, power and efficiency) was measured at 50W/cm^2 as the module slowly cools down to room temperature. In a second phase, the module was placed in a fridge at 5°C , then the performance of the module was measured while the module slowly warmed up to room temperature. In both cases, the relative temperature coefficient for efficiency was found to be $-0.17\%/^\circ\text{C}$.

4.6 Cell Types

Cell Type	Configuration	Efficiency @ 100 → 500 Suns	Strong Points	Weak Points
Silicon Front/Back contact	Single planar junction with one electrical contact on front and one on back	18 - 25%	Relatively simple construction Common substrate material Lowest cost	Front contacts complicate close packing for high concentration
Silicon back contact	Multiple "point" contact junctions Solderable back contacts	20 - 28% (practical limit up to 30%)	No front contacts High efficiency	More expensive than front/back contact version
GaAs Front/back contact	Single planar junction One contact on front, one on back	22 - 28%	High efficiency High Voltage $V_{oc} = 1.10$ volts per cell	More expensive than all of the above.
GaInP/GaAs/Ge Triple front/back contact	3 monolithic series- connected junctions with different band gaps 2 contacts - 1 front, 1 back	30.0 – 40%	Highest efficiency High Voltage 3.15 V/cell	Most expensive

Table 4-3: Possible candidates for 'dense array' CPV (pre 2004)

The back contact silicon cells were chosen as the most "accessible" and best first entry candidate. The efficiency is reasonable (almost twice the average commercial flat plate cell), the back contact connection simplifies connection in a close packed configuration. The researcher developed a concept for a 'back contact' multijunction cell which was subsequently developed by Spectrolab and used for all work post 2004. Figure 4-21 shows the high Quantum Efficiency of a typical triple junction CPV cell that was used in these developments.

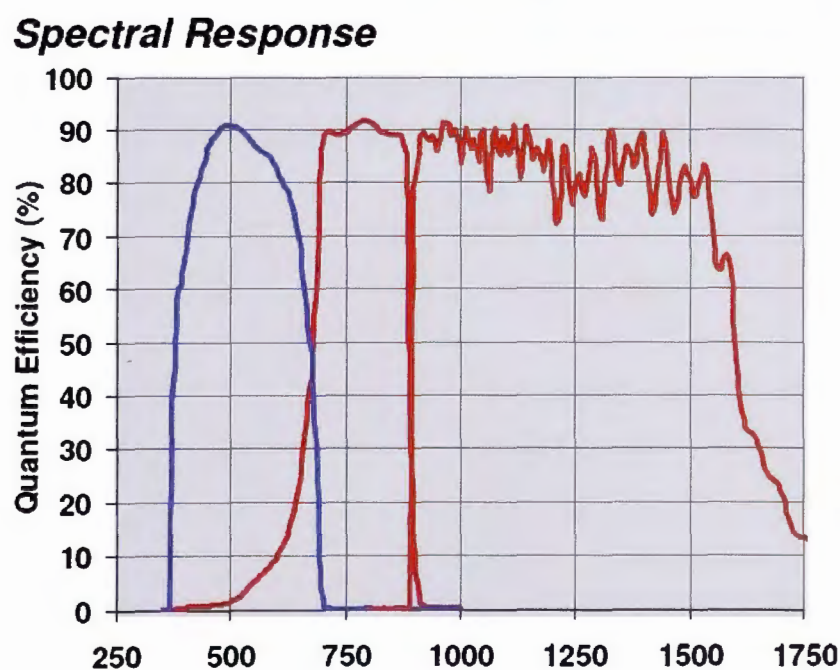


Figure 4-21: Quantum efficiency of a typical triple junction CPV cell used by the researcher

4.7 Future projections for cell efficiency

Figure 4-22 shows the expected concentrator cell efficiency improvements and includes best ‘hero’ cell and also shows the year that the average production efficiency will match that hero performance.

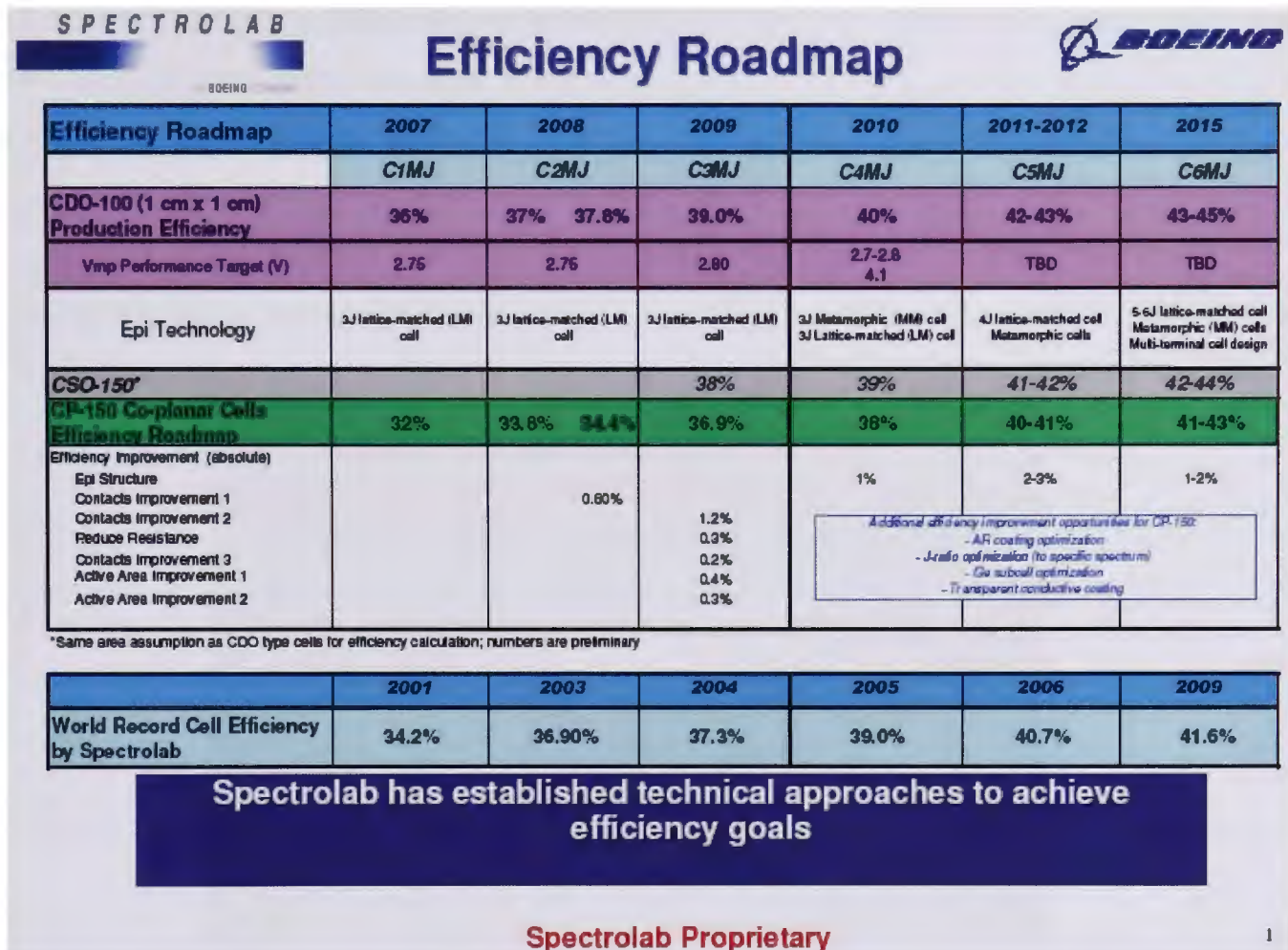


Figure 4-22: Cell efficiency projections by Spectrolab (2009)

CHAPTER 5. 130m² DISH CPV SYSTEM

The 130m² dish design was developed with the following commercial targets:

Highest power output in standard conditions

Highest average output with in all conditions

Designed for manufacture and deployment

Low operation and maintenance

In order to get a feel for the look and relative scale of the components a 1/50th scale model was built by the researcher (see Figure 5-1).



Figure 5-1: 1/50 Scale model of the production 130m² CPV dish

The scale of the full size dish was chosen based on the following requirements:

For utility scale, the requirement was at least tens of kW per unit.

It was big enough to minimise the number of connection points for power and cooling and to generate a reasonable voltage (250V DC).

The mass should be small enough to be lifted by a widely available 45 ton crane.

The aesthetics of the dish were also considered since appearance is an important aspect of being environmentally acceptable. The main features and architecture of the dish are shown in Figure 5-2, 5-3 and 5-4.

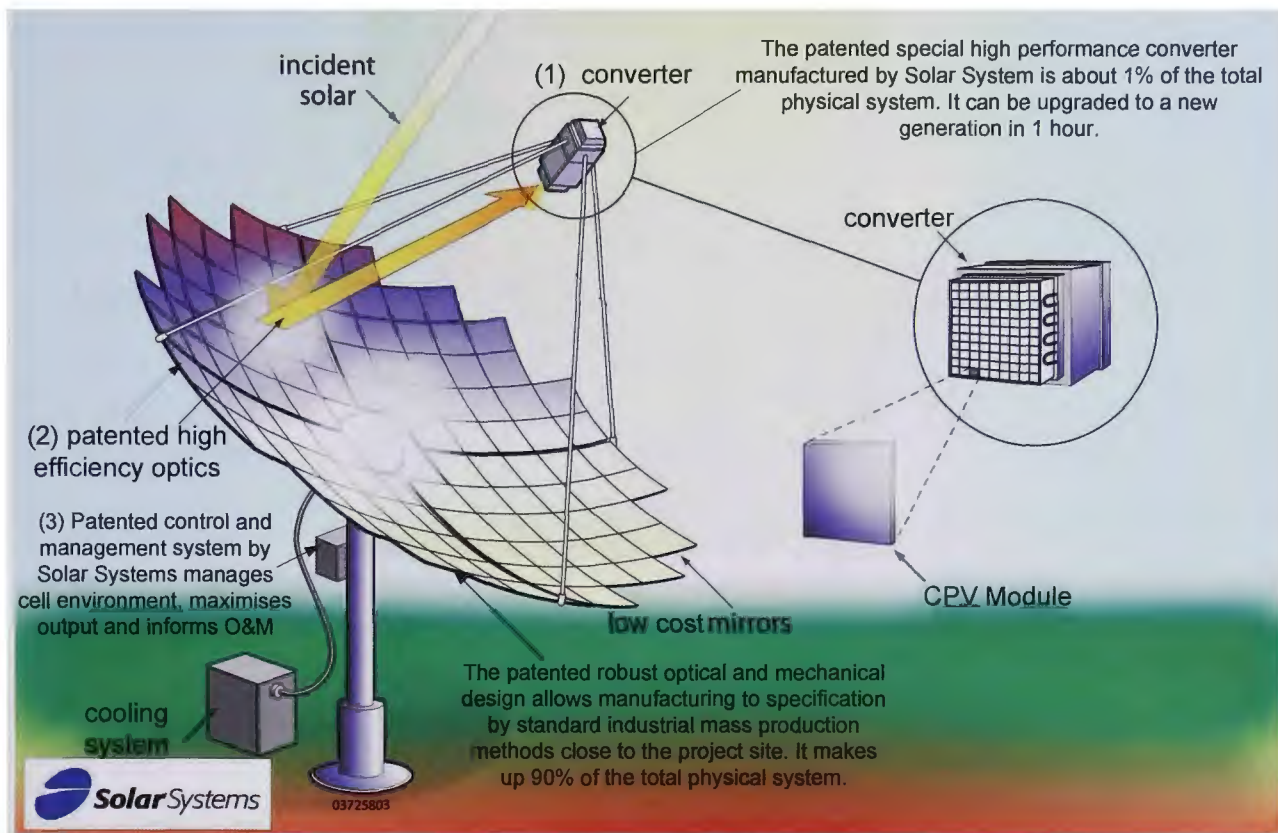


Figure 5-2: Schematic of 130m² CPV dish designed, constructed and tested by the researcher

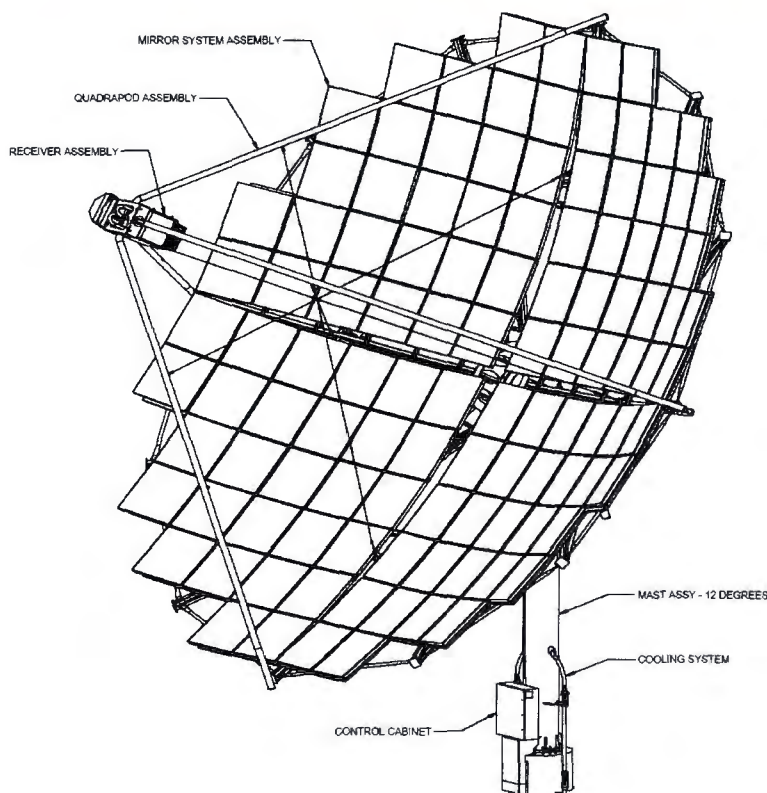


Figure 5-3: Main Components of the CS500, 130m² CPV dish

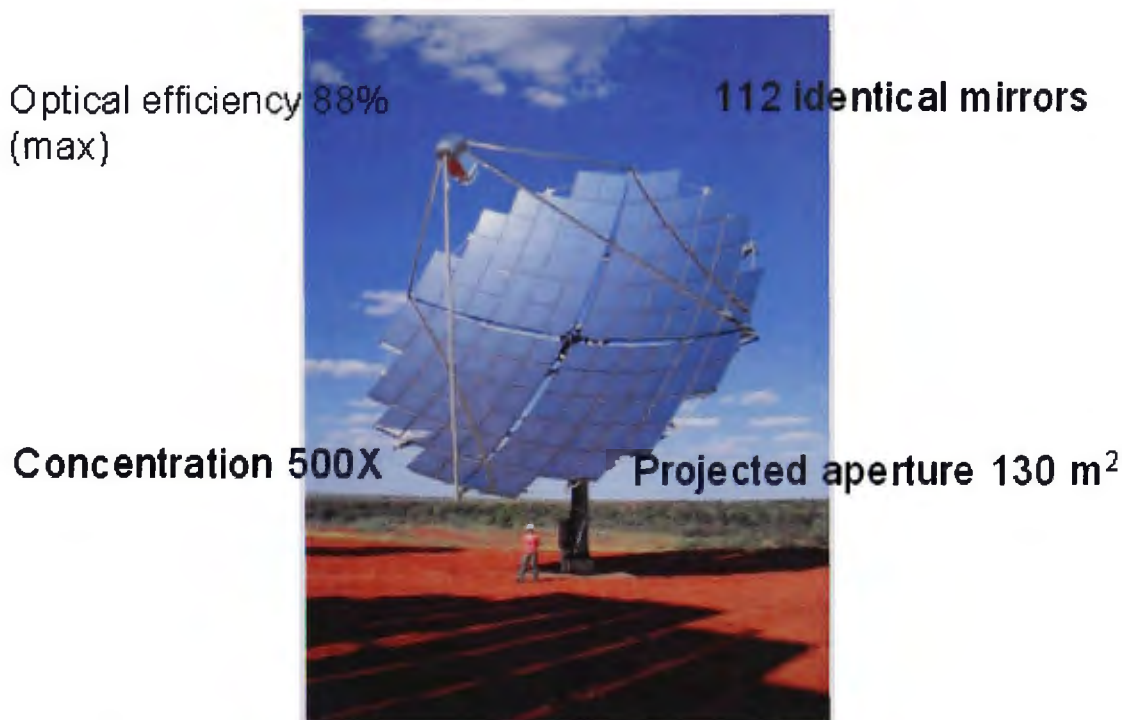


Figure 5-4: Photograph of the researcher with a CS500 dish concentrator PV system

5.1 Primary Optics

The primary optics consists of 112 spherically shaped mirror panels fitted to a paraboloid surface with a focal length of approximately 8 metres. The mirror panels have an individual focal length which is different to the overall paraboloid. The optimisation of the relative focal lengths is part of the art which was developed in this work

5.2 Mirror Panels

The mirror design, size and radius of curvature were chosen for maximum performance and minimum cost. From a performance perspective the following characteristics were targeted:

Highest possible reflectivity with a spectrum that matches the need of multijunction cells, requiring thin (1mm) white (low iron) glass with high quality 1000mg/m² silver coating (See Figure 5-5);

An optimum focal length to give relative beam size at the receiver which has:

- a high intercept resulting in an optical efficiency of approximately 85% (favouring a short focal length)
- an even flux distribution over the receiver face favouring a long focal length
- a high number of mirror facets to achieve statistically significant averaging at the receiver to give an even flux distribution

From a cost perspective, the following characteristics are desirable:

Mirrors on thin glass superstrates (1mm) have low weight and high reflectivity;

Sufficient number of facets so that the quality of each facet does not have to be high – 2mr (milliradians) slope error is acceptable; and

All mirror facets should be the same so that:

- Inventory is minimised
- Assembly errors are eliminated (any mirror can fit anywhere)
- Operation and maintenance is simple
- Gear up for manufacturing is straightforward.

As well as achieving all of the above requirements the mirror panel must be light weight and rigid to prevent slope change. The researcher invented a laminated sandwich of glass, high density polystyrene foam and steel to meet these requirements. It is described in detail in a patent by the researcher (Lasich, 2001, US7550054B2 and Figure 5-6)

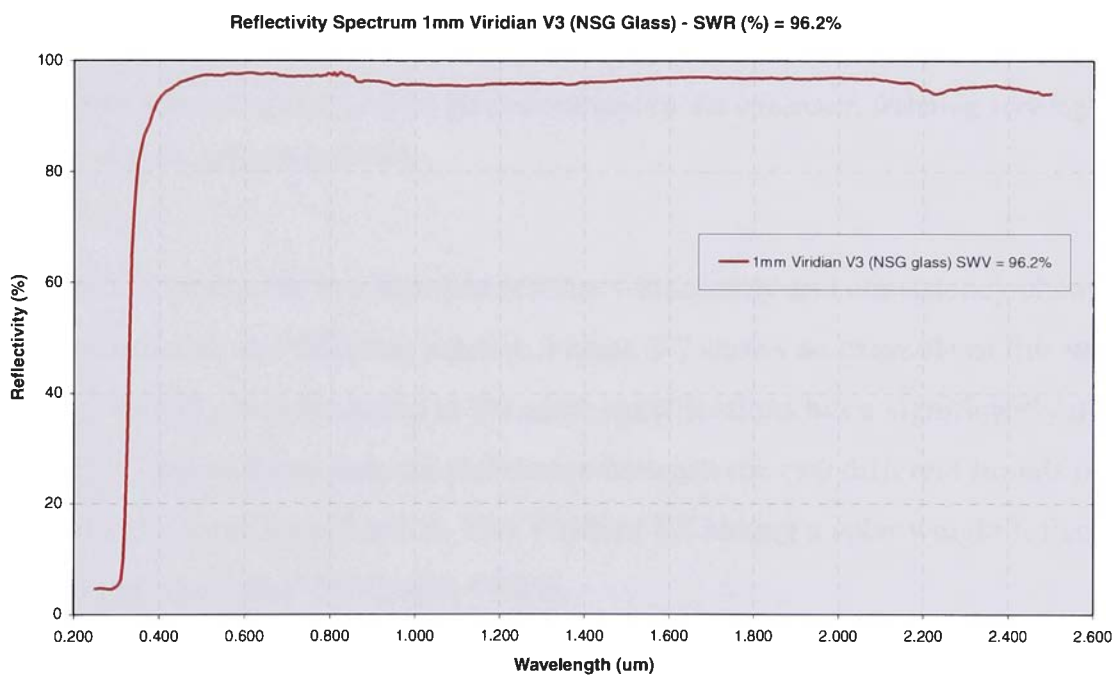


Figure 5-5: Reflectivity spectrum for mirror glass used for the reflective concentrator mirror panel. Note the exceptionally high reflectivity between 350nm and 850 nm which is favourable for a multi-junction concentrator cell which is 'top cell limited'. Refer to Figure 4-4 which shows the external quantum efficiency which must be matched by the mirror.

The mirror panel shown in Figure 5-6 illustrates a very rigid laminated structure consisting of high reflectivity, thin 'back mirrored' glass, ultra high density, expanded, polystyrene foam and a galvanised steel backing.

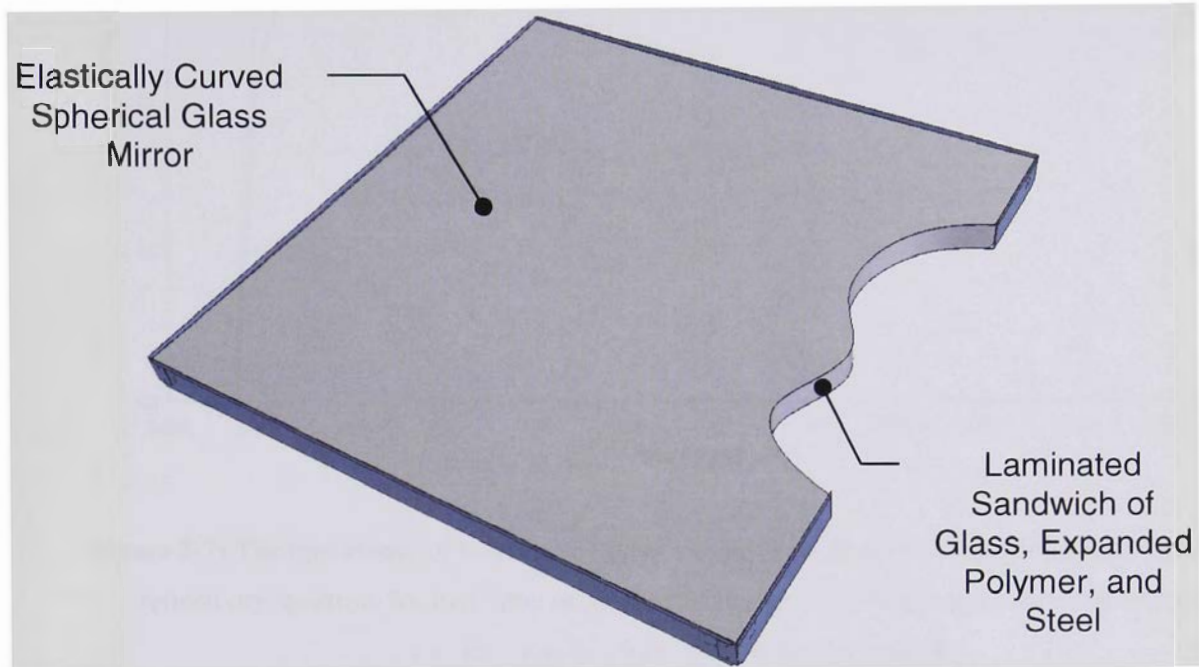


Figure 5-6: Schematics of the mirror panel developed by the researcher, featuring very high rigidity laminate of glass, polymer and steel.

The selection of components is a significant issue with quality and consistency changing from different supplier and different batches. Figure 5-7 shows an example of this where mirror glass nominally manufactured to the same specifications has a significantly different reflectivity. It is interesting to note the difference between the two different brands of glass with essentially the same specification. The Viridian V3 having a solar weight reflectivity of 96.2% and the 'Guardian' NGC with 94.8%.

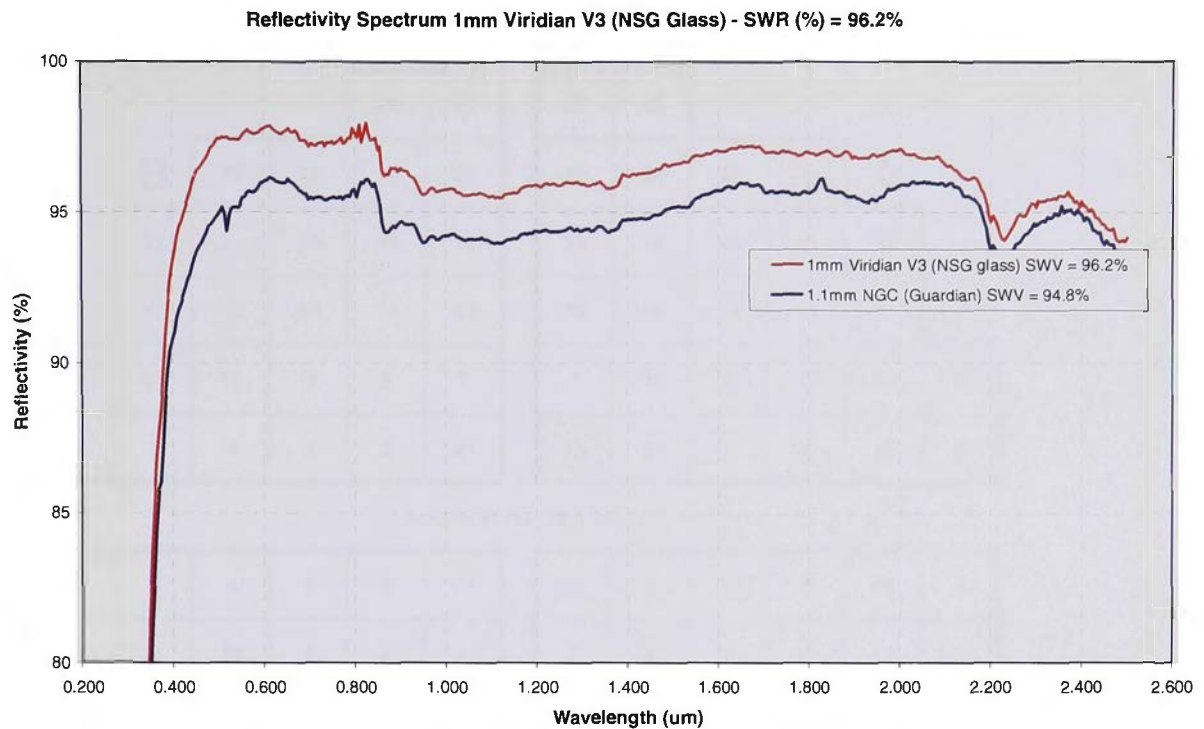


Figure 5-7: The importance of selection of glass composition. There is a significant difference in the reflectivity spectrum for two different mirrors of the same thickness and nominally the same specification, but from two different suppliers.

Quality Assurance

In order to know the optical shape of the mirror for performance prediction using ray trace modeling, QA/QC and performance prediction, the researcher developed a ‘laser mapper’ (Lasich, 2001, AUS 2002244529B2)

This machine scans 900 points on each mirror and produces an array of surface normals in a ‘pan file’ which can be statistically analysed for quality (slope error resulting in beam spread and symmetry assessment). This pan file is used in the ray trace model in Section 5.8. The position of each mirror as positioned on the real dish and in the ray tracer is shown in Figure 5-8.

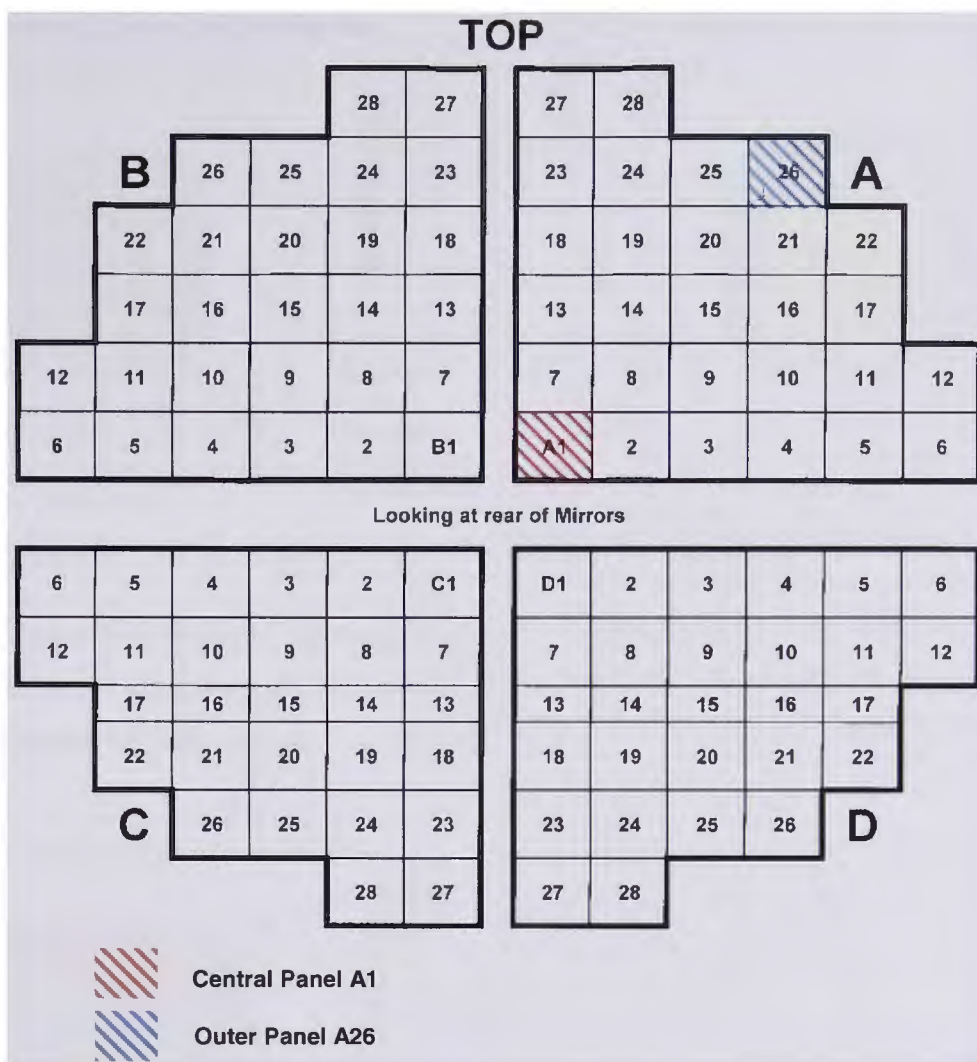


Figure 5-8: Map of mirror panel array on 130m^2 dish concentrator. Ray traces for individual mirrors A1 and A26 are used to illustrate the difference in image size and shape and also the difference between ‘model’ mirror panels with random Gaussian error of 2mr and ‘real mapped’ mirrors with a similar error.

Figures 5-9a to 5-9c show a series of simulated dish images for a dish consisting of 112 mirrors (at focal plane) which illustrates the changes in image with the progressive addition of errors for slope error and pointing error. It can be seen that as some ‘reality’ is introduced the image becomes much more spread and ‘peaky’.

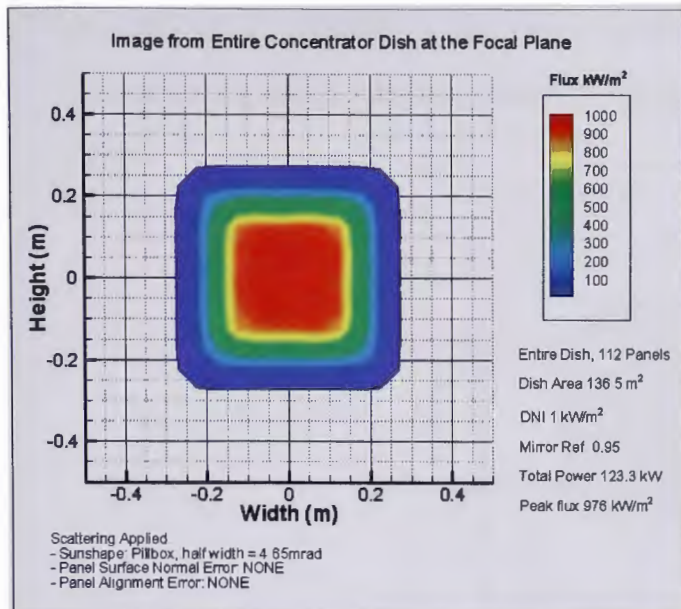


Figure 5-9a: Sun shape only, no errors. The image is at the focal plane and is the result of the parabolic reflector with 112 ‘simulated’ mirror panels.

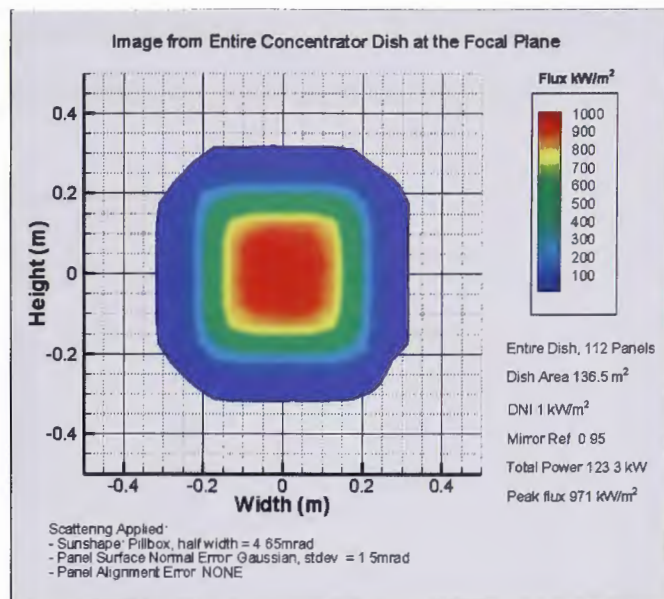


Figure 5-9b: Sun shape with slope error. The image is at the focal plane and is the result of the parabolic reflector with 112 ‘simulated’ mirror panels.

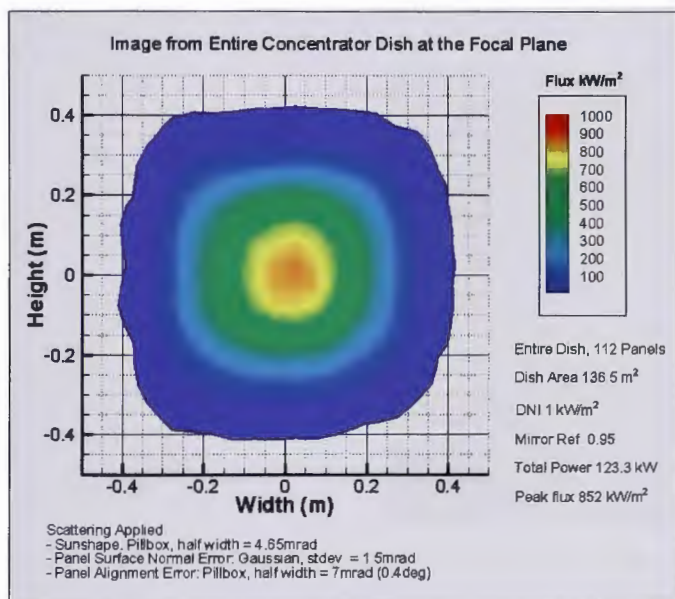


Figure 5-9c: 112 mirrors with sun shape slope error and pointing error. The image is at the focal plane and is the result of the parabolic reflector with 112 ‘simulated’ mirror panels.

Figures 5-10, 5-11a and 5-11b show images for single central (position A1) mirrors. Figure 5-10 is a ‘simulated’ image which uses a pill box sun shape and a Gaussian slope error showing a relatively flat (green) distribution. Figure 5-11a shows a ‘3D’ image of Figure 5-11b. Figure 5-11b is derived from a scan of a ‘real’ production mirror panel and shows a generally similar but much ‘rougher’ image representing the real world effects of

manufacturing tolerances. An important part of the art is to model the optical situation with 'bottom line' characteristics which is measured rather than assumed error distributions.

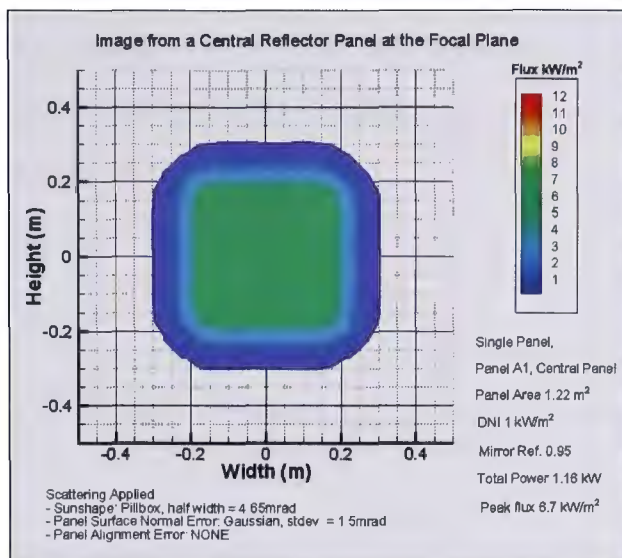


Figure 5-10: Simulated single panel with pill box sun shape and slope error indicating a relatively flat flux distribution.

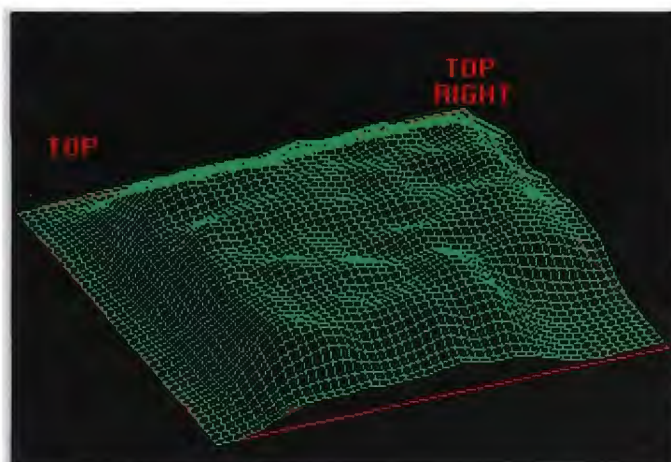


Figure 5-11a: Inner mirror intersects image. Position 1A Note fact of receiver shading in right hand corner.

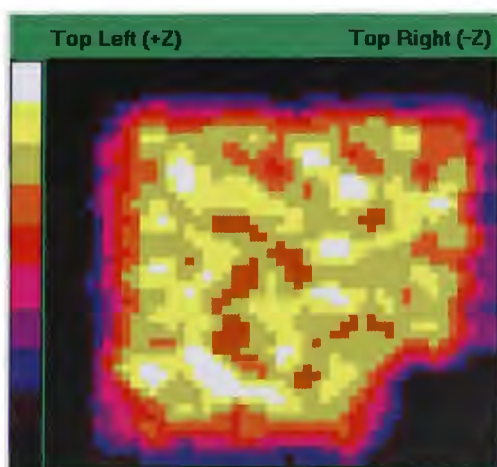


Figure 5-11b: Single inner (1A) panel with sun shape and actual errors as mapped (1A) from a completed mirror. The shading of the receiver can be seen on the bottom right hand corner.

5.3 Dish Frame

The dish frame was designed using state of the art CAD and FEA systems and methods to Standard Building Codes and correlated by wind tunnel tests at Monash University.

Analysis of this area is beyond the scope of this thesis however it can be seen from Figure 5-24 that the structure is sufficiently stiff for 10.0m/s winds to have a negligibly deleterious effect on output. The ripple is approximately 1%.

5.4 Receiver

The receiver (see Figure 5-12) is positioned at the focus of the parabolic collector to receive concentrated typically up to 120kW of light at 500 suns and convert approximately 32% to DC power.

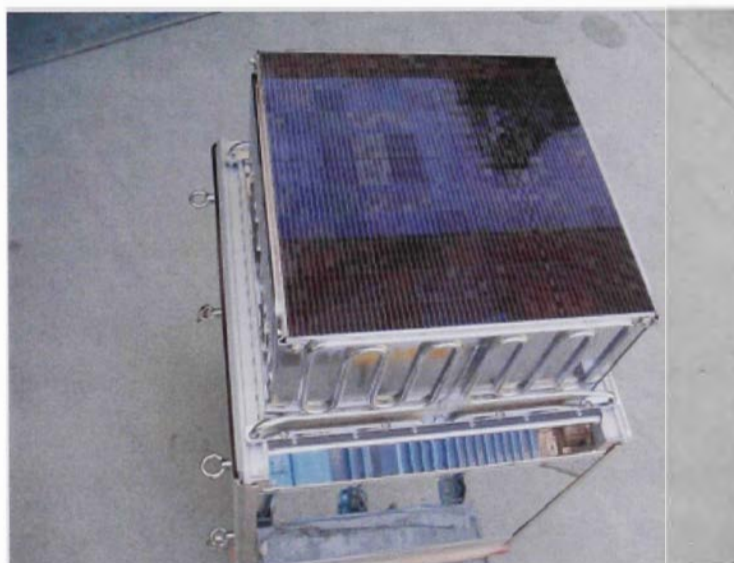


Figure 5-12: Multijunction 35-kWp receiver containing 64 modules

The receiver contains:

secondary optics which are cooled reflective mirrors known as ‘flux modifiers’

64 PV modules each with 24 PV cells and integrated heat sink.

manifolding to provide coolant power and monitoring connections to the 64 modules and flux modifiers.

weatherproof housing to protect components

is robust enough to stand high solar flux

The researcher invented a CPV dense array receiver which incorporates all of these features (Lasich, 2001, US7076965B2)

5.4.1 Secondary Optics

The secondary optics consist of a 4 sided 'kaleidoscope' of cooled high reflectivity (96%) mirrors. The design of the angles, length and position in relation to the focal point of the primary concentrator are key to delivery their function which is to: -

Assist in achieving a high overall bulk optical efficiency of 85%;

Mix the concentrated light to assist in providing a uniform 'flux distribution' of light on the cell face; and

Provide a shroud for weather protection for the PV cells.

The design of the flux modifiers is developed using previous experience, intuition and iterative ray tracing in conjunction with the modelling of the primary optics described in Section 5.8.

5.4.2 Cell Array and Modules

The dense array CPV module must be designed to deal with a number of demanding requirements simultaneously when exposed to 500 suns. It must be capable of:

- Removing unused energy from the solar cells at a rate sufficient to keep the cells cool for a maximum performance and a target of 20 years lifetime. It should be noted that the operational intensities encountered in this application can melt copper as shown in Figure 5-13 which shows a 6 mm thick copper plate which melted in 12 seconds when placed near the focus of the 130m² dish.
- Operating at high voltage. In order to transmit power efficiently a receiver output voltage of 250V+ is required when dealing with 30kW+. The International Electrochemical Committee standard IEC 62108 requires the modules must maintain electrical isolation with a leakage current of smaller than 10mA at two times the operational voltage plus 1000 volts. This equates to 1500 volts.
- Being hermetically sealed to stop the effects of weather.
- Withstanding intense radiation of 500 suns for 20 years without significant degradation of the optical and cell elements.

- Withstanding 40,000 temperature cycles over 20 year lifetimes (This was estimated from one year of solar data that showed approximately 1500 events of solar flux changing from $<250 \text{ W/m}^2$ up to $>800 \text{ W/m}^2$. This was rounded up to 2000 ‘cycles’ per year to allow some margin.)
- Withstand hydraulic pressure of the coolant. The researcher has invented, designed, built and tested a CPV dense array module (Lasich, 2001, US 7076965B2 and 2003, US 1661187).



Figure 5-13: Hole melted in a 6mm thick cooled copper target plate after 12 seconds of exposure to the beam of the 130m^2 dish. The tracks can be seen where the beam traversed ‘on’ and ‘off’ the plate.

The cell array of 1536 cells is made up of 64 modules arranged in a 8x8 array each with 24 cells (see Figure 5-14).

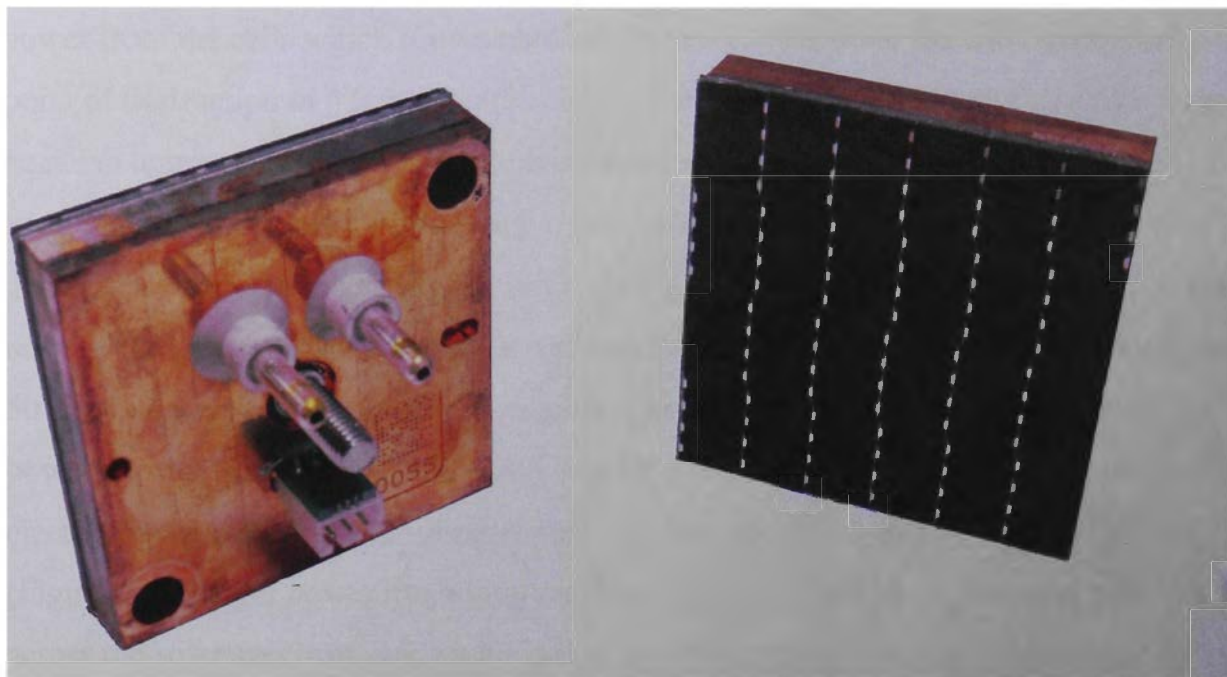


Figure 5-14: CPV Concentration Module with an array of 24 cells and power output of 660 W at 500X concentration under flash test at 21°C

The modules are closely packed into a frame which supplies cooling water, power connections and data acquisition for temperature, voltage and current. The packing factor is 97%, that is 97% of the receiver face is covered by PV cells (This 3% dead space is accounted for in the ray tracer). The average performance of the modules in Receiver No. 61 is 35.7% and the average power was 643W at 500 suns and 21°C in practice at operating conditions of 400 to 500 suns and a cell temperature of 45°C with a less than perfect flux distribution. The receiver has an efficiency of approximately 32% and this means that about 60% of the 100kW+ light power impinging on the cells must be removed (approximately 12% is reflected from the cell face). See Appendix 3. It should be noted that another mode of power loss from the PV cells is 'radiative recombination'. This effect has not included since it is relatively small and difficult to measure.

5.4.3 Heat Sinks and Thermal Considerations

A key to successful operation of CPV systems is the ability to extract the unused thermal power from the cells which if uncooled would normally elevate the cell temperatures to the point of destruction in a few seconds. Not only must the survival be considered but the negative temperature coefficient of power (established in Chapter 4.5, the relative temperature coefficient for efficiency was found to be $-0.17\%/^{\circ}\text{C}$) means that for every ten degrees rise in cell temperature the output power drops by 1.7% relative. The objective is to remove the excess thermal energy at a rate sufficient to keep the cells cool, typically below 50°C while keeping the associated parasitic power to a minimum. The removal of heat at a power density of $50\text{W}/\text{cm}^2$ (500 suns) is quite a challenge when the solar cell must also be electrically isolated from the cooling sink. For the case illustrated by the ‘screen shot’ (Figure 5-29), light power impinging on the cell face is 102 kW the cell face reflectivity across the solar spectrum is 12% including the effect of the cover glass measured by the researcher at NREL. The cooling water flow rate through 64 modules totaled 149 L/min. The modules described in Figure 5-14 are mounted into a ‘receiver’ frame shown in Figures 5-15 and 5-16. This receiver provides manifolding for the coolant supplied to each module.

For the case illustrated in the ‘screen shot’ (Figure 5-29), the thermal (P_{th}) power sunk by the module heat sinks totals 57.2 kW calculated from the coolant flow rate and the temperature rise across the receiver.

$$P_{\text{th}} = \frac{149 \text{ l/m}}{60} \times 5.4 \times 4.281 = 57\text{kW}$$

Thus the power density (W/cm^2) required to be sunk by the heat sinks during nominal operation with DNI (DSR) of $948\text{W}/\text{m}^2$ is

$$W_d = \frac{57000}{64 \text{ modules} \times 36.0\text{cm}^2} = 25 \text{ W}/\text{cm}^2$$

Under worst case conditions when the DNI is at its maximum, for example at $1050\text{W}/\text{m}^2$ and no electrical power is being exported and the dish is clean, the power density to be

extracted is approximately double this at $50\text{W}/\text{cm}^2$. While the design is optimised for the typical condition requiring approximately 25 to $30\text{W}/\text{cm}^2$ to be transferred the design must be able to cope with the worst case conditions.

When considering the desired cell operation temperature, it is necessary to know the power density that will be required to be ‘sunk’ (in W/cm^2) and the ability of the sink to transfer the heat for a given temperature difference between the coolant and the cell, also known as the thermal conductance ‘U’ with units of $\text{W}/\text{cm}^2\text{ }^\circ\text{C}$. This condition is described by the following equation

$$T_{\text{cell}} = T_{\text{in}} + \frac{W_d}{U}$$

Where:

T_{cell} = Average cell temperature ($^\circ\text{C}$)

T_{in} = Inlet coolant temperature ($^\circ\text{C}$) - measured

W_d = thermal power density (W/cm^2) to be transferred

U = Thermal conductance ($\text{W}/\text{cm}^2\text{ }^\circ\text{C}$) determined for typical module in laboratory calibration over a range of coolant flow rates.

It is interesting to note that the ΔT between the coolant inlet ‘water in’ and the ‘average cell temperature’ is just 14°C for an incident radiation intensity of 424 suns (or $42.4\text{ W}/\text{cm}^2$, see cell: $42.4\text{ W}/\text{cm}^2$ in Figure 5-29). In order to understand the system energy balance and thus determine the ‘optical efficiency’, it is useful to know how much power reaches the receiver, denoted as P_{efm} expressed as a percentage of the light which impinges on the primary concentrator.

The optical efficiency

$$R_{\text{Opt}} = \frac{P_{\text{efm}}}{\text{DNI} \times 130\text{m}^2}$$

And

$$P_{\text{efm}} = \frac{P_e + P_{th}}{1 - r}$$

$$\begin{aligned}
 &= \frac{32.8 + 57.2}{1 - \frac{12}{100}} \\
 &= 102 \text{ kW}
 \end{aligned}$$

Where:

P_e = electrical power (kW)

P_{th} = thermal power (kW)

P_{efm} = power entering flux modifier

(approximate power impinging on cell face)

r = reflectivity of cell face = 12%.

DNI = Direct Normal Irradiance = 0.948 kW/m^2

And thus the optical efficiency is

$$R_{Opt} = \frac{102 \times 100}{0.948 \times 130} = 82.7 \%$$

The optical efficiency represents the ability of the mirrored collector to deliver the concentrated sunlight to the receiver. (Note, more recent 'in-house' reflectivity measurements of PV modules indicate the reflectivity is closer to 14% when considering the approach angle of the concentrated light. In this case the R_{Opt} would be about 84.7%)

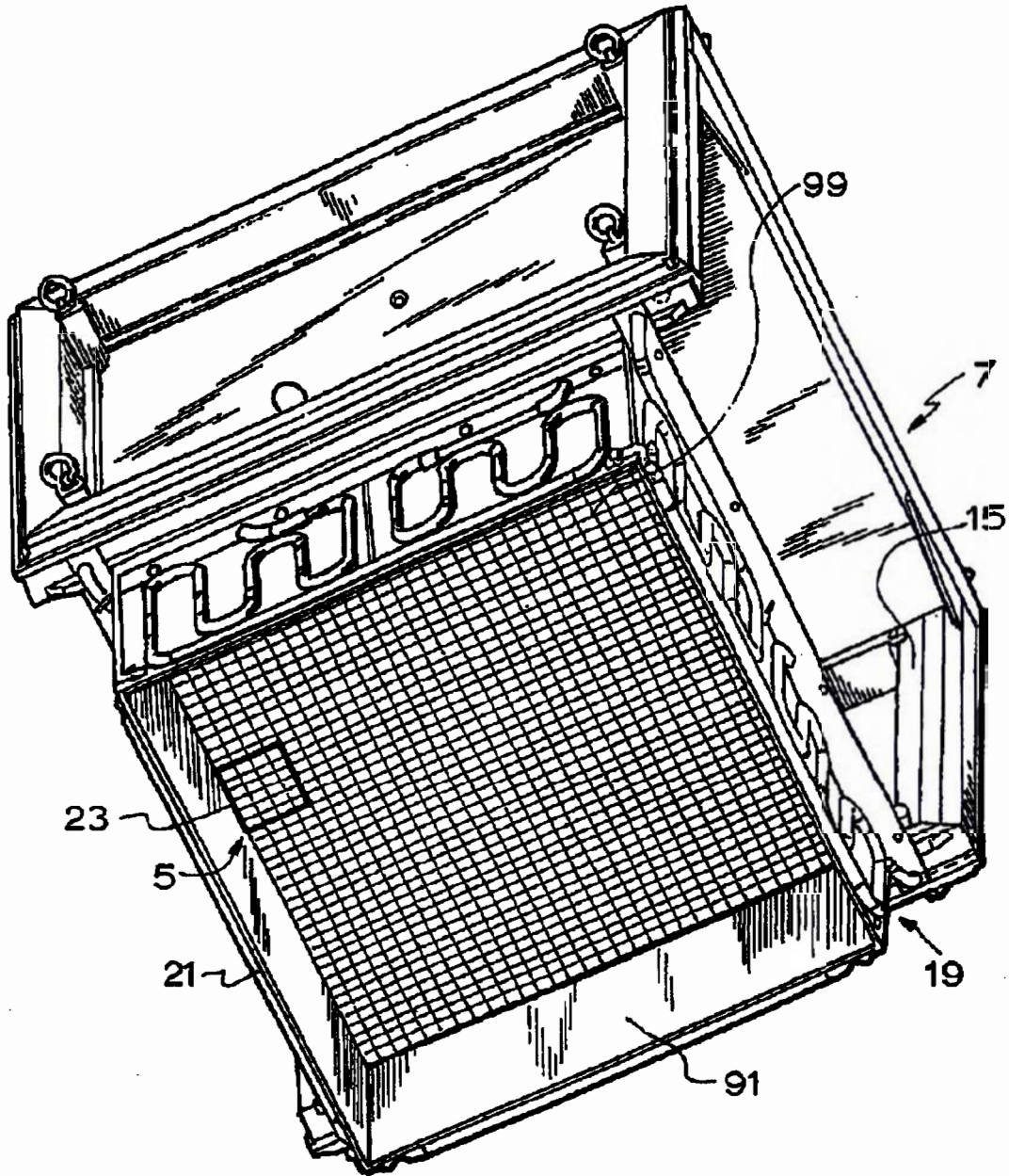


Figure 5-15: Schematic of CPV Receiver showing one (No.23) of 64 modules forming an array of 1536 cells.

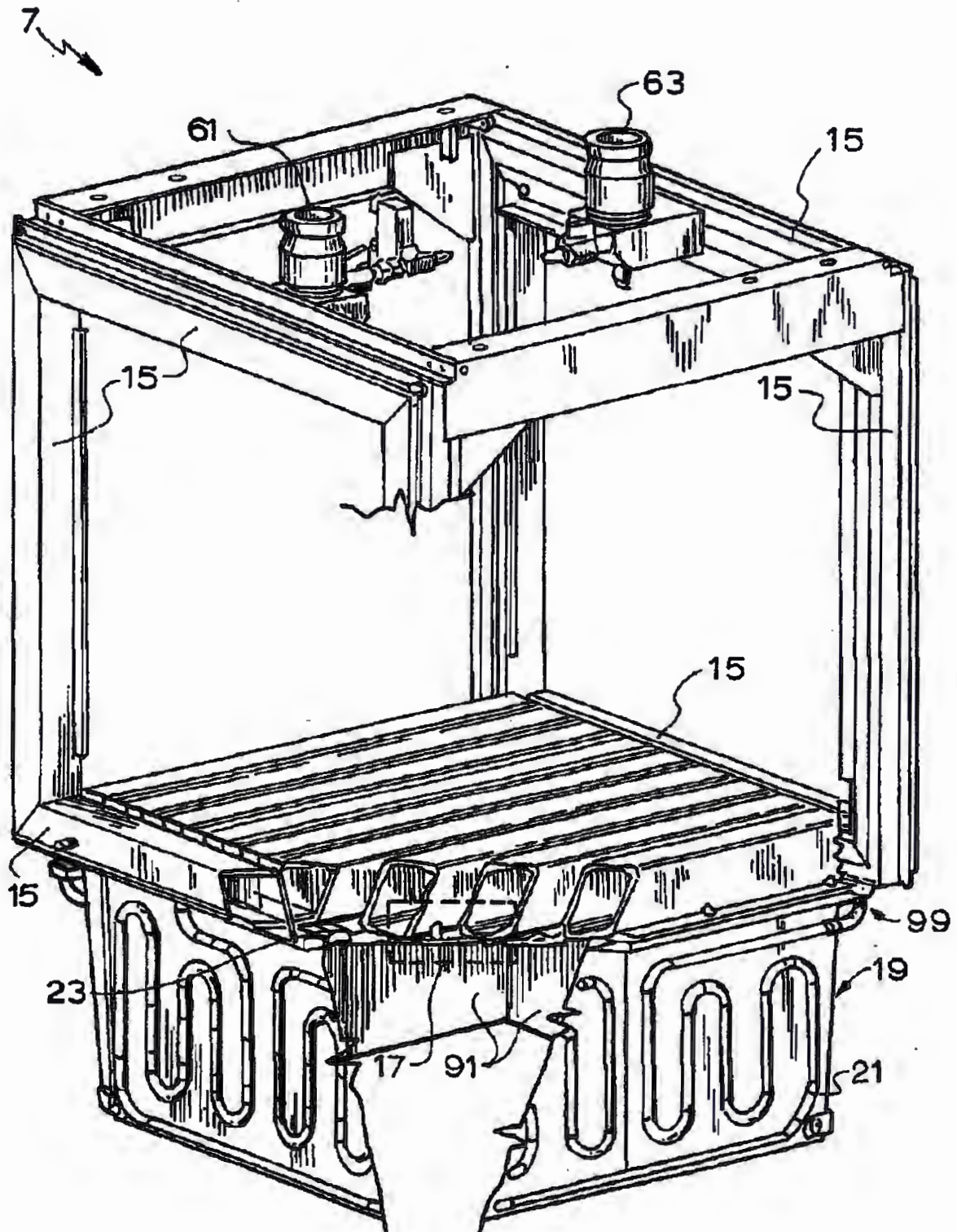


Figure 5-16: Assembly drawing of a typical CPV module developed by the applicant as described in Lasich 2001 US 7076965B2

5.5 Monitoring

A unique facet of this approach to CPV which has all the CPV cells in one small place means that a high level of monitoring can be achieved at a low cost. Figure 5-17, 5-18 and 5-19, show 'screenshots' of the 'flight desk' style control and monitoring human machine interface (HMI) screens designed by the researcher and co-workers. Figure 5-17 shows detail of a single dish with explanatory notes. Figure 5-18 shows detail of a grouped cooling system when 10 dishes are cooled by a central cooling system. Figure 5-19 shows the AC power distribution including inverters, bussing and protection to the point of export to the grid.

Cleaned 31 July 2008

DC Dish power output measured at base of dish under actual operating conditions

Direct normal solar irradiance measured with Class I Pyrheliometer

DC Dish power output corrected to standard operating conditions 'SOC'
 $T_{cell} = 21^{\circ}\text{C}$, $\text{DSR} = 1000 \text{ W/m}^2$ Direct

Dish overall instantaneous DC efficiency sun -> DC Power (excluding pumping and tracking). With these auxiliaries included the DC efficiency is approx 25%)

Receiver efficiency, concentrated light in vs DC electrical output (reading slightly high, should be approximately 32.5%)

Dish optical efficiency; light which enters receiver vs light which is intercepted by dish. (reading slightly low, should be approximately 85%)

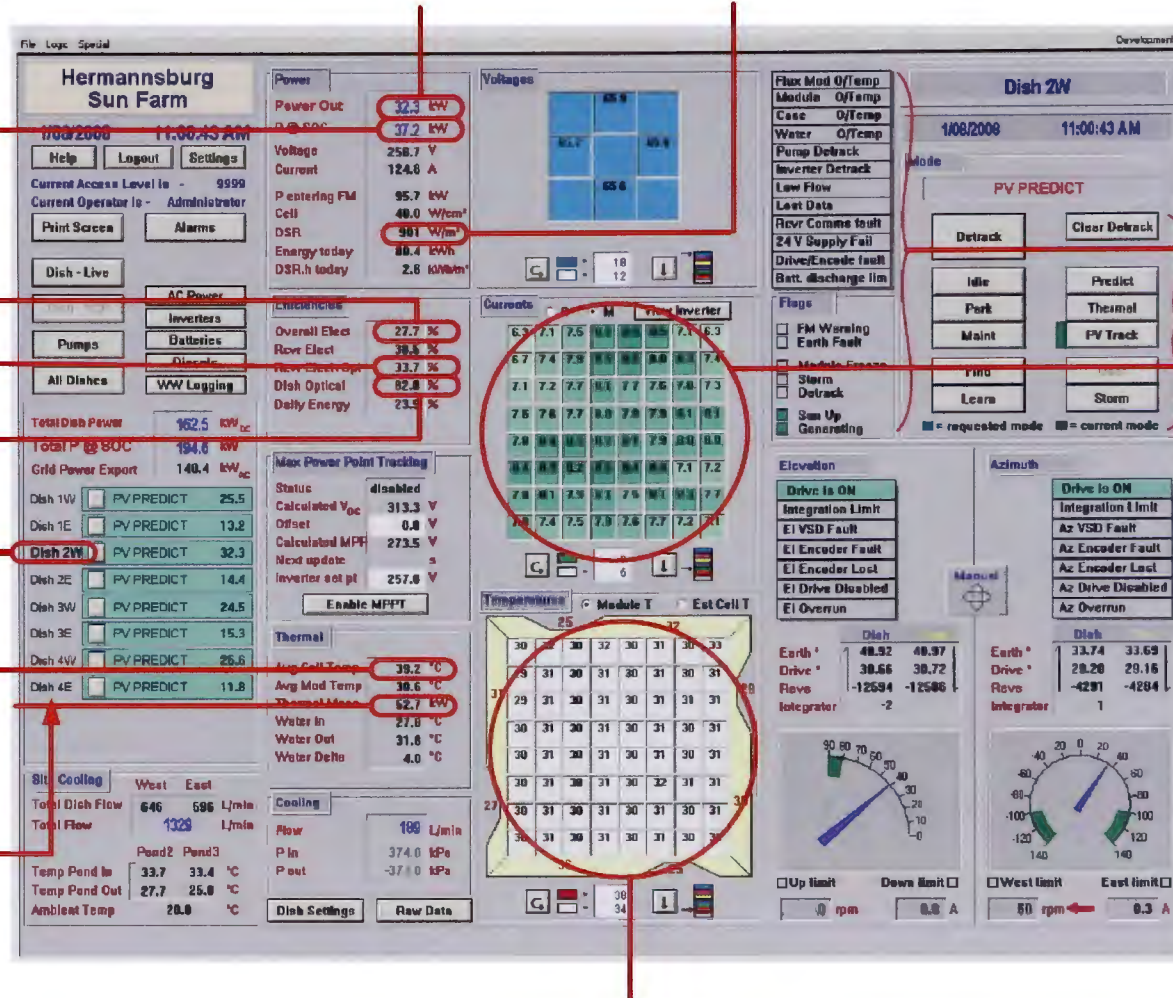
This dish

Average cell temperature at this moment

Thermal energy captured for rejection on cogeneration

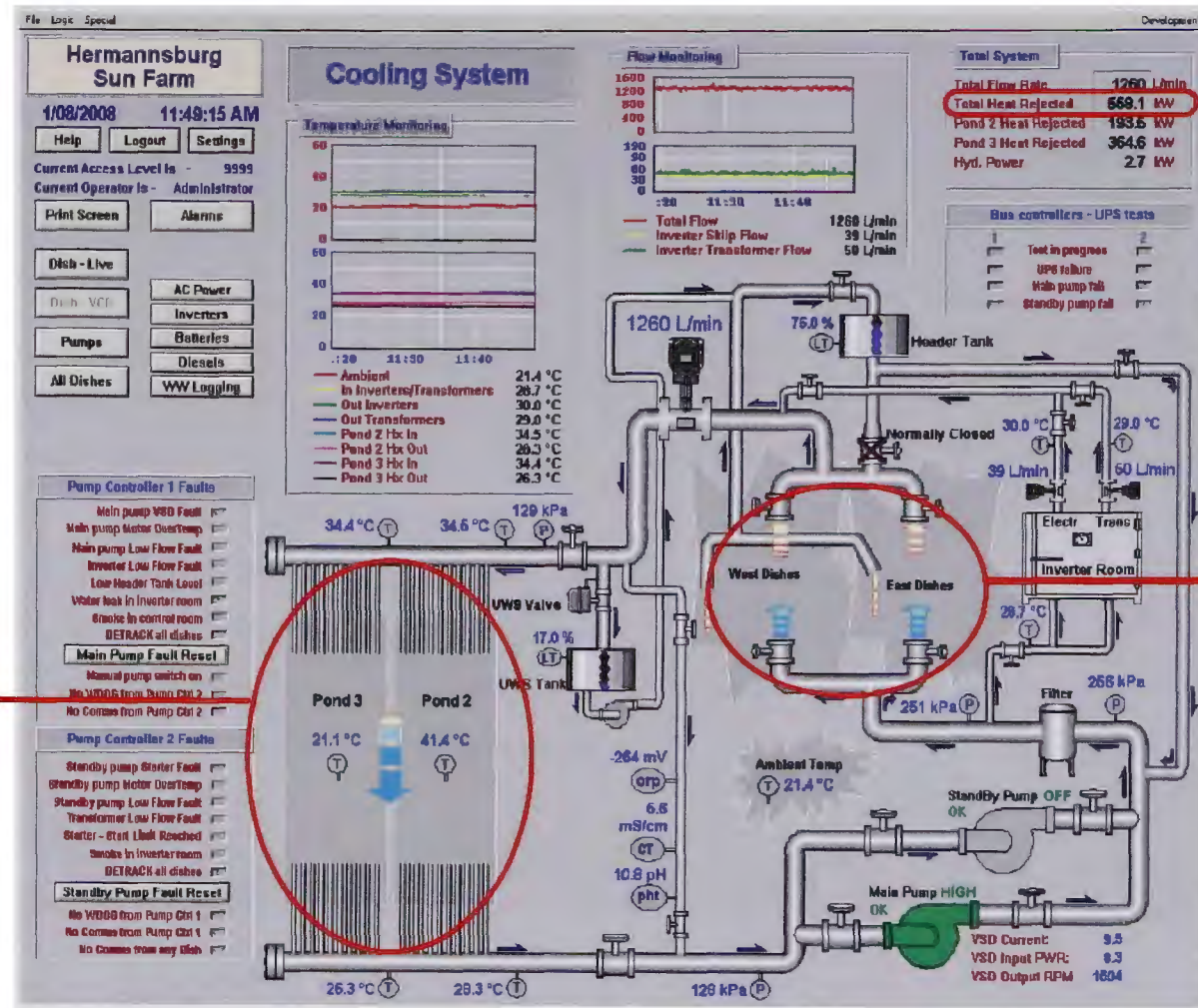
West dishes 1W, 2W, 3W, 4W have multi-junction receivers of several generations. 2W has latest technology.

East dishes have silicon receivers and are connected in parallel with the 'MJ' dishes at a voltage which is preferential for the MJ receivers.



Individual module temperatures

Figure 5-17: Screenshot of Receiver 61 in Dish 2W at Hermansburg. Average module efficiency 35.7%

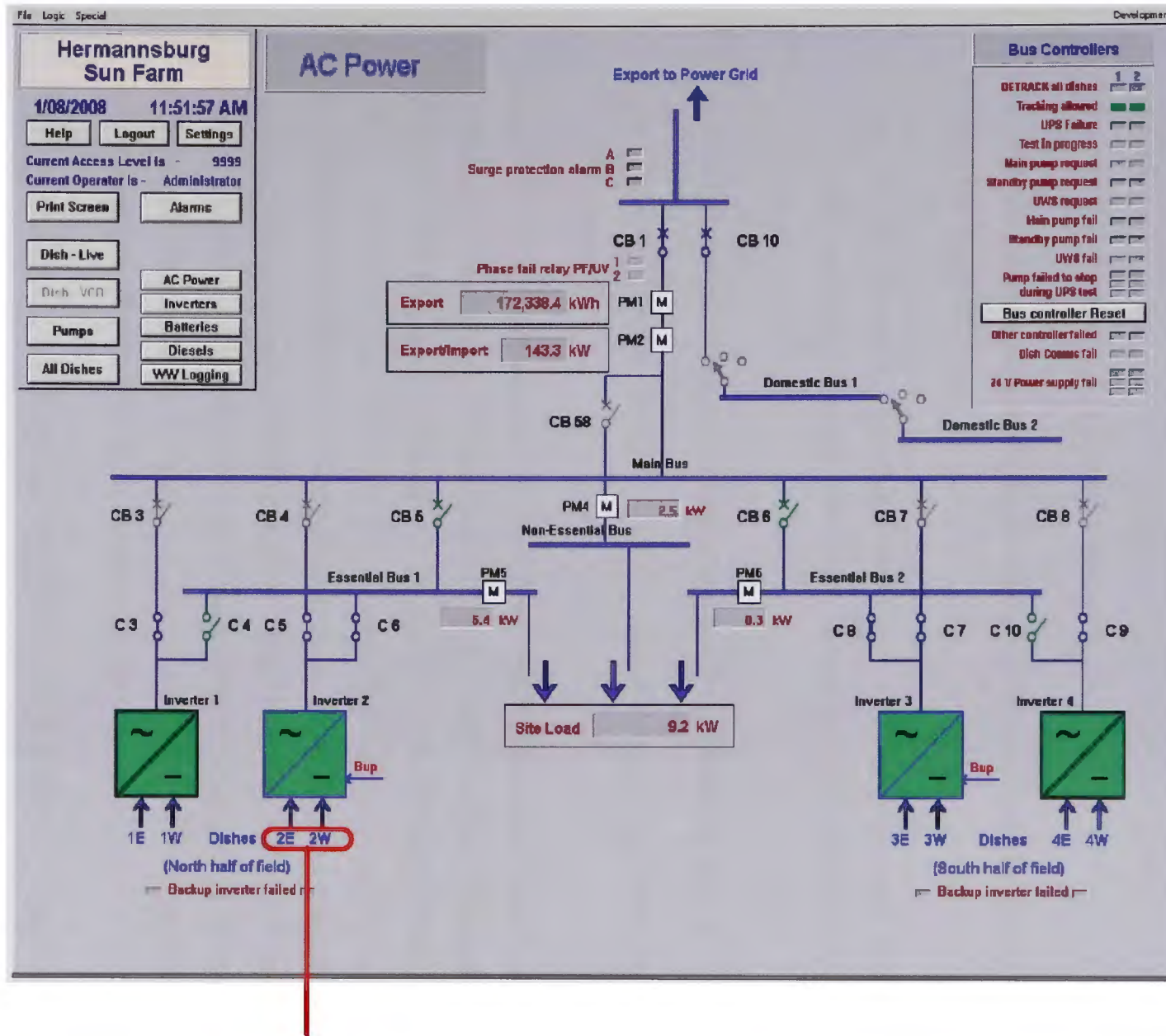


Could be used for cogeneration in an appropriately designed system

Dishes connected in here

Heat rejected into pond. The Mk V dish will use air cooling

Figure 5-18: Cooling system for a field of 8 dishes



Dishes connected to inverters

Figure 5-19: AC power system for a field of 8 dishes with 4 inverters

5.6 Tracking System

The physical arrangement of the tracking system is a modified altitude-azimuth (alt-az) configuration. The azimuth drive is tilted typically at latitude minus 12° . This extends the range of application of the essential design. For example a normal alt-az tracker cannot work within the tropics since a very high (in theory, infinite) azimuth speed is required to stay aligned to the sun as it passes vertically overhead. (Lasich, 2004, US7589302).

The following discussion focuses on the unique control system developed by the researcher to avoid the issues of:

- Having inaccurate tracking typical of ‘sun sensor’ type systems which suffer from alignment issues, tracking ‘false suns’ caused by bright reflections from neighboring clouds.
- High cost of precision mechanics required for accurate tracking.
- Significant power (energy) loss during operation due to inaccurate tracking, causing ‘hunting’.

To maximize the power output from the dish-receiver system (see Figure 5-20), it is necessary to consistently hold the electrical output at the maximum during all operating conditions. This places high demands on the accuracy of the tracking system. If this were to be achieved by using a precision mechanical tracking drive system similar to astronomical telescopes the cost would be prohibitively high for solar applications which still require significant cost reductions to become widely competitive. This has led to consideration of tracking tolerance versus output loss and is characterized by the system ‘acceptance angle’ being the tracking error which allows for a loss of less than 5-10%. Typical acceptance angles range from 0.5° to 1° (Luque-Heredia et al 2009).

The most economical design for a given system is that determined by optimizing the combined effects of tracking system cost, loss in energy output when the acceptance angle is exceeded and any additional costs to increase the system acceptance angle.

The challenge here is to maintain full output over time and keep the cost to a minimum. While it is possible to increase the acceptance angle by, for example, increasing the cell area at the focus, this comes at a significant increase in system cost (and effectively reduces the concentration ratio which is one of the drivers for low cost). During the formulation of

the system design the researcher invented a tracking system (Lasich 2001, AUS2002242487) which can provide accurate tracking with low cost industrial drives and also requires no additional cost at the receiver to increase the acceptance angle. This system uses nominal sun position from an astronomical almanac and uses feed back from the PV receiver to 'trim' the positioning of the dish such that the concentrated solar beam is always precisely aligned on the PV receiver cell array. This is achieved by taking voltage, current and temperature readings (already collected by the monitoring system) and comparing those values which give a direct reading of where the solar beam is positioned on the PV array. Figure 5-21 shows the cell/module array in front of the receiver. For example, the voltages for the top row of modules are compared to the bottom row and the left column compared to the right column (see Figure 5-22). The difference is used to command the drive system to a new (better aligned) position. The new position is detected by the encoders and becomes the new reference position. The encoders and drive motors are in a separate feedback loop to maintain this position in the event of wind or other disturbance. Both axes are controlled in this manner. Consider the elevation control system shown in Figure 5-23. The motor controller loop consisting of amplifier (36), motor (38), encoder (40), position feedback connection (44) and summer (42) ensure that the difference between the actual dish/receiver position (output 44) and the relative direction to the sun is zero. Thus the elevation axis of the dish will follow the sun's position as predicted by the computer (34) which runs the sun position algorithm.

The elevation integrator (46) serves to make small adjustments to calculated solar positions to allow for the mechanical tolerance of the dish and any asymmetric behavior of the optics of the dish (14) or the receiver at (16) (Figure 5-20).

The elevation integrator source is selected by means of an elevation integrator source selector 48. When the source is selected to be 'thermal' 50a, the difference between the top and the bottom flux modifier plate temperature sensor readings 52 and 54 respectively is integrated 46 over time and applied as an offset to the predicted sun position 34 by second elevation adder 58. This causes the dish to move until the integrated value approaches a 'null', that is, the flux modifier plate temperatures are equalized.

When the integrator source is selected to be 'Photovoltaic' (PV) 50b, the sum 60 (see Figure 5-23) of the receiver's voltage due to the top half photovoltaic cell array (28a in Figure 5-22) is compared to the sum 62 of the receiver's voltage due to the bottom half of

the array (28b in Figure 5-22). The resultant voltage is integrated 64, and the dish is moved in elevation until the receiver's array generates a symmetric voltage. This implies that the power generated in the top half of the receiver 16 is the same as the power generated in the bottom half of the receiver 16. This balance gives the maximum power output. Figure 5-24 shows the performance of the tracking system in real life conditions over one full day.

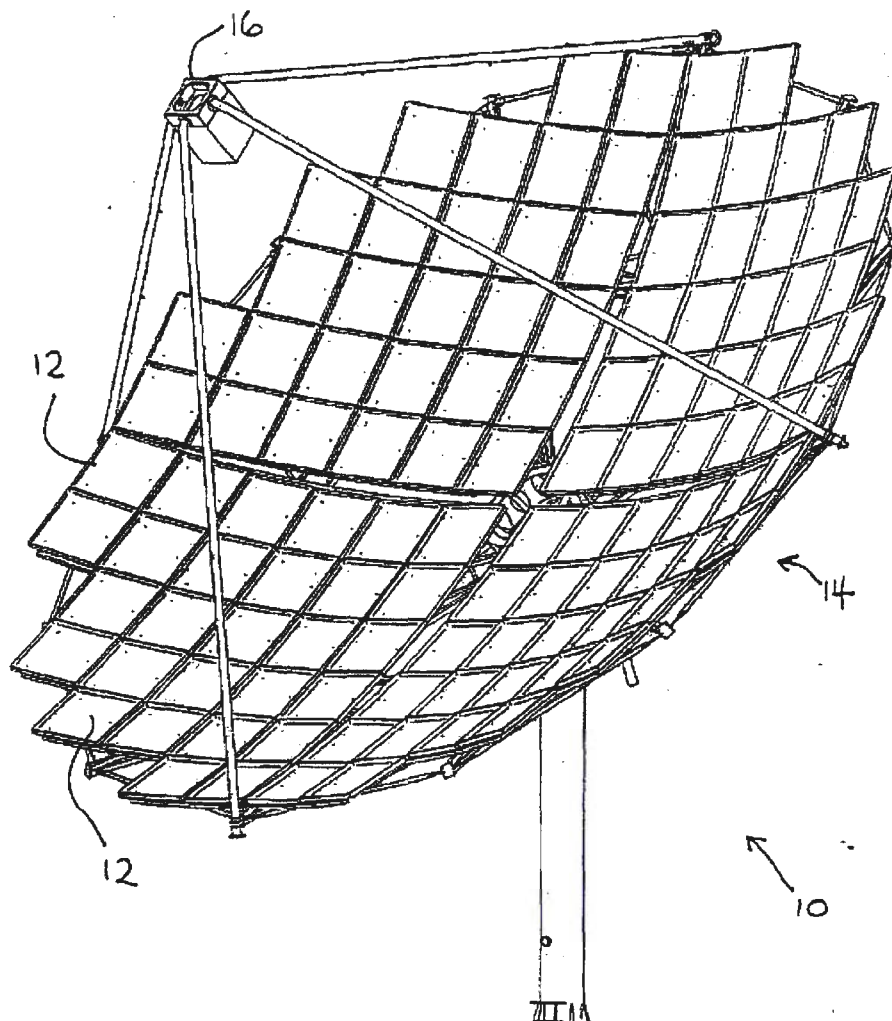


Figure 5-20: 130m² collector dish (14) with individual mirror facets (12) and PV receiver (16) facing the mirror facets.

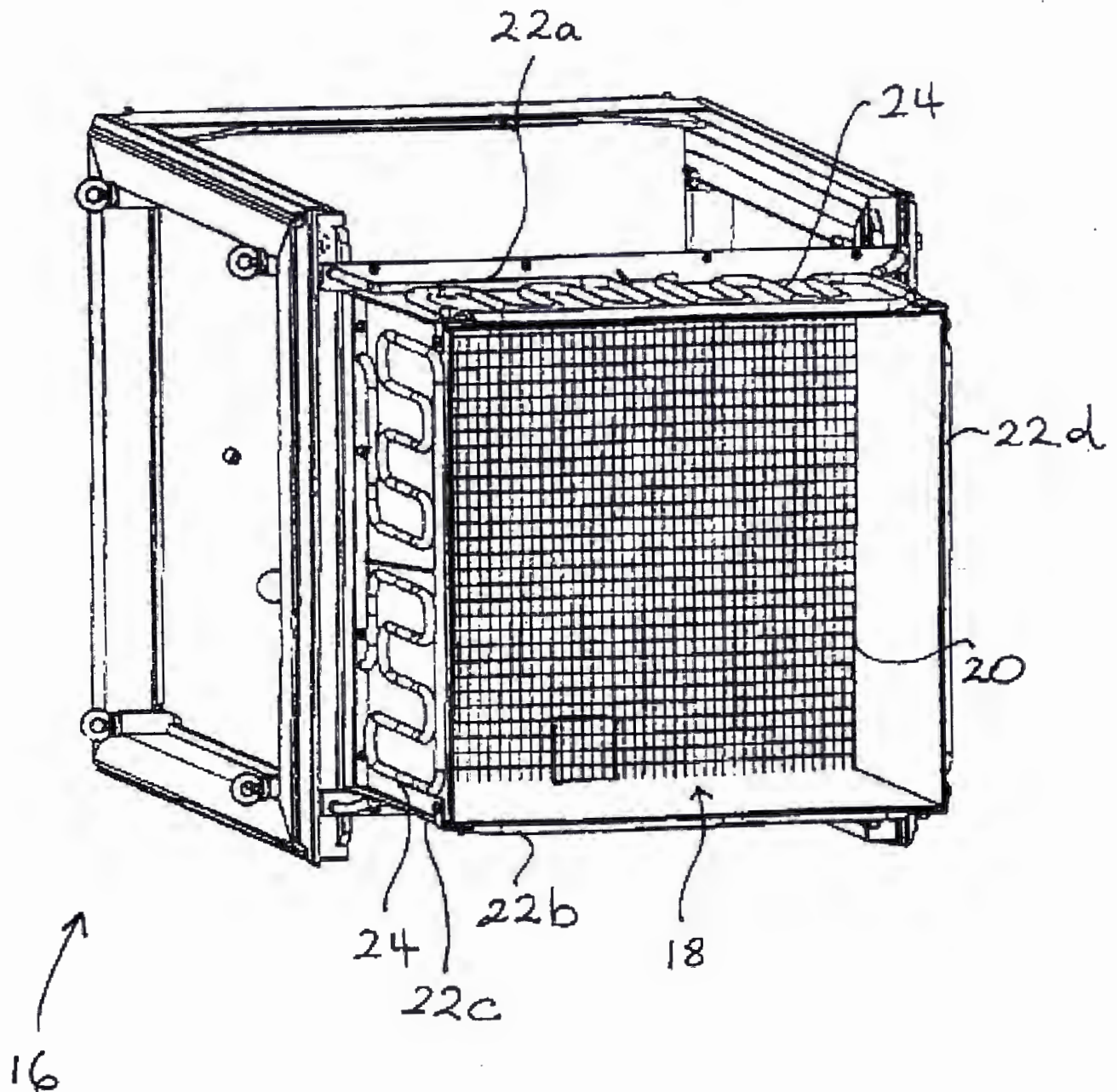


Figure 5-21: Photovoltaic concentration receiver showing the frame populated with an array of 64 modules each with 24 cells (1536 cell) and bordered by 4 flux modifiers (22 a, b, c, d) which form the secondary optics.

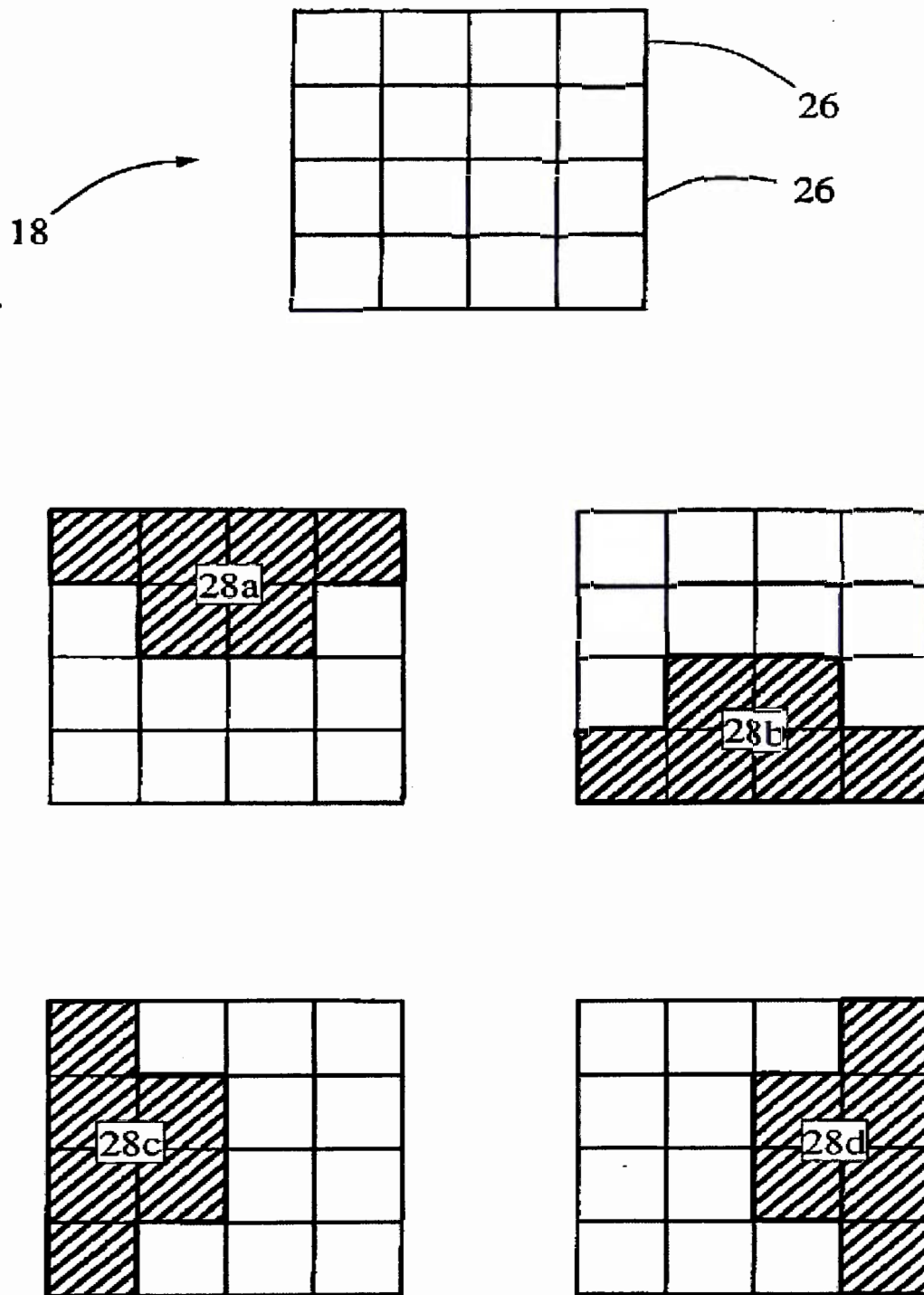


Figure 5-22: Examples of PV module selections for 'PV' feedback tracking. The voltage is compared for top (28a) and bottom (28b) modules to command the elevation integrators. Comparison of the left and right modules commands the azimuth integrators.

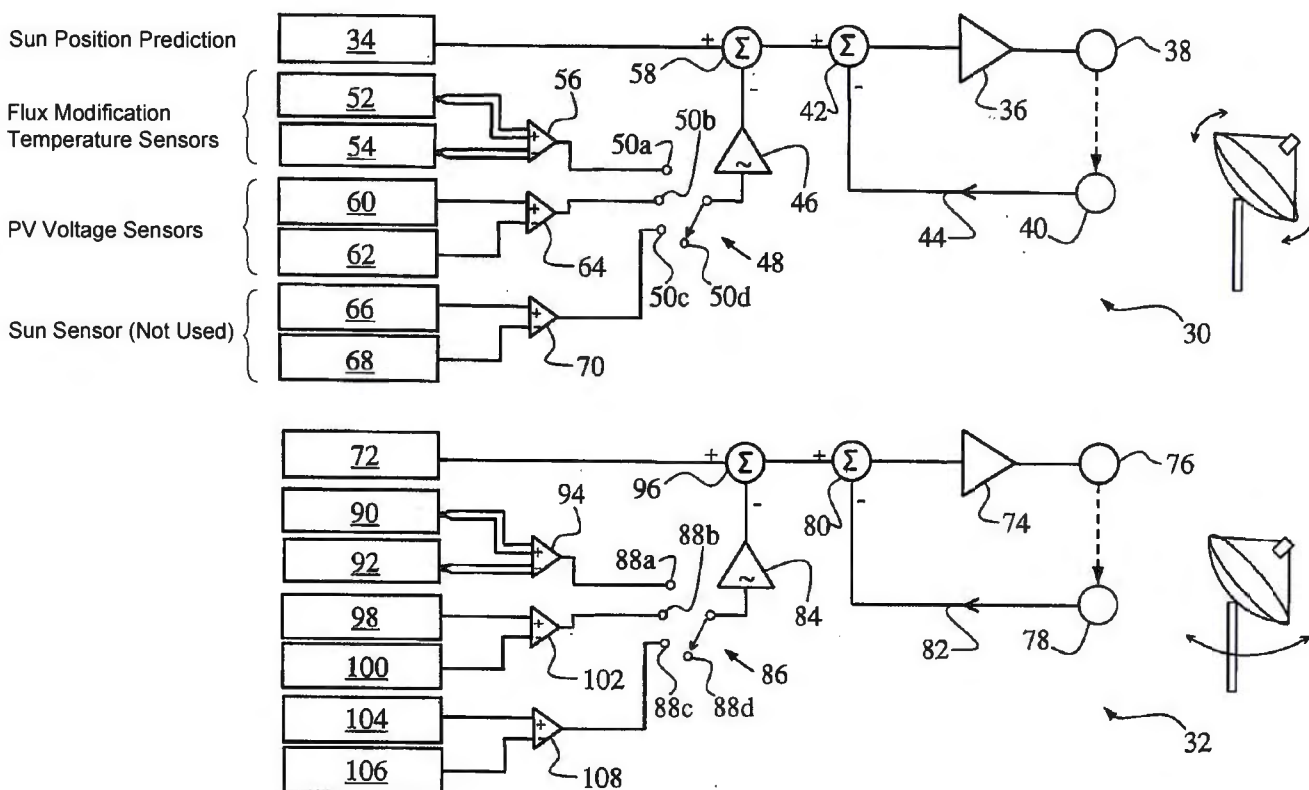


Figure 5-23: Flux modification temperature sensors 52, 54 measure the temperature of flux modifiers 22a and 22b respectively (See Figure 5-14)

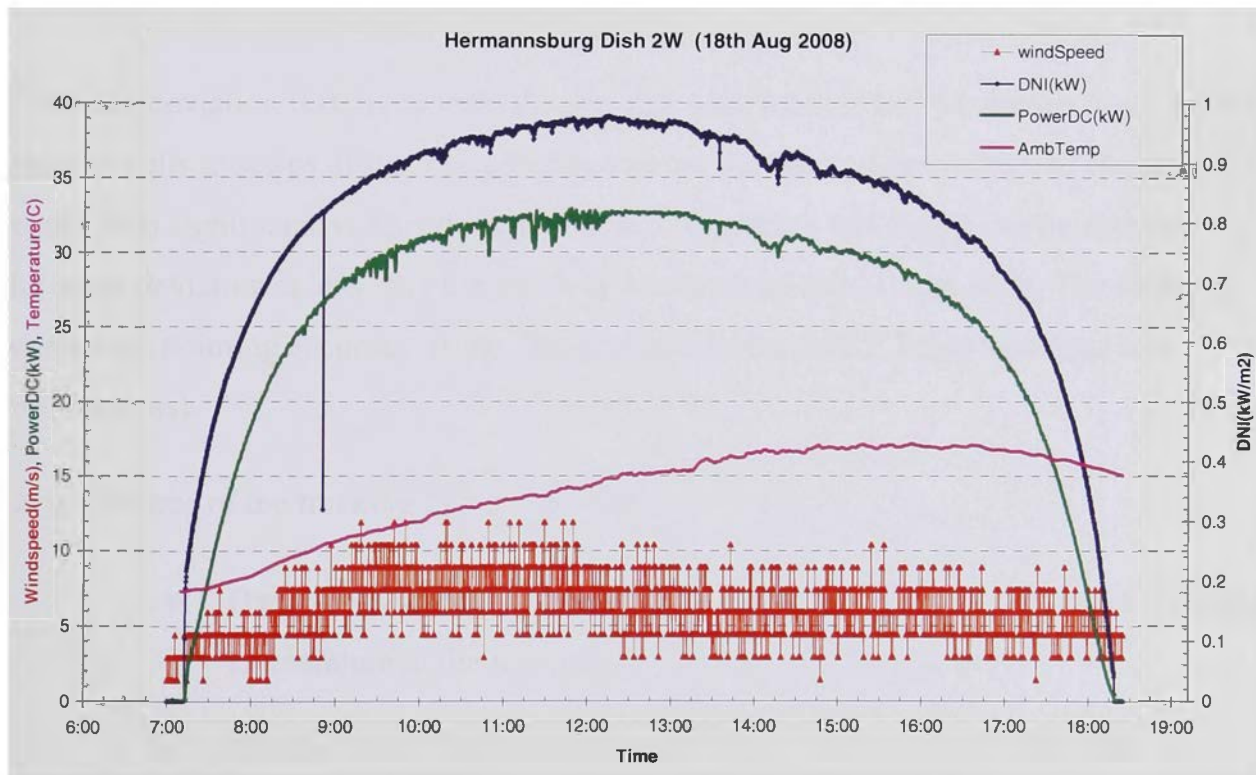


Figure 5-24: Power output of 35kW_{DCSTC} dish 2W Hermannsburg (green) is quite stable when compared to the DNI (Blue) even in significant winds (red) up to 12m/s or 40km/h. This is evidence of the high tracking accuracy from the feedback loop.

The result is a relatively smooth power output profile over a day. See Figure 5-24 which shows stable output during windy conditions. The power ripple is approximately 1% .

It is possible to determine the tracking accuracy by considering the tracking frequency. It takes an average of 12 hours for the sun to traverse 180°. The dish has an average step frequency which has a movement every 6 seconds, thus by simple proportion:

$$180^\circ \times \frac{6.00}{12.0 \times 3600} = 0.025^\circ \text{ or } (0.44\text{mr})$$

This calculation indicates a resolution of tracking movement of 0.025°. As a correlation check, consider the following (Figure 5-25).

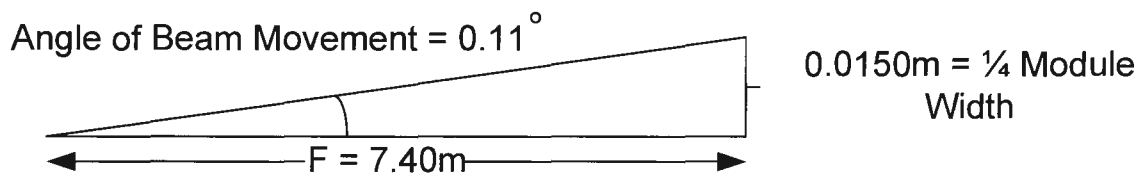


Figure 5-25: Beam Movement Triangle

The beam deviation is derived from the fact that each module has 4 columns (each 1.5cm wide) of cells in series, if just one column was not illuminated the voltage of the modules would drop significantly. This does not occur in operation and thus it can be deduced that the beam deviation is less than the width of 1 column of cells 1.5cm wide. The resulting worse case pointing accuracy of the dish is at maximum 0.055° being less than 1mr (milliradians).

Other features of the tracking system include:

- Over temperature de-track to defocus the dish in the event of excess temperature at the receiver.
- No flow de-track to protect against destruction of uncooled receivers.
- Manual tracking to position the dish at will.
- Dynamic braking to stop overrun during fine tracking steps.

Figure 5-26 and 5-27 show the CPV Receiver 'on sun' and 10 operational CPV dishes.



Figure 5-26: Multijunction 35-kWp CPV Receiver on sun with 102 kW of concentrated 'light power' entering the flux modifier



Figure 5-27: Ten CPV dishes designed by the researcher on sun at Umuwa, South Australia.

5.7 Balance of System

The balance of the system includes conventional industrial components such as an inverter for conversion of DC power to AC power and a fan cooled heat exchanger to reject up to 100kW of heat unused by the receiver. The researcher developed an algorithm for the target set point voltage for the inverter which used cell temperature and the concentration actually impinging on the cell in real time to calculate V_{oc} and then approximate V_{mp} .

5.8 Raytrace Modelling

The ray tracing model was designed to be as realistic as possible in particular using the optical character of the real mirror panels actually used in the dish 2W at Hermannsburg. Each mirror was mapped using a laser mapper developed by the researcher (Lasich, 2001, AUS 2002244529B2).

This mapping produces a 'pan file' which records the slope at 900 points on each panel of size 1.1m x 1.1m. The 112 mirror panels are optically positioned in the mathematical model with an average pointing error of 0.06° being typical as measured by the mirror alignment system described in the above reference. The actual conditions prevailing at the time of measurement (Figure 5-29) are input to the model which predicts an output of 32.8 kW.

The principles of operation of the dish optical model used in the ray tracer are explained in Chapter 3.2. The specific application to a 130m^2 dish with 112 spherical facets fitted to a paraboloidal surface with a target receiver size of 0.23 m^2 is exemplified here.

Each of the 112 mirror facets has been mapped and its 'pan file' loaded into the ray tracer. This gives the 'real' character of the mirrors and no mathematically modelled 'surface' or 'slope' error is added.

A pointing error of 0.06° determined by post mapping of the entire dish is included to add practical reality into the simulation. The position for the receiver was determined by using a method similar to that described in Chapter 3.2 for the 20m^2 dish. The flux distribution is determined at the 'cell face' and a series/parallel model is used to determine the expected receiver performance (see Figure 5-28, shown on the next 5 pages).

An iterative loop is also used to determine the operating condition of each cell with regard to its temperature and impinging light concentration. This is then used to determine the performance of the cell at the condition from the concentration-efficiency characteristic and temperature coefficient. The performance of a module is tied to the output of the lowest performing cell.

Ray trace of 130m² CPV system

Serial Number = 10284.5701

INFORMATION ON RAY-TRACE 10/11/09

Description: 129.7m² Parabolic faceted DISH - @ STC with 112 spherical mirrors

MIRRORS (1.1x1.1m mirrors) - AT 948 W/m² SOLAR INPUT

File name : \\labbpwfile01\home\$\JBLasich\JBL thesis\thesrealXX32.8dat.DAT

Each spherical facet (Panel) contains laser-mapped directional data

Spherical facet (Panel) laserspot files used are: (No. files= 112)

9862a.pan, 9862b.pan, 9863a.pan, 9864a.pan,
 9865a.pan, 9866a.pan, 9867a.pan, 9868a.pan, 9869a.pan,
 9869b.pan, 9870a.pan, 9871a.pan, 9872a.pan, 9873a.pan,
 9874a.pan, 9875a.pan, 9876a.pan, 9877a.pan, 9878a.pan,
 9879a.pan, 9880a.pan, 9881a.pan, 9882a.pan, 9883a.pan,
 9884a.pan, 9885a.pan, 9886a.pan, 9887a.pan, 9888a.pan,
 9889a.pan, 9890a.pan, 9891a.pan, 9892a.pan, 9893a.pan,
 9894a.pan, 9895a.pan, 9896a.pan, 9897a.pan, 9898a.pan,
 9899a.pan, 9900a.pan, 9901a.pan, 9902a.pan, 9903a.pan,
 9904a.pan, 9905a.pan, 9906a.pan, 9907a.pan, 9908a.pan,
 9909a.pan, 9910a.pan, 9911a.pan, 9912a.pan, 9913a.pan,
 9914a.pan, 9915a.pan, 9916a.pan, 9917a.pan, 9918a.pan,
 9919a.pan, 9920a.pan, 9921a.pan, 9922a.pan, 9923a.pan,
 9924a.pan, 9925a.pan, 9926a.pan, 9927a.pan, 9928a.pan,
 9929a.pan, 9930a.pan, 9931a.pan, 9932a.pan, 9933a.pan,
 9934a.pan, 9935a.pan, 9936a.pan, 9937a.pan, 9938a.pan,
 9939a.pan, 9940a.pan, 9941a.pan, 9942a.pan, 9943a.pan,
 9944a.pan, 9944b.pan, 9945a.pan, 9946a.pan, 9947a.pan,
 9948a.pan, 9949a.pan, 9950a.pan, 9951a.pan, 9952a.pan,
 9952b.pan, 9953a.pan, 9954a.pan, 9955a.pan, 9956a.pan,
 9957a.pan, 9958a.pan, 9959a.pan, 9960a.pan, 9961a.pan,
 9962a.pan, 9963a.pan, 9964a.pan, 9965a.pan, 9966a.pan,
 9967a.pan, 9968a.pan, 9969a.pan,

Mirror panel map files

Panellaser spot data has been randomly rotated for each facet
 Panel laser spot data has been pre-loaded and the coordinates of the
 average of 4 outer laser spots have been used to define the spot patterns' center
 Panel laser spot target-mirror distance has been extended (artificially aged) by 4.00m
 Panel laser spot target has been increased by 1.00%
 Average random y-panel tilt (pill box) (deg) = 00.06320
 Average random z-panel tilt (pill box) (deg) = 00.06022
 The following facets have been omitted: (count= 0)
 The following facets have been tilted: (count= 0)

PRIMARY REFLECTOR CHARACTERISTICS:

Primary reflector typefaceted paraboloidal dish with square spherical facets
 Focal length of primary.....(m) 7.4
 Reflector diameter (aperture)(m) 12.8
 Reflector rim angle(deg) 46.77
 Error (1)gauss,(2)pill,(3)parabolic 2
 Mirror facets maximum slope error (degrees)..... 0.01(essentially no added slope error)
 Spherical facet length + height....(m) 1.1
 Spherical facet radius of curvature(m)
 Primary reflectance (%) 94.00
 Shading loss - due to struts etc...(%) 0.00

SECONDARY DEVICE(S):

Secondary reflector type is a flux modifier
 Flux modifier posn. rel. to focus ..(m)-.28
 Flux modifier depth(m).208
 Flux modifier aperture(m).54
 Flux modifier back face(m).48
 Flux modifier reflectivity.....(%)95.

PV ARRAY:

PV cell array efficiency(%) 21.8
 PV cell array matrix..... = 4x 6
 PV module array matrix = 4x 4
 PV sub array matrix = 2x 2
 PV cell array Packing Factor.(x100%).97
 Maximum glass cover reflectivity using reflection formula (%) 100.
 IR glass cover reflectivity(%) 11.4

SAMPLER:

Sampling position(m)-.28

Sampling width(m).48

RAY/TRACE CHARACTERISTICS:

Total number of rays selected = 1000000

Light source used = rays from 1 solar mass
source model is a pill boxIncident watt density(Watts/m²)= 948

Solar diameter used (m)= 1387546000

Max. Incident solar ray half angle ... = 2.65E-01deg. (4.63E+00mRads)

Projected Area of dish raytraced .. (m²)= 129.7

SYSTEM PERFORMANCE RESULTS:

Total number of rays fired at primary 792670

Total pwr incident on primary (Watts)122,925.92

Time taken to do ray trace (minutes) 1

Number of smooths in power matrix 2

Average Watt densty impinging on PV(W/cm²) 43.85

LIGHT POWER STATS

Power entering flux modifier = 104,913.57 Watts

Total power impinging on flux modifier walls = 40,686.34 Watts

Power lost due to glass surface reflection = 1,439.13 Watts

Power lost due to absorption on flux modifier walls (indirect) = 2,433.18 Watts

Power lost due to absorption on flux modifier walls (by counts) = 2,434.73 Watts

Power lost due to absorption on flux modifier walls (primaries) = 2,082.70 Watts

Power lost due to absorption on flux modifier walls (doubles,etc)= 352.03 Watts

Power lost due to unknown mathematical reasons = 0.00 Watts

Total power lost on flux mod. and glass surface reflection = 3,872.31 Watts

Power impinging on dense array = 101,041.27 Watts

Power lost due to IR glass cover reflection (indirect) = 11,518.70 Watts

Power lost due to IR glass cover reflection (by counts) = 11,373.44 Watts

(the IR loss is used in thermal and cell effic. calculations only)

Summary of power impinging of Photovoltaic dense array and power output of series and parallel connected array

The calculation is based on all the cells, modules and sub arrays specified.

We have 4x 6 cells, 4x 4 modules, and 2x 2 arrays

We have 1536 total number of cells

Radiation impinging on receiver (cell) array (CPMPAP) = 101143

PV model is based on Spectro Lab triple junction GaAs high concentrator cells

Average cell efficiency for all parallel combinations (%) =34.87

Highest cell efficiency measured (%) =35.02

Lowest cell efficiency measured (%) =34.81

Cell effic. improvement (estimated for next batch) .. (%) =5.70

The average water temperature through receiver ... (deg.) =30.00

The expected PV cell temperature (deg.) =41.28

The temperature safety factor added to the cell T. (deg.) =0.00

The average water temp includes a heatX temp of ...(deg.) =0.00

The U factor for calculating cell temp (W/cm2/deg.C) =2.60

The Temperature coefficient () = -0.17%/°C.

The flow rate through each module (lpm) =2.30

The cell area is (cm2) =1.50

Power output using calculated cell efficiency and a

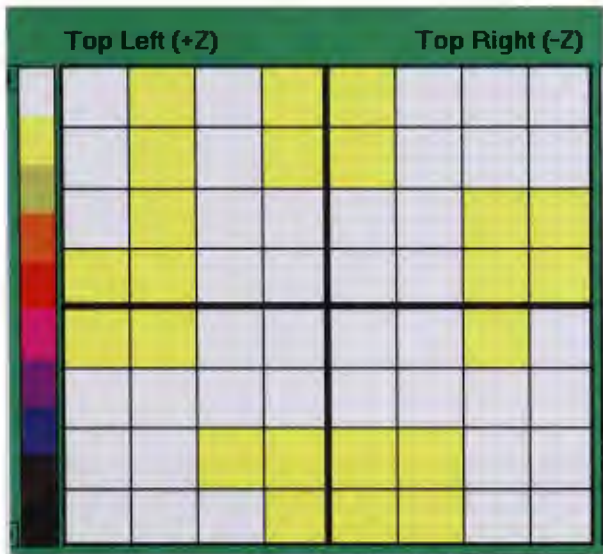
97.00% packing factor and 0.00% cell degradation (Power W) (recvr. effic% (Pin)) (gross effic%)

Cells in series, modules in series, sub arrays in series	=	30074	29.77	24.47	
Cells in parallel, modules in parallel, sub arrays in parallel	=	34210	33.86	27.83	
Cells in series, modules in parallel, sub arrays in parallel	=	33089	32.75	26.92	(This is the configuration used in Receiver 61 in Dish 2W)
Cells in series, modules in parallel, sub arrays in series	=	32773	32.44	26.66	

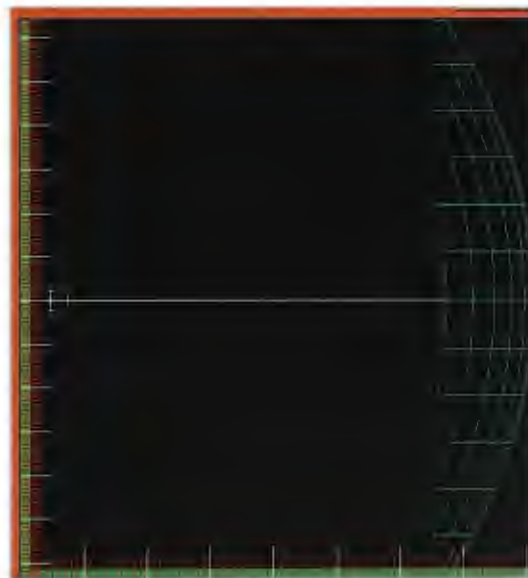
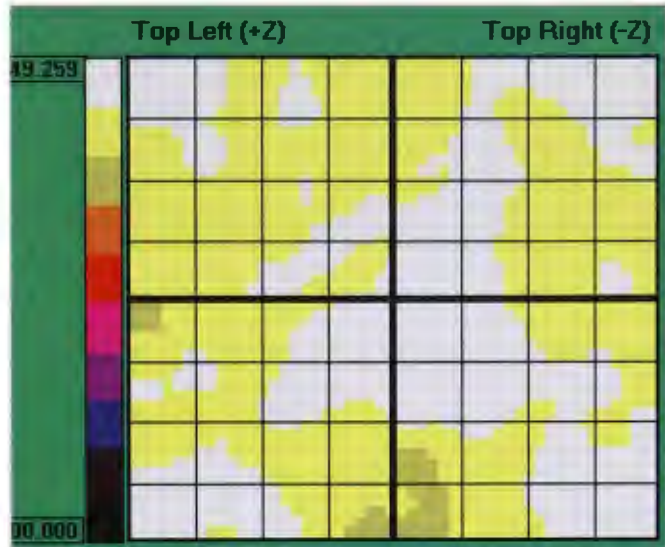
Dish optical efficiency (impinging on array/power in)(%)= 82.20

Figure 5-28: Ray trace of 130m² CPV system showing the modelled performance for the dish using the actual mirror maps for 112 panels (pan files). The predicted output for a series parallel series cell arrangement was 32.77kW and under the same conditions the actual power output was 32.8kW. See Figure 5-29

Cell Map - Power



Cell Map – Power (with Module Grid)

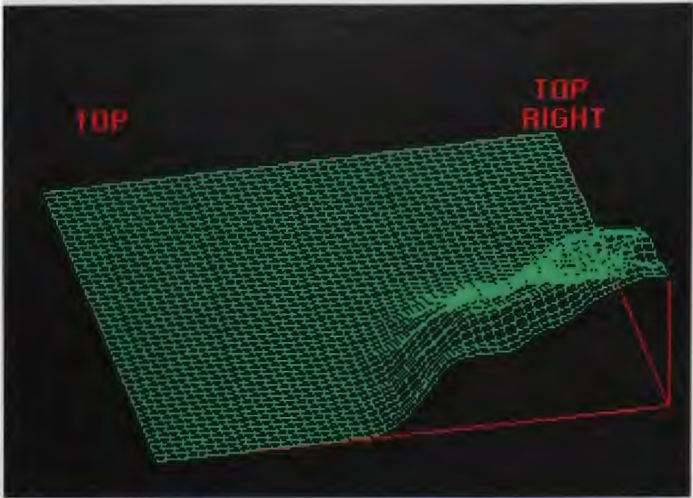


Minor scale = 1cm

Medium scale = 10 cm

Major scale = 1m

Figure 5-28 (Continued): Modelled output for 130m² CPV Dish 2W at Hermannsburg, 2D image.



Outer mirror intersects image from position 26 A (real mapper panel) focussed into corner of receiver.



Modelled flux at cell face (all 112 mirrors)

Figure 5-28 (Continued): Modelled output for 130m² CPV Dish 2W at Hermannsburg, 3D image.

5.9 Actual Performance

Figure 5-29 shows a screenshot from the human machine interface (HMI) for dish 2W, Rx 61 at Hermansburg, 3 June 2009. This records the actual on-sun performance of the dish at operating conditions and cell /module/subarray configuration (cells in series, modules in parallel sub arrays in series). The DC power output is 32.8 kW at a direct normal solar radiation (DSR) of 948W/m^2 , normally called direct normal irradiance (DNI).

It is interesting to compare the output by the ray trace model is 32.77kW (Figure 5-29) for the same conditions. The total DC efficiency is 26.7% with a PV receiver efficiency of 32.4% and an optical efficiency of 82.5%. The average module flash test efficiency was 35.7% at 21°C (shown in Appendix 3).

Allowing for 3% dead space in the receiver one would expect a receiver efficiency of 34.6% which compares well with the receiver flash of 34.8% (see Appendix 3).

When corrected for temperature at the average cell operating temperature of 41.5°C , the average receiver efficiency would be 33.5%. When compared with the measured receiver efficiency of 32.4%, there is a loss of 1.1% absolute which can be attributed to flux distribution losses. This very even flux distribution is also confirmed by the small variation in module current where 90% of the modules are within +/- 10% of the average current (shown in the green matrix of Figure 5-29. (The module with 6.5Amps is not included in this analysis as the module has a failed cell). Since the time of writing a new result has been recorded for a further modification to Dish 2W at Hermansburg and is shown in Appendix 8. With a slight adjustment to the receiver position and a new generation of MJ cells a DC efficiency of 28% at almost full power was achieved.

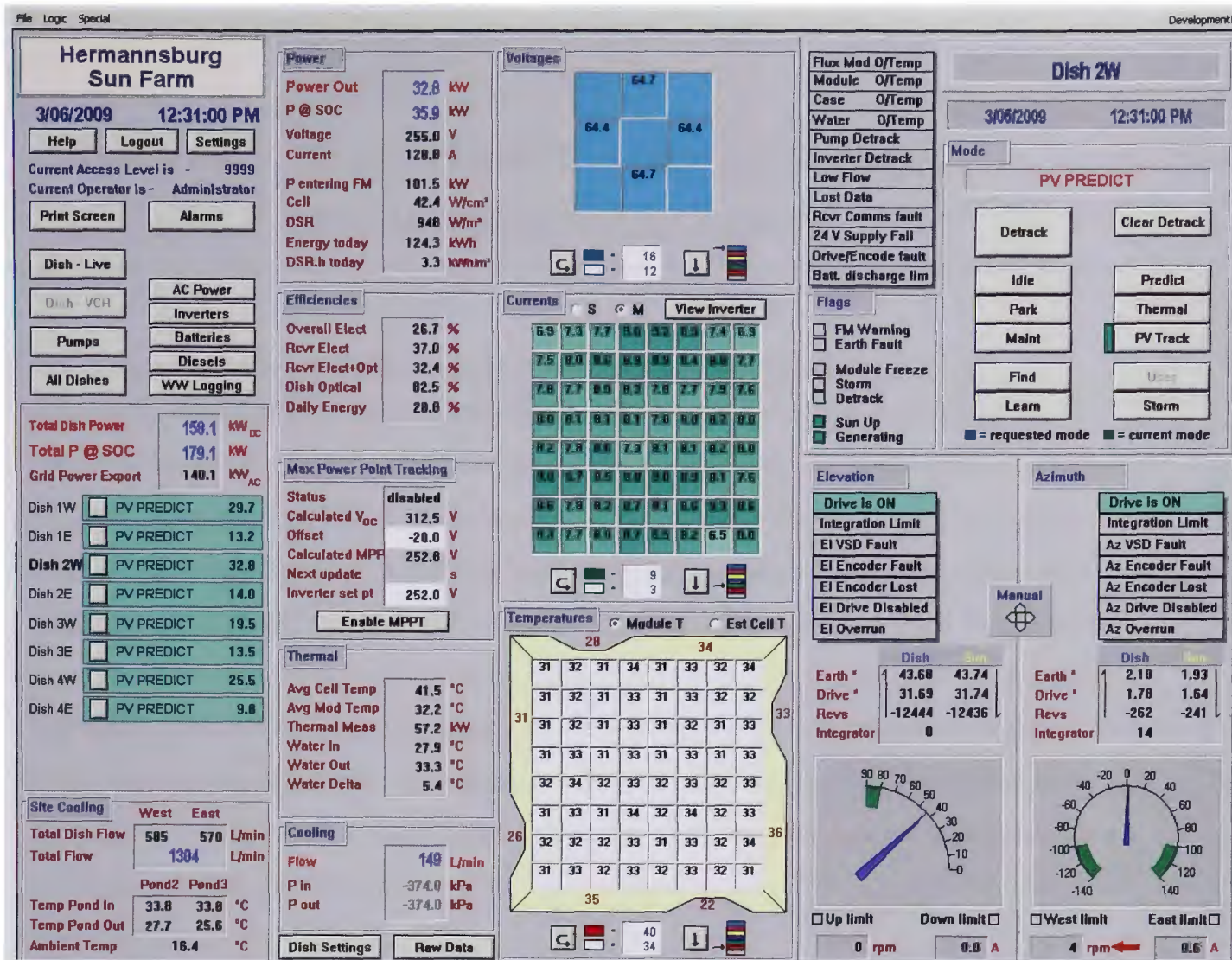


Figure 5-29: ‘Screenshot’ of the human machine interface (HMI) for receiver in dish 2W Hermannsburg showing control and monitoring screen for a 130m² dish. The essential metrics of power, efficiency, temperature and mode of operation are included.

CHAPTER 6. LONG TERM PERFORMANCE/ENERGY PREDICTIONS/ENERGY COST

6.1 Relationship to Instantaneous Performance and Definitions

The operational life of concentrating photovoltaic systems is likely to be measured in decades. However, the researcher has access to data obtained over the short term, that is, up to about three years and we need to be able to predict the performance over a much longer period. First the important terms will be defined and sample calculations necessary to estimate the POWER and ENERGY outputs for a 130m² dish starting with 35% efficient multijunction (MJ) modules in 2008 are shown. Figure 6-1 shows the target performances for dish power, efficiency and energy output through 2012. These increases are driven by improvements in cell/module performances and improvements in the TRANSfer and OPeration (TRANSOP) ‘derate’ factor which account for ‘other’ operational losses for a dish operating in a power station.

The DC ‘name plate’ rating of a dish is $P_{DC\ STC}$ and is roughly equivalent to the flat plate module power at Standard Test Conditions (STC).

The Annual AC Energy Output (kWh/year/dish) for a dish is calculated from the nominal AC power output P_{NAC} , multiplied by the available Direct Normal Irradiance (DNI) and the number of days in the year. ‘ P_{NAC} ’ represents the average annual nominal AC power rating for one dish and allows for all operational, parasitic and field losses (as represented by the TRANSOP). This is the electrical energy that is delivered to the first step-up transformer which will ultimately connect to the grid.

P_{NAC} is a derived metric which is actually determined from long term energy measurements. The DC energy is logged each day along with the DNI. This includes the effect of availability, spectrum, dirt, temperature and shading. The further effects of field losses, parasitics and AC conversion are then added to determine the ‘ P_{NAC} ’.

For example at Alice Springs in 2008 with a dish having a P_{NAC} of 27kW and a DNI of 7.4 kWh/m²/day (i.e. 7.4 nominal peak hours at 1 kW/ m²) and considering one year (365 days) of operation, the annual energy output would be:

$$\begin{aligned} \text{Annual AC Energy Output} &= 27\text{kW} \times 7.4 \text{ hours/day} \times 365 \text{ days/year} \\ &= 72,900 \text{ kWh/year/dish.} \end{aligned}$$

6.2 Nominal Target Performances – 130m² Dish and Modules and Cells

Date	2008	2009	2010	2011	2012
$P_{DC\ STC}$ (kW) measured at base of the dish (efficiency)	35 (27%)	36.5 (28%)	38 (29%)	40 (31%)	42 (32%)
$P_{AC\ STC}$ (kW) measured at the inverter ($P_{AC\ STC}/P_{DC\ STC}$ ratio of 0.915 incl. parasitics but no field losses)	32	33.4 26%	34.8 27%	36.5 28%	38.4 30%
P_{NAC} (kW)* measured at inverter terminals (Annual Average AC Efficiency)	27 (21%)	28.5 (22%)	31 (24%)	32.4 (25%)	34 (26%)
$P_{NAC}/P_{DC\ STC}$ Ratio	0.77	0.78	0.81	0.81	0.81
TRANSOP (see section 6.4)	0.77	0.78	0.81**	0.81	0.81
$P_{typical\ DC}$ (Range) measured at base of dish	24 to 34	25 to 35	27 to 37	29 to 39	31 to 41
$P_{typical\ AC}$ (Range) measured at inverter terminals	20 to 30	21 to 31	23 to 33	25 to 35	27 to 37
Related Module Efficiency (Manufacturing average over full year)***	35%	36.5%	38%	40%	42%

* Accuracy of $\pm 10\%$ Refer to attached conditions pg 2.

* Ratio of $P_{NAC} / P_{DC\ STC}$ ranges from 0.77 in 2008 to 0.81 in 2012 and assumes some improvements in parasitics, availability and 'other'

Energy output per dish per year = $P_{NAC} \times \text{DNI/day} \times 365 \text{ days / year}$ e.g. $27 \times 7.4 \times 365 = 73,000$ kWh/year

** Refer to Sections 6.5 and 6.6

*** Supported by Spectrolab targets see Figure 4-22.

Figure 6-1: Nominal Target Performance – 130m² Dish and Modules and Cells

6.3 Definitions

- **Annual Average AC Efficiency** – AC electrical energy output as a percentage of the solar energy intercepted by the dish over one year.
- **Annual Energy Output (kWh/year/dish)** - the AC electrical energy output for one dish over 1 year.
- **Auxiliaries** – includes all parasitics and losses incurred in the process of generating and delivering AC power to the output terminals. (Typically input terminals of the first step up transformer). These losses are accounted for in TRANSOP.
- **Availability** - percentage of time the dish is generating while the sun is shining.
- **Capacity Factor** - the measure of the energy output over a 24 hour day and depends on P_{NAC} , the name plate rating (either $P_{DC\ STC}$ or $P_{AC\ STC}$) and the DNI

For example, the yearly AC Capacity Factor for 2008 for Alice Springs with a DNI of 7.4 kWh/m²/day, is:-

$$\begin{aligned}
 \text{Capacity factor AC} &= \frac{P_{NAC} \times 365 \times \text{DNI}}{P_{ACSOC} \times 8760\text{hrs/yr}} \\
 &= \frac{27 \times 365 \times 7.40}{31.0 \times 8760} \\
 &= 27\%
 \end{aligned}$$

- **Cell efficiencies** - determined by flash test at 25°C and 500x.
- **DNI** – Direct Normal Irradiance measured in kWh/m²/day (this is a measure of direct solar **energy** delivered per day. The DNI is also equivalent to the number of **peak sun hours** per day at an irradiance of 1000W/m²)
- **Irradiance** – is measure of **solar flux** in W/m² (this is a measure of the solar **power** delivered per m²)
- **Module efficiency** is determined by flash test at 25°C at 500x.

- **$P_{DC\ STC}$ (kW)** – DC power output of one dish corrected to Standard Test Conditions (STC) of $1000W/m^2$ Direct Solar Irradiance and cell temperature of $25^{\circ}C$. Auxiliaries are NOT included. $P_{DC\ STC}$ is approximately equivalent to the ‘name plate’ rating of flat plate systems.
- **P_{NAC}** - is the ‘NOMINAL’ AC power output of one dish and is defined as the ‘Average Annual AC Power’ output measured after the inverter output terminals and allows for field losses, thus P_{NAC} is calculated at the input terminals of the first ‘Step Up’ transformer. (‘Step Up’ transformer losses are NOT included)

P_{NAC} is related to P_{STC} by allowing for TRANSfer and Operation (TRANSOP) losses in a power station.

$$P_{NAC} = P_{DC\ STC} \times TRANSOP$$

The AC **energy** output of a dish is calculated by the equation:

$$\text{Annual AC energy output} = P_{NAC} \times DNI \times 365$$

Section 6.4 shows factors which make up ‘TRANSOP’ target for 2008 and 2010 respectively.

The values stated are derived from Dish 2W under Hermannsburg conditions. P_{NAC} is the ‘pseudo’ power output which represents the AC energy generating capability of a dish. It is derived from the measured energy output divided by the number of kWh of sunlight taken to produce that energy output over a given time. The reverse calculation can be used to estimate the energy output for a given solar input and time. Other performance factors can be applied to this baseline rating to account for temperature and other site or installation specific characteristics.

- **$P_{Typical}$** – is the power observable on any clear sunny day with solar irradiance in the range of 700 to $1050W/m^2$.
- **P_{ACSTC}** – is the AC name plate rating of the dish measured at STC at the inverter of each dish. It includes inverter loss and parasitics but does not include field losses.
- **Peak AC Efficiency** – AC efficiency from sunlight to AC electrical power under peak conditions

- **STC** - Standard Test Conditions of 25°C cell temperature and Direct Normal Solar Irradiance of 1000W/m² A.M. 1.5D
- **TRANSOP** - is the 'derating factor' which allows for losses in OPERATION of dish and TRANSfer of power to AC terminals. Section 6.4 shows factors which make up the TRANSOP factor (see section 6.4).

6.4 TRANSOP Estimated for 130m² Dish for 2008

- Dish availability 97% (non standard operation activities excluded) (approx. 3% loss)
 - Average cell temperature 50°C (approx. 4% loss)
 - Cooling fans 700W (approx. 2.5% loss)
 - Pumping and tracking 1kW (approx. 4% loss)
 - Accumulation of dirt on dishes (approx. 3% loss)
 - Shading for multi-rows of dishes at 40m East West spacing. (approx. 3% loss)
 - Field power collection (approx. 1.5% loss)
 - Inverter efficiency 95% (approx. 5% loss)
- Total 'TRANSOP' =
0.77 for 2008

Total (Multiplicative) TRANSOP = 0.77

During the test period, the following effects may have been present but normally they are small:

- Transients
- High wind during sunny conditions
- Dew or frost on dish
- Measured but uncollectible circum solar radiation
- Cell infant mortality

6.5 EPR and Average System Efficiency

The energy production rate (EPR) is used as a measure of the system performance. The EPR = daily dish DC output kWh/DNI in units of kWh/m²/day. The efficiency = EPR /dish area of 130m². The 'AC' version of 'EPR' allowing for TRANSOP the same as 'P_{NAC}'.

6.6 Energy & Performance Analysis

A new MJ receiver (Rx 56) was installed on March 28th 2007, a few days after the autumn equinox, and monitored for 2 years. During these 16 weeks of autumn and winter, the daily average air mass number was slowly increasing. It was expected that the output power and the daily energy production of the MJ receiver would decrease, not only because the sunlight intensity would be reduced, but also because the solar spectrum would change during this period and would be less favorable to the MJ solar cells that are optimized to a particular spectrum. The solar spectrum was carefully monitored the solar spectrum with a spectrophotometer and calculated the ozone, precipitable water and aerosol optical thickness. This data was entered into our modeling program of the MJ receiver that calculates the expected daily energy production, based on the spectral response of the cells, the location of the concentrator system, the date and the atmospheric parameters (ozone, water and aerosol optical thickness). Figure 6-2 shows that there is a very good agreement between the simulated data and the actual daily energy production divided by the cumulative daily solar irradiance (kWh/kWh/m^2). As a result of the validation of our simulation model, we are now in position to further optimize the spectral response of the solar cells to a particular target solar spectrum for the best annual performance of the system.

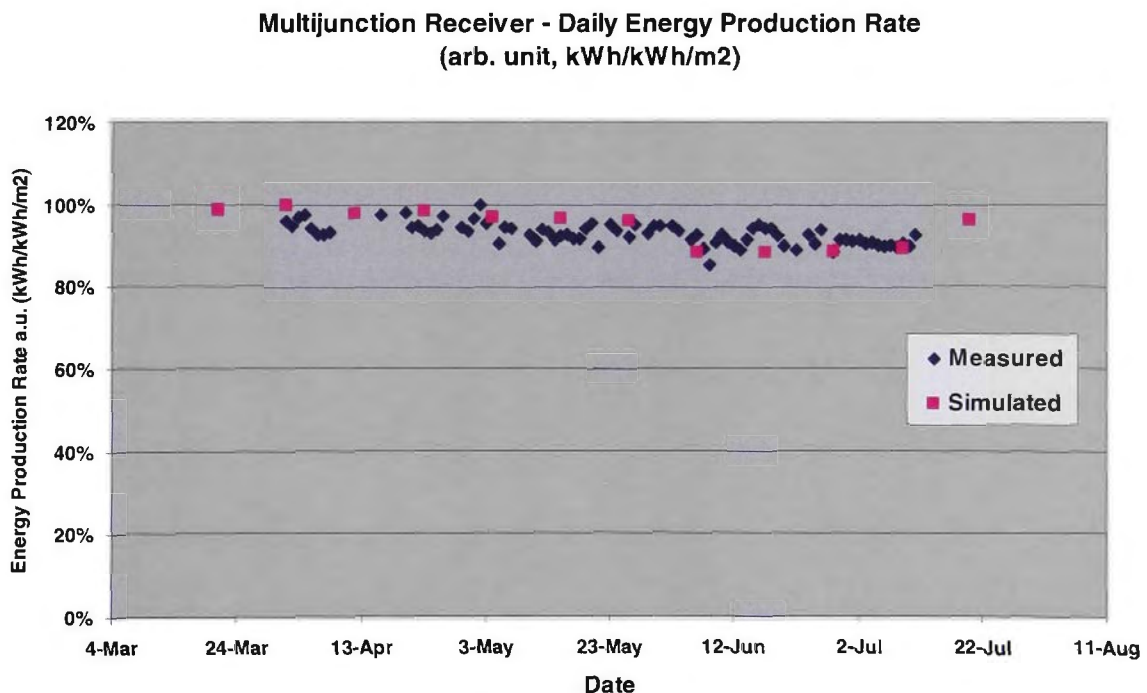


Figure 6-2: Daily energy production rate for modelled and measured output (daily produced energy divided by the daily cumulative solar irradiance) between end of March and mid July. The influence of spectral variation is taken into account in the model for the simulated results.

Data were obtained from the records of power output and dish performance at Hermannsburg (see Figures 6-3 to 6-5). The following steps were then taken:

- The mean optical efficiency was limited against plausible maximum values (specified by the researcher, which were different for both dishes. For 1W this was 0.880 and for 2W the topical efficiency was standardised to 0.830.
- The benchmarked EPR was then calculated as such: $(\text{EPR} \times \text{Benchmark})/(\text{LimitedOptEff})$.
- The non-benchmarked value was calculated as follows without the correction for optical efficiency being made. This was only done for 1W.
- To exclude days when the dish may not have been running for the whole day or the weather was unsuitable for operation, the benchmarked EPR was then limited to values above 20.0 kWh/kWh/m². A subsequent check showed this is valid as values under 20.0 were insignificant.
- A linear fit was then applied to the benchmarked EPR data limited above 20.0.
- Using the equation from the linear fit the Rx efficiency was then calculated by substituting in the initial and final dates the Rx was operational, finding the initial and final EPR values, and then using the following equation:

$$\text{RxEff} = 1 - (\text{finalEPR}/\text{initialEPR}).$$
- The mean values were calculated over the same data as the linear fit with the error associated with a 95.0% confidence interval calculation.

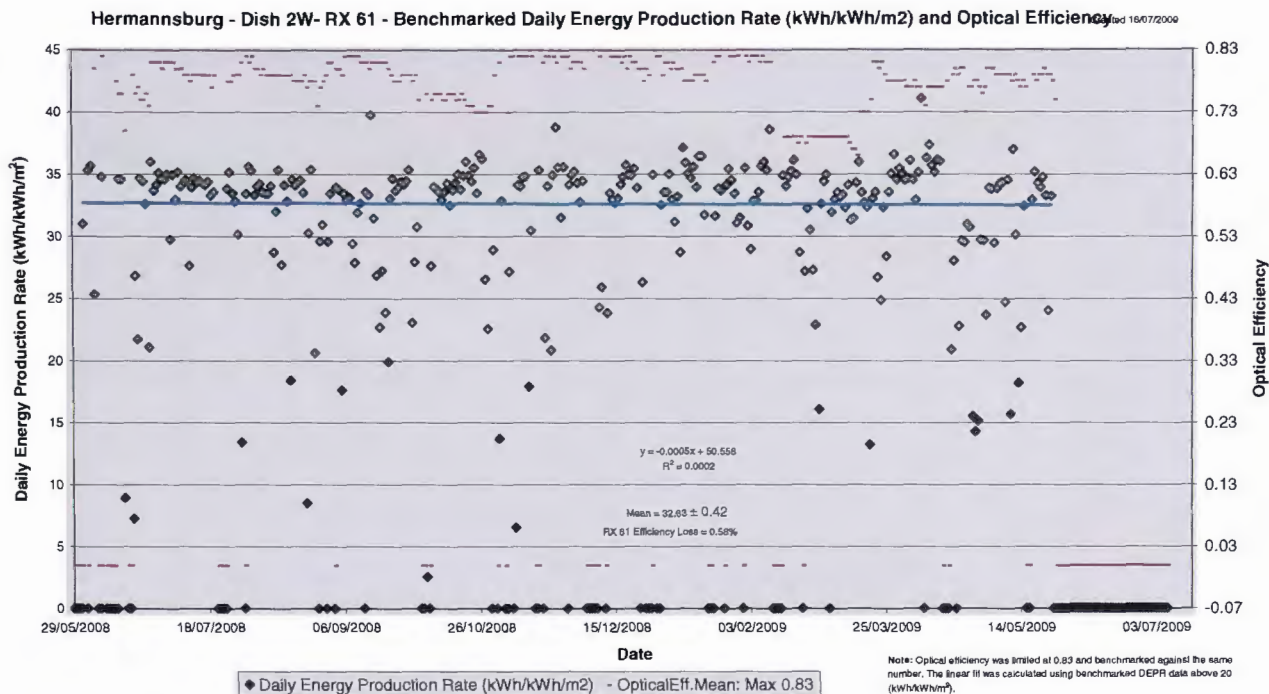


Figure 6-3: Hermansburg Dish 2W Rx 61 - Benchmarked Daily Energy Production Rate Over 1 Year (kWh/kWh/m²). The optical efficiency has been connected to the nominal ‘clean’ value of 83% to show the performance of the CPV receiver. The curve fit indicates a slight degradation over 1 year of 0.58%.

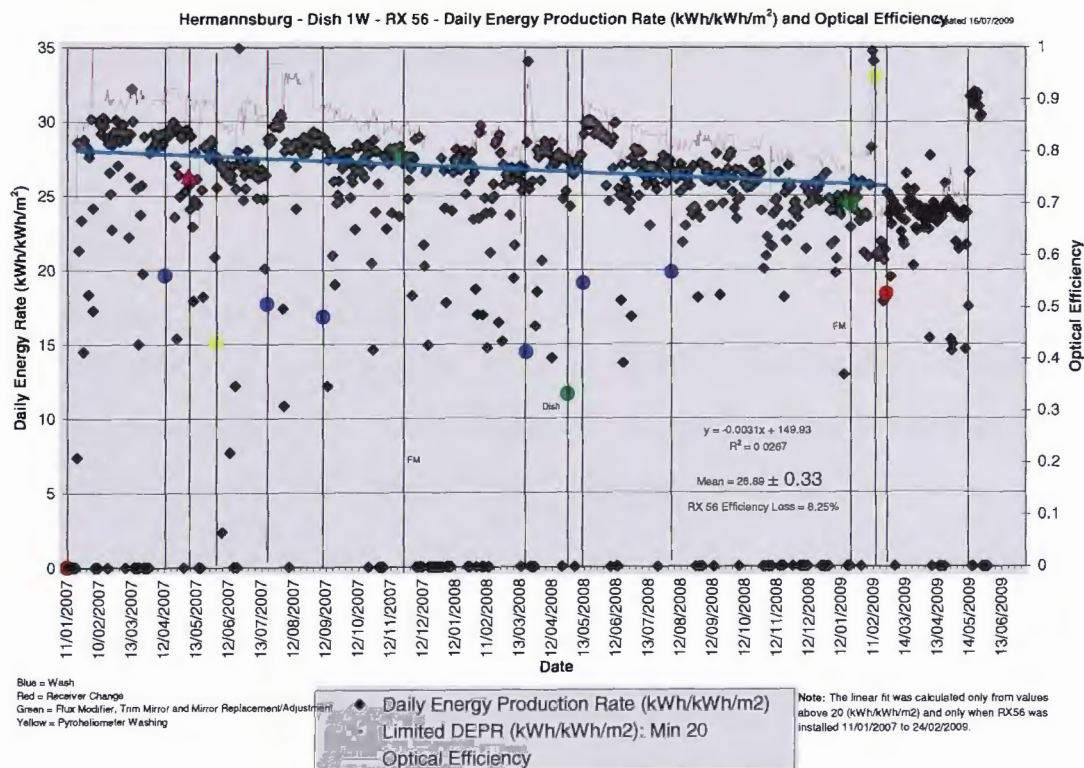


Figure 6-4: Raw data from Hermansburg Dish 1W - Rx 56 - Daily Energy Production Rate and Optical Efficiency Over 2 Years. The blue dots indicate the wash dates. For the period 12/08/08 to 11/02/09 the dish was not washed and the output has dropped by about 8% or approximately 1% per month. This is the ‘typical’ influence of dirt on the mirrors.

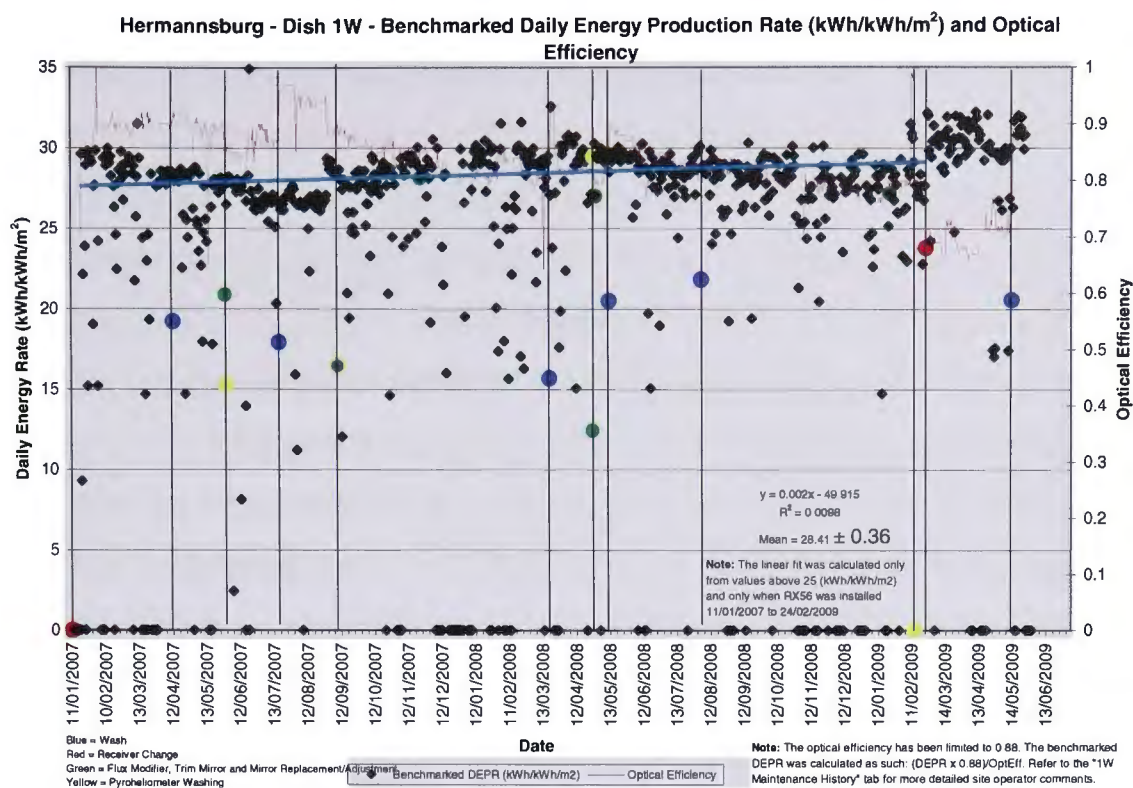


Figure 6-5: Hermannsburg Dish 1W Rx 56 – Benchmarked Daily Energy Production Rate Efficiency Over 2 Years in order to bench mark the CPV receiver performance to optical efficiency was corrected to the nominal ‘clean’ efficiency of 88%. The increase in output over the two years indicates that the ‘availability’ of the dish has improved and the spectral conditions are more favourable. The rise in EPR after 11/02/09 is because a new generation PV receiver was installed.

6.7 Levelised Cost of Energy (LCOE) Model

The concept of LCOE was introduced in the literature review and is explained here in detail. Its purpose is to provide a standard method to compare the cost of energy for a particular scenario against another where the inputs are:-

- The cost of capital, operation and maintenance cost, depreciation, subsidies and tax benefits;
- The average output $P_{NAC} = P_{DCSTC} \times TRANSOP$ as described in Chapter 6.4;
- The ‘DNI’ being the solar resource available at the potential site (kWh/m²/day);
- The nominal name plate rating P_{DCSTC} at the base of the unit; and
- Degradation rate over 20 years.

The example shown in Figure 6-6 compares the researcher's system at small volume <100MW/yr with no 'learning curve' to commercially available 'First Solar' thin film CdTe at 10.6% efficiency and 'SunPower' c-Si at 19.3% efficiency. The average annual 'system efficiency' (of P_{NAC}) used in this calculation is 22.8%. The reported annual average AC system efficiency reported from infield measurements at Hermansburg for dish 2W is 22.5% (Lasich, 2009) – refer to Figures 6-7 to 6-9. While the commercially available flat plate products have been produced at GW scale have many years of learning curve experience, it is evident that the researcher's system (with cost calculated at 60MW/year) is competitive on the basis of LCOE with all 3 cases being within just a few percent of each other. The capital costs used for the flat plate systems were obtained from company data indicating their future cost targets in the next 3 years.

In Chapter 8 where performance enhancements and the effects of 'learning curve' and 'volume' production are modeled, it can be seen that the researcher's CPV system when produced at 0.5 GW/year with a 42% module efficiency or LCOE of \$50/MWh (5c/kWh) may be possible. It should be noted that these calculations use income tax credits as presently available in the USA.

2010 LCOE Analysis - Update	Solar Systems		High Efficiency Silicon
	DA CPV	CdTe Thin Film (TF)	(8i)
Sensitivity Analysis			
Low case module cost per watt	N/A	0.85	1.75
High module cost per watt	N/A	1.00	2.00
Low case module cost per watt		0.85	1.75
Low efficiency	26.93%	10.70%	19.30%
High efficiency	28.04%	11.30%	19.70%
Low efficiency	26.93%	10.70%	19.30%
Cost factor to apply to low efficiency case	4.110%	5.607%	2.073%
GENERATION ASSUMPTIONS			
Solar Radiation			
Las Vegas	7.1	5.4	8.7
Insolation (1000kW/m2)	1000	1000	1000
Desired plant output (DC MW soc)	20.000	20.000	20.000
Generation unit details (i.e. flat plate module or dish)			
Collector length (mm)	1,100.00	1,200.00	1,559.00
Collector width (mm)	1,100.00	600.00	1,046.00
Collectors per generation point	112.00	1.00	1.00
Collector size/generation unit (m ²)	135.52	0.72	1.63
Efficiency (DC soc)	28.04%	10.70%	19.30%
Generation unit output (kW)	38	0.07704	0.314727802
Number of generation points	527	259,606	63,547
Collector area required (m ²)	71,326.32	186,915.89	103,626.94
Real output of each generation point (kW Pnac)	30.9890	0.0629	0.2387
Pnac ratio (AC avg output over DC nameplate)			
Availability	99%	99.50%	99.50%
Standard operating temperature (deg C)	25	25	25
Temperature coefficient/1 degree C loss	0.17%	0.25%	0.38%
Average module temperature (deg C)	45	60	60
Thermal coefficient multiplier	96.60%	91.25%	86.70%
Parasitics			
Cooling	2.50%	0.00%	0.00%
Pumping	2.00%	0.00%	0.00%
Tracking	0.20%	0.00%	0.20%
Mismatch	0.00%	0.50%	0.50%
Dirt loss	3.00%	3.00%	3.00%
Shading loss	3.00%	0.00%	3.00%
Field loss	1.00%	3.00%	2.00%
Inverter efficiency loss	4.00%	4.00%	4.00%
Pnac ratio (AC avg output over DC nameplate)	81.55%	81.60%	75.83%
Systems Efficiency (Pnac)	22.87%	8.73%	14.64%
System Output (MW Pnac)	16.31	16.32	15.17
Generation per annum - year 1 (kWh AC)	42,267,315	38,123,834	48,159,136
Plant life (years)	25	25	25
Annual degradation factor	0.10%	0.80%	1.00%

The annual average system efficiency

2010 LCOE Analysis - Update	Solar Systems		High Efficiency Silicon
	DA CPV	CdTe Thin Film (TF)	(Si)
Average annual output over life of plant (kWh AC)	41,660,121	34,014,559	41,786,017
2010 LCOE Analysis - Update			
O&M Cost Per Annum (\$MM)	877,455,000	748,388,891	709,563,904
O&M Cost as a % of Capital Cost	1.01%	1.00%	0.75%
O&M Cost per square metre of collector	\$12.30	\$4.00	\$6.85
O&M Cost per MWh in year 1	\$20.76	\$19.63	\$14.73
O&M Cost \$ per kW-year (ACsoc) in year 1	\$43.87	\$37.42	\$35.48
Present value of O&M cost	\$12,757,762.54	\$10,881,205.02	\$10,316,708.88
TOTAL LIFE CYCLE COST (TLCC)			
Capital cost net of ITC	\$60,537,001.41	\$52,387,222.35	\$66,225,964.40
PV of MACRS tax shield	-\$25,839,259.25	-\$22,360,655.27	-\$28,267,502.90
PV of O&M cost	\$12,757,762.54	\$10,881,205.02	\$10,316,708.88
TLCC	\$47,455,504.70	\$40,907,772.10	\$48,275,170.38
PV OF GENERATION OVER ASSET LIFE (\$/MWh)	522,794	442,335	548,896
LCOE	\$90.77	\$92.48	\$87.95

Figure 6-6: Comparison of levelized cost of energy for 3 different technologies. The researcher's CPV, CdTe thin film flat plate and high efficiency crystalline silicon flat plate. The analysis shows that the researcher's CPV system (at 60 MW/yr production rate) is competitive with the other two technologies. The baseline performance and cost for the flat plate systems use forward (some what optimistic) projections for very high (GW Scale) volume. The relatively low annual degradation factor for the CPV system allows for some replacement of degraded PV modules and mirrors. This replacement cost was added into the O&M cost for the CPV system. The degradation rate for flat plate systems is derived from warranty statements of representative suppliers and assumes no replacement. The higher O&M cost of \$12.30/m² of the CPV system accounts for this.

The effect of these tax credits is to reduce the LCOE by approximately one third to one half. Without the subsidy the LCOE projected for the CPV system would be approximately 7.5 to 10c/kWh.

Traditional coal fired generation presently has a base cost of approximately 50 to 70 \$/MWh (IEA, 2008). The global carbon capture and storage institute (GCCSI) estimates the increased cost to 'clean up' generation would be up to 78% (The Age, 2009). This would indicate that the roughly comparable cost of clean coal would be 90 to 120 \$/MWh. Other factors to be considered in this comparison included dispatchability and long term supply which have 'downsides' for solar power and coal power respectively.

A brief comparison with another CPV system ‘FlatCon’ developed by Concentrix Solar shows they have achieved an annual average AC efficiency in the range of about 20% over 1 year (Concentrix 2009).

This system has a slightly higher specific weight than the CS500 Dish developed by the researcher and thus one would expect a slightly higher LCOE for the Flatcon system.

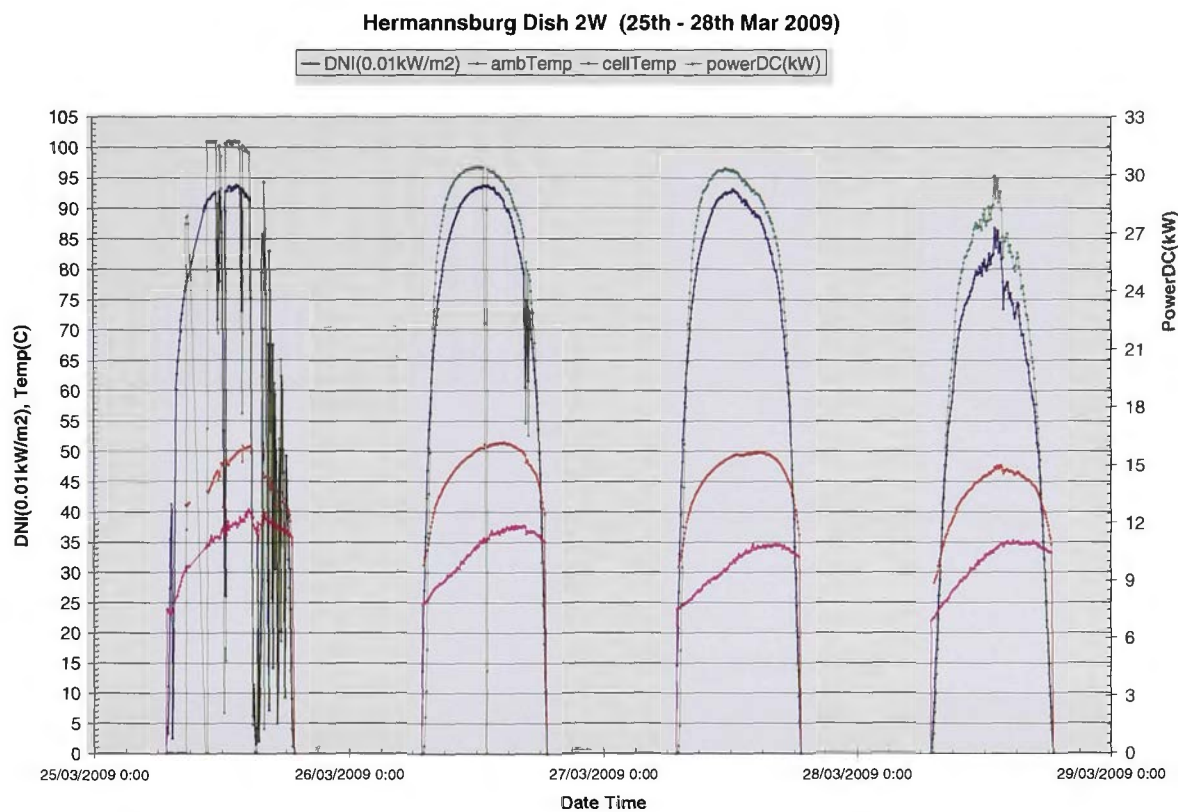


Figure 6-7: 4 Sample days showing comparison of clear and cloudy days

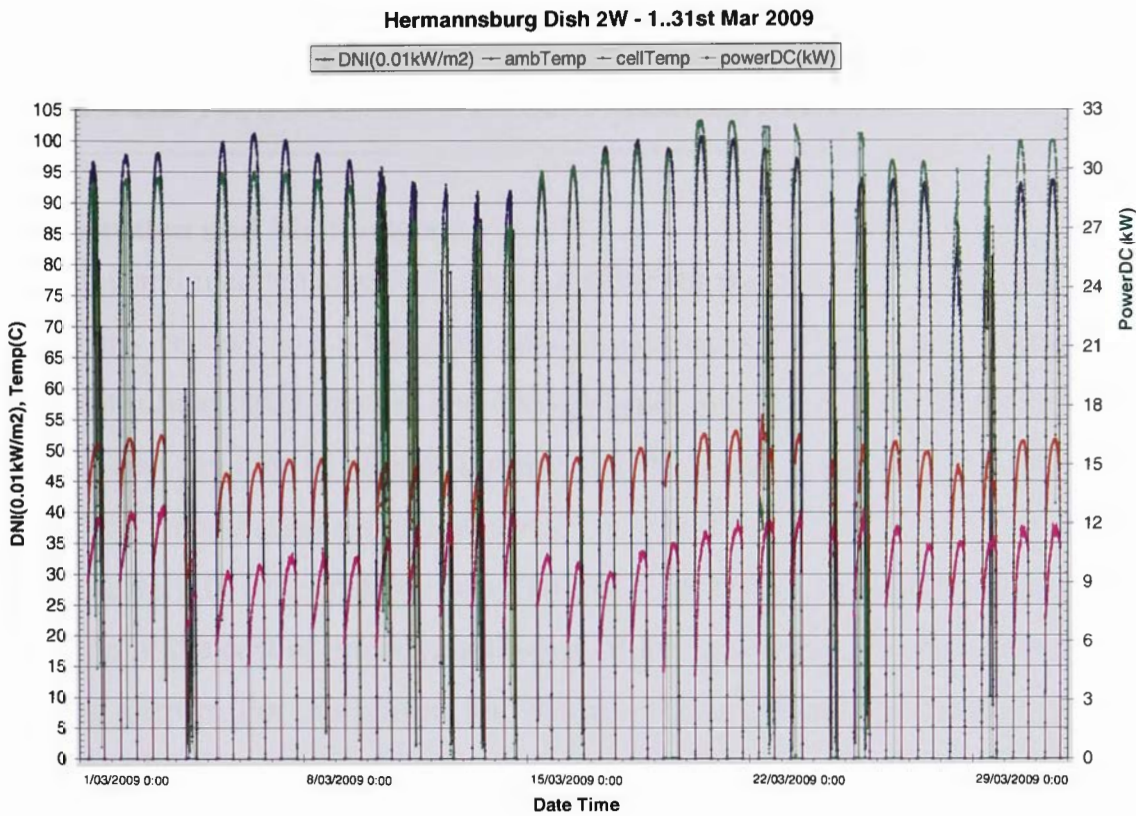


Figure 6-8: One month of operation for Dish 2W at Hermannsburg

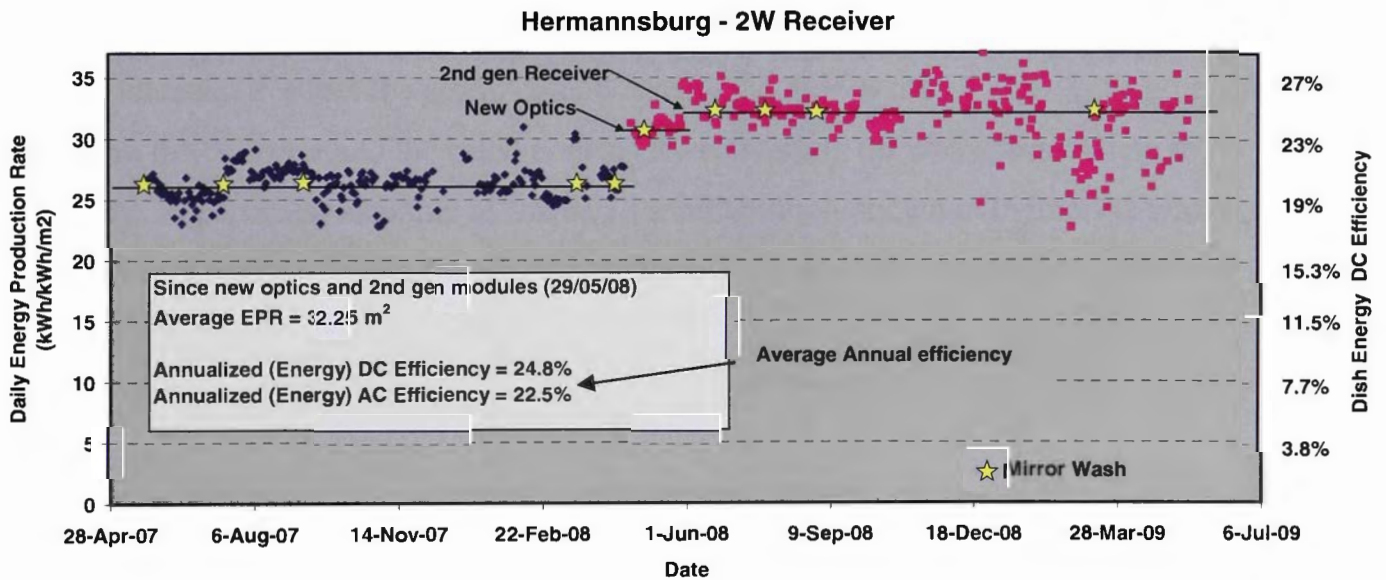


Figure 6-9: Specific Energy Production Rate (EPR) of one dish unit over a two-year period and improvements due to optic re-design and installation of 2nd generation modules.

Yellow stars indicate the dates of mirror wash.

The Annualized (Energy) AC Efficiency of 22.5% allows for availability, dirt, parasitics for cooling & tracking and Inversion.

CHAPTER 7.

RELIABILITY

7.1 Operation and Maintenance

Operation and maintenance costs play a significant part in the LCOE for the technology particularly because it is a recurring cost. A number of CPV companies are getting sufficient infield data to record and classify types and trends in system failures. (Stone, K, 2006) A cost can then be assigned to the 'O&M'. It can be shown that a reduction of \$1000/year in operation and maintenance cost per dish is equal to a capital cost reduction of approximately 10 times that number (\$10,000). Operation and maintenance costs are a reflection of the cost of remedying failures of the system as well as routine costs such as cleaning mirrors. For this reason, knowledge of the expected performance over the prescribed lifetime (typically 20 to 25 years) is very important. The following tests are designed to give an indication of the lifetime/'accelerated lifetime' (or degradation rate) of the component in service.

International standard IEC 62108 (reliability standard) includes a range of accelerated lifetime tests including 'damp heat', 'heat soak', thermal cycling and UV exposure. These tests are intended to stress the active components in the 'power train' of the system i.e. the mirrors on the collector and the cells/modules for converting the concentrated light to electricity. A particular example of 'managing' reliability is shown in Figure 7-2 when a PV receiver can be easily changed for quick O&M or an upgrade with higher performance modules.

7.2 Modules

The CPV module is the key component which dictates reliability and thus the most effort is focused here. It is evident that real infield conditions are not fully represented by these individual tests however they are a good starting point. It is the intention of the researcher to develop some 'combination' tests which will impose the synergistic effect of several stresses simultaneously. The intent would be to have an accelerated test which can predict module performance in the real world over many years.

7.3 Accelerated Testing

The modules assembled with MJ solar cells were extensively tested for reliability through thermal cycling, damp heat, high-temperature soak and on-sun long term exposure testing. In this matter, there is some guidance provided by several technical specifications and international standards. In 2001, the Institute of Electrical and Electronic Engineers (IEEE) produced a first standard for qualification of concentrator PV modules (IEEE Std 1513-2001), which was itself based on earlier recommendations from Jet Propulsion Laboratories and Sandia National Laboratories. In 2008, the International Electrotechnical Commission (IEC) produced a first international standard on concentrator PV modules: IEC 62108-2008 “Concentrator Photovoltaic (CPV) Modules and Assemblies – Design Qualification and Type Approval”. This standard established testing procedures for qualifying CPV modules and assemblies. These testing procedures are essentially accelerated aging tests to ensure long term reliability of the CPV modules. The procedures described in IEC 62108-2008 were followed closest, but in some cases they were modified to suit the particularities of the dense-array CPV modules.

7.4 Damp Heat and High Temperature Soak

It is well established that III-V solar cells are very sensitive to oxygen and moisture and could degrade rapidly due to oxidation of the window top layer. Over the years, manufacturers of solar cells have abandoned the standard AlGaAs window layer material for a more robust and more reliable AlInP layer. In order to test the resistance of encapsulated cells to high-temperature and moisture, the encapsulated MJ modules were submitted to a damp heat test of 1,000 hours at 85°C with a relative humidity greater than 85%RH and with a halogen light bias (~ one sun) in order to generate enough voltage and current to enhance any galvanic corrosion. The MJ modules survived the damp heat test with less than 10% degradation in performance. In another test, the MJ modules survived without any observable degradation a temperature soak at 100°C for more than 1,000 hours.

Solar cell suppliers have also tested the reliability of the MJ solar cells. For example, Spectrolab had applied high temperature soaks to the current MJ solar cells for more than 2,000 hours at temperatures between 140°C and 250°C in nitrogen (N₂) and in air. The efficiency and open-circuit voltage V_{oc} of the cells were measured at regular time intervals. Assuming an activation energy E_a of 0.73 eV, which was previously obtained by measurements at Spectrolab on similar space solar cells, it was possible to calculate the

estimated degradation in performance over 25 years and for a continuous on-sun operation at 70°C, which is about 20°C above the normal operating temperature of the solar cells. The estimated degradation was less than 2% for the currently used MJ solar cells over a 25-year period.

7.5 Thermal Cycling

The testing and modeling of CPV modules is complex and depends on many factors. The challenge is to accelerate ageing in order to predict the future lifetime, while at the same time subject the specimen under test to conditions which would induce a 'real' mode of failure. The researcher conducted many tests with different module designs and under different test regimes. This section relates to a sample of those tests.

The MJ modules were submitted to accelerated ageing testing by subjecting them to thermal cycling. Solar cells in a typical CPV system may undergo about 2,000 shallow thermal cycles per year, between 30°C and 50°C, depending on the location, due to the sun being occluded by clouds. Additionally, the cells may undergo about 365 deep thermal cycles, between 10°C and 50°C, due to the normal daily cycles. Over a 25-year period, the cells would undergo about 50,000 shallow cycles and about 9,125 deep cycles. In particular, in the system developed by the researcher, the cells are actively cooled and are typically operating at a temperature of 45°C. The expected actual temperature difference during these shallow cycles is from the water inlet temperature (20°C to 35°C) to the Normal Operating Cell Temperature (NOCT) of 45°C.

The test was designed to thermally cycle individual modules between 27°C and 72°C, with 800 to 1,000 cycles per day. In order to make sure that the degradation mechanisms are similar to the actual ones, the set points of temperature were selected to be greater but still similar to the actual temperatures seen by the solar modules. The new MJ modules survived more than 45,000 thermal cycles without any significant degradation. A particular version of the modules survived more than 70,000 cycles without significant degradation: less than 10% in efficiency and without significant cracks in the layers of solder. The typical result was in the range of 40,000-50,000 cycles.

In order to estimate the actual acceleration factor, several modules were thermally cycled at a higher temperature difference, 27°C to 92°C. With this higher temperature difference, a

smaller number of cycles would be expected to occur until a 'fail' condition occurred. It was indeed observed that the modules only survived about 10,000 thermal cycles without significant degradation, less than 10% in efficiency and without significant cracks in the solder layers. A number of modules were also cycled at 27°C to 82°C with the typical number of cycles to failure being about 20,000 to 25,000. Observations of these events indicate a very rough rule of thumb, which says that for each increase by 10°C of the temperature cycle range, the number of cycles to failure reduces by a factor of 2. More work needs to be done to develop a useful model to predict module lifetime.

7.6 UV Exposure

Intense UV exposure could degrade CPV modules due to yellowing or browning of the encapsulant material, solarization of the cover glass, or degradation of the cell performance. In any case, the observable degradation is expected to be in the current responsivity only. Due to the very high concentration ratio (468X), it was difficult to find a UV source with sufficiently high intensity to be equivalent to an acceleration factor greater than 1. Therefore, it was decided that an effective UV exposure test would be on the CPV dish with real sun. As described below, MJ modules have been placed under concentrated sunlight (concentration ratio greater than 400X) for more than 3 years in CPV systems installed in the Australian outback without any significant degradation due to intense UV exposure. In particular, there was no observation of solarization of the cover glass or yellowing/browning of the encapsulant material.

7.7 Humidity Freeze tests

Following recommendations from IEC 62108 standard, modules were submitted to 20 cycles of humidity freeze cycles (85% RH, cycles between -40°C and +85°C) 200 cycles between -40°C and 85°C following a pre-cursor dry thermal cycling stress of 200 cycles between -40°C and 85°C, This is considered, along with the Damp Heat test, as the most stringent reliability test. Modules submitted to this test survived acceptably well with performance degradation of less than 8%.

7.8 Observed Cell Degradations

An important research question is to discover if there is any other types of cell degradation that might occur in the field under normal on-sun conditions and that are not observed

during prescribed reliability tests in the IEC 62108 standard. MJ modules and receivers have, at the time of writing this document, been on sun for more than three years. The main mode of degradation of the MJ solar cells observed after long-term real-life on-sun exposure is what is known as “Infant Mortality”. After several years of research, it appears that the “Infant Mortality” failure mode is actually a microscopic electrical shunt created by thermal cycling, probably due to a difference in thermal expansion of metallisation electrical contacts and the GaInP/GaAs/Ge stack of semiconductors. These microscopic electrical shunts evolve over time and after many thermal cycles into a larger electrical shunt that ultimately can completely short-circuit the solar cell. This mechanism of failure has now been successfully duplicated in laboratory but is still under investigation in order to develop a model and a full understanding of the failure mechanism. In any case, this particular reliability problem of the MJ solar cells represents a small loss (about 3% to 6% relative) in performance of a full 35kW receiver as time progresses.

7.9 Mirrors

Coupons of mirrors have been sent to US National Renewable Energy Laboratories (NREL, thanks to Cheryl Kennedy) for accelerated ageing tests, including damp heat, thermal cycling and humidity freeze. The damp heat test was found to be the test which caused the greatest ageing effect and therefore constant required ageing is used as the primary indicator of degradation rate. The specular reflectivity for cone reflection angles of 25mr and 7mr were used as a measure of mirror quality. The measurement in this case is done at a single wavelength of 660 nm and is considered to be a reasonable measure of the effective reflectivity. From the triple junction cells point of view, the multijunction cell is limited by the top junction and 660 nm is just within the response band of the top cell. A more conclusive measurement would assess the whole spectrum, however the researcher’s measurement apparatus was limited to a single wavelength.

Accelerated ageing shown in Figure 7-1 is typically carried out at 85°C and 85% humidity. Correlations with mirrors in the field indicate an acceleration rate of approximately 30X. In this case the best mirrors might have a lifetime of about 15 years with a reflectivity loss of <5%. The worst case samples would be unserviceable after just 2 years.

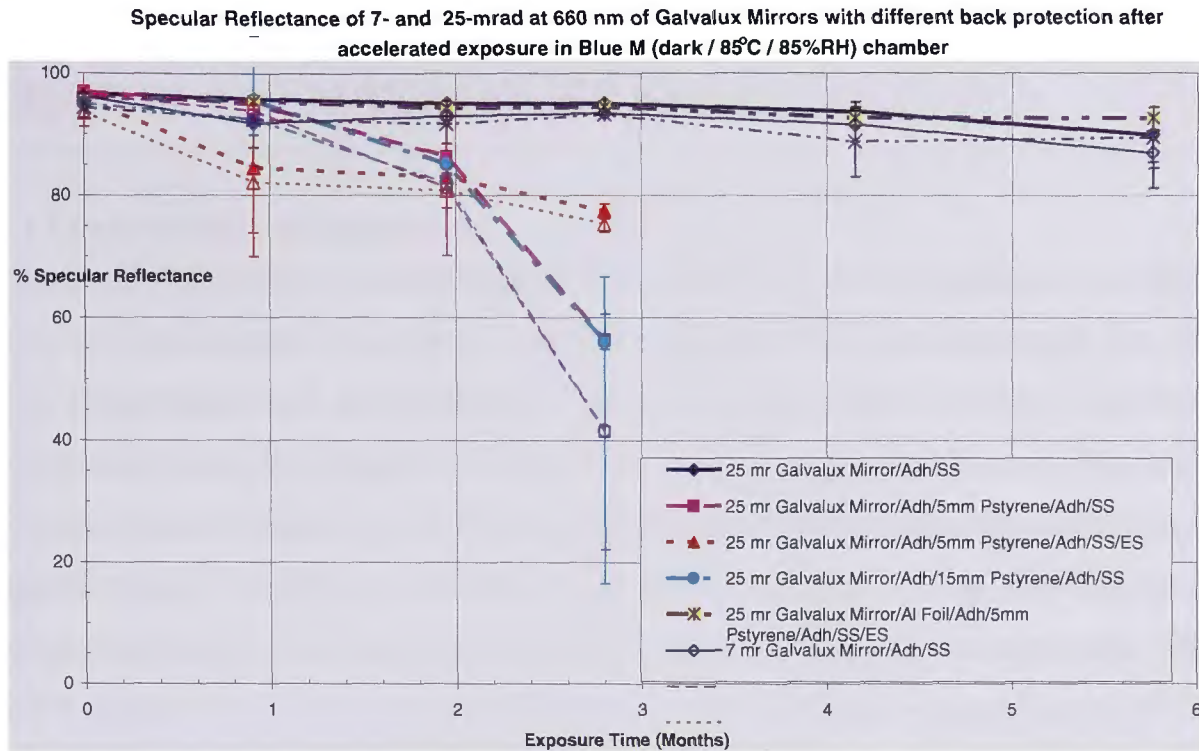


Figure 7-1: Graph shows aging effects for a range of mirror panel configurations under accelerated aging by exposure to 85% humidity and 85°C. The indication is reflectivity.

7.10 Mechanicals

The mechanical reliability is reflected in the system availability. The developmental systems in operation total approximately 1.5MW with an average annual availability of about 95%. After recent improvements, availability of about 99% has been achieved.

7.11 Maintenance

All of the active components are contained in the receiver. A complete 35kW CPV receiver can be exchanged in 30 minutes. See Figure 7.2.



Figure 7-2: Changing a CPV receiver to upgrade to a more efficient PV technology takes only ~ 30 minutes

CHAPTER 8. FUTURE WORK AND PROJECTIONS

8.1 Limits on the Minimum Cost

In assessing the value of a technology, it is necessary to have an insight into the ultimate cost and performance of the system when fully optimised and mass produced. The 130 m² dish concentration unit, as described in Chapter 5, is not perfect or fully developed and an opportunity exists for further performance enhancement and cost reduction. Potential areas of improvement include optical efficiency; reduction of infant mortality and burn in; optimization of control and maximum power point tracking; reduction in parasitic power; power matching of modules in the receiver and increasing the concentration ratio. The table below quantifies the present performance and the possible improvement in each of these areas. Explanatory descriptions are given for each case. To determine the cost of the mass produced unit at 500 MW/year, a 'Learning Curve' model using a representative industry Progress Ratio (PR) was applied in to the baseline cost. Two scenarios were considered to show the sensitivity of (conservative) 90% and (more optimistic) 80% PR. The combined results of the cost reduction and performance enhancement were input the LCOE model to compute reduced cost/kWh of electricity at high volume production shown in Figure 8-2. The limits are reached when the system cost approaches the material cost, that is, the cost of the technology has been paid off.

8.2 Possible Performance Improvements for MkV 130m² Dish

Excluding cell efficiency improvement, shown in Figure 6-1 there is potential for a total of about 20% improvement in dish performance without significant increase in bill of material (BOM) cost. Present estimates are shown in Figure 8.1.

Focus Area	Now (Estimated)	Future (Possible)	Delta (possible gain)	Estimated Time (yrs) to Execute	Additional Cost to Dish
Cell Infant Mortality/ Burn in	4 - 6% loss	1-2%	3-4%	0.5-1	0-1%
Optical Efficiency	84%	88%	4%	0.5	0-1%
Control Maximum Power Point, Tracking Optimisation	97%	98-99%	1-2%	0.5-1	0-0.5%
Parasitics Reduction			1%	0.5-1	0-0.5%
Power Matching	1-4% loss	1-2%	1-2%	1	1%
Increase Concentration Ratio	500x	600x	10% (Net)*	2	6%
Total			20-24%		

* Allows for 6% cost increase

Figure 8-1: ‘Other efficiency’ areas of possible performance improvements for 130m² Dish CPV System presently operating at 500x. These are improvements in system ‘other’ than module improvements.

8.3 Infant Mortality

This would require the collection of failure mode data analysis to correlate field failures/degradation and development of screening methods to avoid the initial degradation of performance of 4-6%. While Dish 2W (after 1 year running with Rx 61) at Hermannsburg is still above its nominal pro-rata P_{DCSTC} output, namely 35.7 kW (for 35.7% efficient modules), the initial performance appears to have been greater than 37kW. If infant mortality/degradation could be isolated, its root cause could be determined and eliminated. The actual output would stay about 3-4% relative above our nominal ratings and thus it would be possible to increase the name plate power rating for P_{DCSTC} and P_{NAC} which would reduce the LCOE.

8.4 Optical Efficiency

Preliminary analysis of the data from 2W obtained at Hermannsburg indicates that while the addition of the long focal length mirrors have increased the overall output (by improving the light flux distribution to the cells) the optical efficiency seems to have reduced from a typical 88% that we expect for a standard dish versus about 83%-84% which is obtained from the long focal length version. It is planned to carry out an optical power audit of 2W Dish at Hermannsburg to determine if this is the case and how much improvement is potentially available. Once this is established a program of further research will be initiated to improve the optical efficiency and this will include optical modeling to determine how much gain could be achieved by varying the parameters of improved mirror alignment, mirror focal length, receiver position, flux modifier length and aperture. Success in this area would increase P_{DCSTC} and P_{NAC} and thus reduce LCOE.

8.5 Increased Concentration Ratio

It is possible to use the same receiver and the balance of system with an increase in the collector size by up to 20% resulting in a concentration ratio of 600 suns. This would increase the output by about 16% with the sub-linearity due to the slight reduction in optical efficiency, higher cell temperature and a less favorable operation point on the concentration verses efficiency curve. The inverter size would be increased by 16% and the cooling system can remain the same size since the module efficiency (at 40%) will offset the increased concentration. With an expected 16% increase in power output and a 6% increase in cost, gives a net improvement of about 10%.

8.6 Control Maximum Power Point, Tracking Optimisation

Presently the Maximum Power Point (MPP) voltage is fixed. An algorithm deriving MPP from cell temperature and concentration ratio has been developed and would optimize the MPP voltage for all conditions. It is possible that by tuning the maximum power point tracking and the dish tracking to match the latest design changes may result in an increase of 1-2% relative energy output. This will not increase the P_{DCSTC} but will increase P_{NAC} and reduce LCOE.

8.7 Parasitics Reduction

The auxiliaries associated with the present systems are not fully optimized. It is possible to adjust the cooling parasitics with output, thus consuming less power.

8.8 Power Matching

It is possible to recover some of the (1-4%) power presently lost in the receiver due to flux variation. The value of this depends on the cost and reliability of additional electronics. A 1% increase in output could justify a cost of \$1,000.

8.9 Enhanced Monitoring, Replacement and Possible Recycling of Cells/Modules

Presently there is about a 1%-2% relative loss in output at a nominal module change-out rate of about 1 module per year. A monitoring system which could automatically identify poorly performing modules and flag them to be changed could mean a higher average of output of 1%-2%. It is possible to recycle the cells/modules so that the receiver is always kept at its maximum output rather than just using the nominal O&M change-out rate which is 0.5 modules/year for the purpose of O&M modeling in the LCOE.

	Units	Year							
		Baseline	2009	2010	2011	2012			
Module efficiency *	%	36.5	36.5	38.0	40.0	42.0	45.0	50.0	
Other Improvements									
Other efficiencies **		1.0	1.03	1.05	1.08	1.1	1.1	1.1	
Increase concentration to 600x		1.0	1.0	1.0	1.1	1.1	1.1	1.1	
Total		1.0	1.0	1.1	1.2	1.2	1.2	1.2	
Total net performance improvement		1.00	1.03	1.09	1.30	1.39	1.49	1.66	
PDCSTC	kW	36.5	37.6	39.9	48	51	54	61	
PACNOC (= PDSTC x 0.85)	kW	31.0	32.0	33.9	40.4	43.2	46.3	51.4	
PNAC (= PDSTC x 0.835)^^	kW	30.5	31.4	33.3	39.7	42.4	45.5	50.5	
Cost/WAC Turn Key at 65MW/yr production rate	US\$/WAC	4.00	3.88	3.66	3.07	2.87	2.68	2.41	
LCOE (from LCOE Model)	US\$/MWh	88.05	85.47	80.54	66.95	63.01	59.51	52.68	
Cost/WAC Installed at 500MW/yr production rate ***	US\$/WAC	2.88	2.80	2.63	2.21	2.07	1.93	1.74	
LCOE (from LCOE Model)	US\$/MWh	70.46	68.40	64.46	53.58	50.43	47.63	42.16	
Cost/WAC Turn Key at 500MW/yr production rate ^	US\$/WAC	2.00	1.94	1.83	1.54	1.44	1.34	1.21	
LCOE (from LCOE Model)	US\$/MWh	56.64	54.99	51.82	43.07	40.54	38.29	33.89	

* Refer to module efficiency in Section 6.1

** Refer to Figure 8-1

*** Refer to Appendix 8, we have assumed a Progress Ratio of 0.9 or 10% cost reduction per doubling of cumulative production which would represent a typical but conservative learning curve for PV systems and other mass produced goods. (Attached)

^This is a progress ratio of 0.8 or 20% cost reduction, which has been typical for the PV industry.

^^ This takes into account TRANSOP losses but excludes dish dirt losses.

Figure 8-2: Summary of effect on LCOE by performance enhancement and 'learning curve' cost reduction.

Tax incentives, as presently available in the USA, are included in these calculations.

It can be seen that using typical Learning Curve Progress ratio's of 0.9 and 0.8 to extrapolate the capital cost/W in US\$/W_{AC} from \$4 to \$2.88 and \$2.00/W respectively gives rise to a range of (subsidised) LCOE's potentially as low as \$40/MWh at a production rate of 500 MW/yr with a module efficiency of 42%. This is competitive with any fossil based power generation cost. If the tax incentives are not included, the LCOE for this technology approaches about \$70/MWh and is competitive with 'clean' coal.

8.10 Other Formats

A dense array CPV system may be deployed in several different formats including dish and central receiver embodiments.

8.11 HCPV

Large CPV power stations using dish technology clearly require a great number of distributed units for utility scale applications. The disadvantage of distributed units is the increased amount of physical infrastructure (wiring, cooling, power conditioning, etc.) and large number of small receivers. The ability to combine many of the active components into large central receivers in a Heliostat Concentrator PV (HCPV) configuration takes advantage of economies of scale, giving potential to significantly reduce system cost, as well as operation and maintenance cost. This is analogous to the advantages of central receivers vs. dishes for solar thermal applications. However, like for solar thermal applications, there is a performance penalty with HCPV due to the nature of heliostat tracking a fixed target (tower located receiver) compared to a dish tracking the sun directly. On the other hand, unlike thermal systems, the efficiency is not dependant on scale and this additional degree of freedom allows much greater flexibility in choosing the size of the 'repeatable optimum field unit'. Performance modelling, correlated by actual test results, and cost estimates by the researcher and co-workers indicate significantly lower capital and energy cost potential with HCPV. The transfer of the essential technology into the heliostat (central receiver) format was successful and achieved the target performance as designed. Much of the dish technology experience, including experience with dense array receivers, mirrors, tracking, control, cooling and management system, has been either directly applied or easily scaled up for the initial demonstration of 140 kWp. In our case, the scaling step has been relatively small to ensure high confidence in a successful

demonstration and to quickly develop an understanding of the performance, operational and cost differences of any new technology, e.g. heliostat structures, controls and CPV receiver response.

The concept of a PV central receiver system was originally presented by Swanson, 1992. Photovoltaic central receiver systems or Heliostat CPV (HCPV) have the potential to be the optimum solar energy generation system for utility scale because it combines all the advantages of CPV (high-efficiency, high capacity factor, low cost). It centralizes the electric generation in a high-power central receiver, avoiding the cost of power and cooling fluid reticulation over a large field, and can have a collector field of heliostat chosen for minimum cost per area. Since the efficiency of HCPV is substantially independent of scale, this technology has considerable scope to minimise the cost by selecting the appropriate power blocks and subsystems with the lowest cost of fabrication, installation and O&M. In general, the total installed cost of a solar power station can be minimised by:

- Minimizing the amount of equipment to be deployed per MWp. This is substantially driven by efficiency and concentration ratio. Our 36cm² dense array module with an efficiency of 37% at 500X (Lasich, 2008) is emerging as the most efficient solar energy converter available.
- Maximizing the proportion of pre-fabricated sub-systems, for example an appropriately sized heliostat can be factory assembled, pre-commissioned and shipped to site as a complete unit. As another example, 1MW-scale HCPV receiver can be pre-assembled in factory and shipped to site in one piece.
- Rationalizing the infrastructure to reduce cost by minimizing field reticulation and cooling. For HCPV, concentrated light is used as the actual transfer medium to bring a large amount of power to a central point. A smaller number of large sub-system blocks are used to convert light to AC electricity. Typically larger components have a lower specific cost per MWp and greater efficiency.

Traditional wisdom is that heliostat fields are typically 20% less efficient than dishes. If we consider just the simple optical efficiency this is generally true. If however a heliostat field is fully optimised for a particular location and adjustments are made to dish efficiency to represent the 'effective' energy generating capacity for a given mirror area, the results are quite different and somewhat surprising.

We see that by the time we collect, convert and connect to the grid the difference is very small (based on these indicative calculations) and probably less than 5% when the sensitivity is tested.

Dish modelled optical efficiency (Typical) = 90%

Modelled **energy weighted** optical efficiency for HCPV = 79%

To obtain a more realistic comparison of the ability of these systems to generate net kWh, the following adjustments shown in Figure 8.3 can be made.

Adjustments to dish performance to compare to HCPV				Factor
Total Mirror Area	=	$\frac{\text{Dish projected area}}{\text{Total mirror area}} = \frac{129.7}{135.5}$		0.957
Field losses	=	$\frac{\text{Dish field losses (1.50\%)}}{\text{Heliostat field losses (0)}} = \frac{0.985}{1.00}$		0.985
Parasitics				
Pump	Dish (Target 2010)	500W	= 2%	0.99
	HCPV large pump with high efficiency		= 1%	
Fan	Dish (Target 2010)		= 2.5%	0.99
	HCPV (Some Wind Cooling)		= 1.5%	
Dirt Cleaning – easier cleaning for HCPV than dish, assume for same cost of washing can get 1% improvement				0.99
Flux distribution?	Same 0%-3%			1.02
Inverter efficiency (larger inverter and higher voltage)				0.99
Shading				0.97
Dish	= 3%			
HCPV shading already included in model = 0%				
Total Derate for Effective Dish Optical Efficiency				0.896

Figure 8-3: Adjustments to dish performance to compare to HCPV

For comparison purposes only this 'derate' of 0.896 could be applied to the dish optical efficiency. This results in an 'Effective' optical efficiency for the Dish of 81%.

Thus it can be seen that there is minimal difference between 'effective' performance of dishes at 81% and HCPV at 79%. This it can be seen that when other factors are taken into account the handicap of the central receiver system in this case is quite small.

Some other advantages of HCPV over Dishes

- Wind loading being less critical implies that the cost in foundations could be reduced;
- Washing is easier – heliostats can be smaller and flatter;
- Complete prefab of receiver and heliostat possible;
- No field wiring if it is solar powered radio controlled;
 - (10W at \$3/W = \$30/heliostat from the solar panel)
- Possibly less fire risk;
- Better co-generation options;
- Ability to use extra heliostats during low intensity hours to keep plant at maximum output;
- Other thermal applications or H₂ generation possible e.g. beam down; and
- Evolving production technology supports high volume repetitive production.

A larger receiver has more options to achieve high voltage (720V could save 1% in MW transmission and inverter loss).

Figures 8-4 and 8-5 show the world's most powerful CPV array and 140 kW central receiver CPV system on sun.



Figure 8-4: The researcher with the world's most powerful CPV array. The array has an area of slightly less than 1m^2 and a power rating of 140kW at 500 suns. The $140\text{kW}_{\text{DC STC}}$ system achieved specified performance with a peak DC efficiency of 25% including optical losses.



Figure 8-5: 140kW central receiver system on sun.

8.12 Small Domestic

A small CPV dish as shown in fig 8-6 is capable of producing 500W of electricity and 1000W of heat. This configuration could find economic application for small domestic sites where the 'thermal' power has high volume.

8.13 Other Applications

Concentrated solar radiation can produce very high temperatures of more than 2000°C or more (Lasich 2008) capable of driving many industrial processes which require heat. The researcher recorded a peak flux of approximately 2000 suns using the 'wand' in the small dish (fig.8-6) and melted Zirconia which melts at above 2200deg C. For example, 'calcining' cement is a major consumer of energy which could be driven directly from concentrated solar power. In this manner the overall energy efficiency can be greatly enhanced by avoiding the energy conversion step of producing electricity. The efficiency of this approach could be above 50%.

Another approach is to apply components that are developed for CPV to other 'non solar' applications. For example the CPV receiver could be used for thermophotovoltaic (TPV) applications where the solar cells are driven by another light source such as radiation from a selective emitter heated by natural gas.

8.14 Cogeneration

8.14.1 PV Power and Low Temperature Heat

It is relatively simple to use the low temperature heat (40⁰C) contained in the cooling water. This is only of value if there is a matching use e.g. fish farm requiring low grade heat for the hatching pond operating at 28°C.

8.14.2 Spectrum Splitting

High Temperature Heat

This method of obtaining high temperature heat simultaneously with PV generation was invented and demonstrated by the researcher. (See Lasich 1993, AUS731495). The system splits out long wavelength light at wavelengths longer than 1.1µm and refocuses it to a light

guide which can pipe the light to a point of use. A temperature of 1000°C can be achieved by using this technique.

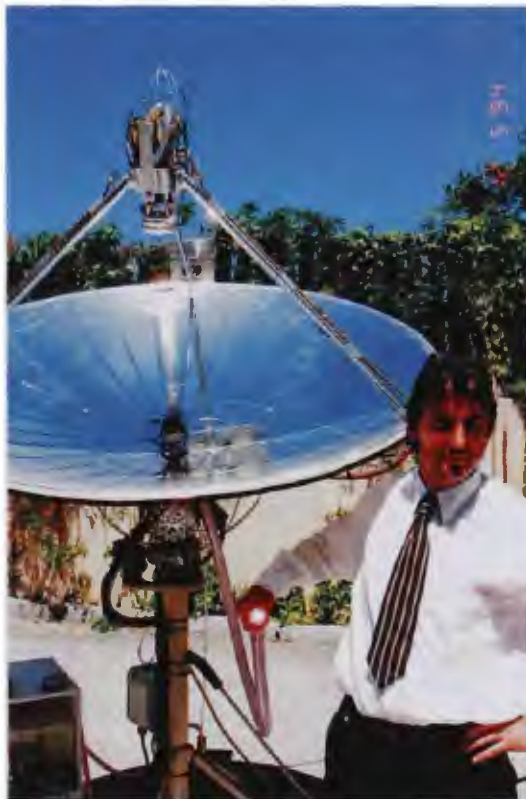


Figure 8-6: The researcher demonstrating a small CPV dish with a spectrum splitter invented by the researcher (Lasich, 1993). Piped light is produced at the same time CPV power is being produced.

Hydrogen

The above method may also be used to provide DC electricity and heat simultaneously to drive an ultra high efficiency hydrogen electrolysis process (see Figure 8-7). This has been demonstrated by the researcher and is described in Patent No AUS731495 and McConnell, Lasich and Elam, 2005.

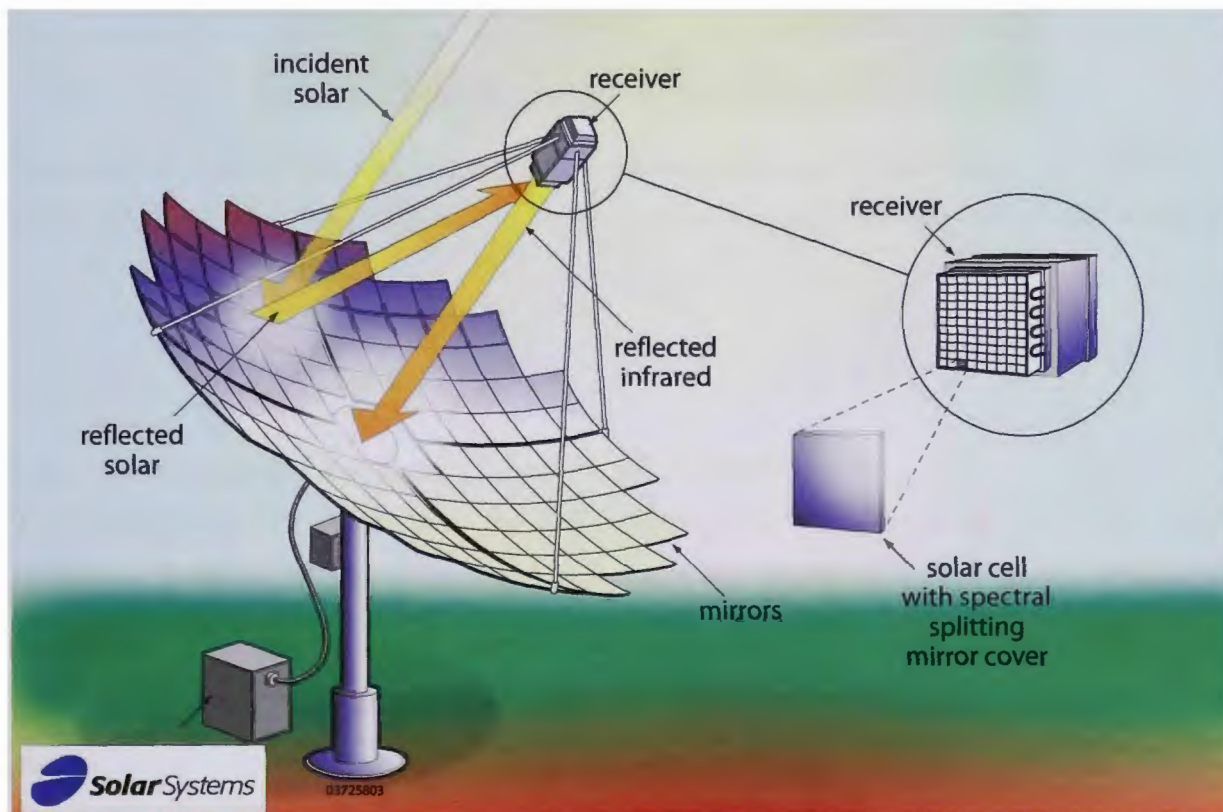


Figure 8-7: Shows basic principles of CPV dish system with spectrum splitter which reflects infrared radiation to be collected of the vertex of the dish

8.15 Thermal Applications

In this case only heat was generated from the concentrated beam to reform natural gas to produce hydrogen. The peak concentration was 1500 suns. The solar thermal dish in Figure 8-8 was optimised to operate at approximately 1000 suns for hydrogen production by reforming natural gas at 750°C (Edwards, 2002).



Figure 8-8: Hydrogen Dish designed and built by the researcher and co-workers for the CSIRO to reform natural gas at 750 deg C to make hydrogen. The black louvers are to regulate the concentrated solar power.

8.16 Correlation of Efficiency Improvements with Sales

It is noted by the researcher (Lasich, 2007) that there appeared to be a correlation between advancing system efficiency and market demand for the system, with the log of annual production over time being roughly proportional to the efficiency increase. If this relationship could be established, it could provide a strong supporting argument for investment in improving system efficiency. This could in turn increase the penetration into the market and accelerate the use of clean renewable solar power.

8.17 Embedded Energy and Energy Payback Ratio

The researcher has made an estimate of the ‘embedded energy’ in the 130m² dish system, with the resulting payback time being approximately 1 year with an ‘energy payback ratio’ over 25 years of approximately 20 times. This estimate appears to be supported by (Peharz, 2005) who estimates 0.9 years for the ‘Flatcon concentrator system’. It is interesting to note that according to (Meijer, 2003) and (Gagnon, 2005) this would place concentrator systems as being similar to wind power and more favorable than flat plate PV which has a payback time of 3 to 6 years. It is also interesting to note the inherent design which reduces embedded energy also minimizes product rollout constraints due to exotic material availability, with annual production rates of several TW/year being possible at 500 suns.(Kurtz.S.2008)

CHAPTER 9. PROJECTS DESIGNED AND BUILT BY THE RESEARCHER AND CO-WORKERS

The CPV technology developed by the research has been deployed in 5 power stations in central Australia with a total of almost 1 MWp installed. At the time of writing the total energy generated from these plants is more than 3 GWh with 1.5 GWh being generated from multijunction CPV dishes and central receiver. The power station sites are, in chronological order:

- *White Cliffs, New South Wales*
 - 14 parabolic dishes (1980's solar thermal systems, reconfigured in 1998 for PV generation, retired in 2004)
 - 250X optical concentration (25 W/cm²)
 - Point-Contact silicon cells
 - Total peak DC power: 40 kW
 - Returned field experience, demonstrated 20% efficiency and gave insight for future developments

- *Fosterville, Victoria*
 - Testing facility of Solar Systems
 - 2 parabolic dishes of 20 kWp each
 - Point-Contact silicon cells at 45 W/cm²
 - Used for system development and R&D

- *Pitjantjatjara, South Australia*
 - 10 parabolic dishes installed since 2002,
 - Total peak DC power: 360 kWp

- *Hermannsburg, Northern Territory* (See Figure 9-1)
 - 8 parabolic dishes installed since 2005
 - Total peak DC power: 190 kWp

- *Yuendumu, Northern Territory*
 - 10 parabolic dishes installed since 2005
 - Total peak DC power: 240 kWp

- *Lajamanu, Northern Territory:*
 - 12 parabolic dishes installed since 2006
 - Total peak DC power: 290 kWp



Figure 9-1: Hermannsburg 190 kWp power station. Dish 2W discussed in Chapter 5 is second from the right.

CHAPTER 10. CONCLUSIONS

The hypothesis was that there is a new pathway to lower the cost of solar power and to prove that a high concentration PV system with a separate collector and ‘dense array’ receiver could be shown to work reliably, achieve high efficiency and have the potential for low cost. If this hypothesis were to be satisfied a number of challenges had to be met including:

- Developing and cooling a photovoltaic receiver which could work efficiently and reliably in a concentrated light beam which can melt steel
- Developing the first ‘back contact’ multijunction CPV cell
- Developing and correlating a realistic ray tracing/receiver model
- Developing an optical system which can deliver an evenly distributed light beam to the PV cells at 500 suns intensity
- Tracking and managing the system to maintain high performance over long periods of varied weather conditions and loads
- Monitoring and measuring the performance and reliability of these subsystems requiring new techniques and metrics to be developed

All of the above problems were solved resulting in a new ‘reflective-dense array’ technology with a peak DC STC efficiency of more than 28% at 36kW. The researcher believes this system may have the highest long term performance published for any solar power system at 22% average annual AC efficiency (Lasich, 2009) and the system:

- Has operated for 6 years with quantified output (using multijunction cells for the last 3 years) producing over 4 GWh in total with 1.5 GWh from multijunction cells.
- Has potential for low capital cost $\$4/W_{AC}$ at 50MW/year and less than $\$2/W$ at 500MW/year with an unsubsidised LCOE at $\$100/MWh$. This is competitive with coal fired power stations which account for their pollution.

- Has a maximum scope for continued improvement in performance since the efficiency of a small area of cells can continue to increase at the present rate of 1% absolute per year with little influence on the system cost.
- Has scope for two different formats of CPV as a dish or central receiver and has diverse application for cogeneration or other high value applications such as hydrogen production for storage or fuel. The peak efficiency for cogeneration is estimated to be 60%.

During the journey of this research, a number of other discoveries were made in relation to this unique CPV system with reflective collector optics and a separate receiver/energy converter, including:

- Containment of all the complex components of CVP modules, monitoring and secondary optics in a small demountable receiver
- Has a very low manufacturing cost at less than one tenth of the plant cost for a 'one sun' PV module plant for a given production rate.
- Can be fully monitored and managed 'on line' at low cost resulting in reduced O&M and high average efficiency
- Can be simply upgraded by changing the receiver in less than one hour.
- Reflective optics with a single receiver are more efficient than refractive optics with many targets because; 1. Mirrors have a reflectivity of 95% whereas lenses have transmission up to 90%, 2. Alignment is less critical for many mirrors aimed at a single target and 3. Feedback can be used to almost perfectly align a single solar beam with the needs of a single array of CPV cells.
- CPV systems have the lowest embodied energy of any solar power system (approx 1 year) being comparable to wind turbines but with a far greater resource available.
- With the power output of the CPV modules being more than 1000 times greater than the typical thin film module (of the same area), CPV is unlikely to be constrained by limited supplies of exotic materials.

- The modular dense array receiver can be deployed at any scale from a single module 500W receiver in a small dish to a 256 modules in a 140kW receiver for a central receiver. With 40% efficient cells a 1 MW dense array is just 6 m². This allows a great degree of pre-fabrication and pre-commissioning for large scale roll out.
- Reflective concentrator systems with a high power single beam as developed by the researcher for CPV are versatile and can be used for other applications which do not include PV. This gives greater value to the concentrator system technology.
- The 140 kW central receiver 'HCPV' system produced a peak DC efficiency of 25% (equivalent to 22 % AC) which is possibly the highest efficiency recorded for a central receiver system.

The sum of these findings is that a CPV system with reflective optics and a separate dense array PV receiver is the most efficient of any solar power technology and has a clear pathway to a competitive cost. With its unique potential for continuous improvement and diverse application this is likely to be one of those technologies which can take our world one step closer to the 'balance' we need for sustained occupation of this planet

Also during the period of this research (10 years) there has been considerable change in the 'other' two components of the 'critical mass' referred to in the introduction, namely: social awareness of energy and pollution issues are now topics aired daily in the media and are discussed by and concern the public at large. Today 46 countries have publically stated their greenhouse reduction targets (The Age, 3 November 2009).

- Traditional energy costs have also increased considerably with the oil price more than doubling since writing the introduction.
- A second part of the 'technical solution' on the demand side has also received considerable attention with energy efficiency being supported by governments and embraced by consumers.

I think the state of affairs is well reflected by the economics editor in *The Age*, 21 November 2009 who stated 'Nationally, some 30,000 MW of future power projects are on the drawing board, of those 10,000 MW are from wind, along with 9,500 MW from gas and 3250 MW of coal'. With just 10% of new projects planned to be coal fired perhaps the world *is* turning.

CHAPTER 11. REFERENCES

- Avallone EA and Baumeister, T (Eds), 1987, *Mark's Standard Handbook for Mechanical Engineers*, McGraw Hill, USA.
- Bird, R. E., "A Simple Spectral Model for Direct Normal and Diffuse Horizontal Irradiance," *Solar Energy*, Vol. 32, 1984, pp. 461-471
- Blakers, A, Green, M, Leo, T, Outhred, M, and Robins, B, 1991, *The Role of Photovoltaics in Reducing Greenhouse Gas Emission*, for the Department of the Arts, Sport, Environment, Tourism and Territories.
- BP Global, 2009, *Statistical Review of World Energy 2009 Report*, BP Global
- BP Solar, 1994, Products and Specifications Summary, *Efficiency of BP270 = 11.1% (\pm 5%) at Standard Conditions of 100m W/cm^2 (ie 1000 W/m^2) Light Intensity (AM 1.5) at $25\text{ }^\circ\text{C}$ Cell Temperature, Measured at the + - Braids in the Junction Box.*
- Braun, HW, 1992, 'Solar Stirling Gensets for Large-scale Hydrogen Production', *Solar Energy Technology*, SED, ASME, USA, Vol 13 , pp 21-31.
- British Petroleum 2009, *Statistical Review of World Energy*
- Burgess E.L. and D.A. Pritchard, 1978, "Performance of a One Kilowatt Concentrator Photovoltaic Array Utilizing Active Cooling", *proc. 13th IEEE Photovoltaic Specialists Conference*, pp.1121-1124
- Ceramic Fuel Cells Limited, 1994, *Highlights 1994*, Clayton, Victoria.
- Charters, WWS, March 1995, Lecture *Renewable Fuels*, University of Melbourne
- Cleeve A.X., Lasich J.B., Skinner R.A, "Making Concentrated Photovoltaics a Competitive Reality", *The 4th Renewable Energy Technologies & Remote Area Power Supplies Conference 1998 Drivers and Markets for Renewables*.
- Concentrix marketing presentation, 2009 "The new generation of solar power"
- Coventry J.S., Blakers A., Franklin E., Burgess G., 2009, *Analysis of the Radiation Flux Profile Along a PV Through Concentrator*.
- Curzon, F.L. and Ahlborn, B., 1975, *Am. J. Phys.*, 43:22
- Czanderna A.W., 2006, "Encapsulation of PV Modules Using Ethylene Vinyl Acetate Copolymer as a Pottant: A Critical Review", *Solar Energy and Materials and Solar Cells*, Elsevier Science, Vol. 43, Issue 2.

- Davenport, R L, 1992 'Design & Fabrication of a Photovoltaic Dish Concentrator System', *Solar Engineering*, ASME, Vol 1
- Duffie, J.A. and Beckman, W.A., 1991, *Solar Engineering of Thermal Processes*, John Wiley & Sons Inc.
- Dunn, PD and Reay, DA, 1982, *Heat Pipes*, Pergamon Press.
- Edwards J.H., Badwal S.P.S, Duffy G.J., Lasich J.B., Ganakas G., 2002, "The Application of Solid State Ionic Technology for Novel Methods of Energy Generation and Supply", *Solid Ionic States*.
- Flowers, L, Dodge, D, Swezey, B, and Swisher, R, 1992, 'Utility Scale Wind Energy Update', *1993 American Solar Energy Society Conference Proceedings*, pp 177-183.
- Freidman, D.J et al, 1988, '1-eV GaInNAs Solar Cells for Ultra high efficiency Multi Junction devices', NREL
- Friedman D.J., Kurtz S.R., Sinha K., McMahon W.E., Kramer C.M., Olson J.M, Lasich J.B., Cleeve A.X., Connaughton I., 1996, "On-Sun Concentrator Performance of GaInP/GaAs Tandem Cells", *25th IEEE Photovoltaic Specialist Conference*, pp 73-75.
- Friedman, D.J., 2007, "National Solar Technology Roadmap: Concentrator PV", Dan Friedman. Participants included: National Renewable Energy Laboratory, Sandia National Laboratories, U.S. Department of Energy, University and private-industry experts – DRAFT.
- Gagnon, L., 2005 Hydro-Québec Direction – Environnement July 2005
- Garbousian, V, Personal Communication.
- Gilchrist, G, 1994, "*The Big Switch - Clean Energy for the Twenty-first Century*", Allen & Unwin
- Green M., Emery K., King D.L., Hishikawa Y., Warta W., 2006, "Solar Cell Efficiency Tables (Version 27)", *Progress in Photovoltaics*, Vol. 14, pp. 45
- Green M.A., Emery K., Hishikawa Y., Warta W., January 2009, "Solar Cell Efficiency Tables", *Progress in Photovoltaics*, Wiley Interscience, Vol. 17, Issue 1, pp. 85-94,
- Green, M A and Emery, K, 1993, "Solar Cell Efficiency Tables", *Progress In Photovoltaics: Research and Applications*, Vol 1, pp 225-227
- Heller, P *et al* 2000, "Eurodish the Next Milestone to Decrease the Costs of Dish Stirling Systems Towards Competitiveness", DLR Platforming Solar de Almeria.
- Henry, C.H., 1980, Limiting Efficiencies of Ideal Single and Multiple Energy Gap Terrestrial Solar Cells, *J. Appl. Phys.*, Vol. 51, pp. 4494

- Hock, S, Boer, K W (ed.), 1992, "The Future of Utility-Scale Wind Power", *Advances in Solar Energy*, ASES, Volume 7.
- Holl, R J and DeMeo, EA, 1990, *Advances in Solar Energy, An Annual Review of Research and Development*, Plenum Press, New York, Volume 6.
- Hoy, R and Osborne, J, 1993, "Review of Renewable Energy Technologies for the Generation of Electricity in Victoria", SECV Report No ENU/93/13.
- International Energy Agency (IEA), *Key World Energy Statistics*, 2009.
- Jamal, M A and Muaddi, J A, 1992, "Spectral Response and Efficiency of a Silicon Solar Cell Below Water Surface", *Solar Energy*, Vol 49, No 1, pp 29-33.
- Johnston, G, 1993, "Focal Region Characterisation of Paraboloidal Dish Concentrators", *ANZES Conference*, Perth.
- Jordan, D, BP Solarex, 2000, "Photovoltaics", *6th Renewable Energy Technology and RAPS Conference*. ESAA.
- Kaneff, S *et al*, 2000, "Multi-Megawatt dish based solar thermal electricity generating plant with optional co-generation", Energy Research Centre, ANU/Anutech.
- Kaneff, S, 1992, *Paraboloidal Dishes of 400 m² Aperture and Larger*, ANU Canberra.
- Kaneff, S, 1991, *The White Cliffs Project Overview for the period 1979 - 1989*, for the Office of Energy.
- Kearney, D, 1991, 'Status of the SEGS Plants', *Solar World Congress 1991*, Pergamon Press, Vol. 1, Part 1.
- Kearney, D, *et al*, 1991, "Status of SEGS Plants", *Solar World Congress*, Pergamon Press, pp. 545-550.
- Keyes, B., 2007, "National Solar Technology Roadmap: Film-Silicon PV", Brian Keyes. Participants included: National Renewable Energy Laboratory, Sandia National Laboratories, U.S. Department of Energy, University and private-industry experts – DRAFT.
- King R.R. *et al.*, 2005, "Pathways to 40%-Efficient Concentrator Photovoltaics", *Proc. 20th European Photovoltaic Solar Energy Conf.*, Barcelona, pp. 6-10
- King R.R., D. C. Law, C. M. Fetzer, R. A. Sherif, K. M. Edmondson, S. Kurtz, G. S. Kinsey, H. L. Cotal, D. D. Krut, J. H. Ermer, and N. H. Karam, June 2005, "Pathways to 40%-Efficient Concentrator Photovoltaics". *Proc. 20th European Photovoltaic Solar Energy Conference*, pp.10-11.
- King, R.R. *et al*, 2007, "40 % efficient metamorphic GaInP/GaInAs/Ge multijunction solar cells", *Appl. Phys. Lett.* 90, pp 183516

- Kinsey G.S. et al., 2006, "Multijunction Solar Cells for Dense Array Concentrators", *Proc. 4th World Conference on Photovoltaic Energy Conversion*, Hawaii
- Kinsey G.S., Sheriff R., Piechen Pien, Cotal H., King R., Brandt R., Wise W., Labios E., Wan K., Haddad M., Lacey J., Fetzer C., Verlinden P., Lasich J. and Karam N., 2006, "Multijunction Solar Cells for Dense Array Concentrators", *Proc. 4th World Conference on Photovoltaic Energy Conversion*, Hawaii.
- Kreith F, Goswami D. Y., 2007, *Handbook of Energy Efficiency and Renewable Energy*, CRC Press Taylor & Francis Group, USA.
- Kreith, F, 1992, "Solar Thermal Systems in Least Cost Energy Analyser", *ASES Proceedings*.
- Kurtz, S., 2008, "Opportunities and Challenges for Development of a Mature Concentrating Photovoltaic Industry", NREL/TP-520-43208
- Kurtz, S., Lewandowski, A. and Hayden, H., 2004, *Recent Progress and Future Potential for Concentrating Photovoltaic Power Systems*, NREL/CP-520-36330, 2004
- Landsberg, P.T. and Markvart, T., 2003, *Practical Handbook of Photovoltaics – Fundamentals and Applications*, Elsevier Advanced Technology, Oxford
- Landsberg P.T. and Badescu, V., 1998, 'Solar Energy Conversion: List of Efficiencies and Some Theoretical Consideration', *Prog. Quantum Electronics*, Vol. 2, pp. 211-231.
- Lasich J.B., 1975, 'An Investigation of a Solar Concentration – Solar Cell System'.
- Lasich J.B., "Photovoltaic Concentrator Systems for RAPS"
- Lasich J.B., Birch J., 2008, "Australian Hydrogen Technology for Solar Power on Demand and Transport", *17th World Hydrogen Energy Conference*
- Lasich J.B., Thorpe G.R., 1996, "An Advanced Solar Co-Generation for Remote Communities", *Conference on Engineering in Agriculture and Food Processing*, Paper No. SEAg 96/027
- Lasich J.B., Verlinden P.J. and Holland D., 2007, "Opportunities for Widespread Implementation of Concentrator Photovoltaic (CPV) Systems", *4th ICSC Conference*, El Escorial, Spain
- Lasich J.B., Verlinden P.J., Lewandowski A., Edwards D., Kendall H., Thomas I., Carter S., Wakeman P., Varfolomeev I., Wright M. and Metzke R., 2008, "Large Scale CPV Systems Using Multijunction III-V Solar Cells", *International Conference on Solar Concentrators for the Generation of Electricity*, Palm Desert, California

- Lasich J.B., Verlinden P.J., Lewandowski A., Edwards D., Kendall H., Carter S., Thomas I., Wakeman P., Wright M., Hertaeg W., Metzke R., Daly M., Santin M., Neumann A., Wilson A., Caprihan A., Stedwell M., 2009, "World's First Demonstration of a 140kWp Heliostat Concentrator PV (HCPV) System", *34th IEEE Photovoltaic Specialist Conference*.
- Lasich, J B, Cleeve, A, Kaila, N, Ganakas, G, Timmons, M, Venkatasubramanian, R, Colpitts, T and Hill, J, 1994, "Close-Packed Cell Arrays for Dish Concentrators", *First World Photovoltaic Conference*, Hawaii, Vol II, pp. 1938-1941
- Lee H.S., N.J. Ekins-Daukes, M. Yamaguchi, K. Araki, T. Egami, Y. Miyazaki, M. Hiramatsu and Y. Kemmoku, June 2005, "The Temperature Coefficient in 3-J Concentrator Cell by Outdoor Test with 550X Dome-Shaped Fresnel Lens", *Proc. 20th European Photovoltaic Solar Energy Conference*, pp. 10-11.
- Lillington D., Spectrolab, 1999, personal communication.
- Luque-Heredia I. *et al*, 2009, "Tracking System: Performance Issues and Design for CPV Applications", *2nd Concentrated Photovoltaic Summit*.
- Luzzi, A, et al, 2000, "Projected system efficiencies for Dish Solar Thermal", ANU/ANUTECH.
- Mamuram I and Helm P, 1992, "Photovoltaic System Technology", CISE, Italy.
- Mancini T. R., 1968, "Solar-Electric Dish Stirling System Development", Sandia National Laboratories.
- Mandatory Renewable Energy Target (MRET), Australian Government, 2004.
- Markvart, T. and Castaner, L., 2003, *Practical handbook of photovoltaics: fundamentals and applications*, UK Elsevier Science Ltd.
- Maycock, P D, 1993, *Photovoltaic Technology, Performance, Cost and Market Forecast, 1990-2010*, Paul Maycock, Consultant, Casanova, Va.
- Meijer, A., Huijbregts, M.A.J., Schermer, J.J. and Reijnders, L., Progress in Photovoltaics: Research and Applications *Prog. Photovolt: Res. Appl.* 2003; **11**:275-287 (DOI: 10.1002/pip.489) "Life-cycle Assessment of Photovoltaic Modules: Comparison of mc-Si, InGaP and InGaP/mc-Si Solar Modules"
- McConnell R.D., Lasich J.B. and Elam C., 2005, "A Hybrid Solar Concentrator PV System for the Electrolytic Production of Hydrogen", *Proceedings of the 20th European Photovoltaics Solar Energy Conference*.

- Morales, I and de la Rusa, F F, 1992, "Hydrogen Peroxide Photoproduction by Immobilized Cells of the Blue-Green Algae *Arabeena Variabilis*; A Way to Solar Energy Conversion", *Solar Energy* Vol. 49, No. 1, pp 41-46.
- Müser, H.A., 1957, "*Thermodynamische Behandlung von Elektronenprozessen in Halbleiterrandschichten*", *Z. Phys.* 148, pp. 380 in German.
- Myers, D.R., 2000, *An Excel Spreadsheet implementation done by Daryl Myers using equations from the technical report* (Bird and Riordan, 1984), <http://rredc.nrel.gov/solar/models/spectral/>.
- Nijs, J, Mertens, R, Van Oversraeten, R , Szlufcik, J, Hukin, D and Frisson, L, 1997, *Energy Payback Time of Crystalline Silicon Solar Modules: in Advances in solar Energy*, American Solar Energy Society, Boulder, Colorado, Volume II, pp 291-347.
- Noren Products Inc., 1994, *Heat Pipe Data*, California, USA.
- (Northern Territory Power and Water Authority, 2002, personal communication.
- Osuna et al, 2000 "INABENSA, CIEMAT/DER-PSA PSIO: A 10MW Solar Tower power plant for Southern Spain".
- Pacheco, JE et al, 2000, "Summary of the Solar Two Test and Evaluation Program", Sandia National Laboratories.
- Perharz, G., Dimoth, F., 2005 "Energy payback time of the high concentration PV systems FLATCON" *Progress in Photovoltaics: Research and applications* Wiley Interscience.
- Photon International, 2007
- Rabl, A, 1985, *Active Solar Collectors and their Applications*, Oxford University Press, New York.
- Renewable Energy Target (RET) Amendment, Australian Government, 2009.
- Roy, S, Jana, A.K. and Bhowmik, B.B., 1992, "Kinetics of Temperature-Dependent Photoinduced redox reactions in a Photoelectrochemical cell", *Solar Energy*, Vol. 48, No. 4, pp 215-219.
- Sandia, 1991, *Parabolic Dish Photovoltaic Concentration Development*, Contract No 05-4239E, Albuquerque, NM.
- Sherif R. Spectrolab Program
- Shockley W. and Queisser, H.J., 1961, "Detailed Balance Limit of Efficiency of P-N Junction Solar Cells", *J. Appl. Phys.*, Vol. 32, pp. 510
- Siefer G., P. Abbott, T. Schlegl and A.W. Bett, June, 2005, "Determination of the Temperature Coefficients of Various III-V Solar Cells, *Proc. 20th European Photovoltaic Solar Energy Conference*, pp. 10-11.

- Siemens Solar Energy Products Catalogue, 1994, "Efficiency of M110 = 12.7% at 1000 W/m² Solar Irradiance, 25 °C Cell Temperature and Solar Spectral Irradiance per ASTM E892".
- Slade A., Garboushian V., Oct. 2005, "27.6% Efficient Silicon Concentrator Cell for Mass Production", *Proc. 15th Int'l Photovoltaic Science and Engineering Conference*, Beijing
- Smeltink J.F.H., Blakers A.W., Coventry J., 2005, *A 40kW Roof Mounted PV Thermal Concentrator System*.
- Sopori, B., 2007, "National Solar Technology Roadmap: Wafer Silicon PV", Bhushan Sopori. Participants included: National Renewable Energy Laboratory, Sandia National Laboratories, U.S. Department of Energy, University and private-industry experts – DRAFT.
- Stone, KW et al, 2000, "Boeing: 'Performance of the SES Stirling dish'"
- Stone, KW, Garboushian, V, Boehm, R, Hurt, R, Gray, A, Hayden, H, 2006. '*Analysis of five years of field performance of the Amonix high concentration PV system*'.
- Strahan, D., 2007, 'The Lost Oil Shock', John Murray, London, pp. 36-56
- Swanson R.M., 1992, "Photovoltaic Central Receiver Systems", *Solar Engineering*, The American Society of Mechanical Engineers, Book No. G0656B, pp. 1067-1070
- Swanson R.M., 2000, "The Promise of Concentrators", *Progress in Photovoltaics Res. Appl.*, Volume 8, pp. 93-111
- Swanson, R and Sinton, R, 1990, *Advances in Solar Energy. An Annual Review of Research and Development*, Plenum Press, New York, Volume 6
- Swanson R., et al, 1988, 'Simplified Designs for High Efficiency Concentrator Cells' *Sandia Report*, Sandia National Laboratories, 8AN88-0522.
- Swanson, R.M., 1992, "Photovoltaic Central Receiver System, Sunnyvale, California, USA", *Solar Engineering*, ASME, Vol. 2.
- The Age, 21 November 2009, 'Era of Coal Power Passes'.
- The Age, 2009, 'Clean Coal Tehnology Would Make Electricity Up to 78% More Expensive'
- The Age, 2009 "Clean' Power to Lift Demands on Dams', pp.1
- The Energy Supply Association of Australia, Annual Report 2007
- Thornton, J, De Blasio, R and Taylor, R, 1992, "Recent advances in Photovoltaic Applications for Utilities", *Advances in Solar Energy*, Volume 7, Ch 2.

- Verlinden P.J. and Lasich J.B., 2008, "Energy Rating of Concentrator PV Systems Using Multi-Junction III-V Solar Cells", *33rd IEEE PVSC Conference*, San Diego
- Verlinden P.J., Lewandowski A., Bingham C., Kinsey G.S., Sherif R.A. and Lasich J.B., 2006, "Performance and Reliability of Multijunction III-V Modules for Concentrator Dish and Central Receiver Applications", *Proceedings of 4th World Conference on Photovoltaic energy Conversion*, Hawaii, pp. 592-597
- Verlinden P.J., Lewandowski A., Kendall H., Carter S., Cheah K., Varfolomeev I., Watts D., Volk M., Thomas I., Wakeman P., Neumann A., Gizinski P., Modra D., Turner D. and Lasich J.B., 2008, "Update on two-year performance of 120 kW concentrator PV systems using multi-junction III-V solar cells and parabolic dish reflective optics", *33rd IEEE PVSC Conference*, San Diego.
- Verlinden P.J., R.M. Swanson, R.A. Crane, K. Wickham and J. Perkins, 1995, "A 26.8% Efficient Concentrator Point-Contact Solar Cell", *Proc. 13th European Photovoltaic Solar Energy Conference*, Nice
- Verlinden P.J., Terao A., Smith D.D., McIntosh K., Swanson R.M., Ganakas G. and Lasich J.B., 2001 "Will We Have a 20%-Efficient (PTC) Photovoltaic System?", *Proc. 17th European Photovoltaic Solar Energy Conference*
- Verlinden, P, Swanson, RM, Sinton, R & Crane, RA, 1991, "Single Wafer Integrated 140W Silicon Concentrator Module", *Proceedings of the Twenty Second IEEE Photovoltaic Specialists' Conference*.
- Von Roedern, B., 2008, "The Role of Polycrystalline Thin-Film PV Technologies in Competitive PV Module Markets" Preprint B. von Roedern and H.S. Ullal, National Renewable Energy Laboratory. Presented at the 33rd IEEE Photovoltaic Specialists Conference Sandiego, California May 11-16, 2008.
- Von Roedern, B., 2008, "The Role of Polycrystalline Thin-Film PV Technologies for Achieving Mid-Term Market-Competitive PV Modules" B. von Roedern, K. Zweibel, and H.S. Ullal. Prepared for the 31st IEEE Photovoltaics Specialists Conference and Exhibition, Lake Buena Vista, Florida January 3-7, 2005.
- Von Roedern, B., 2007, "National Solar Technology Roadmap: CIGS PV", Bolko von Roedern. Participants included: National Renewable Energy Laboratory, Sandia National Laboratories, U.S. Department of Energy, University and private-industry experts – DRAFT.
- Wenger, H.J., Jennings, C. and Iannucci, J.J., 1990, "Carrisa Plains PV power plant performance", *Conference Record of the Twenty First IEEE*, Vol 2, pp. 844

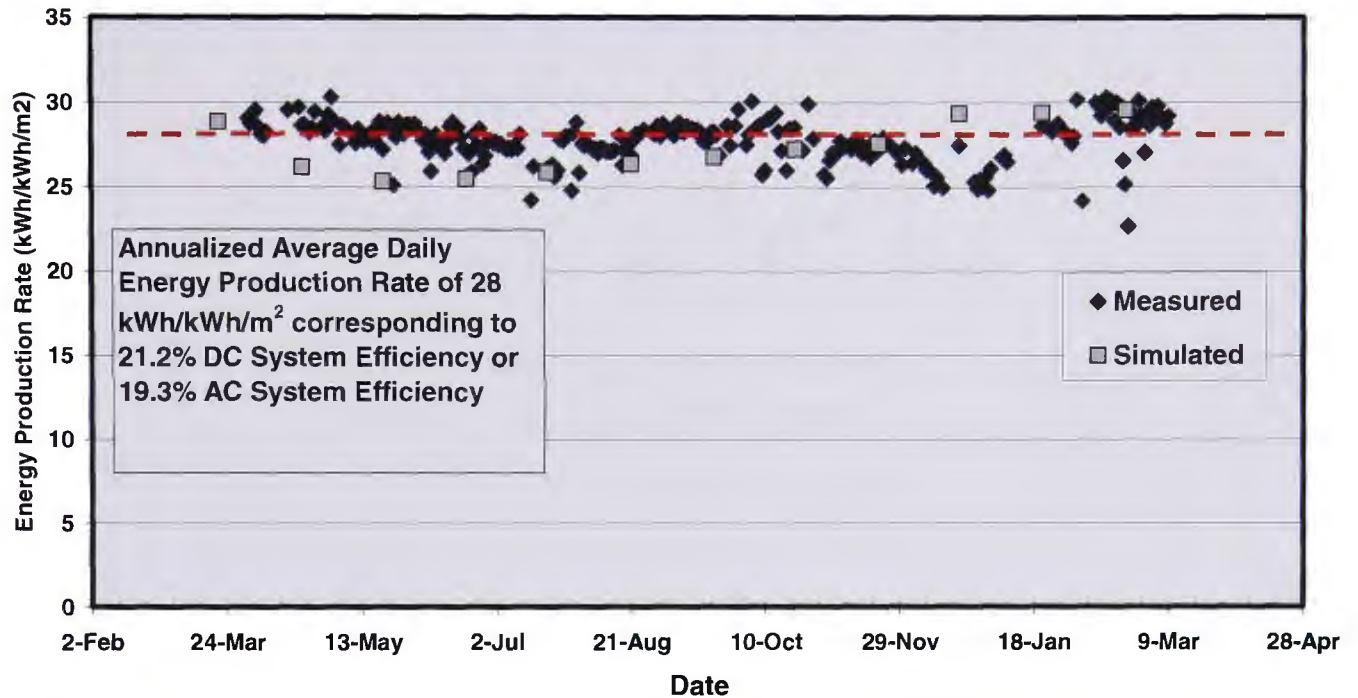
- Werner, J.H., Kolodinski S. and Queisser H.J., 1994, "Novel Optimization Principles and Efficiency Limits for Semiconductor Solar Cells", *Phys. Rev. Lett.*, Vol 72, pp. 3851
- Werthen, J, 1994, Personal communication.
- Wiser, R., Banbose, G., Peterman, C., and Darahouth, N., 'Tracking the Sun II: The installed cost of photovoltaics in the U.S. from 1998 to 2008", Environmental Technologies division, Lawrence Berkeley National Laboratory.
- Yogev, A et al 1998, "Solar 'Tower Reflector' Systems: A New Approach for High-Temperature Solar Plants", *International Journal of Hydrogen Energy*, Elsevier Science Ltd, Vol 23, No 4, pp 239-245.

Patents

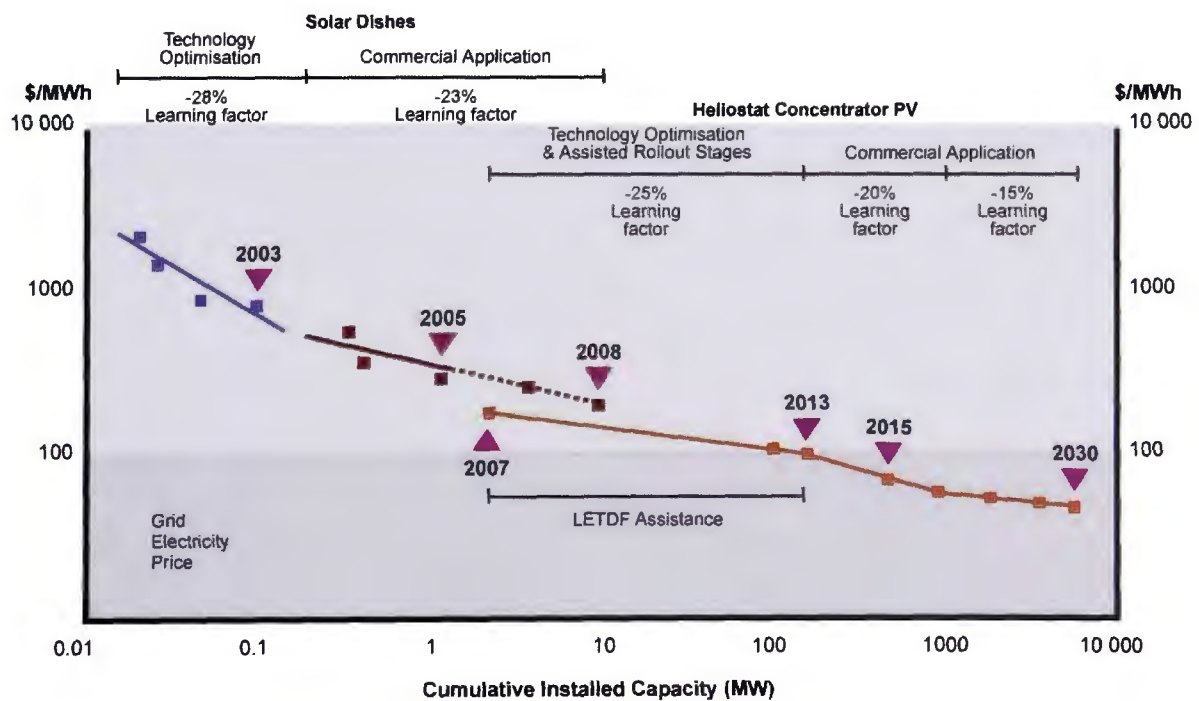
- Lasich J.B., 1993, *Apparatus for Separating Solar Radiation into Longer and Shorter Wavelength Components*, AUS Patent No. 731495
- Lasich J.B., 1993, *Production of Hydrogen from Solar Radiation at High Efficiency*, US Patent No. 5658448
- Lasich J.B., 2001, *Cooling Circuit for Receiver of Solar Radiation*, US Patent No. 7076965B2
- Lasich J.B., 2001, *Solar Tracking System*, AUS Patent No. 200224287
- Lasich J.B., 2001, *Solar Mirror Testing and Alignment*, AUS Patent No. 2002244529B2
- Lasich J.B., 2001, *A Method of Manufacturing Mirrors for a Dish Reflector*, US Patent No: US7550054B2
- Lasich J.B., 2003, *Bypass Diode for Photovoltaic Cells*, AU Patent No. 2004239803
- Lasich J.B., 2003, *Extracting Heat from An Object*, WO Patent Application No. 1661187
- Lasich J.B., 2004, *A Tracking System*, US Patent Application No.US7589302

CHAPTER 12. APPENDICES

Appendix 1 Multijunction Receiver – Daily Energy Production Rate (kWh/kWh/m²)



Appendix 2 Cost Reduction Curve



***Appendix 3 Module Performance for Receiver 61 Using Xenon Flash Test at 500 Suns
and 21oC***

The average module temperature is 35.7°C

Ave Power	643.4	Watts
-----------	-------	-------

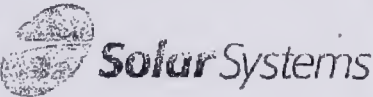
Low	622.69	Watts
-----	--------	-------

High	659.15	Watts
------	--------	-------

Std Deviation	10.1631166	
---------------	------------	--

Appendix 3 cont'd.

Certificate of Performance for multijunction receiver.

CERTIFICATE OF PERFORMANCE		
 		
Date; Time 22/05/2008 11:00:00 AM		
Receiver Serial Number 61		
Operator Name 1		
Cell Temperature During Measurement 18		
Comments 1 module t ds1820		
	As Measured	Corrected 50 (W/cm²) at 21 (oC)
	Voc (V) 310.0	Voc (V) 308.8
	Isc (A) 162.3	Isc (A) 162.9
	Vmp (V) 257.7	Vmp (V) 256.4
	Imp (A) 155.3	Imp (A) 156.4
	FFm (%) 79.5%	FF (%) 79.7%
	Efficiency (%) 34.8	Efficiency (%) 34.8
	Intensity (W/cm²) 50	Output Power (W) 40098.9

Appendix 4 CPV Companies (These tables are a work in progress, since data varies rapidly)

BLANK

Appendix 5 Flat Plate PV (High Efficiency)

SUNPOWER™
315 SOLAR PANEL
EXCEPTIONAL EFFICIENCY AND PERFORMANCE

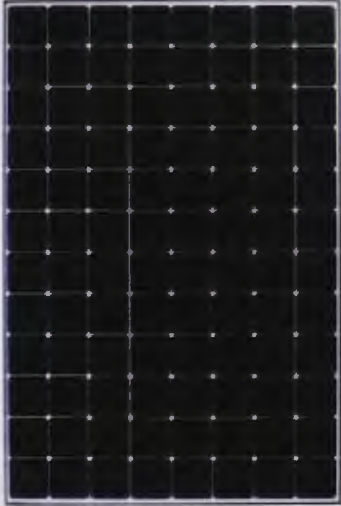
BENEFITS

Highest Efficiency
SunPower™ Solar Panels are the most efficient photovoltaic panels on the market today.

More Power
Our panels produce more power in the same amount of space—up to 50% more than conventional designs and 100% more than thin film solar panels.

Reduced Installation Cost
More power per panel means fewer panels per install. This saves both time and money.

Reliable and Robust Design
Proven materials, tempered front glass, and a sturdy anodized frame allow panel to operate reliably in multiple mounting configurations.



The planet's most powerful solar panel.

The SunPower™ 315 Solar Panel provides today's highest efficiency and performance. Utilizing 96 back-contact solar cells, the SunPower 315 delivers a total panel conversion efficiency of 19.3%. The 315 panel's reduced voltage-temperature coefficient, anti-reflective glass and exceptional low-light performance attributes provide outstanding energy delivery per peak power watt.

SunPower's High Efficiency Advantage - Up to Twice the Power

	Thin Film	Conventional	SunPower
Peak Watts / Panel	65	215	315
Efficiency	9.0%	12.8%	19.3%
Peak Watts / ft² (m²)	8 (90)	12 (128)	18 (193)

About SunPower

SunPower designs, manufactures and delivers high-performance solar electric technology worldwide. Our high-efficiency solar cells generate up to 50% more power than conventional solar cells. Our high-performance solar panels, roof tiles and trackers deliver significantly more energy than competing systems.



SPR-315E-WHT-D



SUNPOWER

315 SOLAR PANEL

EXCEPTIONAL EFFICIENCY AND PERFORMANCE

Electrical Data

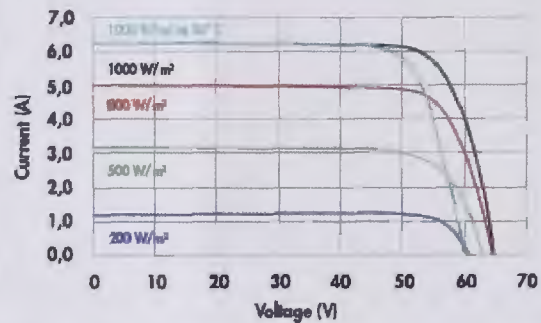
Measured at Standard Test Conditions (STC): irradiance of 1000W/m², AM 1.5, and cell temperature 25° C

Peak Power (+5/-3%)	P _{max}	315 W
Rated Voltage	V _{mpp}	54.7 V
Rated Current	I _{mpp}	5.76 A
Open Circuit Voltage	V _{oc}	64.6 V
Short Circuit Current	I _{sc}	6.14 A
Maximum System Voltage	UL	600 V
Temperature Coefficients	Power	-0.38% / K
	Voltage (V _{oc})	-176.6mV / K
	Current (I _{sc})	3.5mA / K
NOCT		45° C +/-2° C
Series Fuse Rating		15 A

Mechanical Data

Solar Cells	96 SunPower all-back contact monocrystalline
Front Glass	High transmission tempered glass with anti-reflective (AR) coating
Junction Box	IP-65 rated with 3 bypass diodes Dimensions: 32 x 155 x 128 (mm)
Output Cables	1000mm length cables / MultiContact (MC4) connectors
Frame	Anodized aluminum alloy type 6063 (black); stacking pins
Weight	41.0 lbs (18.6 kg)

I-V Curve



Current/voltage characteristics with dependence on irradiance and module temperature.

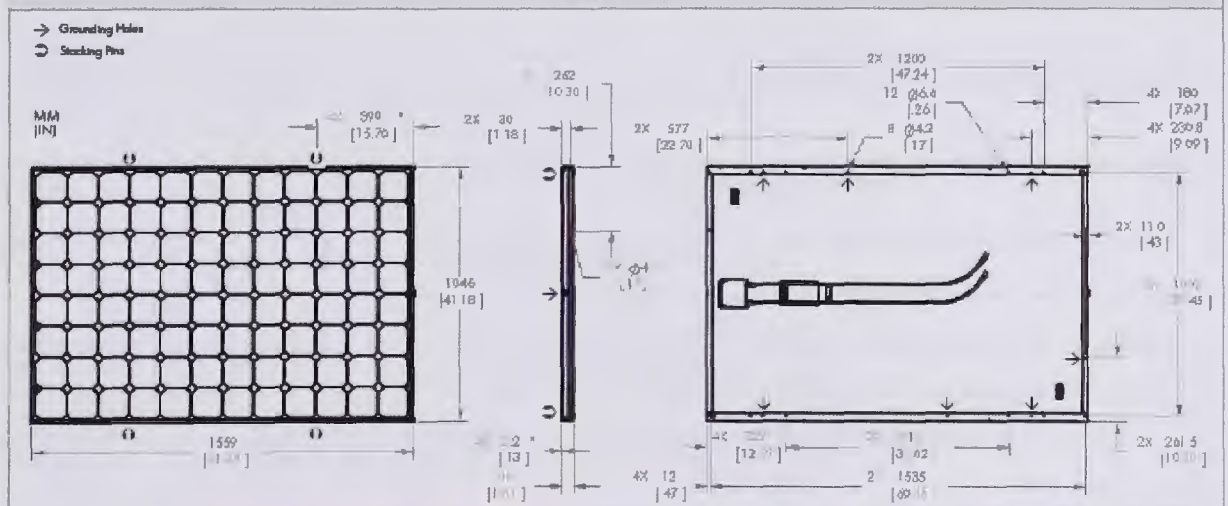
Tested Operating Conditions

Temperature	-40° F to +185° F (-40° C to + 85° C)
Max load	50 psf 245 kg/m ² (2400 Pa) front and back – e.g. wind
Impact Resistance	Hail 1 in (25 mm) at 52mph (23 m/s)

Warranties and Certifications

Warranties	25 year limited power warranty 10 year limited product warranty
Certifications	Tested to UL 1703. Class C Fire Rating

Dimensions



CAUTION: READ SAFETY AND INSTALLATION INSTRUCTIONS BEFORE USING THE PRODUCT.

Visit sunpowercorp.com for details.

SUNPOWER and the SUNPOWER logo are trademarks or registered trademarks of SunPower Corporation.
© May 2009 SunPower Corporation. All rights reserved. Specifications included in this datasheet are subject to change without notice.

sunpowercorp.com
Document #001-52265 Rev*A / ITR_EN



BP 4175

175 Watt Photovoltaic Module

High-efficiency photovoltaic module using silicon nitride monocrystalline silicon cells.

Performance

Rated power (P_{max})	175W
Power tolerance	$\pm 5\%$
Nominal voltage	24V
Limited Warranty ¹	25 years

Configuration

BP 4175B	Framed module with output cables and polarized Multicontact (MC) connectors
----------	---



Electrical Characteristics ²	BP 4175
Maximum power (P_{max}) ³	175W
Voltage at Pmax (V_{mp})	35.7V
Current at Pmax (I_{mp})	4.9A
Warranted minimum P_{max}	168.5W
Short-circuit current (I_{sc})	5.4A
Open-circuit voltage (V_{oc})	44.0V
Temperature coefficient of I_{sc}	(0.065 \pm 0.015)%/°C
Temperature coefficient of V_{oc}	-(160 \pm 10)mV/°C
Temperature coefficient of power	-(0.5 \pm 0.05)%/°C
NOCT (Air 20°C; Sun 0.8kW/m ² ; wind 1m/s)	47 \pm 2°C
Maximum series fuse rating	15A (S, L)
Maximum system voltage	600V (U.S. NEC & IEC 61215 rating)

Mechanical Characteristics

Dimensions	Length: 1595mm (62.8") Width: 790mm (31.1") Depth: 50mm (1.97")
Weight	15.4 kg (34.0 pounds)
Solar Cells	72 cells (125mm x 125mm) in a 6x12 matrix connected in series
Output Cables	RHW AWG# 12 (3.3mm) cable with polarized weatherproof DC rated Multicontact connectors; asymmetrical lengths - 1250mm (-) and 800mm (+)
Diodes	IntegraBus™ technology includes Schottky by-pass diodes integrated into the printed circuit board bus
Construction	Front: High-transmission 3mm (1/8 th inch) tempered glass; Back: Tedlar; Encapsulant: EVA
Frame	Bronze anodized aluminum alloy type 6063T6 Universal frame

1. Module Warranty: 25-year limited warranty of 80% power output; 12-year limited warranty of 90% power output; 5-year limited warranty of materials and workmanship. See your local representative for full terms of these warranties.
2. These data represent the performance of typical BP 4175 products, and are based on measurements made in accordance with ASTM E1036 corrected to SRC (STC.)
3. During the stabilization process that occurs during the first few months of deployment, module power may decrease by up to 3% from typical P_{max} .

Quality and Safety

ESTI Module power measurements calibrated to World Radiometric Reference through ESTI (European Solar Test Installation at Ispra, Italy)



Listed by Underwriter's Laboratories for electrical and fire safety (Class C fire rating)

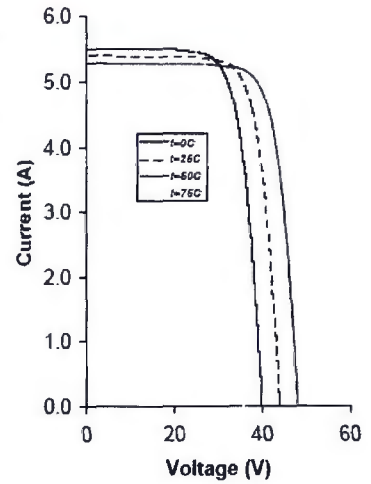


Certified to IEC 61215 standards by ASU/PTL

Qualification Test Parameters

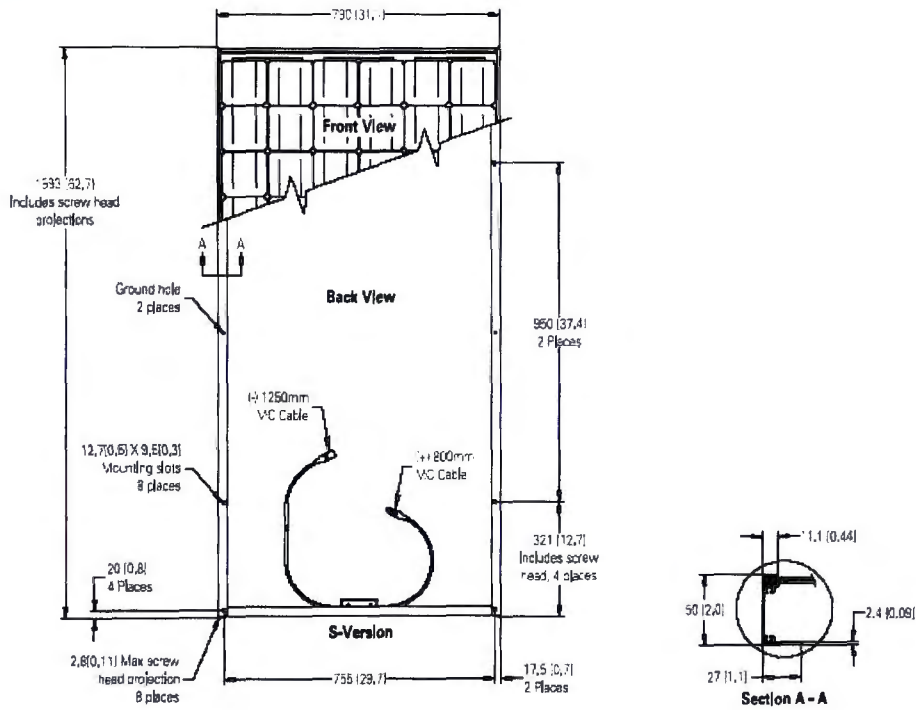
Temperature cycling range	-40°C to +85°C (-40°F to 185°F)
Humidity freeze, damp heat	85% RH
Static load front and back (e.g. wind)	50psf (2400 pascals)
Front loading (e.g. snow)	113psf (5400 pascals)
Hailstone impact	25mm (1 inch) at 23 m/s (52mph)

BP 4175 I-V Curves



Module Diagram

Dimensions in brackets are in inches. Un-bracketed dimensions are in millimeters. Overall tolerances ±3mm (1/8")



Self-tapping grounding screw, instruction sheet, and warranty document included with each module.

Note: This publication summarizes product warranty and specifications, which are subject to change without notice. Additional information may be found on our web site: www.bpsolar.com

Appendix 6 Flat Plate PV Module 'Thin Film' Example

Solar modules

FIRST SOLAR – FS-262 / FS-265 / FS-267 / FS-270 / FS-272 / FS-275

Solar modules are the key element of every solar power system as they convert sunlight into electricity. Their quality, reliability and performance are therefore critical for the yield and profit of your system. Solar modules based on thin-film technology absorb a particularly wide spectrum of sunlight. This enables the effective use of the sun's power – even under less than ideal sunlight conditions.

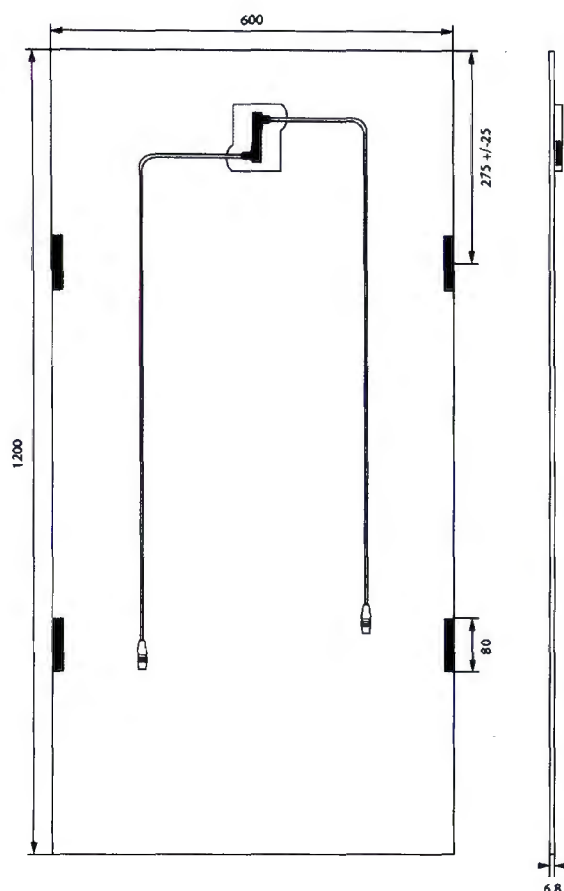


The advantages at a glance:

- 62.5; 65; 67.5; 70; 72.5 and 75 Wp power output available
- Tested independently from the manufacturer
- Reliable power generation through high temperature tolerance and high performance, even in diffuse sunlight
- High efficiency and stable output power provide reliably high performance over a period of many years
- 25-year performance guarantee* at 80 % of the minimal rated power output
- 10-year performance guarantee* at 90 % of the minimal rated power output
- Frameless solar module
- Pre-funded end-of-life take back and recycling

* The manufacturer's warranty conditions apply

Parameters



Mechanical parameters

Length [mm]	1200
Width [mm]	600
Depth [mm]	6.8
Depth with connection socket [mm]	19.9
Weight [kg]	12
Connection socket (manufacturer)	First Solar
Positive cable (manufacturer/length [mm]/cable cross-section [mm ²])	General Cable/610/3.2
Negative cable (manufacturer/length [mm]/cable cross-section [mm ²])	General Cable/610/3.2
Plug connector (manufacturer/type)	Multi-contact/MC3
Front cover (material/thickness [mm])	Tempered glass/3.2
Cell type (quantity/technology)	116/CdS/CdTe
Cell embedding (material)	Ethylene vinyl acetate (EVA) with edge seal
Rear cover (material/thickness [mm])	Tempered glass/3.2
Frame (material/profile type)	Frameless

Warranties

Product warranty	5-year product limited warranty*
Performance guarantee	10 years at 90% of the minimal rated power output* 25 years at 80% the minimal rated power output*

* The manufacturer's warranty conditions apply

Qualifications and Certificates

IEC 61646

TÜV safety class II



First Solar has consistently focused on thin-film technology and is one of the international leading manufacturers of solar modules, primarily in the larger solar power plant sector. The company manufactures solar modules using a highly-developed semi-conductor coating process that reduces module manufacturing costs whilst ensuring high performance yields in the field.



Parameters

Electrical parameters

Electrical parameters for STC (1000 W/m², 25 (+/- 2)°C, AM 1.5 according to EN 6090-4)

Article number	100285	100284	100287	100288	100270	100271
Power output [P _{mpp}]	62.50	65.00	67.50	70.00	72.50	75.00
Power output tolerances [%]	+/- 5	+/- 5	+/- 5	+/- 5	+/- 5	+/- 5
Efficiency [%]	8.68	9.03	9.38	9.72	10.07	10.42
Max. voltage V _{mpp} [V]	62.50	63.70	64.60	67.10	67.90	69.40
Max. current I _{mpp} [A]	1.00	1.02	1.05	1.04	1.07	1.08
Open circuit voltage V _{oc} [V]	86.00	87.00	87.00	89.00	90.00	92.00
Short circuit current I _{sc} [A]	1.17	1.17	1.18	1.19	1.19	1.20

Electrical parameters for 800 W/m², NOCT, AM 1.5 NOCT = Nominal Operating Cell Temperature, cell temperature under nominal operating conditions

Max. power output P _{max} [Wp]	46.90	48.80	50.60	52.50	54.40	56.30
Max. voltage V _{max} [V]	59.00	60.00	61.00	63.00	64.00	66.00
Max. current I _{mpp} [A]	0.80	0.82	0.84	0.83	0.85	0.85
Open circuit voltage V _{oc} [V]	80.00	81.00	80.00	83.00	83.00	86.40
Short circuit current I _{sc} [A]	0.96	0.96	0.97	0.97	0.97	0.97
Reverse current loading capability I _r [A]						2
Max. permissible system voltage V _{max} [V]						1000

Efficiency variance from 1000 W/m² to 200 W/m² (T_{module} = 25° C), + 2 (Increase!)

Parameters of the thermal characteristics

NOCT [° C]	45
Temperature coefficient of the short circuit current I _{sc} [%/K]	+ 0.04
Temperature coefficient of the open circuit voltage V _{oc} [%/K]	- 0.25
Temperature coefficient of the MPP power P _{mpp} [%/K]	- 0.25

Operating conditions

Max. operating temperature [° C]	- 40 to + 85
Max. snow load [Pa]	according to IEC 61646
Max. wind load [Pa]	according to IEC 61646

Subject to modifications and errors

Appendix 7 Experience curve (also known as learning curve)

The General Form of the Experience Curve is the Power Curve

- $P(t) = P(0) \times [q(t)/q(0)]^{-b}$

Where:

$P(t)$ = average price of a product at time t

$q(t)$ = cumulative production at time t

b = learning coefficient

- $PR = 2^{-b}$

Where:

PR = progress ratio. For each doubling of cumulative production the MC decreases by $(1-PR)$ percent.

R. M. Margolis, HDGC Seminar, Oct. 16, 2002, page 6

Application of Progress Ratio to Dish Costs

From R. M. Margolis, *'Experience Curves and Photovoltaic Technology Policy'* (Margolis, HDGC Seminar, Oct 16 2002) of 10% cost reduction per cumulative production output doubling (being the Progress Ratio (PR) of 0.9%, typical of this type of product), we have:-

$$PR = 2^{-b} \quad \text{where } PR = 0.9$$

$$\ln(0.9) = -b \ln 2$$

$$b = -\frac{\ln(0.9)}{\ln 2}$$

$$b = 0.16$$

If the cost is \$4.00/W at 65 MW, then the cost $P(t)$ for 500MW is:-

$$P(t) = P(0) \times [q(t)/q(0)]^{-b}$$

$$= 3.90 \times (500/65)^{-0.16}$$

$$= 3.9 \times 0.72$$

$$= \$2.88$$

If the Progress Ratio (PR) = 0.8 (for 20% cost reduction per cumulative production output doubling):-

$$PR = 0.8 = 2^{-b}$$

$$b = -\left(\frac{\ln 0.8}{\ln 2}\right) = \left(-\frac{0.22}{0.65}\right) = 0.34$$

$$P(t) = 3.9 \times (7.69)^{-0.34}$$

$$= 3.9 \times 0.5$$

$$= \$2.00/W \text{ at } 500 \text{ MW/annum}$$

CHAPTER 13. LIST OF ACRONYMS

- 2W – Solar dish ‘2-West’ at Hermannsburg power station
- A/W – Amps per Watt
- AC – Alternating Current
- AOD – Aerosol Optical Depth
- AM – Air Mass
- BoS – Balance of System
- CAD – Computer Aided Design
- CCS – Carbon Capture and Storage
- CdTe – Cadmium Telluride, thin film PV
- CSG – Crystal Silicon on Glass
- C_{\max} – Peak concentration ratio
- C_{opt} – Optimum concentration ratio
- CPV – Concentrator Photovoltaic
- CSP – Concentrating Solar Power
- CST – Concentrating Solar Thermal
- DC – Direct Current
- Dish 1W – Solar dish 1-West at Hermannsburg Solar Power Station
- Dish 2W – Solar dish 2-West at Hermannsburg Solar Power Station
- DNI – Direct Normal Irradiance, $\text{kWh}/\text{m}^2/\text{day}$, solar radiation from the sun’s direction
- DSR – Direct Solar Radiation, W/m^2
- E_g – Bandgap
- EPR – Energy Production Rate, $\text{kWh}_e/\text{kWh}_{\text{ph}}/\text{m}^2$
- EQE – External Quantum Efficiency
- EVA – Ethylene Vinyl Acetate
- FEA – Finite Element Analysis
- FM – Flux Modifier
- GaAs – Gallium Arsenide, PV cell material
- GaInP/GaInAs/Ge – Layers of triple junction PV cell
- GW – Gigawatts
- GWh – Gigawatt hours
- HCPV – Heliostat Concentrator PV (will be referred to as C2PV in future)

HMI – Human Machine Interface
 kW – kilowatts
 kWh – kilowatt hours
 kWh_e – kilowatt hours electrical output
 kWh_{ph} – kilowatt hours of photonic energy incident on a collector
 LCOE – Levelised Cost of Energy
 LED – Light Emitting Diode
 MPP – Maximum Power Point
 MJ – Multijunction PV cell
 MW – Megawatts
 MWh – Megawatt hours
 NOCT – Normal Operating Cell Temperature
 NREL – National Renewable Energy Laboratory (US)
 N-S – North-South
 n-type – type of semiconductor
 O&M – Operations and Maintenance
 p-n junction – Interface where two types of semiconductor material meet
 P_{NAC} – Nominal AC power output
 WOT – Water Optical Thickness
 p-type – type of semiconductor material
 PV – Photovoltaic
 QA/QC – Quality Assurance/Quality Control
 R_s – Series resistance
 R_{sh} – Shunt resistance
 R_x – Receiver
 SEGS – Solar Energy Generating System plant in California, US
 SOC – Standard Operating Conditions at 1000W/m² and 25 deg C
 STC – Standard Test Conditions of 1000W/m² and 25 deg C
 S_R – Spectral response
 T_{cell} – Average cell temperature (°C)
 TRANSOP – ‘Derating factor’ which allows for operation and power transfer losses
 V_{MP} – Voltage at maximum power point
 V_{oC} – Open circuit voltage
 W – Watts

**The Design and Optimisation of a Reflective Concentrator
Photovoltaic Generation System**

Volume II

Supporting Publications

By John Lasich, BSc

Centre for Environmental Safety and Risk Engineering

Victoria University

Melbourne, Australia

2009

The work presented in Volume I of this thesis is supported by 16 publications, 7 full patents awarded to the candidate and 2 patent applications.

Table of Contents

1. PUBLISHED PAPERS

- 1.1 Lasich, J B, Cleeve, A, Kaila, N, Ganakas, G, Timmons, M, Venkatasubramanian, R, Colpitts, T and Hill, J, 1994, "Close-Packed Cell Arrays for Dish Concentrators", First World Photovoltaic Conference, Hawaii, Vol II, pp. 1938-1941
- 1.2 Cleeve A.X., Lasich J.B., Skinner R.A, 1996, "Making Concentrated Photovoltaics a Competitive Reality", The 4th Renewable Energy Technologies & Remote Area Power Supplies Conference Drivers and Markets for Renewables
- 1.3 Lasich J.B., Thorpe G.R., 1996, "An Advanced Solar Co-Generation for Remote Communities", Conference on Engineering in Agriculture and Food Processing, Paper No. SEAg 96/027
- 1.4 Friedman D.J., Kurtz S.R., Sinha K., McMahan W.E., Kramer C.M., Olson J.M, Lasich J.B., Cleeve A.X., Connaughton I., 1996, "On-Sun Concentrator Performance of GaInP/GaAs Tandem Cells", 25th IEEE Photovoltaic Specialist Conference, pp 73-75
- 1.5 Lasich J.B., 2000, "Photovoltaic Concentrator Systems for RAPS"
- 1.6 Verlinden P.J., Terao A., Smith D.D., McIntosh K., Swanson R.M., Ganakas G. and Lasich J.B., 2001 "Will We Have a 20 %-Efficient (PTC) Photovoltaic System?", Proc. 17th European Photovoltaic Solar Energy Conference
- 1.7 Edwards J.H., Badwal S.P.S, Duffy G.J., Lasich J.B., Ganakas G., 2002, "The Application of Solid State Ionic Technology for Novel Methods of Energy Generation and Supply", Solid Ionic States
- 1.8 McConnell R.D., Lasich J.B. and Elam C., 2005, "A Hybrid Solar Concentrator PV System for the Electrolytic Production of Hydrogen", Proceedings of the 20th European Photovoltaics Solar Energy Conference.
- 1.9 Kinsey G.S., Sheriff R., Piechen Pien, Cotal H., King R., Brandt R., Wise W., Labios E., Wan K., Haddad M., Lacey J., Fetzer C., Verlinden P., Lasich J. and Karam N., 2006, "Multijunction Solar Cells for Dense Array Concentrators", Proc. 4th World Conference on Photovoltaic Energy Conversion, Hawaii
- 1.10 Verlinden P.J., Lewandowski A., Bingham C., Kinsey G.S., Sherif R.A. and Lasich J.B., 2006, "Performance and Reliability of Multijunction III-V Modules for Concentrator Dish and Central Receiver Applications", Proceedings of 4th World Conference on Photovoltaic energy Conversion, Hawaii, pp. 592-597
- 1.11 Lasich J.B., Verlinden P.J. and Holland D., 2007, "Opportunities for Widespread Implementation of Concentrator Photovoltaic (CPV) Systems", 4th ICSC Conference, El Escorial, Spain
- 1.12 Lasich J.B., Birch J., 2008, "Australian Hydrogen Technology for Solar Power on Demand and Transport", 17th World Hydrogen Energy Conference

- 1.13 Lasich J.B., Verlinden P.J., Lewandowski A., Edwards D., Kendall H., Thomas I., Carter S., Wakeman P., Varfolomeev I., Wright M. and Metzke R., 2008, "Large Scale CPV systems using multijunction III-V solar cells" International Conference on Solar Concentrators for the Generation of Electricity, Palm Desert, California
- 1.14 Verlinden P.J. and Lasich J.B., 2008, "Energy rating of concentrator PV systems using multi-junction III-V solar cells", 33rd IEEE PVSC Conference, San Diego
- 1.15 Verlinden P.J., Lewandowski A., Kendall H., Carter S., Cheah K., Varfolomeev I., Watts D., Volk M., Thomas I., Wakeman P., Neumann A., Gizinski P., Modra D., Turner D. and Lasich J.B., 2008, "Update on two-year performance of 120 kW concentrator PV systems using multi-junction III-V solar cells and parabolic dish reflective optics", 33rd IEEE PVSC Conference, San Diego
- 1.16 Lasich J.B., Verlinden P.J., Lewandowski A., Edwards D., Kendall H., Carter S., Thomas I., Wakeman P., Wright M., Hertaeg W., Metzke R., Daly M., Santin M., Neumann A., Wilson A., Caprihan A., Stedwell M., 2009, "World's First Demonstration of a 140kWp Heliostat Concentrator PV (HCPV) System", 34th IEEE Photovoltaic Specialist Conference.

2. PATENTS

- 2.1 Lasich J.B., 1993, "Apparatus for Separating Solar Radiation into Longer and Shorter Wavelength Components", Patent No. 731495, Australia
- 2.2 Lasich J.B., 1993, "Production of Hydrogen from Solar Radiation at High Efficiency", Patent No. 5658448, USA
- 2.3 Lasich J.B., 2001, "Cooling Circuit for Receiver of Solar Radiation", Patent No. 7076965B2, USA
- 2.4 Lasich J.B., 2001, "Solar Tracking System", Patent No. 200224287, Australia
- 2.5 Lasich J.B., 2001, "Solar Mirror Testing and Alignment", Patent No. 2002244529B2, Australia
- 2.6 Lasich J.B., 2001, "A Method of Manufacturing Mirrors for a Dish Reflector", Patent No: US7550054B2, USA
- 2.7 Lasich J.B., 2003, "Bypass Diode for Photovoltaic Cells", Patent No. 2004239803, Australia
- 2.8 Lasich J.B., 2003, "Extracting Heat from An Object", Patent Application No. 1661187, World International Property Organisation (also known as WO 2005/022652 A1)
- 2.9 Lasich J.B., 2004, "A Tracking System", Patent Application No. US7589302, USA

1. Published Papers

- 1.1 Lasich, J B, Cleeve, A, Kaila, N, Ganakas, G, Timmons, M, Venkatasubramanian, R, Colpitts, T and Hill, J, 1994, "Close-Packed Cell Arrays for Dish Concentrators", *First World Photovoltaic Conference, Hawaii, Vol II*, pp. 1938-1941

CLOSE-PACKED CELL ARRAYS FOR DISH CONCENTRATORS

J.B. Lasich, A. Cleeve, N. Kaila, G. Ganakas
Solar Research Corporation Pty. Ltd.,
6 Luton Lane, Hawthorn, Victoria 3122, Australia

M. Timmons, R Venkatasubramanian, T. Colpitts, J. Hills
Research Triangle Institute, RTP, USA

INTRODUCTION

Globally, 60 MW of photovoltaic (PV) equipment per year is sold and produces a revenue of about half a billion dollars. As a percentage of the 5,000 billion⁽¹⁾ or more dollars revenue generated from conventional energy, this is about 0.01%. Rather than take the view that PV is insignificant, we see a very large market yet to be tapped. To be a contender for a significant portion of this diverse and expanding market, an installed system cost of about US\$3.00 per watt must be achieved. At this level, with appropriate financial security, PV power plants of suitable scale can be commercially financed. PV/Dish Concentrator Systems offer an avenue to this \$3/watt goal and beyond, having the greatest scope for efficiency improvement and cogeneration. **

Although PV concentrator systems are complex relative to flat-plate systems, they are simple when compared to solar thermal (steam) systems - a technology which is the most advanced of any solar-electric technology.

The two main components of the system under development are:

1. PV modules with close-packed cells for "stacking" into fully active receivers of any scale.
2. Parabolic dish concentrator system with supports and interface.

The advantages of this approach are many and include the following:

Advantages of a dish concentration system are:

- requires smallest receiver of any concentration system; the advantages of a small receiver are that each has a small area of expensive PV cells, the cooling system is small, and the units are serviceable - receivers can be exchanged and serviced in-house,
- dish technology is developing well for thermal applications; steam, Stirling and thermochemical programs are producing excellent dish systems,
- PV cells operate more efficiently at the higher concentrations available with a dish,
- the highly concentrated beam facilitates the option to split and redirect the unused part of the spectrum (mostly IR) effectively for cogeneration applications,
- the entire system efficiency may be upgraded at a fraction of system cost by upgrading the receivers only.

Advantages of a GaAs receiver are:

- high efficiency - in excess of 28% has been recorded,
- high cell voltage - requiring fewer series-connected cells to produce useful voltage,
- high concentration - GaAs cells have been run at more than 2000 suns⁽²⁾
- GaAs can be used as the lower cell of a cascade tandem where, for instance, GaInP₂ may be grown on top using the same technology - efficiencies of the order of 32% at 500 suns, AM1.5 are expected⁽³⁾;
- a significant portion of the solar spectrum, 38%, is still available for co-generation. (Methods of separation, concentration, and utilisation of IR have been demonstrated by Solar Research Corporation.)

Advantages of a Silicon receiver are:

- High efficiency in excess of 25% has been recorded.
- Abundant low cost materials for large scale applications,
- most developed technology (advanced back contact silicon cells facilitate close packing)⁽⁴⁾,
- medium concentration : 200-300 Suns relaxes performance requirements of concentrator/tracking system.
- 25% of the spectrum is still available for cogeneration.

SYSTEM REQUIREMENTS

To demonstrate the concept, a system consisting of a 1.5m parabolic dish, a 36-cell GaAs module and a 10-cell Si module have been built and are shown schematically in Figures 1 & 2.

Incorporation of the components into a system provided many new challenges, including the development and optimisation of: the dish concentrator, flux modifier, cell array, cell-heat sink interface and heat sink. Specific considerations and developments for each component include:

Dish:

Size, rim angle, mirror type, tracker accuracy, general tolerances applicable to PV receivers.

Flux Modifier:

This component delivers the necessary even, flat solar flux distribution to the PV receiver, straightens the rays improving absorption and increases the apparent size of the cell array, thus maximising system efficiency, and reducing the required tracking accuracy.

Heat Sink:

The Heat sink is capable of sinking high heat flux (Typically 50 W/cm²) of thermal energy from the cells and maintain cell temperatures below 50°C. Constraints include: low pressure drop, high heat transfer coefficient and small footprint.

Cell-Heat Sink Interface:

To cool and electrically isolate the PV cells from the heat sink, a metallised ceramic substrate has been developed to provide a high heat transfer area for cell mounting and electrical interconnection. This component is bonded directly onto the heat sink. Thermal mismatch between the metal and ceramic has been accommodated by proprietary design.

Cells/Array:

To maximise power transmission, a large number of small, series connected cells are required to provide high voltage and relatively low currents at high solar concentrations. The problem of close packing many small cells was overcome by using interconnected n-p and p-n GaAs cells. The Silicon receiver relies on a monolithic array of back contacted cells.

SYSTEM PERFORMANCE

A 1.5 m diameter dish has been designed, fabricated and tested with both Si back contact cells and GaAs cells. Table 2 shows the performance of the receivers. Electrical efficiency around the 20% mark have been achieved generally, and for Case 3, a cogeneration system was run simultaneously producing 135 W thermal and developing 1100°C in a separate receiver. The overall efficiency of the two receivers was 31.8%.

The measured heat sink thermal conductance is approximately 1.7 W/cm²/°C @ 1.5 l/min, and the pumping (for cooling) required less than 2 per cent of the power while maintaining cell temperatures about or below 50°C. The flux modifier has been tested; showing a highly uniform delivery of solar energy to the cells which is reflected in a 60% improvement in receiver output.

The p-n and n-p GaAs cells have been fabricated, modelled and actual performances (average for 18 cells of each polarity to be mounted in the array) are shown in Table 1.

Table 1

Cell	V _{oc} (V)	I _{sc} (mA)	FF (%)	η (%)
p-n (Measured)	1.022	6.07	83.6	24.2
p-n (Modelled)	1.046	5.68	88.5	25.0
n-p (Measured)	1.000	5.95	85.0	23.5
n-p (Modelled)	1.046	5.73	83.7	23.9

The GaAs efficiencies are based on active device area (including grid), and the currents are matched to within 2 per cent.

CONCLUSIONS

The concept for a dish PV concentration system has been successfully demonstrated in a 1.5-m-diameter dish system. A single close packed Silicon array produced more than 200 Watts with an efficiency of 22% at 239 suns and a GaAs module produced 85 Watts with an efficiency of 18.3% efficiency at 381 suns.

We believe these are the highest on sun efficiencies recorded for close-packed series connected high voltage concentrator modules at high concentration. (8V for Si and 40V for GaAs).

Complete receiver efficiencies in excess of 20% are expected to be produced within the course of our R&D program. A 16 V Silicon module is under development.

The series connection of the n-p and p-n GaAs cells has been successfully demonstrated with good current matching and an average of V_{oc} = 1.1 volts per cell. A packing factor of 0.88 has been achieved and it is expected to reach 0.96.

Utilising the IR component from dish PV, it is possible to achieve even greater overall efficiencies from synergistic processes. Total receiver efficiencies of 31.8% have been demonstrated for a combination of electricity and high grade heat (1100°C) outputs. At this temperature the heat has high value and can be used to - produce super-heated steam - power a furnace - operate low band gap solar cells - drive a thermo-chemical reaction, to name a few applications.

The receiver modules are self-contained with all components being within the shadow of the cells. This allows modular stacking into receivers of any scale.

To prove this concept at a substantial level, a 5-m-diameter dish has also been commissioned for large-scale tests (3 kW electric, 2 kW thermal). A 100 kW system using a 400 m² dish is also contemplated.

Using high efficiency receivers, costing less than 20% of total system value, the well-known economies of scale for the remainder of the system, i.e. steel, concrete, glass and plastic, will assist with the financial leverage required to commercialise the product.

- (1) BP Statistical Review of World Energy, June 1992.
- (2) Solar Research Corporation Pty Ltd., unpublished data.
- (3) Research Triangle Institute, unpublished data.
- (4) Cells supplied by SunPower Corporation.

System Description & Performance

Table 2

GaAs Module	Case No	V _{oc} Volts	I _{sc} Amps	FF	Power Watts	C _r ^{*4} Suns	Module efficiency %	Module Temp °C	Packing Factor	Irradiance W/m ² Direct
Cell arrangement alternate series connection of 18 n-p cells with 18 p-n cells Module size 3.2 cm x 3.2 cm Flux Modifiers used	1	39.75	2.25	0.8 ^{*1}	71.5	381	18.3	44.0	0.88	836
	2	39.7	2.67 ^{*3}	0.8 ^{*1}	85.0	469	17.7	32.5	0.88	982

Silicon Module	Case No	V _{load} Volts	V _{oc} Volts	I _{load} Amps	I _{sc} Amps	FF	Power Watts	C _r Suns	Module efficiency %	Cell Temp °C	Packing Factor	Irradiance W/m ² direct
10 back contact Cells series connected. Module size 6 cm x 6 cm Flux Modification used	3	6.40	≈ 7.9	29.2	33.0		187 ^{*2}	282	18.4	30	0.96	933
	4	6.23	-	30.5	-		190	239	22.1	34	0.96	793
	5	6.30	-	30.9	-		195	248	21.7	34	0.96	815
	6	6.35	7.97	32.7	35.1	0.74	207	264	21.8	29	0.96	867

*1 To be confirmed.
Fill Factor (FF) for unconnected cells averaged 0.835. A FF of 0.8 has been assumed under series connection

*2 Simultaneously with this electrical production, infra-red radiation was split from the primary beam and refocused to simultaneously generate a temperature of 1100 °C in a separate secondary receiver. This thermal power was later measured to be at least 135 Watts.

This approximates to a thermal receiver efficiency of 13.4% based upon the incoming flux to the primary receiver of 1008 W.

The total receiver efficiency is thus 31.8%.

*3 Sublinearity ≈ 96.4%

*4 1 Sun = 1000 W/m² Direct.

** The systems described herein are substantially protected by local and foreign patents or patents pending and exclusive rights are owned by Solar Systems Pty Ltd.
These systems must not be reproduced without the prior consent of Solar Systems Pty Ltd.

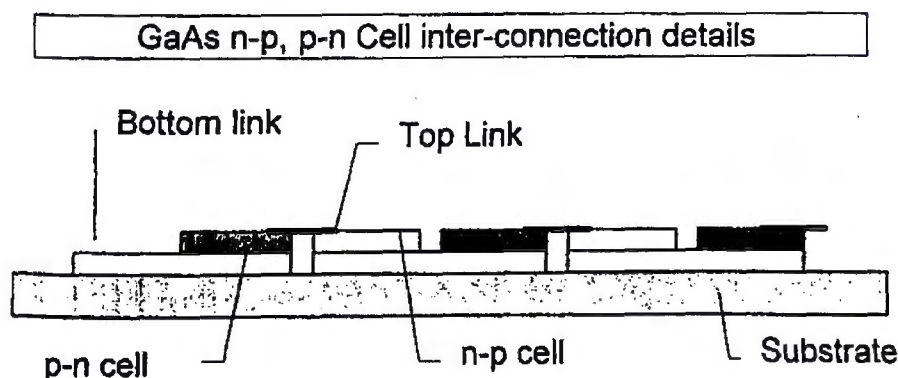


Figure 1

PV CONCENTRATOR COGENERATION SYSTEM

DISH
CONCENTRATOR
(2 AXIS TRACKING)

SUN RAYS

GREGORIAN LENS, TO
REFOCUS UNUSED PART
OF SPECTRUM
(CASEGRAINIEN LENS IS
ALSO POSSIBLE)

FLUX MODIFIER

CONE/LIGHT GUIDE
RECEIVER

HEAT SINK

COOLING CIRCUIT

POWER OUT

LIGHT GUIDE

PRIMARY RECEIVER
(ELECTRICAL EFFICIENCY
~ 20%)

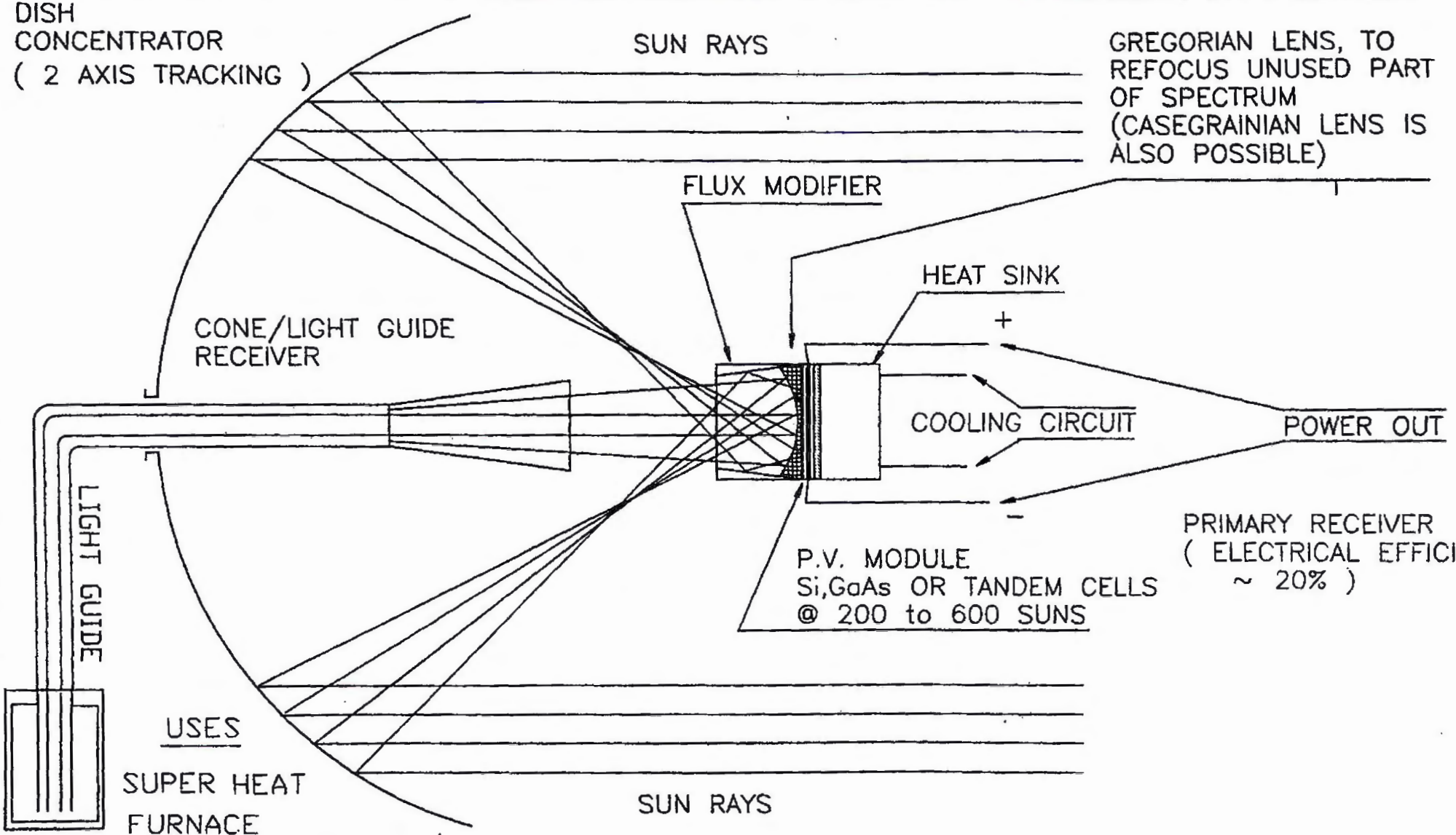
P.V. MODULE
Si,GaAs OR TANDEM CELLS
@ 200 to 600 SUNS

USES
SUPER HEAT
FURNACE

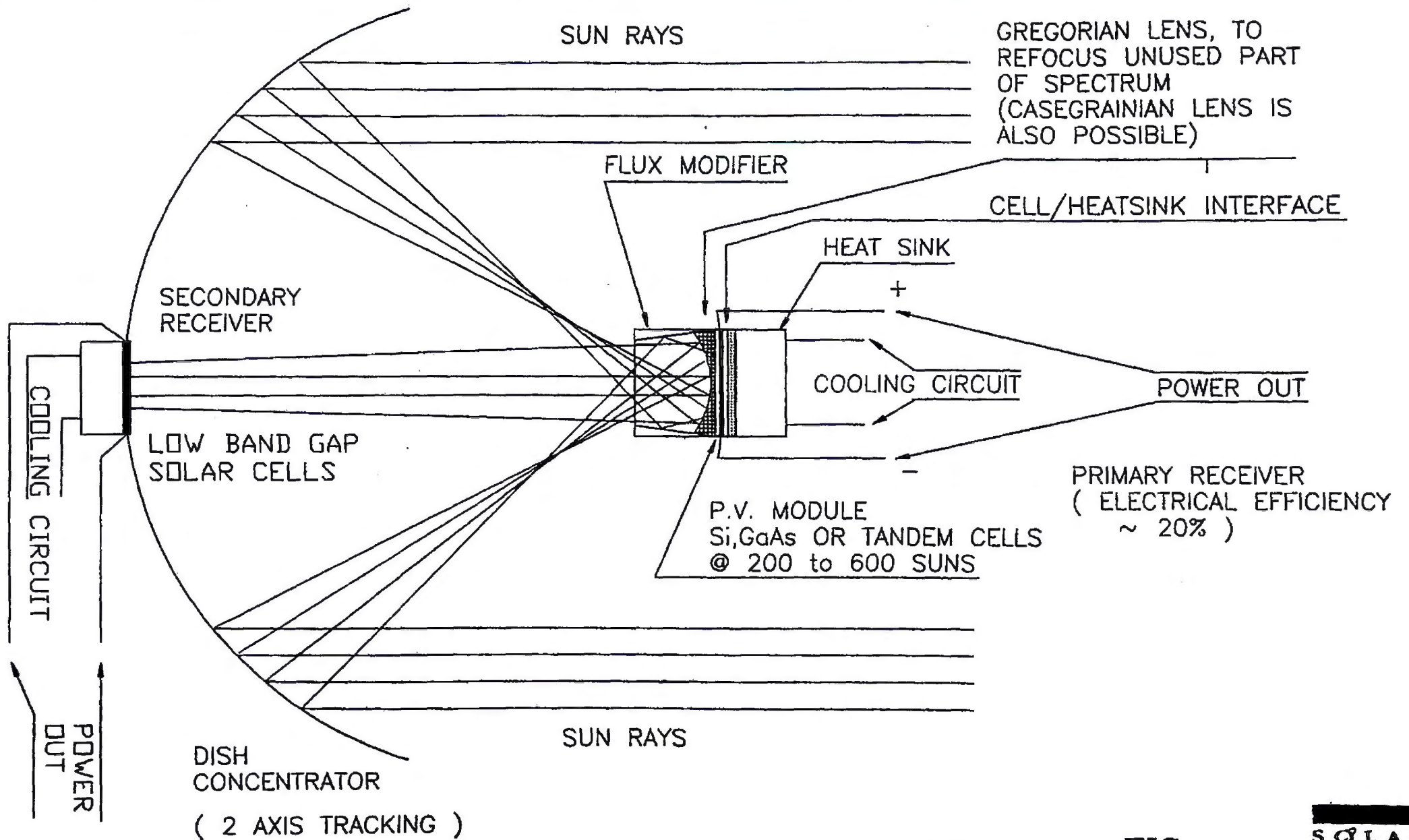
SUN RAYS

LOW BAND GAP SOLAR CELLS
THERMO CHEMICAL PROCESS

PATENT PENDING. FIG. 2.

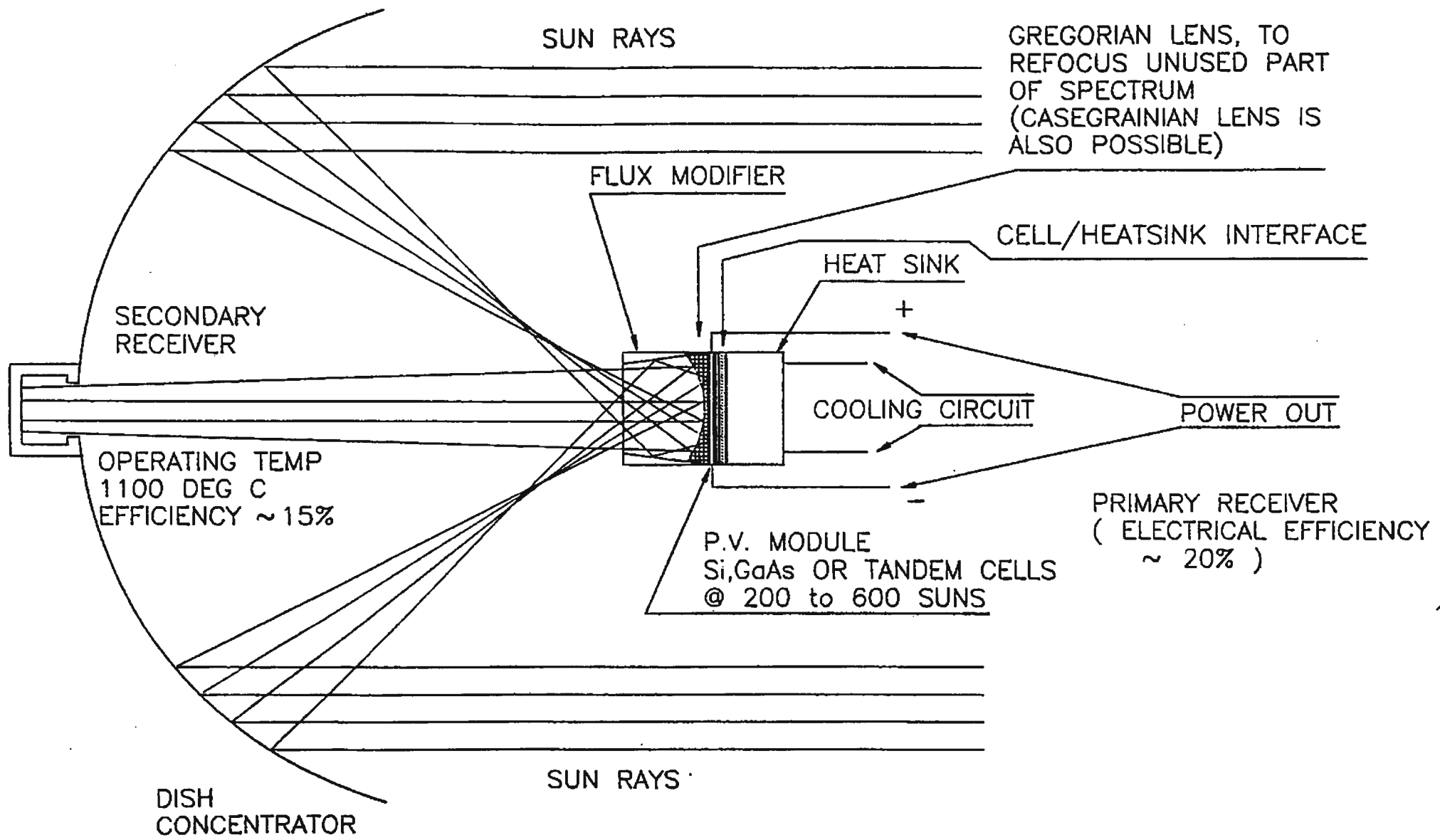


PV CONCENTRATOR COGENERATION SYSTEM

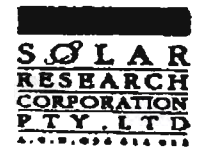


PATENT PENDING FIG

PV CONCENTRATOR COGENERATION SYSTEM



PATENT PENDING FIG



- 1.2 Cleeve A.X., Lasich J.B., Skinner R.A, 1996, “Making Concentrated Photovoltaics a Competitive Reality”, *The 4th Renewable Energy Technologies & Remote Area Power Supplies Conference Drivers and Markets for Renewables*

The 4th Renewable Energy Technologies & Remote Area Power Supplies Conference

Session 6: Turning Renewables into Commercial Realities

MAKING CONCENTRATED PHOTOVOLTAICS A COMPETITIVE REALITY

Solar Systems Pty Ltd

A X Cleeve, Chief Executive Officer
J B Lasich, Director, Technical Services
R A Skinner, Administration & Information Services

Abstract:

The market reality for electricity produced using photovoltaic technologies is that it must meet the customers' requirements. The likely customers are not in the main the consumers of the electricity, rather they are the utilities and mining companies that provide the power at subsidised prices to the consumers. These utility and mining company customers require that the electricity generated meets their commercial disciplines by being, amongst other things:

- 1) Economical
- 2) Reliable, and
- 3) Continuously available

Solar Systems has designed a concentrating photovoltaic device which it intends to build, own and operate to provide economical, reliable electricity initially in parallel with and later in substitution for diesel fired remote area power supply (RAPS) systems.

In the medium term Solar Systems expects its price structures to allow grid connected sales at competitive prices per kWh.

MAKING CONCENTRATED PHOTOVOLTAICS A COMPETITIVE REALITY

The common refrain from the marketplace, familiar to all in the renewable energy field is that "it would be great to use more renewable energy, but it is too expensive to do so".

Hearing this, an intelligent observer would believe that at the end of a vigorous debate based on a well researched analysis, all the relevant parties had agreed that the value to the community of renewable electricity is indisputably less than the value of traditional fossil fuel electricity.

This is not what has occurred.

Confusion abounds because various groups speak about different things. Three different scenarios spring quickly to mind:

1. *Capital cost*

Item A costs \$10,

Item B costs \$8

therefore A is more expensive than B.

2. *Life Cycle Cost*

Item A costs \$20 for 5 years service

Item B costs \$25 for 5 years service

therefore A is cheaper than B

3. *Life Cycle Cost including externalities*

Item A costs \$20 for 5 years service plus \$10 to detoxify the site

Item B costs \$25 for 5 years service plus \$2 to landscape the area

therefore A is more expensive than B.

MAKING CONCENTRATED PHOTOVOLTAICS A COMPETITIVE REALITY

It is suggested that:

1. **Capital cost** - is only useful when it is assumed that the items to be purchased are effectively identical and hence the only relevant differentiation is by price. An example of this is a can of Coke is cheaper say at Safeway than at Target. This sort of analysis is not useful when the products are significantly different.
2. **Life cycle cost** – the focus is on the goods or services to be provided and the process attempts to determine all the relevant actual costs and hence indicate which of the available choices is better. This is how business attempts to inform its decision making and determine the cost of its operations over time.
3. **Life cycle cost with externalities** - This is life cycle costing with costs attributed to items that might not be immediately obvious as costs. Examples might be the cost of reinstating toxic soil at a facility used to distribute chemical products or the landscaping of a mining site after removal of the ore. The analysis here is really no different than two above except that further elements have been introduced to the cost equation by community pressure (usually by legislation). This is how an independent party would view the cost question. It is a broader community view as opposed to the more narrow focus of the business community.

What is in fact meant when the refrain “it’s too expensive” is heard is somewhere between Capital Cost and Life Cycle Cost Analysis. It is simply that a kWhr of electricity generated using say diesel fuel is cheaper than a kWhr generated by say flat plate photovoltaic means taking account of all the usual suspects of direct financial costs (Life Cycle Cost which does not include various externalities such as pollution). But not all the suspects are interviewed. The suspects that cause the most trouble are excluded from the financial equation because they are too difficult to locate or too politically sensitive to estimate.

MAKING CONCENTRATED PHOTOVOLTAICS A COMPETITIVE REALITY

For a group interested in commerce rather than politics the choice is stark – be cheaper than the competition on the present basis of financial analysis or don't bother.

The question then is this - do markets exist where photovoltaic technologies can be cheaper on the standard financial analysis basis than the traditional sources of power? The answer is clearly YES!

Where these opportunities are to be found varies for each specific technology.

Solar Systems has focused its attention on concentrator photovoltaic systems and has identified an initial market for its products in the supplementation and subsequent replacement of the diesel fired electrical generation systems that abound in Australia and many other parts of the world.

Electrical energy production by diesel fired generating equipment is probably the most expensive electricity in common commercial use and represents a large and growing market. It seems logical then that the early market entry for concentrator photovoltaic systems will be in conjunction with and eventually in substitution for diesel fired generation systems.

Other factors that will assist concentrator PV in gaining a commercial foothold in parallel with diesel include:

1. ***The convenient load profile:***

The solar resource and the peak load on electrical systems are often coincident.

2. ***High Insolation***

The fact that diesel systems are often found in regions of high insolation (including high direct radiation suitable for concentrator systems).

3. ***Low Operations & Maintenance Costs***

Less intensive operations and maintenance requirements will also lend a hand.

MAKING CONCENTRATED PHOTOVOLTAICS A COMPETITIVE REALITY

In the first instance, photovoltaic systems will be economically justified by lower costs consisting of a combination of operational and capital savings:

Operational savings:

1. Diesel fuel saving
2. Lower operations & maintenance costs, and

Capital savings:

1. Extending the life of existing plant
2. Postponing the need for further capacity expenditure.

Systems scale ranges from kW's to several MW's and Solar Systems has identified (as have others) many such installations totalling tens of MW's in the north west of Australia alone.

The word that has been used to date is **WILL**

That is: Concentrator photovoltaics **will** enter the market supplementing and then replacing diesel generation systems. Initially the solar component **will** provide some of the daylight power requirement with balance and night requirements continuing to be provided by the diesel system. The economic justification **will** be provided by the savings in fuel, operations & maintenance costs, plant life extension and capital savings.

But: At present an electrical power generator seeking to include photovoltaics in its range of generation options would not be able to justify the expense on purely economic grounds. Indeed it is likely that a financial analysis of the sort usually conducted would indicate that presently available photovoltaic systems were roughly twice the price of the diesel option.

MAKING CONCENTRATED PHOTOVOLTAICS A COMPETITIVE REALITY

Solar Systems conducted an extensive analysis of the markets in Australia and overseas and the customers' requirements when first considering a substantial investment in solar energy. The fundamental observation was:

Price is everything.

- It is how society makes comparisons between worthwhile and not worthwhile.
- It provides the forum into which all relevant considerations can be placed if agreement is reached on inclusion.
- As more and more elements of cost are included price as a determinant will favour renewables.

Other important issues were:

1. Most power providers (utilities or mining companies) subsidise diesel power in particular, and remote power in general. The benefit of cheaper remote power generation technology will accrue to the generator or its shareholders (usually the State or Territory Government) through lower subsidy costs.
2. The budgets available for development and deployment of new technology are vanishingly small.
3. Utility shareholders (whether government or private) plan to utilise less rather than more capital and seek to maximise returns through outsourcing, parallel marketing opportunities and plant life extension.
4. They are risk averse.

MAKING CONCENTRATED PHOTOVOLTAICS A COMPETITIVE REALITY

Solar Systems' conclusions were:

1. Concentrator PV had the potential to be a major business opportunity (publicly listed company > AUD \$100 million market capitalisation in 10 years, 1992 to 2002).
2. To justify the employment of capital in competition with other opportunities, significant rates of return on capital are required. Property development, software development and financial services, three areas where Solar Systems founding shareholders had profitable activities, all generate high rates of return and compete for shareholders' available funds. Capital required for the task exceeded \$20 million.
3. Risk would have to be assumed by Solar Systems.
4. Build, own, operate (BOO) was the only realistic model which could meet all the customer's requirements.
5. Significant expenditure would always be required in ongoing research and development and product development activities.
6. It is difficult to see the benefits of any new technology without full and careful analysis. Customers cannot, will not and should not have to undertake their own new technology education. As providers of competing technologies, it is our responsibility to demonstrate the benefits and to take the risks to satisfy the customer's requirements.

MAKING CONCENTRATED PHOTOVOLTAICS A COMPETITIVE REALITY

The company's research had revealed customer requirements for RAPS to be:

1. Provide a consistently cheaper alternative to the market leader diesel.
2. The cost of the equipment and its installation must be met by the technology provider
3. Operations & maintenance requirements must be provided by the technologist and should not displace existing workers.
4. The risk of technology failure must remain with the technology provider.

Having defined the market and the customers' requirements, Solar Systems committed itself in 1992 to establish the technology, the manufacturing facilities, the marketing program and the financial services systems to deliver the customer the required service.

1. Technology Review

Solar Systems shareholders had been active in renewable energy since 1977 and had a detailed understanding of the "state of play". After appointing an appropriate advisory team a detailed technology review was undertaken including a worldwide study tour and a detailed database search which concluded that the most prospective technology was concentrator photovoltaic technology.

It was considered that this technology represented the best method of combining high efficiency electricity production, thermal co-generation and storage systems.

This would allow initial market penetration in the short term and a significant medium and long term product train.

The long term objective was a reversible hydrogen fuel-cell electrical production system driven by high efficiency solar means.

MAKING CONCENTRATED PHOTOVOLTAICS A COMPETITIVE REALITY

2. Market Entry Target

Through experience in other commercial fields in local and overseas markets, particularly the Philippines, Malaysia, Indonesia and Thailand, it was clear that the first possible market entry point would be substitution of diesel power because of its high cost of generation. Analysis and discussions with prospective customers revealed that the price per kWhr was believed to start at slightly under AUD\$0.20 and range upwards quite rapidly. I use the word "believed" because in many cases, there was no empirical evidence of the actual cost of generation as no appropriate records were kept. In some cases, plant life and operations & maintenance costs were assumed to be the manufacturers' recommended level or to cost nothing. The most expensive diesel systems then provide the initial market entry point.

3. Research & Development Program

In the period 1992-1997, Solar Systems undertook an extensive research and development program in Australia and overseas – particularly in the United States of America. The ongoing program was specifically designed to produce a product that could generate electricity more cheaply than a typical diesel fired system could. In addition, the system had to be capable of accepting later developed improvements such as retrofitting of the inevitable improvements in solar cell efficiency and planned add on storage and co-generation systems. The system had to be modular to allow for installation growth and attention was focused on price reductions through a combination of higher system efficiency and ease of manufacture. The technology developed was a concentrator photovoltaic system operating in excess of 250 Suns which leverages the cheap laser-aligned, computer-controlled steel and glass reflectors and Infra Red Reflection and Recovery (IRRR) optics systems against the expensive, but highly efficient receiver.

4. Design

The culmination of the research and development program resulted in a design which has the necessary qualities, capacity and capability to enable Solar Systems to enter and maintain a position in the market.

MAKING CONCENTRATED PHOTOVOLTAICS A COMPETITIVE REALITY

Namely:

- Modular design which allows efficient manufacturing and installation over a wide range of scales.
- Ability to be simply updated with new technology.
- Ability to expand into co-generation and high efficiency systems through the use of synergistic add-ons.

The research and development and design programs produced the required results and the company has spent the last nine months finalising pre-production issues for the initial release device designated the Solar Systems SS20. Solar Systems is now engaged in marketing its ability to deliver solar energy to the marketplace at prices significantly cheaper than many diesel power installations.

5. The Manufacturing Process

In order to achieve the initial price points and assure future competitiveness, Solar Systems has spent several years on manufacturing issues to ensure the lowest cost of manufacture and deployment. This entails a fully automated production process at the company's own manufacturing facility and also at partnering facilities in specialist outsourced locations. In addition, expert dedicated deployment teams equipped with appropriately designed assembly and erection tools complete the process.

6. Design the Financial Options

In addition to its substantial technical and administrative staff, Solar Systems' in-house accountants, lawyers, intellectual property specialist and structured finance operatives, ably supported by the best available external consultants and bankers, have designed and had approved by the National Australia Bank Ltd a financing option that ensures that no capital expenditure is involved in the decision to add solar energy to the customer's energy generation mix. This arrangement ensures that the

MAKING CONCENTRATED PHOTOVOLTAICS A COMPETITIVE REALITY

only risk assumed by the customer is the risk that the customer will not be able to on-sell the power purchased. This risk is faced whether the power in question was generated by solar or fossil fuel means.

7. Work with the customer to satisfy its requirements

Solar Systems is now approaching various utilities and other power generators offering its unique package. This involves a teamwork approach consisting of the following:

- the customer suggesting possible sites for solar supplementation to existing diesel generation capacity
- Solar Systems and the customer calculating current diesel generation costs.
- Solar Systems then puts forward a proposal in relation to the level of solar power that should be installed, taking account of usage patterns and the available solar resource.
- Finally, a tariff and contract period for the Independent Power Producer agreement that underpins the finance option is negotiated.

Currently, Solar Systems is involved in a number of negotiations aimed at securing the first agreement to install SS20's in the field.

8. Marketing

In June of this year Solar Systems will launch the SS20. The launch will be supported by an appropriately targeted marketing program both in Australia and overseas. Elements of the plan include

- Site demonstration visits to Solar Systems' Fosterville demonstration and testing facility to view the SS20 device.
- Indicative cost analysis for generators over various contract periods.
- Examination of the advertising and cross-promotional benefits of using solar power.

MAKING CONCENTRATED PHOTOVOLTAICS A COMPETITIVE REALITY

- Demonstration of products to be introduced over the next few years.

9. The Future

Solar Systems has a current product phase which commences with the SS20 and which will culminate with the delivery of the patented solar hydrogen electrical generation and storage system (Hytemp). All elements of this system have been demonstrated, including

- High efficiency infra-red reflection and recovery (IRRR).
- Light-guide technology.
- Fuel cell production and consumption of H₂.
- High efficiency III-V receiver.

Work is continuing and customers will be kept up to date on product availability times and system upgrade options.

In addition to the hydrogen program Solar Systems is involved in various longer term research and development projects.

Conclusion

Solar Systems is now in the business of offering solar electric power at prices demonstrably lower in cents per kWhr terms than many current diesel installations.

The company is undertaking a systematic approach to obtaining orders and is well staffed, well capitalised and has the necessary technical skills to deliver a quality product and an excellent customer service.

The future will produce many technical innovations which have been designed to be retrofitted to the early installations and when achieved, will open broader markets for Solar Systems' concentrator photovoltaic technologies.

- 1.3 Lasich J.B., Thorpe G.R., 1996, “An Advanced Solar Co-Generation for Remote Communities”, *Conference on Engineering in Agriculture and Food Processing*, Paper No. SEAg 96/027

An Advanced Solar Co-Generator For Remote Communities

J B Lasich¹ and G R Thorpe²

¹Solar Research Corporation Pty Ltd and

²Department of Civil Engineering, Victoria University

COPY

1. INTRODUCTION

In remote off-grid areas electrical energy is traditionally provided for individuals or communities by diesel generators. Often fuel is transported over long distances and thus the ultimate cost of the generated electricity is high with the cost ranging from 20 to 80 cents/kWhr. In Australia, flat plate PV electricity generation systems are practical and economical for areas where high fuel and maintenance costs exist for diesel systems. With PV panel costs of approximately \$8/peak only a small part of this market is accessible by solar.

To expand the applicability (reach) of solar photovoltaic systems it is necessary to reduce their cost and improve their versatility. A new system using dish concentrators, high efficiency PV receivers and infra-red separation optics for co-generated heat production has been devised and is under test at SRC. The use of concentration to replace high cost solar cells with low cost mirrors and the by-product heat have the potential to reduce solar power costs to \$4/watt or less. This paper explains the concept - describes the system and indicates likely performance outcomes from early tests.

2. DESIGN PHILOSOPHY

A market survey by Blakers et al (1991) has concluded that if the cost of photovoltaic power was reduced from the present \$8/watt to \$4/watt the potential market would expand by a factor of ten to an estimated \$1.2 billion.

There is thus considerable incentive for reducing the cost of solar generated power.

The approach to reducing solar power generation cost is three-fold:

- (i) To reduce the cost of the solar collection system by substituting mirrored glass at \$300/m² for solar cells which cost \$1000/m². In order to significantly reduce the cost of the Solar Cell component the photovoltaic receiver must be small in relation to the collector area. This necessarily requires using high concentration of solar energy. The receiver area is approximately 1/300th of the collector (concentrator) area and thus the concentration ratio is 300x and the PV receiver is subject to a light intensity of 300 suns.

The receiver must be actively cooled and be of special design to dissipate the heat and deliver the high power density associated with the intense beam. Figure 1 shows a schematic of the main system components.

All of the sunlight which is intercepted by the Mirror Dish Concentrator is directed to the receiver at the focal point and converted to electricity. The system is automatically aligned to the sun. Figure 2 shows a photograph of a 1.6m² Dish PV concentrator system.

- (ii) To increase the system efficiency. At high concentration 200 Suns+, the area of the solar cell is less than 1% of the collector area. This allows a relatively high cost per unit area solar cell of high performance to be used with only an incremental increase in system price. Cells with more than double

the efficiency of commercially available flat plate products have been demonstrated in the concentrator system.

Figure 3 shows a commercially available Flat plate PV panel having an efficiency of approximately 10%. 2.5m² of this type of Flat plate module will deliver 250 watts of full sun. Figure 4 shows the SRC high efficiency high concentration module also rated at 250 W - however with an efficiency greater than 20% of 300 suns. The area required is just 0.0036m². (The module is 600 times more powerful per unit area)

Super high efficiency tandem cells of GaIP/GaIAS have been tested at 28% efficiency on sun. Figure 5 shows Tandems on sun (green plate).

- (iii) The recovery of useful thermal energy from the system by separation of a substantial portion of the normally unused infra-red radiation from the solar beam before it reaches the solar cells. This contributes to lower cell temperature and allows the generation of high value heat (70 °C +) simultaneously.

Figure 6 shows the 1.6m² PV Concentrator dish system with optical infra-red separation system. The IR (and some visible) light is shown being emitted simultaneously with electricity production. Combined efficiencies of 30% were demonstrated using similar technology and temperatures of 1100 °C+ have been developed from the intense by product heat.

3. SYSTEM DESCRIPTION

A Dish Concentrator, photovoltaic receiver and heat transfer/rejection system are the main sub systems. The Mirror consists of mirrored facets attached to a parabolic dish which are aligned by Laser direction to a pre-determined configuration for even accuracy and suitable power distribution to the Flux modifier and ultimately the

PV receiver.

The Flux modifier redistributes the light from the dish beam to provide an even flux distribution at the cell face. The receiver for a 20m² Dish has an area of .06m² and consists of modules which are close packed such that the receiver face is 99% active. The receiver has features as described below:

(i) Active cooling for the solar cells provides a low operating temperature to protect the cells and maximise the power output. To achieve this an integrated photovoltaic module has been developed which includes:

- series circuit for cell connection
- intimate thermal connection to cooling heat exchanger while maintaining electrical isolation of live components
- high efficiency, low pressure drop heatsink
- connection terminals, bypass diode and mounting stud
- >99% packing factor

The modules may be connected in series/parallel to provide the desired voltage/current characteristics. The DC power produced may be stored in batteries and/or connected to an inverter for AC output.

(ii) IR makes an insignificant contribution to the production of PV electricity, it adds considerably to the thermal load on the cells. For this reason, an IR filter is placed in front of the cells, and the heat absorbed by this filter may be used to provide, for example, hot water. A further variant uses IR reflection and reconcentration to a light guide which has been used to produce temperatures of 1100 °C.

(iii) The solar radiation flux must be uniform if the arrays of PV cells are to operate with a high efficiency. For this reason software has been developed to design a flux modifier that ensures a very high uniformity of radiation flux striking the array of cells. The typical shape of an un-modified beam is shown in fig.

The modified beam is shown in fig.

4. THE PERFORMANCE OF A LARGE SCALE SYSTEM

The design philosophy has been realised by the construction of a dish concentrator system at Fosterville, Victoria. The system consists essentially of a 5m diameter parabolic collector dish. The silicon solar cells are mounted in the form of an array that has dimensions of 240mm by 240mm. The intensity of solar radiation on the array of cells is 270 suns. The parabolic dish is fitted with a tracking system that can follow the sun with an accuracy of $\pm .1^\circ$. Preliminary results from the system indicate that it is capable of providing : 3.0 kW @ 240V AC of electricity and 2.5 kW of heat at a total efficiency of approximately 30%.

5. CONCLUSION

The high efficiencies necessary to effect a cost reduction are being realised. When system performance is optimised the unit will be costed. This will provide a direct measure of the cost of power for this system. It is planned to market the system in 1997.

REFERENCES

Blakers, A, Green, M, Leo, T, Outhred, H and Robins, B, 1991 The Role of Photovoltaics in Reducing Greenhouse Gas Emissions, Australian Government Publishing Service.

- 1.4 Friedman D.J., Kurtz S.R., Sinha K., McMahon W.E.,
Kramer C.M., Olson J.M, Lasich J.B., Cleeve A.X.,
Connaughton I., 1996, “On-Sun Concentrator
Performance of GaInP/GaAs Tandem Cells”, *25th IEEE
Photovoltaic Specialist Conference*, pp 73-75

COPY

**On-Sun Concentrator Performance
of GaInP/GaAs Tandem Cells**

**Reference: Twenty Fifth IEEE
Photovoltaic Specialists Conference 1996**

Pages 73 - 75

ON-SUN CONCENTRATOR PERFORMANCE OF GaInP/GaAs TANDEM CELLS

D. J. Friedman S. R. Kurtz, K. Sinha, W. E. McMahon, C.M.Kramer, and J. M. Olson
National Renewable Energy Laboratory, 1617 Cole Blvd., Golden, CO 80401

J. B. Lasich, A. X. Cleeve, and I. Connaughton
Solar Research Corporation Pty. Ltd, 6 Luton Lane, Hawthorn, Victoria 3122, Australia

ABSTRACT

The GaInP/GaAs concentrator device has been adapted for and tested in a prototype "real-world" concentrator power system. The device achieved an on-sun efficiency of $27\% \pm 1\%$ in the range of approximately 80-400 suns with device operating temperatures of 32°C to 50°C . We discuss ways of further improving this performance for future devices.

INTRODUCTION

The monolithic two-terminal GaInP/GaAs solar cell [1] is a promising candidate for application in terrestrial concentrator power systems, due to its demonstrated efficiency in excess of 30% for concentrations in the range of 100-300 suns [2]. This device has been adapted for evaluation on-sun in a parabolic-reflector concentrator system [3], the first measurement of this device under real-world concentrator conditions. This paper describes the necessary adaptations, presents the on-sun measurement results, and compares these results with the modeled behavior to aid in predicting the performance of future generations of the device.

DEVICE REQUIREMENTS AND GRID DESIGN

The requirements for a device usable in the concentrator system are more stringent than for devices measured on a simulator. To obtain acceptable signal to noise in the concentrator system, a device with an effective size of 1.0 cm^2 is used. This device, a top view of which is pictured in Fig. 1, consists of four 0.25-cm^2 "subdevices" on a single wafer, processed and mesa-etched for electrical isolation so that the subdevices can be tested individually if desired. Each subdevice has a bus bar on only one side of the device. For the on-sun testing, the bus bars of the four subdevices are connected electrically to give a device that is thus actually a 1.0-cm^2 -illuminated-area device with bus bars on opposite sides of the device. In contrast, the original GaInP/GaAs concentrator device [2] was 0.1 cm^2 . For ease of soldering contacts to the bus bars, the bus bars are 0.75 mm wide.

The ultimate concentration goal for this application is 500 suns. However, the requirement of the large device size as described above puts heavy demands on the grid fingers of the front metallization. A highly conductive, narrow, thick (and thus, high-aspect-ratio) finger with good contact resistivity is called for. For the first iteration of the

device, a Au-plated front-contact metallization is used for convenience. This metallization is limited in the conductivity, narrowness, and height of the grid fingers it can provide — a significant limitation for high-concentration devices, especially for the grid-finger lengths of the device shown in Fig. 1. Typical resistivity for the Au-plated metallization is $5 \times 10^{-6}\ \Omega\text{-cm}$, more than twice the tabulated bulk Au resistivity of $2.2 \times 10^{-6}\ \Omega\text{-cm}$. The difference is due to the relatively grainy character of the metal deposited in the electroplating process. In principle, limitations in the grid finger resistivity can be compensated for by increasing the thickness of the finger. However, for the plated metallization, the thickness is limited by the photoresist thickness to about $2.5\ \mu\text{m}$. Increasing the finger conductance by increasing the finger width must be balanced against the grid-coverage shadow loss; for this reason, narrow high-aspect-ratio grid fingers are preferred. The plated-metallization process, however, cannot reliably produce grid finger widths significantly below $10\ \mu\text{m}$, and the limitations of the finger thickness and conductivity for this metallization diminish the importance of narrower grids. Finally, I^2R losses due to the emitter sheet resistance (about $200\ \Omega/\text{sq}$ for the top cell of the device

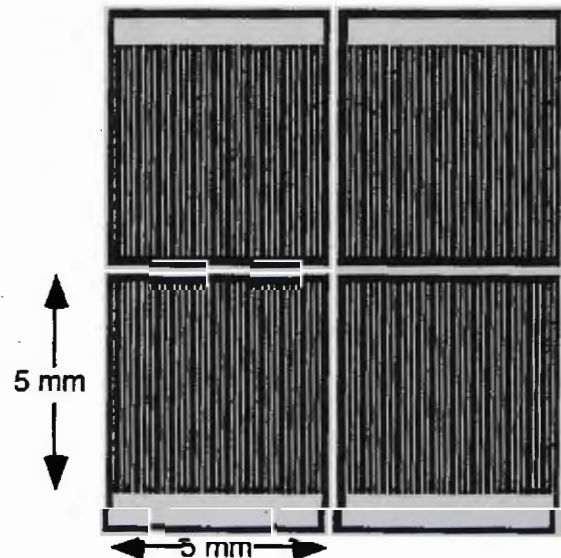


Fig. 1. Schematic top view of the device. The subdevices are electrically isolated with a mesa etch, so the area between them is not photoactive. All four bus bars were connected electrically for testing, resulting in an effectively 1-cm^2 device. Grid fingers are $10\ \mu\text{m}$ wide and are spaced $150\ \mu\text{m}$ apart.

described here) demand that grid fingers be spaced close together. This emitter sheet resistance loss combined with the grid-finger resistivity loss (plus several other loss terms [2] of less importance for the device described here) must be balanced against the grid-coverage shadow loss to arrive at a final grid design.

The initial iteration of the device has grids optimized for a lower concentration of 200 suns; the optimal grid spacing at this concentration for the plated metallization is 150 μm . Even at this lower concentration, the deficiency of the plated metallization limits the device efficiency. Future iterations of the device will use an evaporated metallization that should overcome the grid-finger limitations of the plated grids, permitting fingers 3 μm wide and 5 μm thick, or better. The evaporated metallization also provides grid-finger resistivities much closer to the book values (i.e., much lower than the plated metallization provides), due to the superior density and grain structure provided by the evaporation process.

DESIGN OF TOP CELL

The on-sun spectrum is, of course, not precisely the ASTM E891 standard AM1.5 direct spectrum, and indeed it varies during the day. For the series-connected tandem device described here, the ideal top-cell thickness depends on the spectrum. This dependence arises because the top-cell thickness determines the relative photocurrents of the top and bottom cells; the tandem cell photocurrent is maximized when the top and bottom cell photocurrents are matched, because the tandem current is limited by the series connection to the lesser of the two subcell photocurrents [4].

For the first iteration of the device, we have chosen to design for the standard AM1.5 direct spectrum, with a top-cell thickness of 1.0 μm . Future iterations of the device may be tuned to some time-average of the actual incident spectrum. A detailed discussion of the performance of multijunction devices as a function of variations in the incident spectrum is given elsewhere [5,6]. The overall conclusion of these works is that spectrum fluctuations affect the performance of series-connected tandems more than the performance of 1-junction devices, but that the overall performance advantage of the tandem is not changed by this efficiency fluctuation.

DEVICE MEASUREMENT AND PERFORMANCE

The wafer was mounted on a receiver substrate with good thermal contact to cooling water. The light flux onto the receiver region was apertured so that only a well-defined area on the wafer is illuminated. The flow and temperature of the receiver cooling water were precisely measured, permitting a direct calorimetric measurement of the incident flux given the reflectance of the device. Thus no assumptions about the linearity of the short-circuit current (J_{sc}) with concentration need be made, in contrast to typical simulator measurements. This is not a trivial issue, because nonlinear response has been reported for GaAs solar cells [7]. Nor are spectral corrections needed, because the actual solar spectrum is being used.

The temperature of the device was not held at 25°C, the conventional simulator-measurement reporting temperature, but rather was allowed to reach the

temperature it would operate at if the concentrator system were being used to generate power. Therefore, no temperature correction need be applied to the device performance parameters to predict the device performance under actual operating conditions. However, the device temperature must be taken into account in the modeling of the device behavior.

Figure 2 shows the measured concentration-dependent open-circuit voltage (V_{oc}), fill factor, and efficiency. For V_{oc} , the open symbols show what V_{oc} would be at 25°C, using a temperature coefficient of -3.9 mV/°C as measured for this device. For comparison with the data, the dashed lines show the modeled behavior. V_{oc} is modeled by assuming an effective ideality factor of $n=2$, appropriate for a series-connected tandem with ideal ($n=1$) top and bottom cells. The calculated V_{oc} describes the temperature-corrected measurements very well. The fill factor (FF) is modeled by calculating I-V curves [8], with the addition of an effective series resistance [2,9]. The measured fill-factor data points appear to be consistent with the modeled curve, to the degree to which the two can be compared given the scatter in the measurements.

The linearity of J_{sc} at concentration C is given by the ratio of the one-sun-normalized J_{sc} to the concentration, $(1/C) J_{sc}(C)/J_{sc}(1)$. The concentration C is given by the ratio of the calorimetrically-measured photon energy flux $\Phi(C)$ to its one-sun value: $C=\Phi(C)/\Phi(1)$. The measured J_{sc} linearity is shown in Fig. 3. The difference between the measurements and the ideal-linearity case is presumably due almost entirely to noise in the measurement of Φ , because the linearity would not be expected to vary as nonmonotonically with C as the data of Fig. 3 does. Thus a

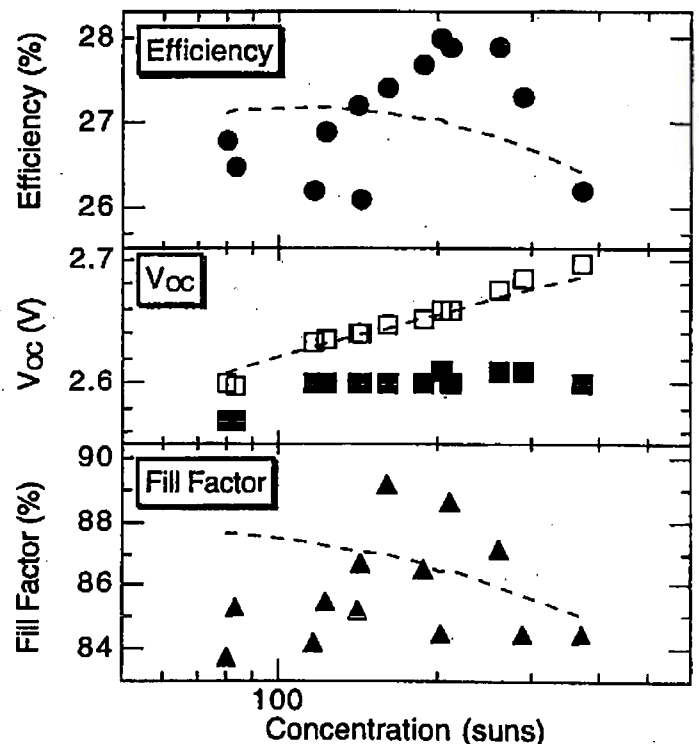


Fig. 2. On-sun performance of the device, "MA215". The data are shown as the filled symbols. The open squares show V_{oc} corrected to 25°C operating temperature. The dashed lines show the modeled behavior, including temperature correction for V_{oc} (but not for FF).

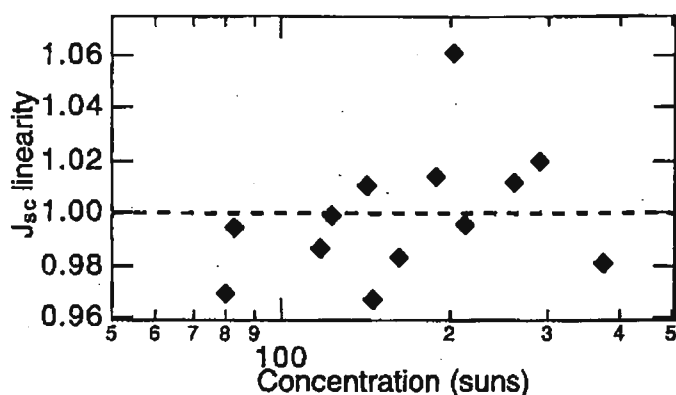


Fig. 3. J_{sc} linearity. The dashed line represents the case of perfect linearity.

determination of the device nonlinearity awaits data with better signal to noise in Φ . Working with larger device areas should help with this measurement.

Finally, the measured efficiency shown in Fig. 2 is given by $J_{sc}V_{oc}FF/\Phi$. The modeled efficiency, which uses the temperature-corrected V_{oc} , is shown for comparison. The efficiency data appear to have a maximum with concentration that is much sharper than the modeled curve. However, this is most likely an artifact of the noise in the FF and Φ data. From the scatter in the data, we estimate a relative uncertainty of about 2% in the FF and Φ measurements, giving a relative uncertainty (not including systematic errors, which are hard to quantify) of about 3% (i.e., about 1% absolute) in the efficiency numbers. With these error bars, we can summarize the peak performance of the device as $27\% \pm 1\%$ in the range of approximately 80-400 suns. The modeling suggests that the efficiencies are in the lower end of this range. It should be emphasized that the efficiencies in this concentration range are achieved with device operating temperatures of as high as 50°C .

FUTURE WORK

The most important direction for improving the performance of future devices will be the adoption of an evaporated-metal/lift-off front grid metallization. Modeling a device with this improved metallization, at 500 suns a gain on the order of 6% in the relative cell performance (about 2% in absolute efficiency) can be expected. Better current-matching of the top and bottom cells to the solar spectrum being used may also lead to a further improvement in the device efficiency. Fabricating 1-cm^2 devices without the mesa-etch division into four subdevices will reduce perimeter recombination by a factor of two.

To optimize total module efficiency, a single bus bar running down the center of the cell would reduce the total cell area compared to the two side bus bars used in the device shown in Fig. 1. The single-central-bus-bar configuration does not change the effective lengths of the grid fingers, and so the performance of such a device should not suffer compared to that of the present two-bus-bar design. Future work will include the examination of this bus bar design.

ACKNOWLEDGMENTS

This work was supported by the U.S. Department of Energy contract No. DE-AC36-83CH10093.

REFERENCES

- [1] K.A. Bertness, S.R. Kurtz, D.J. Friedman, A.E. Kibbler, C. Kramer, and J.M. Olson, "29.5%-efficient GaInP/GaAs tandem solar cells", *Appl. Phys. Lett.* **65**, 1994, pp. 989-991.
- [2] D.J. Friedman, S.R. Kurtz, K.A. Bertness, A.E. Kibbler, C. Kramer, J.M. Olson, D.L. King, B.R. Hansen, and J.K. Snyder, "GaInP/GaAs monolithic tandem concentrator cells", *1st World Conference on Photovoltaic Energy Conversion*, 1994, pp. 1829-1832.
- [3] J.B. Lasich, A. Cløeve, N. Kaila, G. Ganakas, M. Timmons, R. Venkatasubramanian, T. Colpitts, and J. Hills, "Close-packed cell arrays for dish concentrators", *1st WCPEC*, 1994, pp. 1938-1941.
- [4] J.M. Olson, S.R. Kurtz, A.E. Kibbler, and P. Faine, "A 27.3% efficient Ga_{0.5}In_{0.5}P/GaAs tandem solar cell", *Appl. Phys. Lett.* **56**, 1990, pp. 623-625.
- [5] S.R. Kurtz, J.M. Olson, and P. Faine, "The difference between standard and average efficiencies of multijunction compared with single-junction concentrator cells", *Solar Cells* **30**, 1991, pp. 501-513.
- [6] P. Faine, S.R. Kurtz, C. Riordan, and J.M. Olson, "The influence of spectral solar irradiance variations on the performance of selected single-junction and multijunction solar cells", *Solar Cells* **31**, 1991, pp. 259-278.
- [7] G. Stryi-Hipp, A. Schoenecker, K. Schitterer, K. Bücher, and K. Heidler, "Precision spectral response and I-V characterization of concentrator cells", *Proceedings of the 23rd IEEE Photovoltaic Specialists Conference*, 1993, pp. 303-308.
- [8] S.R. Kurtz, P. Faine, and J.M. Olson, "Modeling of two-junction, series-connected tandem solar cells using top-cell thickness as an adjustable parameter", *J. Appl. Phys.* **68**, 1990, pp. 1890-1895.
- [9] T.A. Gessert and T.J. Coutts, "Grid metallization and antireflection coating optimization for concentrator and one-sun photovoltaic solar cells", *J. Vac. Sci. Technol. A* **10**, 1992, pp. 2013-2024.

1.5 Lasich J.B., 2000, “Photovoltaic Concentrator Systems
for RAPS”

PHOTOVOLTAIC CONCENTRATOR SYSTEMS FOR RAPS

John B LASICH

Solar Systems Pty Ltd, 6 Luton Lane, Hawthorn, AUSTRALIA 3122

ABSTRACT

Solar energy has the potential to be the perfect source for all of our energy needs providing infinitely renewable power with virtually zero material or thermal pollution during operation.

As great as this potential is however, an almost insignificant fraction of our energy is provided directly from this source. The reason is the perceived high cost. Analysis of this "cost" reveals two apparent reasons - technological immaturity and cultural perception.

The technological causes stem from the difficulties associated with capturing, converting and storing a dilute and intermittent energy source. The cultural barrier comes from our current sense of 'value'.

Our present culture is to value most highly that which we can "acquire today and pay for tomorrow". Presently, with solar power one pays today and receives the benefits tomorrow.

One method of addressing both problems is by reducing the capital cost of a solar power system to a level where a financier can profit from financing the product into a market, thus allowing a customer in that market to have the service today, and pay as he or she consumes in cents/kWh. This now provides a direct comparison such that a relatively simple judgement can be made to determine if solar power is cheaper.

The whole problem may thus be reduced to one of a technical nature, with financial events following (once there is profit to be made). To address the technical problems, the activities of solar power generation may be considered as a two-step process of collection and conversion, it is then possible to identify clear targets for improvement by cost reduction and efficiency increases.

The use of a dish solar concentrator focusing to a small high power photovoltaic receiver provides for both of these benefits, as well as the additional bonus of synergistic cogeneration via spectrum splitting, which is unique to this combination of components.

To achieve these benefits the technical barriers which have been broken include - development of optics for the even illumination and production of a close-packed, high voltage, high power PV receiver operating at 45 °C in a solar beam which would normally melt steel.

At a production rate of just a few megawatts, the cost of AC power production from this technology is about 30 cents/kWhr. This approximates to less than \$5.00/Watt of nameplate rating for fixed flat PV plate panels.

This is economic as a fuel saver for most diesel and many end of grid applications where finance can be arranged.

INTRODUCTION

Solar energy has the potential to be the perfect source for all of our energy needs providing infinitely renewable power with virtually zero material or thermal pollution during operation.

The earth receives 7×10^{17} kWh/year (Avallone and Baumeister, 1987) of radiant energy from the sun, which is 7,000 times more energy than we presently consume - clearly an ample resource.

With a solar energy system having an efficiency of 25%, an area 600 km square located in the Australian Desert, would be sufficient to supply the world's energy needs. It is thus evident that solar radiation could supply all our energy, while reducing pollution problems during humankind's likely habitation of the planet.

It appears that scientific evidence and deduction however, are not sufficient to bring about acceptance and adoption of such a change by us even for our own good.

As great as this potential is, an almost insignificant fraction of our energy is provided directly from this source. One of the main reasons is the perceived high cost. Analysis of this "cost" reveals two apparent components - technological immaturity and cultural perception.

The technological causes stem from the difficulties associated with capturing, converting and storing a dilute and intermittent energy source. While these problems are solvable, it takes time for ideas and concepts to reach the market place.

The cultural barrier derives from our current sense of 'value'.

Our present culture (ably assisted by financial institutions) is to value most highly that which we can "acquire today and pay for tomorrow". Conversely, the very nature of solar energy is that all the cost is up-front - the energy is delivered free later.

One method of addressing both problems is to reduce the capital cost and increase the size of a solar power system to a level where a financier can profit from financing the product into a market, thus allowing that customer to have the service today, and pay as he consumes in cents/kWhr.

In fact, a critical mass of four components are ALL needed to facilitate the substantial uptake of renewable energy. These are social conscience, improvements in new technology, government support and the increased cost of traditional energies due to the addition of "externalities". These components will provide a progressively more favourable market place.

While three of these elements may be beyond the scope of individual influence, and are controlled by global economics and political forces, an individual effort may significantly influence the renewable technology component.

To achieve this worthwhile goal, it is necessary to enlist the inspiration of invention and impetus of commerce. 'Allow individuals to profit today from the use of new energy practices which will benefit us all in the future and a pathway will be found to the solution.'

The objective is thus to produce a solar energy conversion system which is competitive in price and performance with present expectations. This product must achieve entry into the most accessible market (where existing costs are highest) and have the continuing potential for versatility and improvement to enter other larger energy markets in the future.

If this can be achieved a substantial market is open to those who are successful and our energy and pollution problems will be solved for the long term.

• If just 10% of the Australian Government's 2% greenhouse proposal for renewable energy was met at \$5/Watt, the value is of the order of \$1 - 2 billion.

Philosophy

In order to begin the exploitation of the ideal resource of solar energy for wide application, it is necessary to reduce the cost of utilisation to a point where technology is competitive with traditional forms in certain markets. Typically, this will be the remote area power supply or RAPS in sunny locations. An analysis of the cost of generating electricity using diesel shows that the cost is frequently more than 30 cents/kWhr. To enter this market, solar power must achieve a similar or lower cost.

Possible avenues to this goal of cost reduction include:

- 1) Increasing the system efficiency
- 2) Reducing the cost of the system

To address the technical problems, the activities of solar power generation may be broken down into a two-step process of collection and conversion. It is then possible to identify clear targets for improvement by cost reduction and efficiency increases.

The use of a dish concentrator with a photovoltaic receiver provides for both of these benefits, as well as the additional bonus of synergistic cogeneration via spectrum splitting, which is unique to this combination of components.

The underlying philosophy for achieving objectives outlined above is based on the following premises:

Solar radiation is a very dilute energy source and a large area of solar flux must be intercepted to capture useful amounts of energy.

This "large area" requirement is the major contributor to the cost of all solar energy conversion systems.

The present photovoltaic panels for example, have the area of conversion device (solar cell) equal to the collection area. The sophisticated and intense processing required to produce a solar cell makes the conversion devices expensive and thus the entire panel is even more expensive.

Furthermore, a substantial part of the energy which has been collected (at great expense) is wasted, e.g. flat plate photovoltaic systems (solar panels) with efficiencies of typically 12% waste 88% of the intercepted solar energy.

When viewed from this perspective, it is clear that while a high cost is paid to intercept the solar radiation, we do not fully capitalise on this energy which has been intercepted. The energy conversion step is grossly inefficient, particularly in the production of electricity - the highest value energy form.

Efforts to increase conversion efficiency over a large area (equal to collection area) will lead to substantial cost increases and may not improve the cost per unit output.

A solution to this problem lies in the use of energy concentration in which the solar energy collector is large and cheap (mirrors) and the energy converter (PV receiver) is small and highly efficient. For example, the solar energy converter for a parabolic dish solar concentrator may have an area that is only 0.2% of the size of the collector and still deliver excellent performance. An efficiency of more than double that of most existing commercial PV panels has been achieved for concentrator receivers. (Lasich, et al, 1994)

This scenario allows for a relatively large expenditure per unit area of energy conversion device to produce a high efficiency converter, which has the effect of increasing the entire system efficiency, but at small marginal increase in system cost.

The remainder of the system (mirrors) is concerned only with energy collection and has a cost an order of magnitude less per square metre than active devices, such as solar cells.

While conceptually this approach is straightforward, many complicated practical issues must be overcome to achieve the benefits, these include:

- Delivering an even radiation intensity to a large number of series connected PV cells in a small receiver.
- Guaranteeing the survival and optimal (low temperature) operation of the PV cells in a solar beam which would normally melt steel.
- Delivery of high voltage and acceptable current from a small solar panel while maintaining 99.8% packing factor and cell isolation.
- Providing accurate tracking and control.

Having established the problems, which must be solved to achieve the potential benefits of dish - PV concentrator systems, our company has developed a range of technologies to provide the solutions.

THE TECHNOLOGY

The essential components are shown in Figure 1 and include the dish concentrator 1., which concentrates all the solar energy which falls on it to the PV receiver 2., which is cooled by a heat rejection system 3., and the whole unit is directed and governed by the tracking/control system 4. Depending on the application a combination of inverter generation - battery storage may also be included 5.

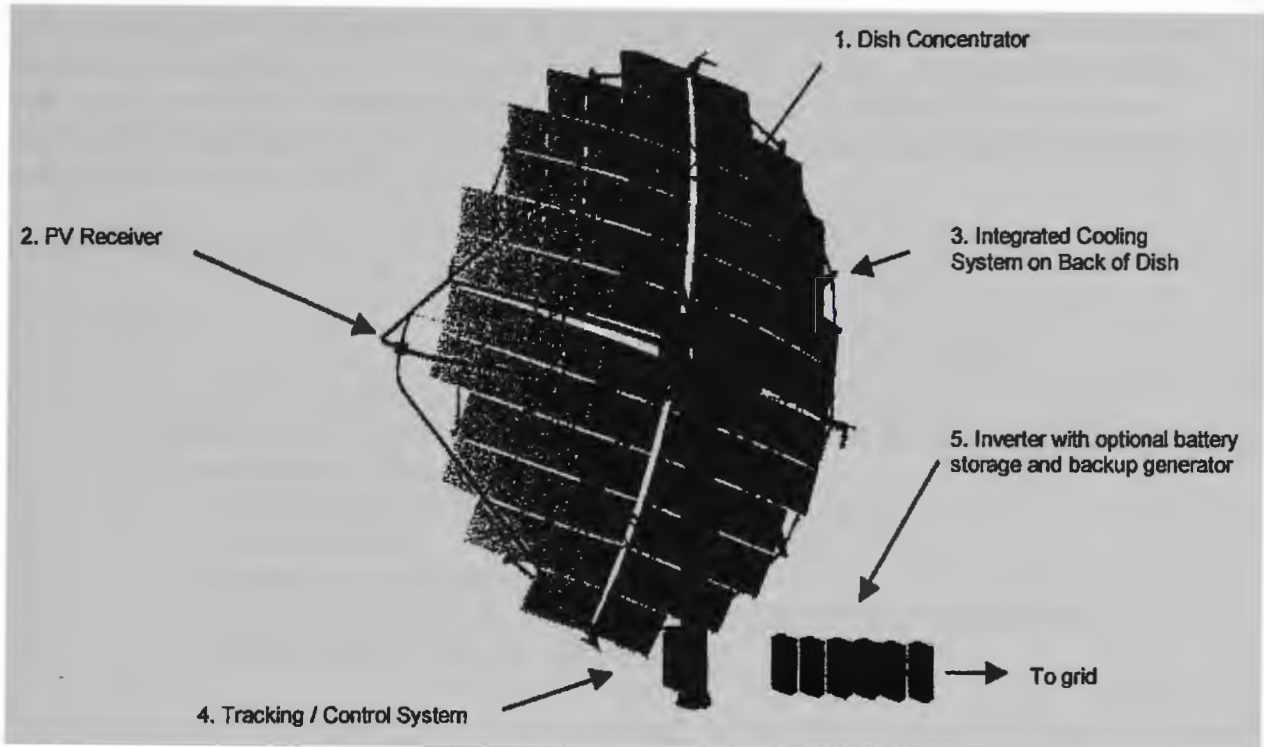


Figure 1 The SS20 Unit

Dish Solar Concentrator

The requirement

The requirement is for the most efficient Dish Concentrator at low cost with a predictable beam characteristic, which may be optically manipulated to produce an even flux distribution on the flat plane of a solar cell array positioned near the focus.

The final concentration ratio at the primary focus should be approximately 300 to 500 Suns @ 1000 W/m² Direct Solar Radiation Input.

For co-generation, the primary optics should be such that secondary and tertiary optics will work efficiently allowing for simple robust methods of spectrum splitting and collection of the 'split' energy at a second focus.

The system should be modular to facilitate maximum flexibility in production, deployment and operation.

Design of Components:

To deliver the characteristics prescribed above, the design of components for subsystems of a dish concentrator must include the following characteristics:

Mirrors

To achieve the objectives of low cost and consistent quality require the mirror system to consist of mirror sections, which are square, modular and all of the same spherical section. Square mirrors are low cost because mirrors can be constructed from components, which are normally supplied square, such as glass and steel. Modularity allows for repetitive production and flexibility of design and construction. Appropriately positioned spherical sections can approach a paraboloid very closely if each section is approximately 1% of the total area.

Photovoltaic Receiver

The receiver must :

- Withstand high solar flux to several thousand Suns.
- Be optically matched to the dish to provide the appropriate intensity and flux distribution.
- Have close-packed PV modules which have:
 - cell packing density 99%
 - no front contacts
 - excellent electrical isolation.
 - excellent thermal conductivity for removal of intense energy from cell face.
 - means of removing high intensity heat.

The PV receiver shown in Figure 2 achieves the above requirements.

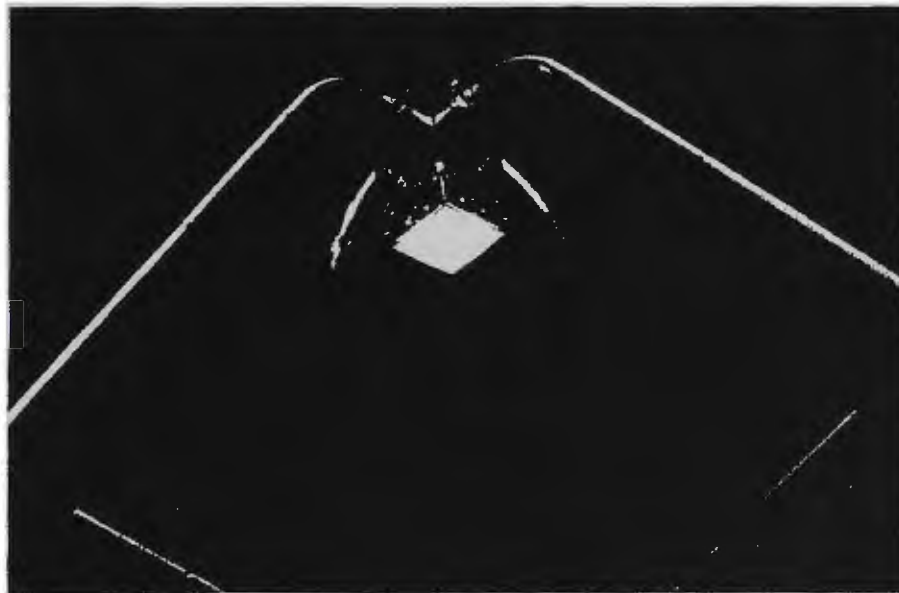


Figure 2 SS20 Receiver View - 'on sun'

The main components of the receiver include:

- A "flux modifier" to assist in optical matching of dish and photovoltaic receiver.
- A close-packed array of PV concentrator modules which contain:
 - High efficiency solar cells designed for operation at 300 Suns @ 99.8% packing factor.
 - A metallised ceramic substrate which provides a series circuit for high voltage inter-connection of cells and excellent electrical isolation as well as
 - Excellent heat transfer to a high performance actively cooled heat sink. See Figure 3.
- Data Acquisition System to monitor the receiver conditions such as module voltage, module temperature, coolant flow, etc. This information is also used in the Control programs.

A photovoltaic concentrator module designed for 330 suns operation is shown in figure 3.

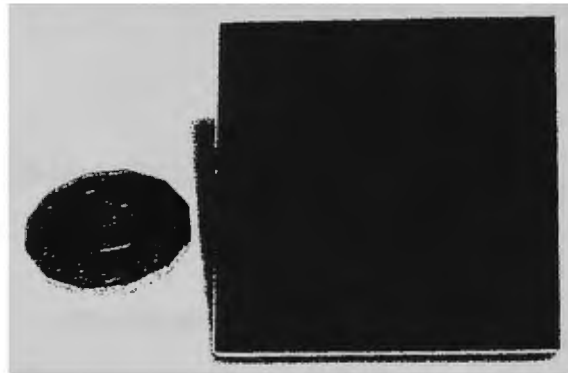


Figure 3 A 280 Watt PV Concentrator Module

Control System

The Control System must be intelligent and self-educating to optimize power output, maximize reliability and minimize dependence on operators.

The integrated software controlled tracking system developed by Solar systems takes account of

- | | | |
|--|---|--|
| Location, time and system geometry for | - | Predictive Tracking |
| Sun position for | - | Sun Tracking |
| Receiver Conditions for | - | Power optimization and Self-preservation |
| Wind Speed and Direction | - | For safe parking in high winds |

All of which are considered in the control loops for dealing with varied weather conditions, wear and tear and the need for maximum power.

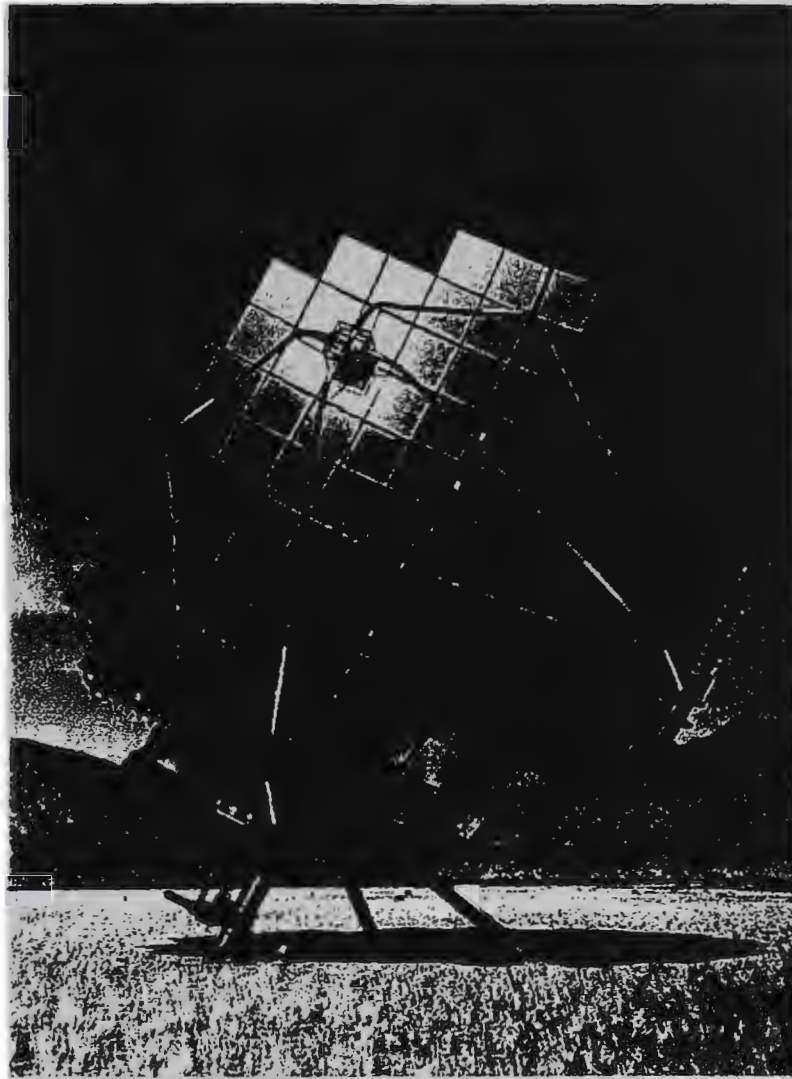


Figure 4 The 20 kW SS20 Dish - PV Unit

Heat Rejection

A considerable amount of heat must be rejected - Figure 4 shows a PV concentrator with a Heat rejection system integrated as part of the dish frame. Some of this energy may also be reflected away from the receiver. This reduces the heat load and allows for the capture and re-concentration of IR radiation to produce high grade heat for co-generation. Solar Systems has developed a patented system which can deliver high grade heat for activities such as - desalination, process heating, operation of a stirling engine, production of hydrogen and illuminating a second Low Band Gap PV receiver to produce more DC power. Our tests have shown efficiencies of 30-40% are practically achievable.

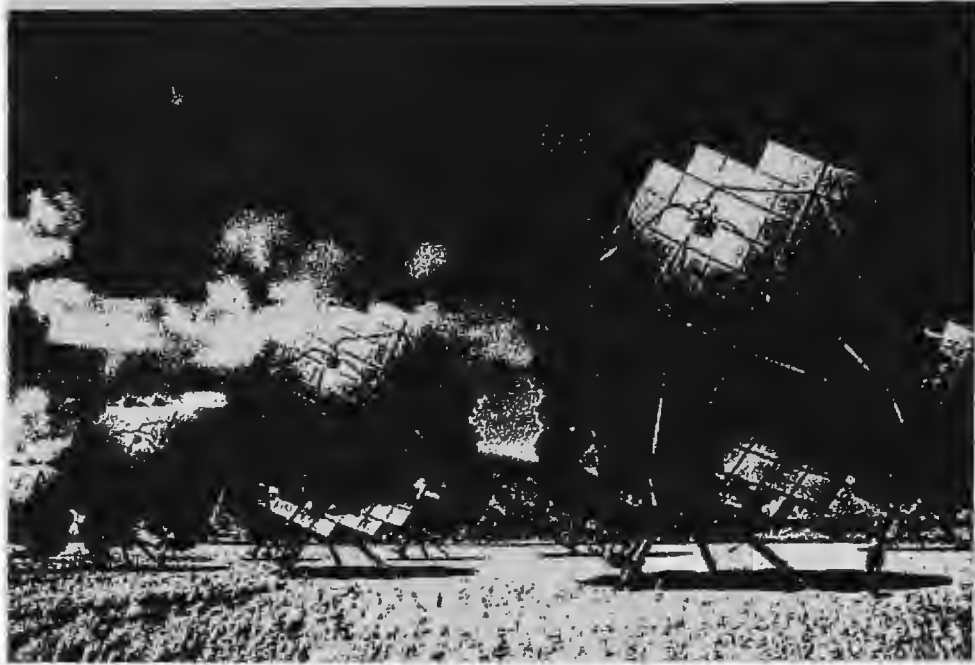


Figure 5 A Field of SS20 Dish Concentrators

CONCLUSION

At quantities of a few megawatts, the Solar Systems PV Concentrator System can produce power for less than 30 cents/kWhr, being cheaper than diesel generation in most instances and economic for end of grid connection. In the near future receiver improvements and co-generation will reduce the system cost further, increase the diversity of application and thus deliver a product ready for entry into larger, broader markets.

Figure 5 shows a "scientist's" impression of mainstream solar power.

ACKNOWLEDGEMENTS

I gratefully acknowledge Adrian Cleeve, Rosemary Skinner, George Ganakas and all the staff at Solar Systems Pty Ltd who have so ably supported the author during this work over the last seven years.

REFERENCES

AVALLONE, E.A. and BAUMEISTER, T. (Eds) 1987, *Mark's Standard Handbook for Mechanical Engineers*, McGraw Hill, USA.

LASICH, J. B., CLEEVE, A., KAILA, N., GANAKAS, G., TIMMONS, M., VENKATASUBRAMANIAN, R., COLPITTS, T. AND HILL, J., 1994, "*Close-Packed Cell Arrays for Dish Concentrators*", First World Photovoltaic Conference, Hawaii, November 1994.

1.6 Verlinden P.J., Terao A., Smith D.D., McIntosh K.,
Swanson R.M., Ganakas G. and Lasich J.B., 2001 “Will
We Have a 20%-Efficient (PTC) Photovoltaic
System?”, *Proc. 17th European Photovoltaic Solar
Energy Conference*

WILL WE HAVE A 20%-EFFICIENT (PTC) PHOTOVOLTAIC SYSTEM?

P.J. Verlinden, A. Terao, D.D. Smith, K. McIntosh, R.M. Swanson, G. Ganakas* and J.B. Lasich*

SunPower Corporation
430 Indio Way
Sunnyvale, CA 94085, USA
Tel: +1-408-991-0900
Fax: +1-408-739-7713
e-mail: pverlinden@sunpowercorp.com

*Solar Systems Pty Ltd.
6 Luton Lane
Hawthorn, Victoria 3122, Australia
Tel: +61-3-9819-9544
Fax: +61-3-9819-9063
e-mail: gganakas@solarsystems.com.au

ABSTRACT: This paper discusses the importance of solar cell efficiency to reduce the overall cost of electricity produced by photovoltaics. A large-scale demonstration of a concentrator PV system in White Cliffs, Australia is presented. The concentrator system, based on reflective dish and Point-Contact silicon solar cells, has a PTC efficiency of 20.02%.

Keywords: High-efficiency - 1: Concentrators - 2: PV system - 3

1. INTRODUCTION

There is a very common practice within the photovoltaic community, from both industry and research, to price every component of a photovoltaic system in terms of dollar per peak power ($\$/W_p$). This practice is generally used throughout the whole value chain, from bulk starting material (for example silicon feedstock in the case of silicon technologies) to system pricing. Since every developer is usually focussing on only one element of the value chain, this practice may not end up to the most economical PV system. At the end, what really counts is the cost of energy ($\$/kWh$). For example, a research team developing a new process for solar cell manufacturing may choose or not choose a particular technology based only on the additional cost of this particular technology and the additional power produced by the solar cell under Standard Rating Conditions (SRC). If the ratio of those is greater than the current cost of manufacturing solar cells, the idea may be abandoned. If this research team had a larger view, they would realize that the increase in efficiency has a tremendous effect on the whole value chain. This is particularly true and well known for concentrator systems where the cost of solar cells is a very small portion of the whole system cost and, therefore, the cell efficiency has a great impact on the cost of the produced solar electricity. It is also very true for flat-plate systems because a large part of the overall system cost is proportional to the area of the system. The realization of this leverage, that the solar cell efficiency has to reduce the cost of PV systems, is possible if the PV industry becomes fully vertically integrated or if collaborative design and implementation is increased across the whole PV value chain.

The purpose of this paper is to present the reasons why efficiency is a very important parameter in the final cost calculation of PV solar electricity, to analyse the potential of the different commercially available PV technologies, and to present the first large-scale demonstration of a cost-effective PV system to reach 20% efficiency under PVUSA Testing Conditions (PTC).

2. PV SYSTEM COST

Although we have the habit to price each element of a PV system in terms of dollar per peak power, the largest part of the cost is actually more proportional to the system area and less proportional to the peak power. Table 1 A-B shows a non-exhaustive list of the components of a PV system and their cost relationship to the area of the system or the peak power.

Table 1-A: Components of the cost of a PV system that are more proportional to the area than the peak power of the system (Not all the components apply to all PV technologies.)

Component of a PV System	Cost is more proportional to area
Bulk Starting Material	- silicon feedstock - gases - chemicals - substrates
Wafer	- ingot pulling or casting - slicing - etching
Solar Cell Manufacturing	- labour - film deposition - screen printing - diffusion - anneal - etching - testing
Module	- tabbing and stringing - laser scribing - glass, EVA, Tedlar lamination - frame, junction box - testing - packaging
Installation	- shipping - mounting structure - labour - field wiring
Maintenance	- cleaning

Table 1-B: Components of the cost of a PV system that are more proportional to the peak power than the area of the system

Component of a PV	Cost is more proportional to
-------------------	------------------------------

System	peak power
Balance of System	- inverter, controller
	- battery
	- breaker
Monitoring	- monitoring equipment

In order to illustrate how much leverage the efficiency has over the overall system cost, let's take the following example. A typical residential roof-top grid-connected PV system without backup batteries costs between US\$8 and US\$12 per peak Watt. The cost of solar cell manufacturing, excluding the starting material and the lamination, represents only 20% of the total module cost [7] and around 7% of the total cost of the PV system. On the other side, the inverter, breakers and controller also represent less than 10% of the whole system cost. There is also a fix cost for every installation, about 10% for a typical roof-top system. Therefore, all the other components represent more than 73% of the PV system cost and their cost is proportional to the area of the system. Assuming that the efficiency of the system is mostly determined by the solar cell manufacturing technology, an increase of the solar cell efficiency by 50% would reduce the system area by a factor equal to 1.5, and would be economically profitable even if the technology to produce it is up to 4.4 times more expensive.

This type of reasoning is well understood by a fully vertically integrated PV company or if collaborative design and implementation across the value chain is achieved within the PV industry.

3. TEMPERATURE COEFFICIENT

There is another fundamental reason why efficiency is important for reducing the cost of solar electricity. All existing commercially available flat-plate PV modules are rated under Standard Rating Conditions (SRC), i.e. 1000 W/m², AM1.5G and 25°C cell temperature. These are laboratory-type conditions and are quite unrealistic. In order to calculate the amount of energy that the PV system will produce over one typical year, one need to use a complete performance model that includes, among others, temperature coefficients, spectral coefficients, and wind coefficients, as the one developed by D. King [4]. A much more realistic rating is the one used by PVUSA. In the PVUSA Testing Conditions (PTC), the PV modules or systems are tested under real conditions: AM1.5G, 1000 W/m², 20°C ambient temperature and 1 m/sec wind speed. The modules with the best thermal management design and the cells with the lowest temperature coefficient will be the ones with the smallest difference between the SRC and the PTC ratings. Also, the cells with the highest efficiency have the lowest temperature coefficient.

It is well known that the efficiency temperature coefficient of a solar cell is mostly impacted by the voltage reduction when the temperature of the junction increases, but this voltage temperature coefficient is not a constant. It decreases as the voltage of the cell increases. In fact, it is almost proportional to the difference between the voltage of the cell and the bandgap of the material. In V_{oc} condition, we know that:

$$V_{oc} = kT/q \cdot \ln \left\{ I_{sc} / I_0 + 1 \right\} (1)$$

where I₀ is the saturation current of the cell which is proportional to the square of the intrinsic carrier density, n_i². Also, it is well known that:

$$n_i^2 \sim T^3 \cdot \exp(-E_g/k.T) \quad (2)$$

The derivative of V_{oc} with respect to temperature then becomes:

$$dV_{oc}/dT = - \{ (E_g/q - V_{oc}) + 3kT/q \} / T \quad (3)$$

The dominant part of this equation is (E_g/q - V_{oc}), and we can see that the voltage temperature coefficient is smaller for high-efficiency solar cells with large open-circuit voltages than for low-efficiency cells. For example, a typical flat-plate silicon solar cell would have a voltage temperature coefficient between -2.2 and -2.6 mV/°C, whereas a 22% efficiency silicon solar cell has a temperature coefficient between -1.6 and -1.8 mV/°C, and a concentrator silicon solar cell has a temperature coefficient between -1.28 and -1.34 mV/°C depending on the concentration ratio.

4. MODULE EFFICIENCY

Although the record efficiency for a laboratory silicon solar cell has reached 24.7 % (crystalline FZ Silicon solar cell fabricated by UNSW and measured at one sun with a designated aperture) [1], the efficiency of commercially available flat plate PV modules is still in the range of 5% to 12% (measured under PVUSA Testing Conditions, PTC) [4]. Flat plate PV modules over 20% efficient have been demonstrated [1-2,6]. However, the fabrication cost of these modules is far beyond what is acceptable for terrestrial application. Only concentrator modules have so far demonstrated promising results to attain 170 W/m² or 20% PTC efficiency at reasonable cost [3]. Of course comparing efficiencies of flat-plate and concentrator systems is difficult. In first approximation, and if both modules are placed on 2-axis trackers, we could say that a 20% efficient concentrator system would be equivalent to a 17% flat plate system due to the difference between direct (850 W/m²) and global (1000 W/m²) irradiance.

Table 2 summarizes the record SRC efficiencies for most of the commercially available PV technologies, measured sometimes on very small cells or with designated aperture or even uncut from the wafer to avoid edge recombination. The data for record SRC efficiencies for cells and modules are from the "Solar Cell Efficiency Tables" [1]. The right column gives the best PTC efficiencies for commercial PV modules and the data are extracted from the Sandia I-V Tracer program and their most recent database [4]. The PTC efficiency of the Concentrator III-V module was reported by M. O'Neill et al. [5] and corresponds to a prototype module with linear-focus Fresnel lens and multijunction III-V cells. Finally, the PTC efficiency of the concentrator silicon module is from this work and corresponds to a 19.75 m² concentrator dish with a dense-array receiver made of silicon solar cells.

One has to note that the PTC efficiencies reported in Table 2 are for the entire module area and includes the losses due to packing density, frame and other non-active

area of the modules, which could represent up to 30% of the module. Figures 1, 2 and 3 present the PTC efficiency of several PV modules as a function of the module area, for mono-crystalline silicon, multi-crystalline silicon and thin film respectively

Table 2: Record laboratory cell efficiency of different technologies measured at Standard Rating Conditions (SRC, AM1.5, 1000 W/m², 25C cell temperature) and best commercially available, cost-effective, module efficiency measured at PVUSA Testing Conditions (PTC, AM1.5, 1000 W/m², 20C ambient temperature, 1 m/sec wind speed)

Technology	Record SRC Cell Efficiency	Record SRC Module Efficiency	Best PTC Module Efficiency
Mono-Crystalline Si	24.7 %	22.7 %	11.7 %
Multi-Crystalline Si	19.8 %	15.3 %	11.2 %
Silicon Film	16.6 %	-	7.23 %
a-Si	12.7 %	10.4 %	5.88 %
CIS	18.2 %	12.1 %	8.27 %
CdTe	16.0 %	10.7 %	6.65 %
Conc. Si	28.3 %	N/A	20.0 %
Conc. III-V	32.4 %	N/A	25 %

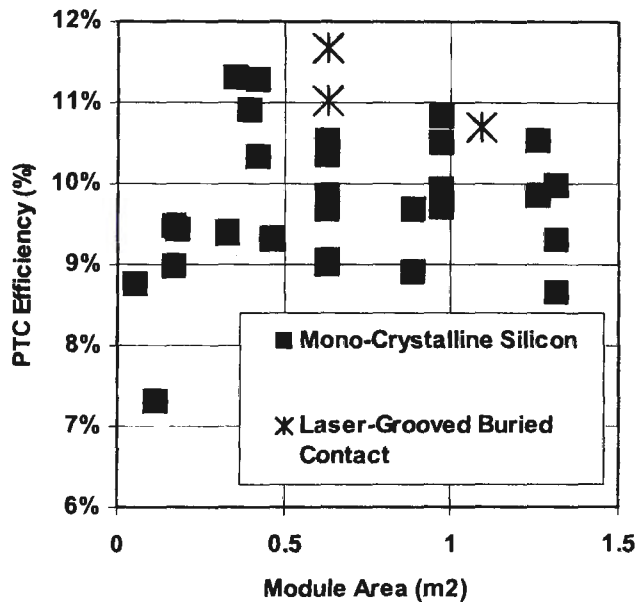


Figure 1: PTC efficiency of commercial PV modules with mono-crystalline silicon technology

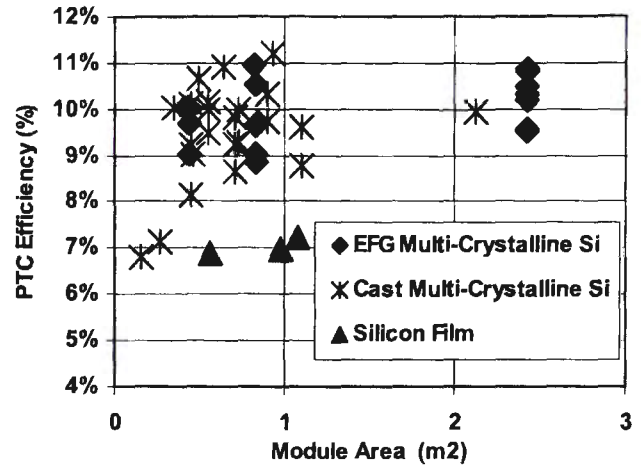


Figure 2: PTC efficiency of commercial PV modules with multi-crystalline silicon technology

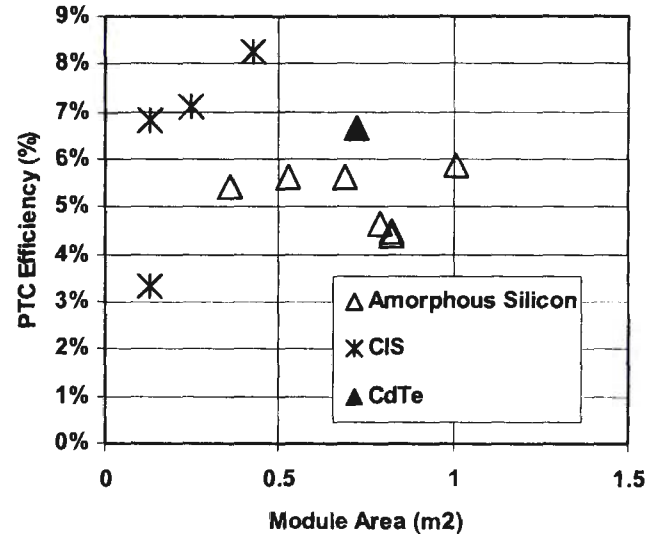


Figure 3: PTC efficiency of commercial PV modules with thin-film technology

5. HIGH-EFFICIENCY CONCENTRATOR SYSTEMS

5.1 Description of the concentrator PV system

Solar Systems Pty Ltd. has developed concentrator photovoltaic systems since 1990. The concentrator PV system is designed around a parabolic reflective dish, concentrating sunlight about 340 times (250X optical concentration) onto a photovoltaic receiver. The 24 x 24 cm receiver is composed of a dense array of 16 PV modules (6 x 6 cm) assembled by Solar Systems using dense-array cells fabricated by SunPower Corporation.

The first large-scale proof of concept is a power plant operated by Solar Systems in White Cliffs, NSW, Australia. The power plant is composed of 14 parabolic concentrators, of almost 20 m² in area, that have been refurbished from a previous solar thermal experiment. In 1998, the reflective surface of the dishes and the old thermal receivers were replaced with new mirrors and photovoltaic receivers. The picture in Figure 4 shows a partial view of the entire power plant.



Figure 4: Partial view of the 14-dish photovoltaic power plant at White Cliffs, NSW, Australia, operated by Solar Systems. The result data presented in this paper are from the dish in front of this picture.

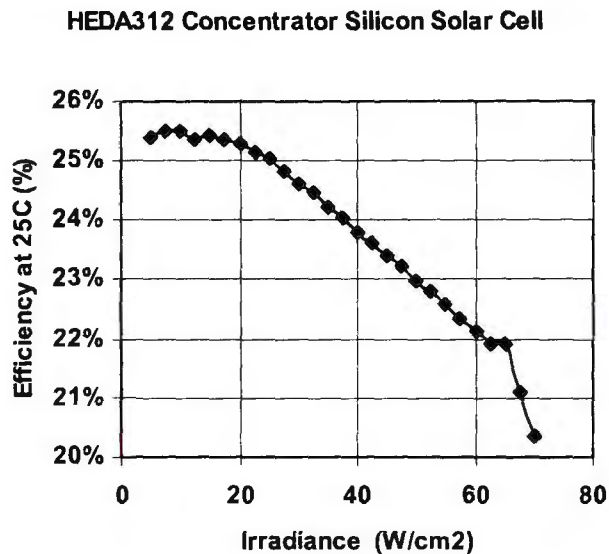


Figure 5: Efficiency of HEDA312 concentrator silicon solar cell for dense-array application vs. irradiance



Figure 6: Photovoltaic dense-array receiver assembled by Solar Systems, composed of 384 series-connected silicon backside contact (Point-Contact) HEDA312 solar cells from SunPower Corporation.

The silicon solar cells used on the receivers are HEDA312, Point-Contact solar cells from SunPower. The

cells are 1.0 x 1.5 cm and are specially designed for dense array application. A typical HEDA312 solar cell efficiency at 25°C is presented in Figure 5. The PV modules are built by laminating the solar cells onto a 6 x 6 cm ceramic substrate forming a dense array of 24 series-connected cells. The ceramic substrate is attached on a water cold plate for active cooling of the dense array. The solar cells are then protected by a thin AR-coated cover glass that is attached to the solar cell surface with RTV silicone.

The PV receiver of each dish is composed of 16 modules, each with 24 solar cells, forming a total of 384 series-connected solar cells. A picture of a receiver while in operation is shown in Figures 6 and 7.

5.2 Results

The following data (Table 3) has been taken from Dish No. 2 of the White Cliffs power plant on April 5, 2001 at 10:40 AM. The conditions were very similar to PVUSA Testing Conditions (PTC), i.e. 850 W/m², 20°C ambient temperature and 1 m/sec wind speed. In this case, the wind speed is not relevant because the receiver is actively water cooled, with the water being pumped from a very large water reservoir with an almost constant temperature.

The overall DC electrical efficiency is 20.02 % under conditions that are very similar to PTC, and without accounting for the parasitic power losses. Table 4 gives the value of the different parasitic power losses per dish. Taking into account the parasitic power losses, the overall system efficiency (DC) is 19.32 %. We believe that this is the first large-scale demonstration of a cost-effective photovoltaic system with a PTC efficiency greater than 20%.

5.3 Incident Power Density on Receiver

The total thermal power P_{Th} on the receiver is calculated from the water temperature difference ΔT_w between inlet and outlet of the cold plate manifold.

$$P_{Th} = \Delta T_w \cdot Q_w \cdot H_w = 9,098.7 \text{ W} \quad (4)$$

where Q_w is the cooling water flow rate in the receiver and H_w is the specific heat of water (4.186 J/g.K).

The total incident power density P_{in} impinging on the receiver can be calculated from the total thermal power P_{Th} and the total output electrical power P_{out} as follows:

$$P_{in} = (P_{out} + P_{Th}) / \{(1 - R) \cdot A_R\} \quad (5)$$

$$= 25.26 \text{ W/cm}^2$$

where R is the integrated reflectance from the cover glass surface and from the solar cell (front and back surface), and A_R is the receiver area (576 cm²). The reflectance of the receiver was calculated to be 13.78 %, from thermal reflection measurement (11.4%) and from simulations of radiation losses at high angle of incidence (2.7%). The incident power on the receiver is 14,552 W.



Figure 7: Photovoltaic receiver of Dish #2 while in operation. The incident power density is 25.3 W/cm^2 in average. One can notice the “flux modifier” in front of the solar cells.

Table 3: Measurement data from Dish No. 2

Data	Symbol	Value	Accuracy
Ambient Temperature	T_A	19.7°C	$\pm 1.0^\circ \text{C}$
Direct Normal Irradiation	DNI	872 W/m^2	$\pm 3\%$ Class 1 Pyroheliometer
Water Flow Rate	Q_w	33.44 lpm	$\pm 5.0\%$
Dish Area	A_D	19.75 m^2	
Receiver Area	A_R	576 cm^2	
Delta Temperature (In-Out)	ΔT_w	3.9°C	$\pm 0.1^\circ \text{C}$
DC Power Output	P_{out}	$3,448 \text{ W}$	$\pm 2.0\%$
DC system efficiency	η_{DC}	20.02%	$\pm 5.0\%$

Table 4: Parasitic power loss per dish

Power Loss	Value	Accuracy
Control Electronics	30 W	$\pm 5 \text{ W}$
Water Pumping	86 W	$\pm 1.5\%$
Tracking Motors		
Azimuth	1.28 W	$\pm 2\%$
Elevation	3.52 W	$\pm 2\%$
TOTAL	120.8 W	$\pm 10 \text{ W}$

5.4 Receiver Electrical Efficiency

The efficiency of the receiver, i.e. the efficiency of the 384 series-connected solar cells, at operating temperature is calculated as follows:

$$\eta_R = P_{out} / (P_{in} \cdot A_R) \quad (6)$$

$$= 23.7\%$$

The average cell temperature, calculated from the water temperature and the temperature drop across the ceramic substrate and the cold plate, is 38.52°C .

For comparison to the outdoor efficiency results, we also have measured efficiencies at cell and module level. For this receiver, the typical cell efficiency, measured at SunPower with a flash testing system, was 25% at 25 W/cm^2 and 25°C . Considering a relative temperature coefficient of $-0.003/^\circ \text{C}$, the typical cell efficiency would be 24.0% at 25 W/cm^2 and 38.5°C . One should note that these reported cell efficiencies are for non-encapsulated solar cells. Since the anti-reflection coating is optimised for an RTV encapsulant, we have to expect that the efficiency of encapsulated solar cells with AR coated cover glass will be higher than the efficiency of non-encapsulated solar cells, due to a better match of the refractive indexes and a better light trapping.

Before mounting the modules in the receiver, indoor flash testing (at Solar Systems) of the least efficient module showed an efficiency of 26.5% at 25.0 W/cm^2 and 21°C . Considering a relative temperature coefficient of $-0.0038/^\circ \text{C}$, this module efficiency would be 24.7% at 25 W/cm^2 and 39°C .

Comparing the module efficiency (24.7%) to the receiver efficiency (23.7%) allows calculating the power losses, mostly due to light non-uniformity. There is an estimated relative loss of 4.1% in power due to light non-uniformity. This is very good considering, for example, that the cell efficiency varies from 25.3% at 10 W/cm^2 to 23% at 50 W/cm^2 .

5.5 Solar Cell Temperature

The temperature of the solar cells has been calculated from the average module temperature, $T_{mod} = 27.4^\circ \text{C}$, measured with thermocouples attached to the backside of the ceramic substrates, and from the variation of open-circuit voltage of the array with the incident power density. A previously measured open-circuit voltage temperature coefficient of $-1.3 \text{ mV}/^\circ \text{C}$ per cell, or $-500 \text{ mV}/^\circ \text{C}$ for the array, allowed us to determine the U-factor and to derive the average cell temperature by the following formula:

$$T_{cell} = T_{mod} + P_{in} / U\text{-factor} \quad (7)$$

where the U-factor has been measured to be $2.216 \text{ W/cm}^2 \cdot \text{K}$.

5.6 Concentrator Optical Efficiency

The concentrator optical efficiency is calculated from the ratio of the incident power on the receiver and the incident power on the dish:

$$\eta_{opt} = (P_{in} \cdot A_R) / (DNI \cdot A_D) \quad (8)$$

$$= 84.4\%$$

The optical efficiency of the dish calculated from several previous tests has shown to be around 86%. This value is only 2% relatively higher than this particular test value of 84.4%. The difference is probably due to the 5% accuracy in the water flow rate measurement.

The results of the performance calculations are summarized in table 5.

Table 5: Summary of the performance and operating conditions of the PV concentrator system at 872 W/m^2 .

Parameter	Symbol	Value	Accuracy
Dish Optical	η_{opt}	84.4%	$\pm 5.0\%$

Efficiency			
DC System Efficiency	η_{DC}	20.02 %	± 5.0 %
System Efficiency with Parasitic	η_{DC^*}	19.32 %	± 5.0 %
Receiver Efficiency	η_R	23.7 %	± 5.0 %
Module Efficiency	η_{mod}	24.7 %	± 5.0 %
Cell Efficiency	η_{cell}	24.0 %	± 5.0 %
Average Cell Temperature	T_{cell}	38.52°C	± 2.0 °C
Average Module Temperature	T_{mod}	27.4°C	± 5.0 %
Inc. Power Density	P_{in}	25.26 W/cm ²	± 5.0 %
Inc. Power on Dish	$P_{in} \cdot A_D$	17,222 W	± 3.0 %
Inc. Power on Receiver	$P_{in} \cdot A_R$	14,552 W	± 5.0 %
Total Thermal Power	P_{Th}	9,098.7 W	± 5.0 %
DC Electrical Power	P_{out}	3,448 W	± 2.0 %

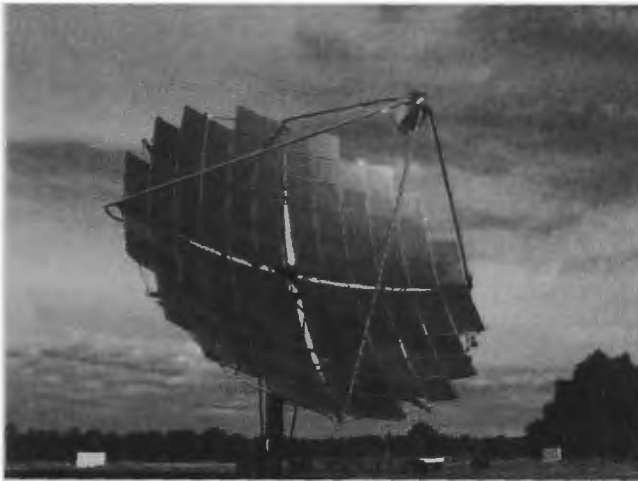


Figure 8: Solar Systems large-area (130 m²), high-efficiency concentrator PV system with 24 kW rated power.

5.7 Recent Concentrator Development

The power plant at White Cliffs is the first large-scale demonstration of high-efficiency PV concentrator systems. It is an excellent proof of concept. Solar Systems has recently developed a larger concentrator PV system that will be soon deployed in the Australian outback. The concentrator has a projected aperture of 130 m² and concentrates the sunlight onto a 48 x 48 cm receiver with a 560X concentration ratio (50 W/cm²). The DC power output of this new concentrator system is 24 kW. Figure 8 shows a picture of the large area concentrator system.

6. CONCLUSIONS

Most of the components in the cost of a PV system are proportional to the area of the system and the solar cell processing cost represents a small portion of the overall system cost. Therefore, the cell efficiency has a large impact on the cost of energy produced by photovoltaics. Not only the use of high-efficiency solar cells allows reducing the PV system area, but also higher efficiency cells have a lower efficiency temperature coefficient and make PV modules with higher PTC efficiency.

The efficiency of commercially available flat plate PV modules is still in the range of 5% to 12% (measured under PVUSA Testing Conditions) far behind the record efficiencies of laboratory cells. Only concentrator PV systems have, so far, demonstrated high-efficiency, above 20%, or 170 W/m² for comparison with flat-plate, under PVUSA Testing Conditions, in a cost-effective way.

We also reported the performances of a concentrator PV system, based on reflective parabolic dish and silicon Point-Contact solar cells, in a large-scale demonstration in White Cliffs, Australia. The concentrator system has an overall efficiency of 20.02% under testing conditions that are very similar to PTC. We believe this the first time that a cost-effective concentrator PV system with such high efficiency has been demonstrated.

REFERENCES

- [1] M.A. Green, K. Emery, D.L. King, S. Igari and W. Warta, "Solar Cell efficiency Tables", Progress in Photovoltaics, Vol. 9-1, 2001, pp. 49-56
- [2] P.J. Verlinden, R.A. Crane, R.M. Swanson, T. Iwata, K. Handa, H. Ogasa and D.L. King, "A 21.6% Efficient Photovoltaic Module with Backside Contact Silicon Solar Cells", 12th European PV Solar Energy Conference, 1994, pp. 1304-1306
- [3] P.J. Verlinden, R.M. Swanson, R.A. Crane, K. Wickham and J. Perkins, "A 26.8% Efficient Concentrator Point-Contact Solar Cell", 13th European PV Solar Energy Conference, 1995, pp. 1582-1585
- [4] D.L. King, Sandia Photovoltaic Performance Model I-V Curve Tracer, Module Database, 2001
- [5] M.J. O'Neill, A.J. McDanal, H.L. Cotal, R. Sudharsanan, D.D. Krut, J.H. Ermer, N.H. Karam and D.R. Lillington, "Development of Terrestrial Concentrator Modules Incorporating High-Efficiency Multi-Junction Cells", 28th IEEE PVSC Conference, pp. 1161-1164
- [6] J. Zhao, A. Wang, F. Yun, G. Zhang, D.M. Roche, S.R. Wenham and M.A. Green, "20,000 PERL silicon cells for the 1996 World Solar Challenge solar car race", Progress in Photovoltaic, 1997, 5, pp. 269-276
- [7] T.L. Jester, "Specific PVMAT R&D on Siemens CZ Silicon Product Manufacturing", 28th IEEE PVSC Conference, pp. 1399-1402

1.7 Edwards J.H., Badwal S.P.S, Duffy G.J., Lasich J.B.,
Ganakas G., 2002, “The Application of Solid State
Ionic Technology for Novel Methods of Energy
Generation and Supply”, *Solid Ionic States*

22/7/02



ELSEVIER

Solid State Ionics 8559 (2002) xxx-xxx

SOLID STATE IONICS

www.elsevier.com/locate/ssi

The application of solid state ionic technology for novel methods of energy generation and supply

J.H. Edwards^a, S.P.S Badwal^{b,*}, G.J. Duffy^a, J. Lasich^c, G. Ganakas^c

^aCSIRO, Energy Technology, P.O. Box 136, North Ryde, NSW 1670, Australia

^bCSIRO Manufacturing Science and Technology, Private Bag 33, Clayton South 3169, Victoria, Australia

^cSolar Systems (Australia) Pty. Ltd., 6 Luton Lane Hawthorn, Victoria 3122, Australia

Abstract

Solid state ionic technologies such as fuel cells, sensors, batteries, supercapacitors, hydrogen generation, storage devices and electrochromic windows are likely to play a major role in extending the life of existing fossil fuel resources by increasing the overall efficiency of energy generation and use. This will lead to a reduction in the emissions of greenhouse gases and pollutants. No single technology in isolation is likely to provide solutions for the energy and environmental needs of future generations. This paper briefly outlines the applications of solid state ionic technologies for sustainable energy generation and summarises key Australian initiatives in this field. It also emphasises the significance of a total systems approach and discusses integration of renewable and solid state ionic technologies for clean and sustainable energy generation.

© 2002 Published by Elsevier Science B.V.

Keywords: Solid state ionics; Energy generation; Renewable energy; Fuel cells; Hydrogen; Distributed generation; Sustainable energy

1. Introduction

Energy generation, which to date has largely been based on fossil fuels, is a major source of anthropogenic greenhouse gas emissions and other pollutants. However, future energy generation must be sustainable in terms of cost, fuel resource availability and environmental acceptability. In addition, energy must be generated and supplied in the form and quality to meet the end-user requirements.

Much effort is being spent on sustainable energy supply through measures such as the development of more efficient energy generation technologies, increased end-use efficiency and greater use of renewable energy sources such as solar, wind, and biomass. At the same time, there is an increased emphasis on small-scale distributed electricity generation. Fuel cells have the potential to play a dominant role in the future distributed energy generation network, with their high fuel conversion efficiencies, and as a clean source of power (significantly lower pollution and greenhouse gas emissions compared to those of conventional, centralised power generation). Furthermore, the use of fuel cells in transport vehicles as an auxiliary power unit or a

* Corresponding author. Tel.: +61-3-9545-2719; fax: +61-3-9545-2720.

E-mail address: Sukhvinder.Badwal@csiro.au (S.P.S. Badwal).

47 replacement for internal combustion engines will
48 bring substantial benefits in terms of clean urban
49 air and by extending the life of existing fossil fuel
50 resources.

51 While solid oxide (SOFC) and polymer electrolyte
52 membrane (PEMFC) fuel cells and oxygen sensors are
53 perhaps the best known and most prominent applica-
54 tions of Solid State Ionics (SSI) in the field of energy
55 generation, other potential areas are starting to
56 emerge. These include hydrogen production from
57 solar energy and novel methods of oxygen separation
58 from air. The latter is a major cost component for the
59 generation of electricity in advanced technologies
60 such as Integrated Gasification Combined Cycle
61 (IGCC) and CO₂ recycle combustion systems. Sub-
62 stantial demand for oxygen also exists for syngas
63 (CO+H₂) production from natural gas. Syngas is a
64 precursor for the production of methanol and higher
65 hydrocarbon liquid fuels.

66 Moreover, no single technology in isolation is
67 likely to fulfill the future energy and environment
68 needs of our society. Furthermore, from a systems
69 point of view, to meet end-user requirements, fuel
70 cells may have to be combined with other technolo-
71 gies, such as advanced energy storage systems based
72 on new batteries and supercapacitors.

73 Efficient and cost-effective energy storage systems
74 are crucial for new load levelling and electricity
75 supply applications, as well as for the wider use of
76 solar and other renewable energy sources in both
77 stationary and mobile power applications. Storage
78 technologies such as advanced batteries and high-
79 power delivery supercapacitors will play key roles,
80 while hydrogen generated from renewable energy is
81 seen as the fuel of the future.

82 The use of solar thermal-fossil energy schemes for
83 hydrogen production in combination with fuel cells is
84 one way of integrating renewable energy with high
85 efficiency power generation. In a major project,
86 CSIRO is demonstrating proof-of-concept for such a
87 technology based on the steam reforming of methane
88 using solar thermal energy to produce solar-enriched
89 hydrogen fuel for use in fuel cells [1,2]. Purely renew-
90 able hydrogen can be generated by the electrolysis of
91 water using PV- or wind-derived electricity. However,
92 this route to date has been hampered by very low
93 overall efficiencies and high costs. One way of improv-
94 ing the efficiency of a solar hydrogen system in the so-

called sun-belt countries is to combine high-temper- 95
ature hybrid solar collectors, which can cogenerate 96
electricity, and high-grade heat with novel high-tem- 97
perature steam electrolysis in solid electrolyte systems. 98

New solid state ionic devices and systems will be 99
essential components of these new technologies, and 100
considerable R&D is being conducted in this area. 101
This paper briefly outlines the main SSI technologies 102
for sustainable energy generation and their potential 103
for centralised and distributed energy generation, 104
transport applications and for advanced hydrogen 105
production and utilisation through the incorporation 106
of new SSI technologies into novel concepts and fully 107
integrated systems. It will also summarise key Aus- 108
tralian initiatives in each of these areas. 109

2. SSI technologies for energy generation, storage 110 and supply 111

SSI technologies that are set to play increasingly 112
important roles in sustainable energy systems include: 113

- fuel cells (PEMFC and SOFC); 114
- advanced batteries (based on Li⁺, Na⁺ and H⁺ 115
conductors); 116
- supercapacitors (polymer membrane capacitors); 117
- ionic-transport membranes (gas separation and 118
chemical reactors); 119
- electrolyzers for hydrogen production (low-temper- 120
ature water electrolysis and high-temperature steam 121
electrolysis); 122
- advanced sensors for process control and safety; 123
- electrochromic smart windows for optical modu- 124
lation and energy-efficient buildings. 125

126
127
Several of these technologies are being commer- 128
cialised now while the others are at various stages of 129
development. All are set to play increasingly impor- 130
tant roles across the entire spectrum of sustainable 131
energy generation and supply. Several projects estab- 132
lished around the world to demonstrate these technol- 133
ogies for energy generation are clearly indicating the 134
significance of a fully integrated approach to com- 135
mercialisation. Although SSI technologies have high 136
efficiencies and environmental benefits in their own 137
right, their integration with other energy generation 138
systems (e.g. cogeneration, tri-generation, renewables,

139 etc) will further improve overall system performance
140 and emissions reduction.

141 142 2.1. SSI technologies in centralised generation

143 In general, most SSI technologies are essentially
144 modular in design. The SOFCs, in particular, have
145 the potential for larger-scale, centralised generation
146 through their suitability for base load generation and
147 for integration with gas turbine and IGCC technol-
148 ogies.

149 The most advanced SOFC technology with poten-
150 tial for centralised generation is the tubular SOFC
151 being developed by Siemens Westinghouse. Proof-of-
152 concept for linking this technology with a small gas
153 turbine is being demonstrated with a 220-kW_e system
154 (200 kW_e SOFC and 20 kW_e microturbine generator).
155 The system is expected to achieve an overall electric
156 efficiency approaching 60%. Plans to scale up this
157 combined cycle technology into the multi-megawatt
158 range are in progress [3].

159 IGCC is regarded as one of the most environ-
160 mentally friendly technologies for power generation
161 from coal. Further increases in efficiency and emis-
162 sion reduction can be achieved by integrating SOFCs
163 with IGCC.

164 Ceramic membranes with high oxygen-ion con-
165 ductivity or mixed ionic/electronic conduction can be
166 used to generate oxygen or for the production of
167 syngas (CO + H₂) by the partial oxidation of methane
168 [4-6]. In particular, membranes with mixed oxygen
169 ion and electronic conductivity have potential appli-
170 cations for large-scale (tonnage) oxygen generation.
171 The electrons in the membrane combine with oxygen
172 in the air to create negatively charged oxygen ions,
173 and the driving force for oxygen-ion transport is
174 provided by the differential partial pressure of oxygen
175 across the membrane at the operating temperature of
176 the device. For oxygen generation, the pressure differ-
177 ence across the membrane is provided by having
178 lower oxygen pressure in the chamber where oxygen
179 is generated or by high pressure on the air side. For
180 syngas production, the process involves combining
181 oxygen separation from air with methane partial
182 oxidation in a single reactor, a considerable advantage
183 over conventional oxygen-generating technologies.
184 The partial pressure differential across the membrane
185 is provided by air being on one side and the natural

gas on the other side of the membrane. Such mem-
brane reactors could be significantly smaller and the
cost of oxygen generation much lower than existing
technologies.

2.2. SSI technologies in distributed energy generation

There is a worldwide trend away from centralised,
coal-fired power generation to smaller-scale distrib-
uted systems based on gas and, where appropriate,
renewable energy. Distributed energy generation sys-
tems are sited at or near the end user location and have
advantages of high efficiency and low cost due to:

- Use of new technologies (e.g. fuel cells and microturbines);
- Ability for cogeneration and tri-generation of electricity, heat and cooling;
- Greatly reduced transmission losses.

Distributed generation, thus, has great potential for
reducing greenhouse gas emissions and represents
huge opportunities for SSI technologies. They will be
an important part of energy supply to industry, com-
mercial buildings and down to individual households.
For example, the smart house concept (Fig. 1) shows
how a fuel cell, combined with suitable technologies
for utilising the waste heat, could be used to supply a
house's total requirements of electricity, hot water and
space heating/cooling. The overall energy efficiency of
such a configuration could approach 90% [7].

Both SOFCs and PEMFCs have the potential of
being the leading technologies over the next 20 years
for use in distributed energy generation systems,
ranging in size from a few kilowatts to megawatts.
Several small-size units to 10 kW_e incorporating
PEMFCs are being demonstrated for the residential
and remote area power supply markets. A 100-kW_e
SOFC generator developed by Siemens Westinghouse
has been tested in The Netherlands for 2 years and
250-kW_e PEMFC systems are being supplied by
Ballard for evaluation in several countries.

In Australia, the planar-type SOFC technology,
being developed by Ceramic Fuel Cells, is targeting
systems at the tens of kilowatt scale for a full range of
distributed energy applications. More than A\$70 mil-
lion has been invested over a 9-year period beginning
in 1992.

186
187
188
189
190
191
192
193
194
195
196
197
198
199
200
201
202
203
204
205
206
207
208
209
210
211
212
213
214
215
216
217
218
219
220
221
222
223
224
225
226
227
228
229
230
231

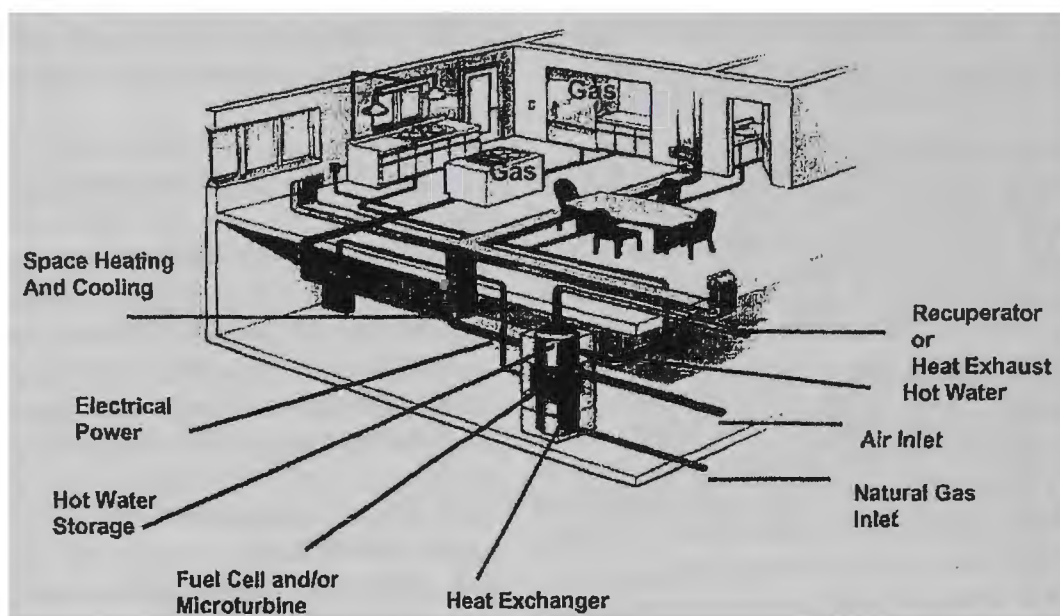


Fig. 1. Smart House Concept described in Ref. [7] and modified by N. Lockhart of CSIRO Energy Technology.

232 The CSIRO Centre for Distributed Energy and
 233 Power (CenDEP) is an association of industry and
 234 government organisations with a common aim of
 235 facilitating distributed generation in Australia. The
 236 Centre will facilitate substantial market penetration
 237 for distributed energy and power generation systems
 238 by providing a focus for technology development and
 239 demonstration, and the associated scientific and engi-
 240 neering research. It will optimise and integrate inno-
 241 vative fossil fuel and renewable energy technologies
 242 in a manner that is commercially relevant, able to
 243 influence government policy and regulation, and will
 244 deliver substantial environmental and greenhouse
 245 benefits.

246 247 2.3. SSI technologies in transport applications

248 SSI technologies are set to play key roles in
 249 future transport systems, both through the use of
 250 advanced supercapacitor/battery systems in hybrid
 251 electric vehicles, and fuel cells to power passenger
 252 cars, buses, light commercial trucks and heavy
 253 transport trucks. Ballard Power Systems/Daimler-
 254 Chrysler is the leading group commercialising
 255 PEMFC technology for the passenger vehicle (50
 256 kW_e) and buses (250-kW_e generator) [8]. Most
 257 major car manufacturers (Ford, General Motors,

DaimlerChrysler, Toyota, Honda, Nissan, Renault, 258
 etc.) are now showing interest in the development 259
 of an all-electric- and/or hybrid-drive trains utilising 260
 fuel cell technology, either in isolation or in combi- 261
 nation with supercapacitors and/or batteries. Both 262
 SOFCs and PEMFCs in the 3–10 kW_e range are 263
 also being considered as auxiliary power units for 264
 automotive applications. 265

The Australian hybrid, electric, low-emissions 266
 vehicle project was established to design and con- 267
 struct parallel- and series-drive, hybrid, electric 268
 vehicles [9]. The parallel-drive ECommodore vehicle 269
 demonstrated the capabilities of CSIRO and Austral- 270
 ian car makers to construct a full-size, hybrid, electric 271
 car, while the series-drive aXcess low-emissions 272
 vehicle demonstrated that CSIRO and Australian 273
 component manufacturers could design and construct 274
 a mid-size car that reduced fuel consumption and 275
 greenhouse gas emissions by 50% and all other 276
 pollutants by 90% [9]. 277

As part of the DaimlerChrysler's Cleaner Urban 278
 Transport for Europe (CUTE) proposal, three Daim- 279
 lerChrysler fuel cell buses are to be tested in Perth 280
 over a 2-year period from late 2002 [10]. Hydrogen 281
 fuel will be produced by BP from refinery waste gases 282
 and a range of hydrogen supply; infrastructure-related 283
 options will be tested. Longer-term hydrogen produc- 284

285 tion will be by steam reforming of natural gas and
286 ultimately, from renewable sources.

287 3. SSI technologies for sustainable hydrogen 288 production

289 Hydrogen for PEMFCs is currently produced by
290 reforming or partial oxidation of fossil fuels such as
291 natural gas and coal. For transport applications and for
292 on-board generation of hydrogen, reforming gasoline
293 and partial oxidation of methanol are other options
294 being considered. These processes are strongly green-
295 house-intensive and not sustainable in the long term,
296 thus, sustainable hydrogen must ultimately be derived
297 from water splitting or electrolysis using renewable
298 energy such as solar, wind, biomass or off-peak
299 hydroelectric power.

300 In the interim, hybrid concepts involving renew-
301 able and fossil energy are important steps towards
302 renewable, energy-based hydrogen production. One
303 such hybrid concept under the development of CSIRO
304 in Australia is briefly described below and is given in
305 more detail elsewhere [1,2].

307 3.1. CSIRO's "towards sustainable energy" project

308 A major project is being undertaken to demonstrate
309 a solar, thermal-gas hybrid energy concept for pro-
310 ducing hydrogen and using it to generate electricity

with potential for high thermal efficiencies and for
greatly reduced CO₂ emissions. The concept features:

- Reforming of CH₄-containing gases using con- 313
centrated solar energy to generate a mixture of 314
CO and H₂. 315
- The further conversion of this gas to H₂ and CO₂ 316
followed by recovery of CO₂ in a concentrated 317
form, as required for any subsequent CO₂ disposal 318
or utilisation scheme. 319
- Use of H₂ for electricity generation in a PEMFC 320
system, as these offer the maximum energy 321
conversion efficiency based on hydrogen fuel. 322

The project involves the construction and oper- 324
ation of a facility to demonstrate the key steps in the 325
technology so that its commercial prospects can be 326
more accurately assessed. The basic steps of the 327
concept are shown in Fig. 2. The gas can be any 328
methane-containing gas such as natural gas, coal 329
seam gas or landfill gas, etc. Solar thermal energy 330
is used to reform the gas to generate a synthesis gas 331
(CO and H₂), which can be used directly as a fuel or 332
as a chemical feed stock containing substantial 333
embodied solar energy. Alternatively, the reformed 334
gas can be further converted, via the water gas shift 335
reaction, to a mixture of CO₂ and H₂. This gas is 336
treated, prior to using the H₂ as a fuel, to recover 337
CO₂ in a concentrated form. This process is greatly 338
facilitated by having high CO₂ partial pressures and 339

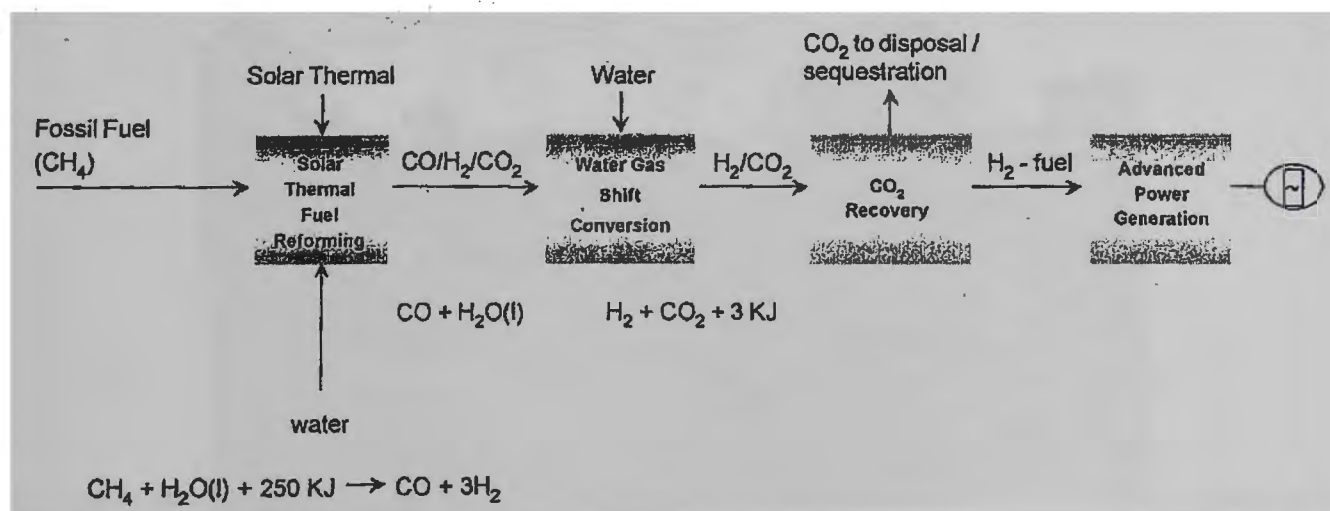


Fig. 2. Process steps for advanced power generation using solar thermal-fossil fuel hybrid concept.

340 relatively small gas volumes, compared with the
 341 alternative of recovering CO₂ from power station
 342 flue gas where the CO₂ is at low partial pressure and
 343 is heavily diluted with nitrogen. The recovered CO₂
 344 can be permanently disposed in various CO₂
 345 "sinks". These include injection into subterranean
 346 cavities or reservoirs such as aquifers, depleted oil
 347 and gas fields, deep unminable coal seams (possibly
 348 to assist in the recovery of coal bed methane) and in
 349 the deep ocean, by far the largest potential CO₂
 350 "sink".

351 The combination of advanced energy conversion
 352 technologies based on H₂ fuel, together with CO₂
 353 disposal, allows the highly efficient utilisation of
 354 fossil fuels with a dramatic reduction in atmospheric
 355 CO₂ emissions.

356 The demonstration facility (Fig. 3) is designed for a
 357 methane feed rate of 44 kW_{th} (Lower Heating Value
 358 basis) and consists of:

- 359 • feed supply and treatment units;
- 360 • a 107-m² paraboloidal, solar, thermal-concentrat-
 361 ing dish;
- 362 • catalytic reactors for steam reforming and water
 363 gas shift;
- 364 • CO₂ separation units;
- 365 • a unit to reduce the CO level in H₂ to <10 ppm;

- a 10-kW_e PEM fuel cell system from Air Liquide/
 DeNora. 366
 367
 368

Supporting this project is also a state-of-the-art
 PEMFC test facility that is being used to test and
 evaluate the performance of PEMFC stacks on a range
 of simulated fuel mixtures. The facility described in
 more detail elsewhere [11] consists of: 373

- test beds with capacity to test up to 3-kW_e size
 PEMFC stacks; 374
 375
- equipment for the fabrication of membrane elec-
 trode assemblies with at least 400 cm² active area
 cells; 376
 377
 378
- all associated gas supply, handling and safety
 equipment. 379
 380

3.2. Hydrogen from renewable energy 382

Hydrogen is widely regarded as the cleanest fuel
 of the future, provided it can be generated using
 renewable rather than fossil energy. A totally sus-
 tainable energy cycle would involve hydrogen gen-
 eration by water electrolysis using electricity
 generated from solar, wind, biomass or off-peak
 hydroelectric sources, its storage/transportation and
 384
 385
 386
 387
 388
 389
 390



Fig. 3. CSIRO's solar thermal-gas hybrid energy demonstration facility.

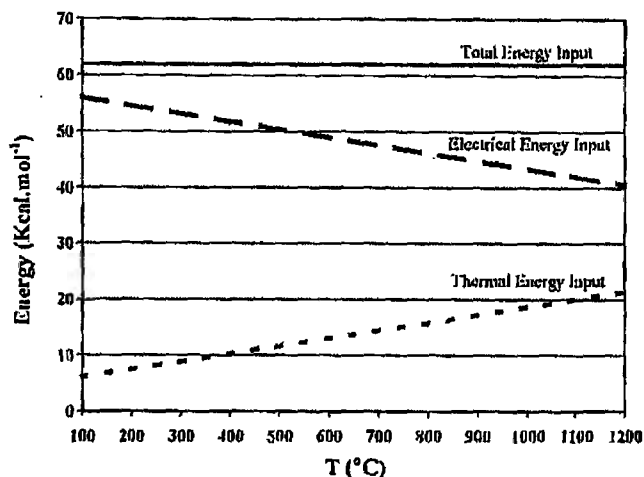


Fig. 4. Theoretical electrical and thermal energy inputs for water decomposition as a function of temperature [13].

purity hydrogen and oxygen when operated in reverse mode [12]. They offer the advantages of being an all-solid-state device with potentially high-conversion efficiency, small footprint and a less hazardous process configuration. However, hydrogen generated by this route is currently uneconomical and substantial effort is required to make the technology viable.

3.3. High-temperature steam electrolysis

High-temperature electrolysis of water has been known for some time to offer advantages in terms of high efficiency, as the electricity required for water splitting can be significantly reduced if it is conducted at elevated temperature [13]. This is shown in Fig. 4, which gives the theoretical electrical and thermal energy inputs for water decomposition as a function of temperature [13]. For example, although the total energy required is essentially independent of temperature, the electrical energy required at 1000 °C is only around 43 kcal

recombination in a hydrogen-based internal combustion engine or in a PEMFC system to generate electricity and heat on site. PEMFCs, with some design considerations, can be used to produce high-

SOLAR HYDROGEN GENERATOR SYSTEM

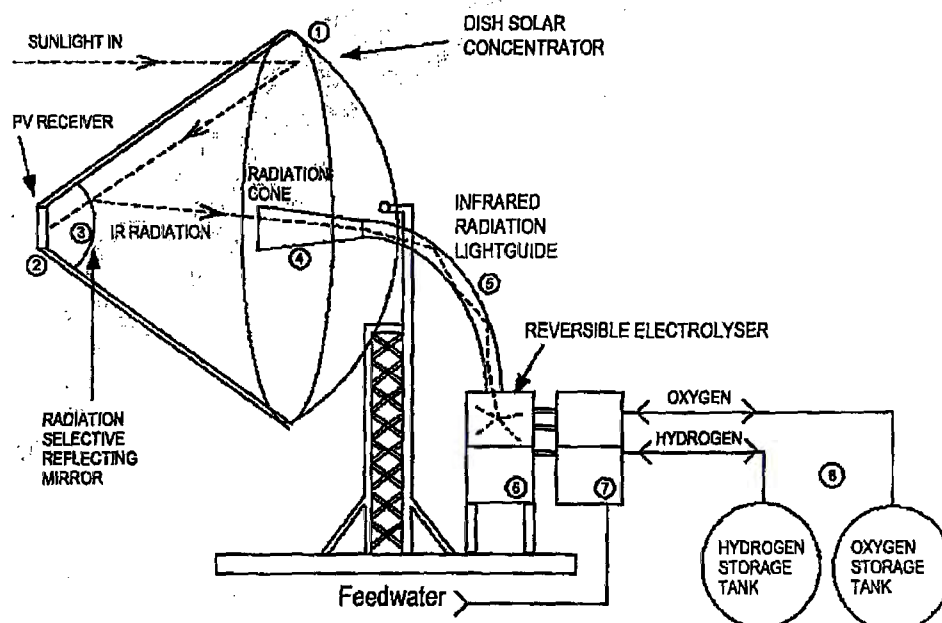


Fig. 5. A block flow diagram of Solar Systems' hydrogen generation system using solar concentration and beam splitting. (1) Tracked parabolic dish concentrator; (2) Photovoltaic receiver; (3) Selective reflecting mirror; (4) Radiation cone; (5) Light guide; (6) Ceramic electrolyser; (7) Heat exchanger/phase separator; (8) Storage vessels.

416 mol⁻¹ compared with 56 kcal mol⁻¹ at 100 °C, a
417 23% reduction.

418 Solar power systems have two technical limitations
419 however, which prevent them from becoming the
420 ideal mainstream energy providers:

- 421 (i) Intermittent operation due to lack of sun during
422 periods of cloud cover and overnight,
423 (ii) Low efficiency (resulting in high power costs).

424

425 In "sun-belt" countries such as Australia, it is
426 possible to use solar energy to provide both the
427 thermal and electrical energy needed for steam elec-
428 trolysis. One potentially attractive method for doing
429 this combines the solar-concentrating and beam-split-
430 ting technologies of Solar SystemsTM with high-temper-
431 ature, ion-conducting membrane technology for steam
432 electrolysis as shown in Fig. 5. This patented solar
433 hydrogen production process is theoretically capable
434 of delivering solutions to both these limitations, that
435 is, providing a continuous power source and operating
436 at a high efficiency [14].

437 In this process, hydrogen is produced from water
438 using solar-generated DC electricity and the cogen-
439 erated heat to drive a ceramic electrolyser. The DC
440 electricity and the cogenerated heat are produced via a
441 single solar concentrator unit to drive a ceramic
442 electrolyser to split water into hydrogen and oxygen.
443 The hydrogen and oxygen can be stored for recon-
444 version to electricity through a fuel cell on demand or
445 exported as a fuel. This system promises high effi-
446 ciency, and the storage of hydrogen eliminates the
447 intermittent nature of solar energy collection from
448 affecting the user, as well as being an energy carrier
449 which can be readily transported to other sites.

450 The generator incorporates a photovoltaic (PV)
451 receiver, a thermal receiver and a large (130 m²),
452 parabolic dish which concentrates, separates and
453 converts solar radiation into electricity and high-
454 grade heat. The electricity and heat may be used
455 directly or converted (at a high efficiency) into
456 hydrogen fuel for storage. In Fig. 5, the tracked
457 parabolic dish concentrator (1) concentrates solar
458 energy to the photovoltaic (PV) receiver (2) via the
459 selective reflecting mirror (3). The infrared (IR)
460 energy is selectively reflected by (3) to the radiation
461 cone (4) which channels IR radiation to the high-
462 temperature electrolyser (6) via the light guide (5) to

463 deliver thermal energy at 1000 °C. Simultaneously,
464 the short wavelengths which pass through (3) excite
465 the photovoltaic (PV) receiver which produces DC
466 electricity, which is also delivered to the electrolyser
467 (6). The hydrogen and oxygen generated in the
468 electrolyser (6) are fed via the heat exchanger/phase
469 separator (7) systems to storage vessels (8). To
470 provide a continuous supply of electricity, the hydro-
471 gen and oxygen may be converted back to electricity
472 through the reversible electrolyser (or a fuel cell).
473 Alternatively, hydrogen may be used for chemical
474 processing in the industry or used directly to fuel
475 transport vehicles.

476 The technique capitalises on the high efficiency
477 and intense beam produced by a large solar concen-
478 trator capable of delivering up to 112-kW radiation
479 to the receiver zone. The present electrical system
480 has a design output of 24 kW and a system effi-

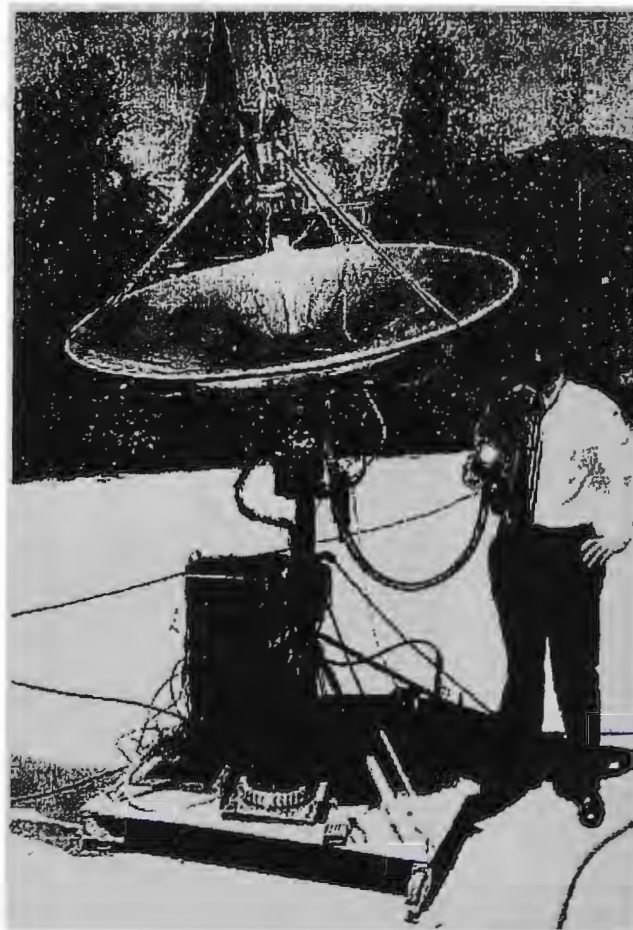


Fig. 6. A solar beam-splitting prototype test unit of Solar Systems.

481 ciency approaching 20% for PV conversion only.
 482 Splitting the spectrum in the intense beam provides
 483 an option to use a second receiver and cogenerate
 484 other energy forms such as high-grade heat. In the
 485 case of high-temperature electrolysis using a zirco-
 486 nia-based cell, all the energy input requirement can
 487 be provided by cogenerated heat from the split solar
 488 spectrum.

489 Fig. 6 is an illustration of a working spectrum-
 490 splitting prototype test unit developed at Solar Sys-
 491 tems. Radiation is concentrated to a primary PV
 492 receiver, where the short wavelength is utilised by
 493 the solar cells and the long wavelength is reflected
 494 through a light guide (being held by the operator). The
 495 infrared radiation is delivered at the end of the guide
 496 (accompanied by some visible light). A temperature of
 497 1100 °C has been achieved using this type of config-
 498 uration.

499 A theoretical efficiency of approximately 50% is
 500 possible using the process described above. Prelimi-
 501 nary experimental results to date show that the major
 502 components will function as required by the concept
 503 and that a practical efficiency of 30% or more is
 504 achievable.

505 4. Other SSI technologies for energy efficiency

506 There are a number of SSI technologies which
 507 are not within the scope of this paper but contribute
 508 directly or indirectly to the energy efficiency. These
 509 include batteries and supercapacitors that are not
 510 continuous sources of power and as such, are not
 511 considered as energy generation devices [15,16].
 512 However, they are important elements in the overall
 513 systems design providing short- or long-term energy
 514 storage when used in combination with other power
 515 generation technologies. Both hydrogen and oxygen
 516 sensors are used widely for safety monitoring,
 517 combustion control and process control/monitoring,
 518 and are key elements in power generation equip-
 519 ment and contribute indirectly to the reduction of
 520 energy consumption and greenhouse gas emissions
 521 [17]. Electrochromic smart windows, although not
 522 in widespread use, have the potential to reduce
 523 energy usage through optical modulation of radia-
 524 tion [18]. Electrochemical membrane reactors based
 525 on solid state ionic systems can provide efficient

and clean routes for the production of chemicals 526
 [6,19]. 527

5. Concluding remarks 528

Solid State Ionic technologies have the potential to 529
 contribute substantially to future energy and environ- 530
 mental needs of our society. Comprehensive SSI 531
 technology R&D programs are tackling the key tech- 532
 nical problems. A combination of renewable and SSI 533
 technologies have the potential to move energy gen- 534
 eration to a totally sustainable energy cycle. However, 535
 future efforts must focus on complete systems devel- 536
 opment and integration for different end user applica- 537
 tions that include: 538

- SSI technologies alone; 539
- integration of SSI with other fossil energy 540
 technologies; 541
- SSI and renewable energy hybrid systems. 542

Each application must address cost, performance, 544
 power quality and reliability, along with grid-interfac- 545
 ing issues. 546

References 547

- [1] J.H. Edwards, G.J. Duffy, R.G. Benito, K.T. Do, N.C. Dave, 548
 R. McNaughton, S.P.S. Badwal, S.P. Jiang, S. Giddey, Renew- 549
 able Energy for the Next Millennium, March 8-10, Sydney, 550
 Australia, 2000. 551
- [2] J.H. Edwards, G.J. Duffy, R.G. Benito, K.T. Do, N.C. Dave, 552
 R. McNaughton, S.P.S. Badwal, Fifth International Conference 553
 on Greenhouse Gas Control Technologies (GHGT-5), August 554
 13-16, Cairns, Australia, 2000, p. 863. 555
- [3] S.C. Singhal, Solid State Ionics 135 (2000) 305. 556
- [4] T.J. Mazanec, Electrochem. Soc. Interface (1996) 46. 557
- [5] S.P.S. Badwal, F.T. Ciacchi, Adv. Mater. 13 (12-13) (2001) 558
 993. 559
- [6] P.N. Dyer, R.E. Richards, S.L. Russek, D.M. Taylor, Solid 560
 State Ionics 134 (2000) 21. 561
- [7] A.C. Lloyd, The power plant in your basement, Sci. Am., July 562
 1999, Adapted by N. Lockhart, CSIRO Energy Technology. 563
- [8] C. Stone, A. Morrison, Solid State Ionics (2002) this volume. 564
- [9] D. Lamb, Seoul 2000 FISTA World Automotive Congress, 565
 June 12-15, Seoul, Korea, 2000, p. 1. 566
- [10] Aust. Energy News (March 2001) 50. 567
- [11] S. Giddey, F.T. Ciacchi, S.P.S. Badwal, V. Zelizko, J.H. Ed- 568
 wards, G.J. Duffy, Solid State Ionics (2002) this volume. 569
- [12] W. Smith, J. Power Sources 86 (2000) 74. 570

ARTICLE IN PRESS

10

J.H. Edwards et al. / Solid State Ionics 8559 (2002) xxx-xxx

- | | | | |
|-----|--|--|-----|
| 571 | [13] J. Padin, T.N. Veziroglu, A. Shahin, <i>Int. J. Hydrogen Energy</i> | [17] W. Göpel, G. Reinhardt, M. Rösch, <i>Solid State Ionics</i> 136– | 577 |
| 572 | 25 (2000) 295. | 137 (2001) 519. | 578 |
| 573 | [14] J. Lasich, <i>The Production of Hydrogen From Solar Radiation</i> | [18] J. Bell, J.P. Matthews, I.I. Skryabin, <i>Solid State Ionics</i> (2002) | 579 |
| 574 | with High Efficiency, US Patent 5658448 (1997). | this volume. | 580 |
| 575 | [15] R.A. Huggins, <i>Solid State Ionics</i> 134 (2000) 179. | [19] P.J. Gellings, H.J.A. Koopmans, A.J. Burggraaf, <i>Appl. Catal.</i> | 581 |
| 576 | [16] R.M. Dell, <i>Solid State Ionics</i> 134 (2000) 139. | 39 (1988) 1. | 582 |